Façade Elements for 3DCP

Structural viability of façade elements manufactured by 3D Concrete Printing

Thesis report

Author

A. (Bram) R.C. Hekker
Delft University of Technology
Faculty of Civil Engineering and Geosciences
Department: Building Engineering

Thesis Committee

Prof. ir. R. Nijsse	TU Delft – Architectural Engineering + Technology
Dr. ir. H.R. Schipper	TU Delft – Civil Engineering and Geosciences
Ir. P.E. Eigenraam	TU Delft – Architectural Engineering + Technology
Ir. J.C. van Wolfswinkel	Movares Nederland B.V. – Structural Design
Theo Voogd	Bruil Beton & Mix – Market and Innovation

Preface

This thesis concludes the research project on the fabrication of façade elements by 3D concrete printing. It forms part of the graduation thesis for the master track Building Engineering at the Technical University of Delft (TU Delft). Additionally, the research was part of a collaborative exploratory research on concrete printing by concrete producer Bruil Beton & Mix and engineering firm Movares B.V. During the course of this research the potential of a small research group with the TU Delft is examined, which will hopefully continue the research.

The collaboration of the two companies lead to a great combination of theoretical research (on structural design) and practical research (on handling concrete). This allowed for research on many aspects, with the opportunity to retrieve advice and information from different disciplines. The possibility of using an actual 3D concrete printer provided a great advantage to the research and made the results much more tangible.

The multidisciplinary approach of the research on this innovative technique was a truly joyful experience for me. The subject fits well into my interests coming from an Architecture bachelor study switching Structural Design master at the Faculty of Civil Engineering. Also, my passions for technological innovation and parametric design were strengthened during the process.

I would like to thank both Bruil and Movares for offering me a place and the tools to conduct the investigation, as well as TU Delft for educating me. Thanks to Jan van Wolfswinkel and Theo Voogd for regulating and providing the means and guidance necessary during the research. With the qualitive feedback and guidance from the graduation committee I was able to complete the thesis in a successful manner. Accordingly, I would like to thank Rob Nijsse, Roel Schipper and Peter Eigenraam for their advice and assessment during the project, giving direction to the thesis and counseling me in the process. Finally, I want to thank my friends and family and all that helped and supported me in the process, including Wim van t Land, Elise Buiter and Eric Barendse.

Bram Hekker,

July 2018

Abstract

The novel technique of 3D Concrete Printing (3DCP) shows great potential in the reduction of labor and material as well as the fabrication of freeform design. Different research institutions and companies recognize this potential and have set up printers to further investigate and develop the technique all over the world. Some pioneering projects showcase the state of the art by producing full scale structures, but otherwise printing of concrete is done mostly in a research lab. In an effort to find whether 3DCP is ready for the current market of the building industry, this thesis performs a viability analysis on the production of façade panels by 3DCP. This research is performed for the University of Technology Delft and Movares Nederland B.V. using the concrete printer from Bruil.

The origins of 3DCP are defined by the development of Additive Manufacturing (AM) in other materials (plastics) as well as the demand for freeform concrete production. Both fields are examined to help understand from where the technique is derived and what its goal and potentials are. Next to the initiators, some of the more advanced researches on the topic are disclosed in order to define the current level of capability of concrete printing.

As this research focusses on testing the viability of 3DCP as production technique for structural verified elements, a case study is performed. Façade design is chosen as the design scope in order to consider the potential benefit of freeform design as well as integration of functions, which are both prominent in a building enclosure. Through analysis of façade designs, typologies and performance requirements, a concept design of a perforated façade panel is defined. Over the course of the case study the fabrication technique and the engineering model influence the design of the panel, and this design process is analyzed for the disciplines of design, engineering and fabrication. The façade panel is designed parametrically to allow façade patterns to be created by customized elements on mass-production scale (mass-customization). This sets the requirement for the engineering models to also be parameterized, for this a software strategy is defined.

Specimen are printed and tested to define material properties of printed concrete and analyze the effect of the additive manufacturing method on the strength and concrete development. Additionally, different forms of reinforcement are implemented in the 3DCP production process and tested on fabrication and structural aspects. Finally, the case study element is produced and load-tested to conclude the research on the feasibility of fabricating and engineering a façade panel by 3DCP. This thesis proves that the technique can produce elements from which the structural behavior (load bearing capacity and failure behavior) can be safely predicted.

Keywords: 3D Concrete Printing, Additive Manufacturing, Digital Fabrication, Façade elements, Product Development, Feasibility Research

Table of Contents

1. Research definition

Challenges arise from the new technique for printing 3D structures from concrete, demanding the building industry to evolve from the repetitive standardized production it is used to. This in turn requires designers to reevaluate the limitations of a 'design for production' concept, the known products and industrial parts, by adapting the design process to the printing production (Strauss, H., 2013). There are still boundaries to be considered for 3D printing since it brings along its own set of limits and possibilities. To encourage the development and implementation of this technique, the roles of the designers and engineers should be taken in to account (van Alphen, J.M.J., 2017, p.20).

Implementing 3D concrete printing (3DCP) in the building construction industry, requires research. Research on the manufacturing technique has been performed by various research groups and companies, these form a good basis for this research. However, as the technique is constantly innovating and renewing, new questions arise.

1.1. Motivation

The great potential of 3DCP is thoroughly reported by previous researchers in multiple research papers. These studies commonly conclude that the promising technique still has many aspects left unexplored. To stimulate the use of 3DCP in practice, the technique needs to be further developed and proven to be useable and applicable by current designers. Once the technique is adopted by designers it can start to live up to its full potentials.

Freeform architecture comes a big step closer to realization when computer driven 3D designs can be developed without compromise of standardization of elements. This form of digital manufacturing also enables the development of freeform designs by computer driven optimizations of structures. These shapes generally contain curvatures that current production methods are either incapable of or would cost a fortune. Optimization can lead to a great reduction in material use, effectively lower the costs and waste in the construction process.

The reduction of manual labor is a potential benefit for structures designed for 3DCP in automated fabrication process. By eliminating the use of molds and in situ pouring of concrete, the construction costs and time are greatly reduced in the future. In turn this will also reduce the health and safety risks on the worksite by reducing the necessity for labor on site. Altogether, the use of 3DCP needs to be stimulated in the building construction industry to gain great profits on all these fields.

1.2. Research objective

The feasibility for 3DCP to become an efficient and used manufacturing technique for façade structures is worth researching. The goal is to show how well the technique can be applied already, reflecting the current level of applicability. If this is the case, this thesis provides a basis for the integration of 3DCP into the construction industry. In the investigation towards this goal, challenges will arise which need to be addressed and overcome in order to lower the barrier for design and construction with 3DCP. These challenges can appear during the design process, but also during the manufacturing process. Concluding relations will be made by expanding the view from single designs to the construction industry as a whole and the role and influence of 3DCP in it.

1.2.1. Hypothesis

Digital manufacturing will impact the construction industry greatly and demands a change in the current design and construction process. A new production chain will (need to) be established in which the role of the designer, engineer and manufacturer will differ from their current function. Rapid manufacturing will demand a file to factory system in which all aspects are considered.

1.2.2. Research thesis questions

The structure of thesis report is guided by the main question and sub questions:

What is the influence of 3D concrete printing on the design and construction process of building envelopes?

- Chapter 2: What is the current state of the art on 3DCP?
  - What are the capabilities and restrictions of the current 3D concrete printer(s)?
  - What variables influence the printing process?
  - What researches have been conducted?
  - What products have been developed using 3DCP?
- Chapter 3: What is demanded from 3DCP façade design?
  - What are the wishes and demands from an architectural perspective?
  - What are the wishes and demands from an engineering perspective?
  - What functional aspects could be assigned to a 3DCP element?
- Chapter 4: What does it take to design and engineer a 3DCP façade element?
  - How are 3D geometry models for printers developed?
  - How are parametric engineering models developed?
  - What are restrictions in design due to the printing process?
- Chapter 5: What can be expected of printed concrete as a structural material?
  - What is the mechanical material behavior of printed concrete?
  - How can printed concrete be strengthened?
  - What components can be integrated in the fabrication process?
- Chapter 6: How is the future design and construction process affected?
  - What requirements should digital design models for 3DCP meet?
  - How should structural analysis be optimized for mass customization?
  - What discipline is involved at what stage of the process?

1.3. Research methodology

In order to accomplish the research objective, the project is divided in three parts and planned in steps. The general approach is to do this by starting with gaining knowledge by investigating what is currently known and done (literature investigation). Then the research is split into two domains: research (theoretical) and development (practical). The first part consists of analyzing and modeling façade designs, the second part is based on a case study, in which a façade element is designed, printed and tested. During the process of this thesis these two phases overlapped and influenced each other, but to form a coherent report they are written consecutively.

Literature investigation forms the initial part of the thesis, here existing researches on topics regarding 3D concrete printing are analyzed. In this part of the process the scope and frame of the thesis are determined and necessary knowledge for the case study is obtained. Furthermore, the investigation phase includes getting acquainted with the printer and its operation, through reading and practice.

During the **Research** and **Development** phase, the focus of the thesis is narrowed to the design and fabrication of façade elements. Requirements and wishes for façade design are correlated with the potentials of 3D concrete printing, the overlap forms the basis for the case study design. For this case study a design is modeled and eventually load tested. Smaller print tests are performed to gain insight on the material and fabrication method. Results from both phases are taken into account with the final case study design and fabrication.

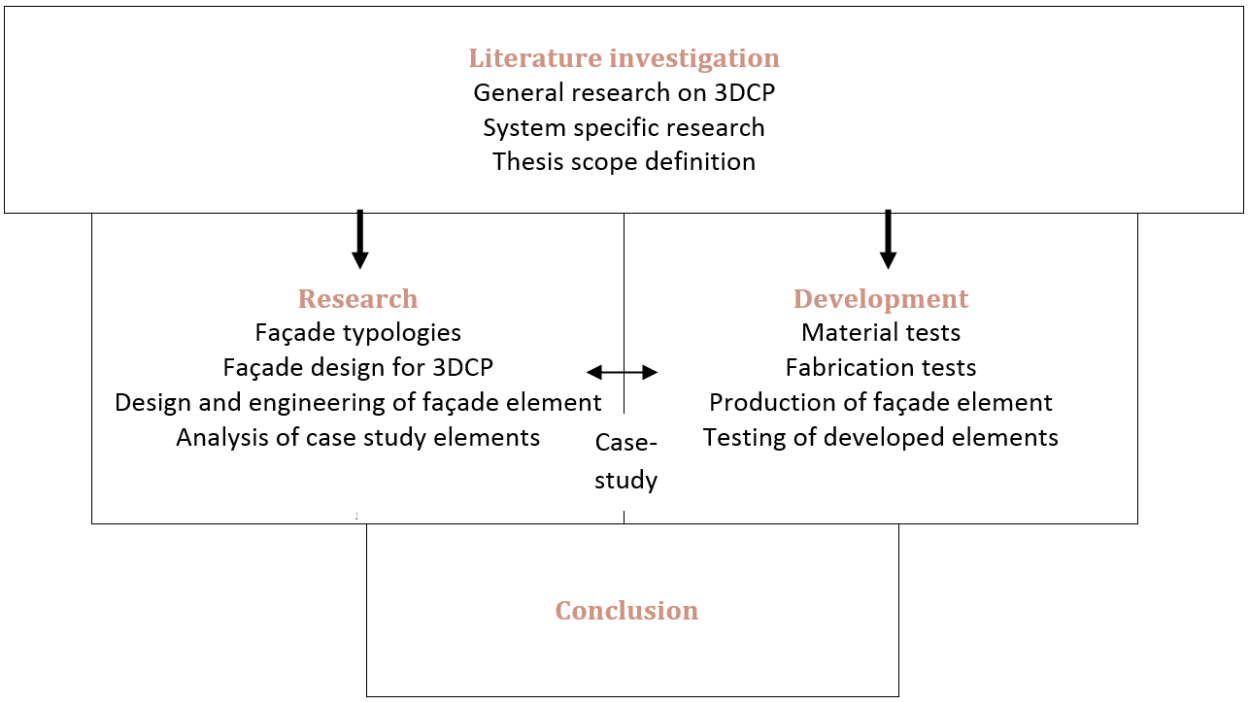

2. Literature Report

Introduction

This thesis report is divided in to several parts following the respective steps in the research process it regards. First is the literature research in which an investigation of literature on studies and experiments regarding 3D Concrete Printing is reported. This part of the report will introduce the technique from its predecessors to its current state. The focus will be structured towards the relevant information for the related design and case study: the design, fabrication and structural qualification of a façade element for 3DCP.

To understand the technique of 3D concrete printing (3DCP), first the origins must be explored. Looking at the bigger picture, the technique is a result of a development that affects society as a whole: digitalization. The world integrates computer use in every aspect of life, “the internet of things” and cryptocurrency are examples of this trend. Additive Manufacturing (and 3D printing) are products from the same trend, aiming to fabricate digitally produced models from digital files. This literature report is structured in the same manner as this scope is narrowed to 3DCP (see Figure 1). Finally, it will expand on the specific 3DCP technique that is subject of this thesis.

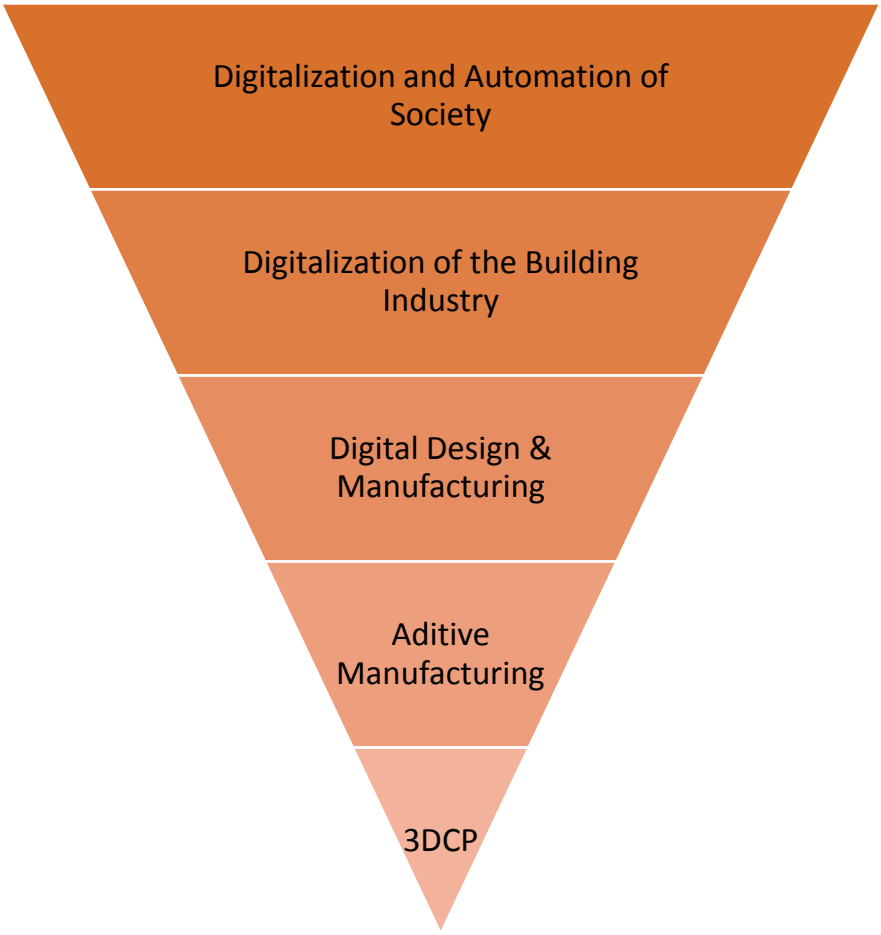

Figure 1: Literature report (chapter 2) structure

2.1. Digitalization of the Building Industry

The current age is becoming more digital every day and this trend is also adapted in the field of architecture by digital modeling. One of the results is freeform shapes with complex geometries which are designed and engineered by advanced computer models. However, fabricating these designs has proven to be a challenge which is either very expensive in production costs or avoided by reducing the complexity of the shape. A new, digital, fabrication technique is demanded that can provide freeform fabrication at the costs of standardized elements (de Witte, 2015, p. 3).

Computer aided design (CAD) brought a liberation in designing complex shapes by making complex 3D models comprehensible and workable for the designer. Along with this software development, the engineering was also influenced by the digitalization. The computing power of the computers increased and far exceeds that of a single structural engineer: digital models can now be structurally analyzed by finite element methods (FEM). Digital design and engineering is common practice in the majority of architectural and engineering firms nowadays (Constanzi, 2016, p. 1).

The construction world reacts slowly to change, but one of the effects of the digital world that can be observed today is the integration of professions. Using a single digital model to transfer information to all parties involved in the design, provides a method for integration of design and construction. Building Information Modeling (BIM) is doing exactly that by linking information from every field to certain parts of the digital model. In this manner every discipline can impose design constraints from their respective fields to the model (Wangler, et al., 2016, p. 74) (Eastman, Teicholz, Sacks, & Liston, 2011, p. 237).

The new designing way can only be realized if the building industry embraces technological upgrades. Therefore, on the other side of the process, production manufacturers are also moving towards a more digital environment: digital manufacturing. Eliminating the manual labor with computer numerically controlled (CNC) machinery, results in a reduction of both costs and errors. In the automotive industry this is proven concept and has automated many production lines. However this technology is not in use or even existent in the construction industry, because the adaption of the techniques to the building constructions is only a recent development (Ding, Wei, & Che, 2014, p. 1) (Wolfs, Bos, van Strien, & Salet, 2017, p. 1).

Figure 2: Heydar Aliyev Center, Baku (2013) by Zaha Hadid Architects

2.1.1. Digital Design

Architectural design without computer is unimaginable in today's world, engineering possibly even more so. Computer modeling has evolved considerably, due to the constant improvement of soft- and hardware, and with it the capabilities of digital design (Kolarevic, 2004, p. 43). This report refers to digital design as designing architecture and structures by using computer modelling software. Some of the characteristics and possibilities of digital design are briefly explained.

Freeform design

Modern architecture as seen today was made possible by digital design. Computer software provides designers and engineers with tools that allow free expressions. Especially with the introduction of three-dimensional modeling, freeform architecture became feasible in theory. But with this freedom in shape, designs took a leap towards geometric complexity (William, 2005, p. 41; Constanzi, 2016).

Due to limitations of the production industry, the digital designs are mostly reduced to standardized elements that represent the original designed shape in a cost-effective manner. Mass production reduces the element price, this is why repetition in design is stimulated. However, the digital design is looking for non-standard, alternatives to the logic of repetition. Architecture of this digital era is developing a new style and a 'new design thinking' (Oxman, 2005, p. 233).

One of the more recent tools that digital design offers to designers is computational design and modeling. Defining a design by (mathematical) relations between variables and restrictions in a model, enables computer analysis of complex systems. In other words, architectural designs can be shaped to best fit the modeled variables, such as daylight entry, circulation of people, acoustics, etc. These digital models are build up from input variables and parameters and their relations with each other and the restrictions (Papalambros & Wide, 2000, p. 5).

The ability to alter a design by changing the input variables, while the relations are maintained, became possible when parametric design was introduced. This form of designing is truly active because it responds to changes in wishes and demands. Parametric software (such as CATIA® and Grasshopper®) allows complex forms to be generated and manipulated in the design process. The interactive and transformable characteristics of parametric design can be useful to more disciplines, such as structural engineers, since it can be a tool for performative design (Woodbury, 2010) (Oxman, 2005, p. 252).

Structural Analysis

Computational modeling also plays a big role in the work of the structural engineer of today, especially in the structural analysis of larger and complex structures. One of ways in which structures can be analyzed is by dividing the design in smaller elements and modeling the restraints, loads and element properties, this is known as Finite Element Modeling and Analysis (FEM and FEA). A well described example is the study of Vizotto (Computational generation of free-form shells in architectural design and civil engineering, 2010), where a freeform structure is designed, optimized and analyzed, with the underlying assumption that it could be fabricated by 3D concrete printing (Contour Crafting).

When parametric design is used to optimize a structure, one or more input parameters are varied, and their relative performance is simulated by multiple iterative calculations (Kolarevic, 2004, p. 141). For example, when the desired behavior is a maximum deflection under a certain load, a parametric structural model can calculate the deformed shape under a certain load. Performance based optimization can than alter the set of design parameters to generate a shape that fulfills the requirements given the set of restraints and relations, this is often referred to as topological optimization (Oxman, 2005, p. 257).

Another type of computational optimization is “Evolutionary” methods (e.g. BESO) or using a soft kill option (SKO) (Mattheck, 1998, p. 238). These methods remove material where it is least effective and recalculate the model under the given design load. The desired performance, for example maximum stress or deflection, is set as a limit which will determine the amount of material that is removed (de Witte, 2015, p. 93). A good example is the optimized grid shell joint of L.P.L. van der Linden (Innovative joints for gridshells: joints designed by topology optimisation and to be produced by additive manufacturing, 2015, p. 16) which is designed and fabricated with additive manufacturing of steel.

Information modeling

As all steps in the design process, the sharing of information also became more digital. With this development another opportunity arose, namely attaching information to models or specific parts thereof (Building Information Modeling, BIM). This allows multiple parties involved in the design process to share their information in one model and create a truly integrated design. However, this does demand a specific type of design process, one in each discipline is actively involved in designing. In practice BIM is used to check designs and possibly dimension elements, rather than used from start to finish (Constanzi, 2016, p. 1) (Rolvink, Mueller, & Coenders, 2014, p. 2).

Because BIM designing is a relative young concept, and software development is fast, the possibilities and use is still growing. Coenders proposes multiple strategies in which parametric and associative design (PAD) can be used as BIM (Parametric and associative design as a strategy for conceptual design and delivery to BIM , 2010). In the prescribed design process, freeform designs could integrate multiple disciplines, and the shape and function of the design could truly go hand in hand. The adaption of PAD as BIM could well be a great step towards the atomization of the design process (Coenders, 2010, p. 2).

When the design model is also interpretable by the manufacturer, the circle is closed and a file to factory cycle is created. With additive manufacturing (AM) this might be closer than traditional fabrication techniques. For production by AM, the 3D model needs to be converted to a print path which the robot arm (of the printer) can follow and depose material on. This is done by slicing the digital geometry in to layers, called G-code, which is then fed to a computer numerically controlled (CNC) machine (Strauss, 2013, p. 31) (Constanzi, 2016, p. 56)

2.1.2. Digital Manufacturing

Digital manufacturing is the latest step in the ever-ongoing industrial revolution, according to many including The Economist (The Third Industrial Revolution, 2012). It started in the 18th century, when the transition from manual labor to machines took place and with the invention steam engines much of the physical labor was industrialized. Then came the automation we know from the assembly line workflow of Henry Ford, introducing mass production. Now the third step in the revolution has emerged: digitalization of the production industry. (Wangler, et al., 2016, p. 1).

Robots (CNC machines) have been in control of the assembly in the automotive industry for some years now and much of the production line for mass production are now fully automated (see Figure 3). With the arrival of Additive Manufacturing (AM, often referred to as 3D printing) a new production technique was introduced. This was firstly primarily used for rapid prototyping by designers but is currently in effect in the production of structural parts in the automotive and aviation industries. In the (building) construction industry AM production techniques are used on an experimental scale only (van der Linden, 2015, p. 19).

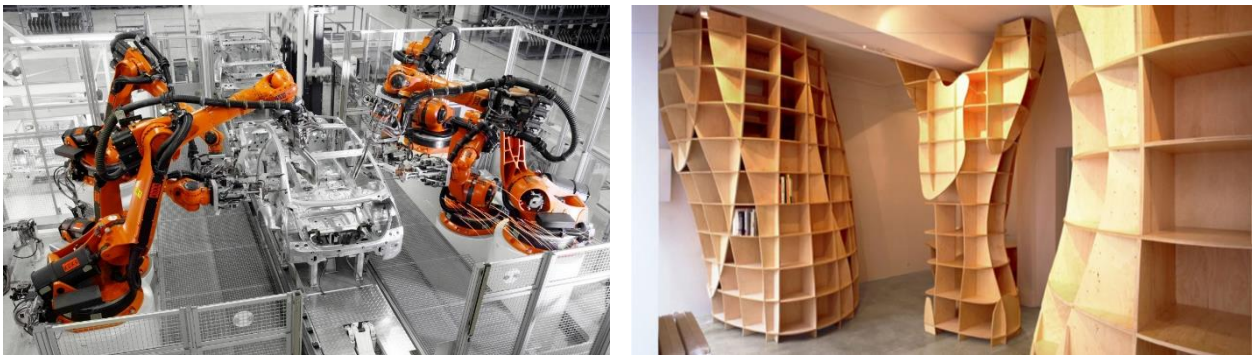

Figure 3: (left) Automated assembly line of the automotive industry (image: www.kuka.com)
(right) Loewy Bookshop furniture by Jakob and MacFalane (Paris), by digital fabrication

One of the advantages of digitalization of production, is the ability to make every element unique without increasing the costs. This type of digital controlled variation results in mass-customization of elements, discarding the necessity for repetition in designs (Kolarevic, 2004, p. 84). Mass-customization, which is a combination of mass production with individual customization, can provide the solution for the complex geometries that are envisioned with parametric design (Strauss, 2013, p. 169). In interior design this type of digital fabrication is already present (Figure 3) as L. Iwamoto shows in her book (Digital Fabrication: Architecture and Material Techniques, 2013). This could be motivator for the manufacturing industry of construction parts to push AM technology and start to develop structural parts for buildings. In order to do so, knowledge on AM techniques needs to be acquired.

Additive Manufacturing

In everyday use the term 3D printing is often used to refer to AM techniques, however in the scientific world Additive Manufacturing summarizes all the production techniques that apply additive methods. In general AM is any production technique that forms three dimensional objects by adding material together in a layered manner, most commonly by gluing or fusing (Strauss, 2013, p. 18) (de Witte, 2015, p. 21). The origins of layered fabrication can be found in photo sculpturing and topological modelling already in 1890, but development in AM really took off from 1951 when Munz invented the Stereo Lithography Apparatus (Bourell, Beaman, Jr., Leu, & Rosen, 2009).

The basis for every AM produced element is a 3D computer model, digitally modeled and then translated (sliced) into coordinates or paths where the selected AM machine needs materialize the object. It then goes into an automated production process where no further tooling is needed, eliminating manual labor. Most systems have a nozzle, from which the material is deposed, fused or glued, which can reach all positions within its given work area, this allows for virtually every freeform shape to be created. However, every technique knows its own restrictions and capabilities of which one of the most influencing factors is the selected material to work with (Strauss, 2013, p. 19) (Volkers, 2010, p. 19).

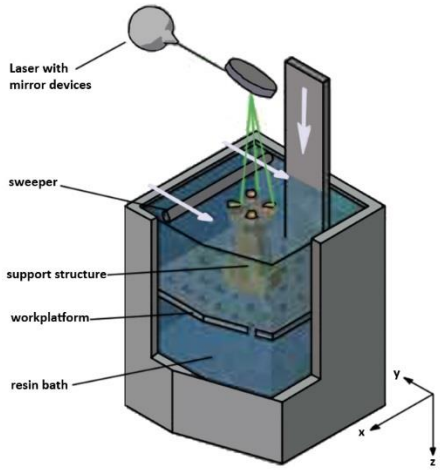

Figure 4: Stereo Lithography Apparatus

Stereo Lithography

The original AM production system is considered to be the Stereo Lithography Apparatus (SLA). This technique builds up models by curing photopolymers (light sensitive plastics) in fluid state with a laser, layer by layer (see Figure 4). Many plastic AM technologies are based on the same principle of binding plastic layer by layer but differ mostly in the selected method of binding. A great overview of AM techniques is given in the doctoral thesis report of H. Strauss (AM Envelope - The potential of Additive Manufacturing for façade construction, 2013, pp. 35-65). However, for this report only two techniques are more relevant to explain the origins of 3D Concrete Printing and are therefore elaborated upon.

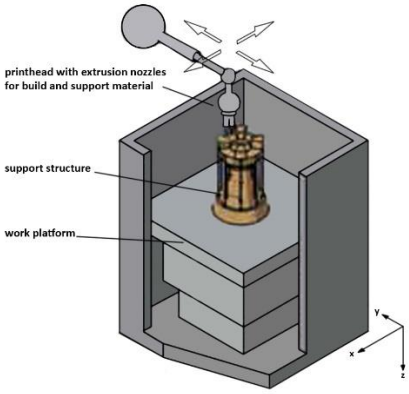

Figure 5; Fused Deposition Modeling

Material Jetting

The technique that is used for Fused Deposition Modeling (FDM) is most additive of AM techniques as it functions by stacking layers of material on top of each other. The system deposes melted material on the work platform which then cures directly due to the lowering of temperature. A next layer is then deposed on top of the semi-solidified material, bonding the layers together. This all takes place in a closed environment, to maintain the correct workable temperature. The nozzle of the printer can move to every coordinate in the xy-plane while the work platform lowers (z-direction) every time a new layer is added (see Figure 5). The outcome is an anisotropic, freeform model (Strauss, 2013, p. 41).

The method of FDM prevents hanging parts to be created because the model is created in an upward development. A solution for this problem is printing (temporary) supporting structures under the cantilevers along with the model. This is already an integrated solution in most FDM software and the polyjet printers, such as the Ultimaker 3, can even depose water solvable plastic (PVA) as support structure. In this manner the supports can be easily removed once the fabrication is finished, without damaging the material (Ultimaker, 2017).

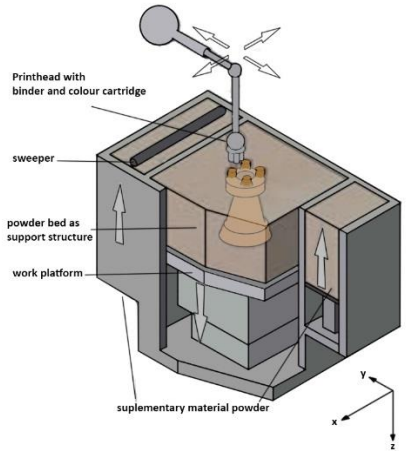

Figure 6: Powder Bed Printing

Binder Jetting

In contrast to FDM, the printing nozzle for printing on powder beds only extrudes the binder material on a powder to solidify material. The nozzle does move in a similar manner, but once one layer is finished an intermediate step is taken. The work platform moves down, and a new layer of powder is disposed on top of the model. The end result is a cube full of powder, in which the designed model is solidified. The powder can be easily removed and reused. For different materials different adhesives (binders) are required, the adhesive can be laced with pigments or ink to introduce color to the model (Strauss, 2013, p. 43).

Construction industry

The opinions on the adaption of AM as a production technique in the building construction industry vary, but many see a great potential in the (near) future. Constanzi and de Witte are conservative in the assumptions of full scale building production using AM, realizing that economically viability and new production complexities have still to be overcome (Constanzi, 2016, p. 11) (de Witte, 2015, p. 3). Strauss and van der Linden are positive on the use of AM for the production of smaller elements (such as joints) from which the building construction industry can benefit (Strauss, 2013, p. 176) (van der Linden, 2015, p. 86).

Most AM techniques use plastics to build their products and this is why these systems are most developed for plastic manufacturing. However, new developments are challenges the techniques to adapt new materials such as textiles (Melnikova, Ehrmann, & Finsterbusch, 2014) and biological materials (Barlett, 2013). For the construction industry the development of structural materials such as steel and concrete are more interesting, but also a development in upscaling the dimensions are requested. Fortunately, many universities and companies are currently developing means to apply AM for steel and concrete for structural parts.

2.2. 3D Printing of Concrete

2.2.1. Origins

Through experiments and researches the number of techniques and materials for additive manufacturing grew. Some of the materials that deemed suitable for AM were clay and ceramics. Due to their hydro plastic behavior, the material is able to be shaped during the manufacturing process and set to a solid shape by drying. The next step was cement and mortar mixes, which enabled bonding between the layers due to chemical reactions in the material. These early developments lead to the believe for some pioneers to further investigate the possibilities in concrete production (de Witte, 2015, p. 76) (Wu, Wang, & Wang, 2016, p. 25).

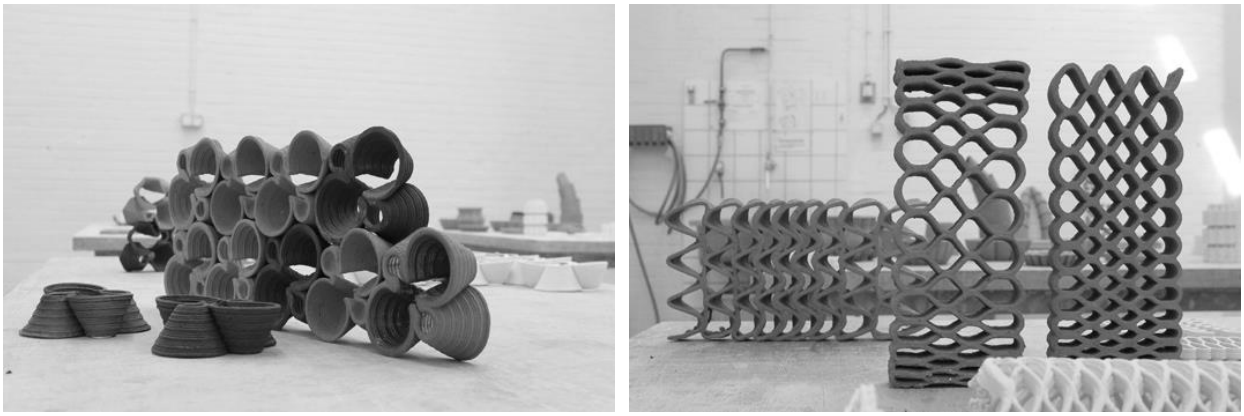

Figure 7: Clay printing by Langenberg

The founding fathers of 3DCP are often considered to be Behrokh Khoshnevis (Contour Crafting) and Enrico Dini (D-Shape). But many adaptations and variations of the technique for concrete have been developed since, each with their own set of parameters, possibilities and challenges. This innovative technique is still researched and developed to this day, this is why many of the 3DCP installations are related or even owned by a University to conduct research on this field. (Salet & Wolfs, Potentials and Challenges in 3D Concrete Printing, 2016, p. 10).

The previously mentioned 3DCP techniques and some of their successors will be explained in more detail in paragraph 2.2.3. But to understand the demands that are set for 3DCP we must first look at the already developed techniques. Production methods with the similar aim to fabricate freeform concrete structures are direct competition for 3DCP which partly determine what direction the technique has to evolve in, in order to find its own place in the construction industry.

2.2.2. Freeform Concrete Production

The wish or demand to manufacture complex geometries as concrete structures is older than the technique for 3DCP. Timber molds are far too expensive and error sensitive for complex shapes and (as with steel formworks) the complexity (curvatures) in shape are limited (Schipper, 2015, p. 12). Therefore, other solutions have already been explored to make custom formworks in order to cast complex concrete elements.

Polystyrene milling

Using robots to control the fabrication of formwork was a logical step to produce custom shaped formwork. One of the ways this is done is by using CNC machine to accurately carve out material to form a mold in which concrete can be casted. Typically, polystyrene foam is used for this procedure, but it is also possible in wood (Wangler, et al., 2016, p. 68). Polystyrene can be milled by chiseling or by drawing hotwires through the foam (Schipper, 2015, p. 13).

Material waste is one of the biggest issues, for any formwork procedure, but in particular for milling because material is removed in order to create the mold. Another downside is the finishing of the concrete. Due to the texture of the foam the concrete will never be completely smooth, although hot wires give better results on this aspect. The form freedom and finishing of the concrete designs vary per system, depending on the CNC machine and its chisel (Constanzi, 2016, p. 15) (Schipper, 2015, p. 14).

Fabric formwork

In an attempt to create more organic shape, more flexible materials were tested, amongst which was textile. The fabric deforms under the pressure of the concrete to shape (double) curved models. Although the surface finish resulting from this procedure is very smooth, problems arise with controlling the final shape which is determined by the stress in the textile. The concrete pressured textile formwork is therefore still very labor intensive (Schipper, 2015, p. 16) (Constanzi, 2016, p. 17).

To control the curvature of the fabric, one can use a plastic mold to limit the deformation, but in extend limiting the form freedom. Another solution is shaping textile with air pressure into pneumatic formwork on which concrete is cast, from which double curved shell elements can be cast. For even more freeform structures, smaller compartments can be pressurized to shape a membrane on which concrete is sprayed (see Figure 8), such as Frank Huijben developed with Vacuumatics (Huijben, 2016).

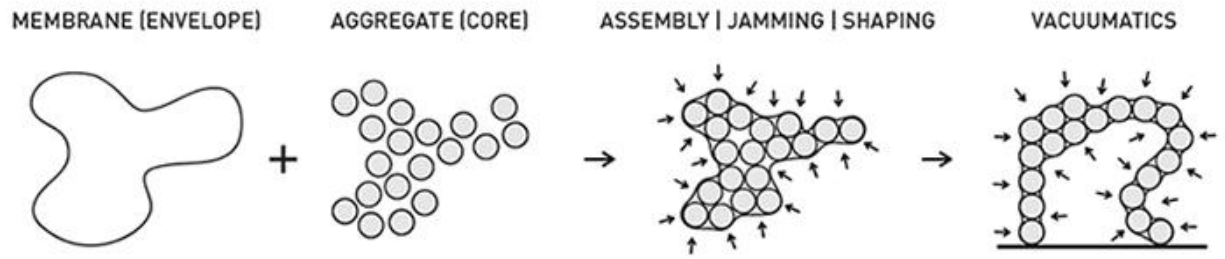

Figure 8: Vacuumatics Frank Huijben (2014)

Flexible molds

Flexibility in molds is a desired characteristic in freeform fabrication, but another issue with molding systems prevents them from becoming a mainstream production technique: labor intensity. This is why more automated adaptable mold were developed, for examples refer to Chapter 4 of Schippers' doctoral thesis (Schipper, 2015, pp. 41-55). The principle is a flexible surface, supported by pistons individually adjustable in height, on which concrete is cast. Due its reusable nature, the waste material is limited, and the production process can be fairly automated. However, the products from this technique "are just curved slabs" as Dennis de Witte describes, and have a constant thickness (de Witte, 2015, p. 87) (Constanzi, 2016, p. 22).

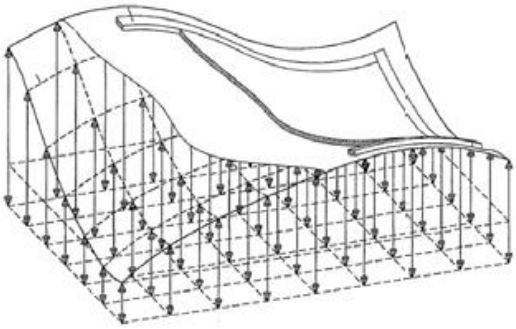

Figure 9: Flexible mold by Koch (1999)

Stay in place formworks

An alternative to custom formworks is shaping the reinforcement and spraying the concrete on the metal bars. The support nets can be bend and curved under force to obtain the correct shape. The surface quality of sprayed concrete usually requires extra finishing services to smoothen the model (de Witte, 2015, p. 116). In an effort to reduce labor, the shaping of the reinforcement was automated by the Mesh Mould procedure, developed at ETH Zurich (Hack, Lauer, Gramazio, & Kohler, 2015). With this

technique a robot bends wires in the desired shape and welds them together to form this stay in place formwork of reinforcement (Wangler, et al., 2016, p. 68).

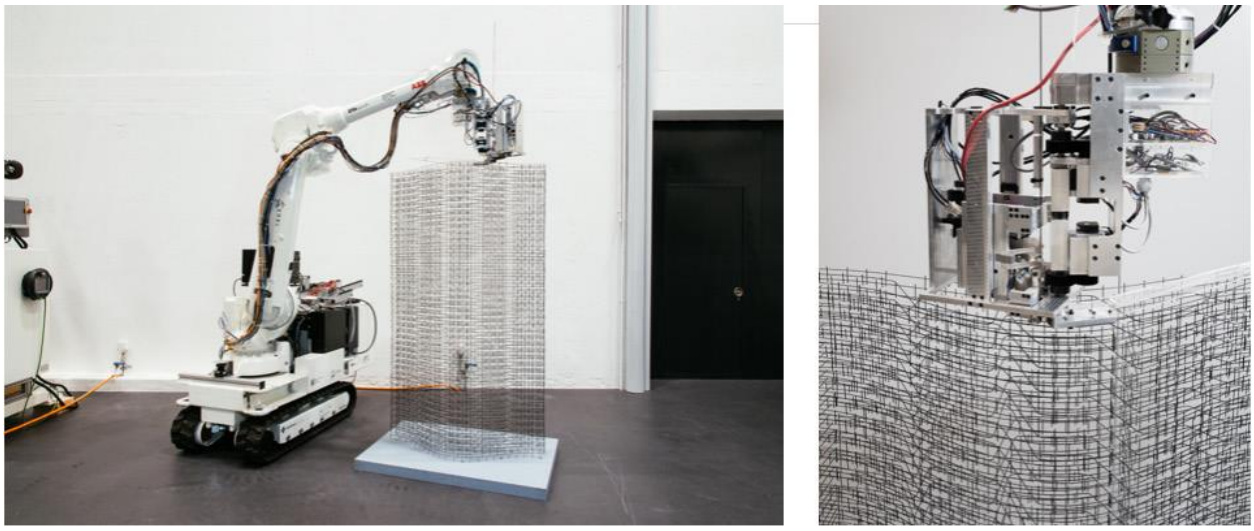

Figure 10: Mesh Mould produced reinforcement as formwork at ETH Zurich

Subtractive Manufacturing

Rather than using CNC machines to mill foam into molds, concrete itself can also be milled, which is referred to as subtractive manufacturing. This very much like an automated process of sculpting concrete where the excess material is removed. This material is reusable in fresh concrete to reduce the material waste. The finishing after milling often requires extra work due to the inhomogeneous properties of concrete (de Witte, 2015, p. 89).

2.2.3. Concrete Additive Manufacturing Techniques

As mentioned before, the pioneers in applying concrete to AM technique are Contour Crafting (Khoshnevis B. , 2004) and D-Shape (patented by E. Dini in 2006). With their inventions the interest in concrete AM grew and others started developing their own systems on the basis of these techniques. First the two techniques are explained in more detail, then the innovations in the 3D Concrete Printing are reviewed.

D-Shape

In 2006 Enrico Dini field a patent for a “method and device for building automatically conglomerate structures” (United States Patentnr. 0148683 A1, 2008). The method and device, which are now referred to as D-Shape, relies on a powder bed printing technique such as described in paragraph 2.1.2. The device places a layer of sand or stone powder on the work platform, after which an inorganic (chlorine based) binder selectively is disposed to bind the powder to a solid form. Similar to the plastic AM technique, the powder acts as support material for the rest of the model (Strauss, 2013, p. 57). The work shows some similarities with the earlier investigation of Joseph Pegna, in which the material properties after printing were topic of research (Exploratory investigation of solid freeform construction, 1997).

The D-Shape was developed to bring 3D printing to the built environment (Monolite, 2017). The projects that are thus far constructed by the printer are sculptures, furniture and building parts (see Figure 11) However, Dini envisions that the printer will be capable of printing buildings full scale and conducted a research on the potential of building an outpost on the moon using Lunar soil (Cesaretti, Dini, de Kestelier, Colla, & Pambaguian, 2012).

The technique shows great potential for developing geometrical complex designs, however there are some drawbacks. Due to the necessity of deposing the material for the entire work platform on every layer, space and material are required in high volumes. It also results in a relatively slow printing process, which after printing still requires a post-processing: removing the powder and (optionally) smoothing the surface (Constanzi, 2016, p. 34) (de Witte, 2015, p. 58).

Figure 11: D-Shape printing: Left: the Radiolaria pavilion and (2008), Right: UnaCasaTuttaDiUnPezzo (by Ferreri, 2010)

Contour Crafting

In 2001 Khoshnevis introduced an automated construction method called Contour Crafting (CC) (Khoshnevis, Russell, Kwon, & Bukkapatnam, 2001). Where D-Shape came from powder bed printing AM technology, Contour Crafting is similar to Fused (or liquid) Deposition Modeling. The entire device consists of multiple assembling robot arms on an operable crane in order to reach every desired location on site. One of the main robots is a computer-controlled nozzle which is fed material (zero slump concrete or mortar mixtures) to depose on the desired destination. The process then builds layer upon layer of extruded concrete to construct the computer designed model (Khoshnevis B. , 2004, p. 7) (Salet & Wolfs, Potentials and Challenges in 3D Concrete Printing, 2016, p. 10).

From the ideology of creating a fully automated building construction machine, which constructs and assembles buildings on site, Khoshnevis designed services to eliminate the need for post-processing. Trowels attached to the nozzle serve to smoothen the surface while the material is still flexible. Machinery was added to place required building components such as reinforcement, lintels and even window sills. The ideology also affects the scale of the operating devices and thereby the resolution of the printed model (Strauss, 2013, p. 56) (Khoshnevis B. , 2004, p. 11).

The concept of CC is extruding the contours of the walls of building in order to fabricate hollow walls, this space can be used for building components and services such as reinforcement, insulation or plumbing. These hollow walls are constructed by applying two (or more) trowels to the nozzle, splitting the stream of material in to two layers at constant width. Where needed the walls can be filled with concrete to add mass, load-bearing strength or to embed the reinforcement, effectively using the contours as formwork (de Witte, 2015, p. 51) (Wangler, et al., 2016, p. 70).

The CC process is characterized by its large-scale construction abilities and the fast rate at which the concrete is extruded. This results in lower resolution and geometric freedom in design compared to the D-Shape technique. Due to nozzle setup (with trowels) and the disability to print slanted walls, the freeform fabrication is limited to a 2-dimensional design that is extruded in vertical direction. Another

side effect of printing large scale is that the concrete (or mortar) should be prevented from hardening too fast in order to obtain good bonding between layers. This problem is tackled by adding plasticizers to the sand and cement mixture (Constanzi, 2016, p. 38) (de Witte, 2015, p. 51).

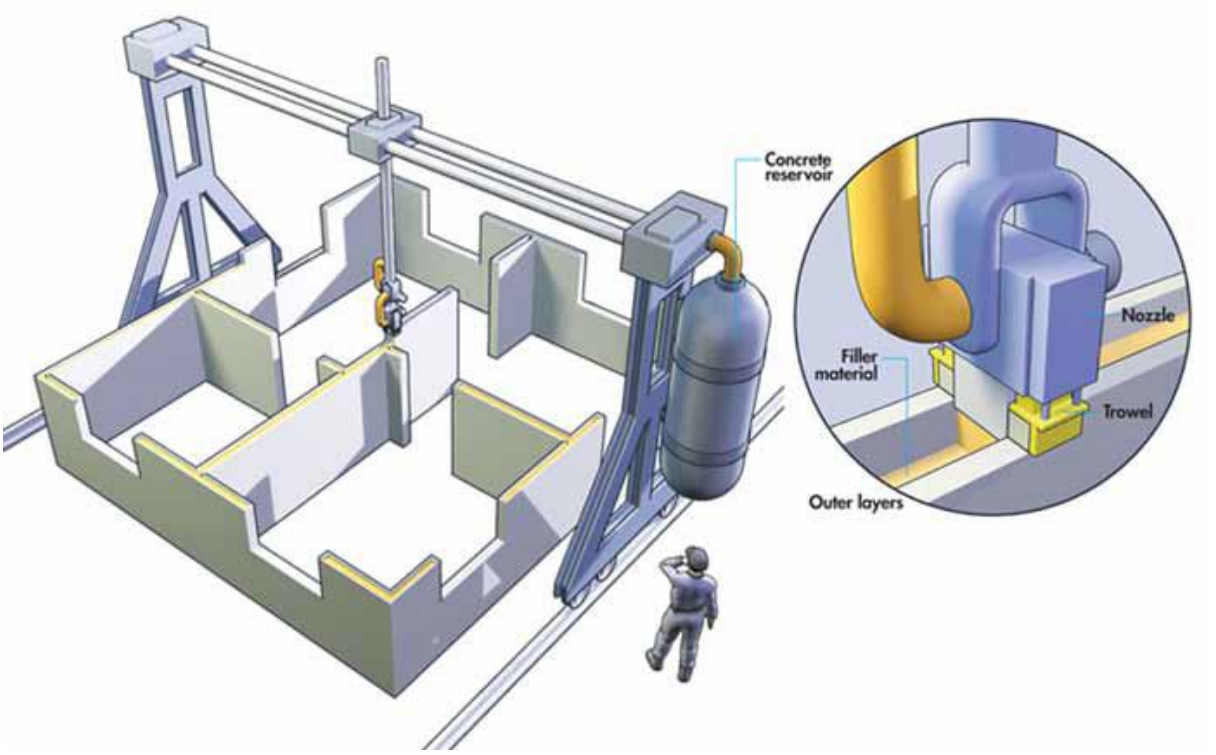

Figure 12: Construction of conventional buildings using CC by Khoshnevis

3D Concrete Printing

The definition of 3DCP is not yet set in stone as different techniques and methods in this field are still developing simultaneously. For this thesis 3DCP refers to all manufacturing techniques that extrude wet cement mortars in an additive fashion. This includes Contour Crafting but excludes D-Shape printing on because it relies on binder jetting of *dry* mixes.

Since the invention of CC, many institutions and companies have developed their own variant of the device. All of them have their own focus and therefore their own advantages and limitations. A division can be made on the basis of the size and resolution of the printers, because a focus on printing full scale buildings requires different printer and material properties than printing elements. (Wangler, et al., 2016, p. 73). Printing a building on full scale on site brings along some challenges. First of all, the printer head or nozzle has to be able to reach the extends of the design, meaning that (in the case of a gantry system) the printer has to be bigger than the building. Secondly, the scale influences the resolution of the prints. Not only are higher print paths desired to fabricated rapidly, but also the machinery size determines the precision of the device.

Printing elements can reduce a number of these issues at the cost of the necessity to assemble the elements. The printing can be performed in a controlled environment, which benefits the material properties. WinSun adapted the CC technique to an element size production, for a rapid construction of 10 houses in one day. Connecting the elements can be performed by post-tensioning as shown in the project 3DCP Water Taxi Stop (van Wolfswinkel, et al., 2017) and 3DCP Bicycle Bridge (Bos, Ahmed, Jutinov, & Salet, 2017).

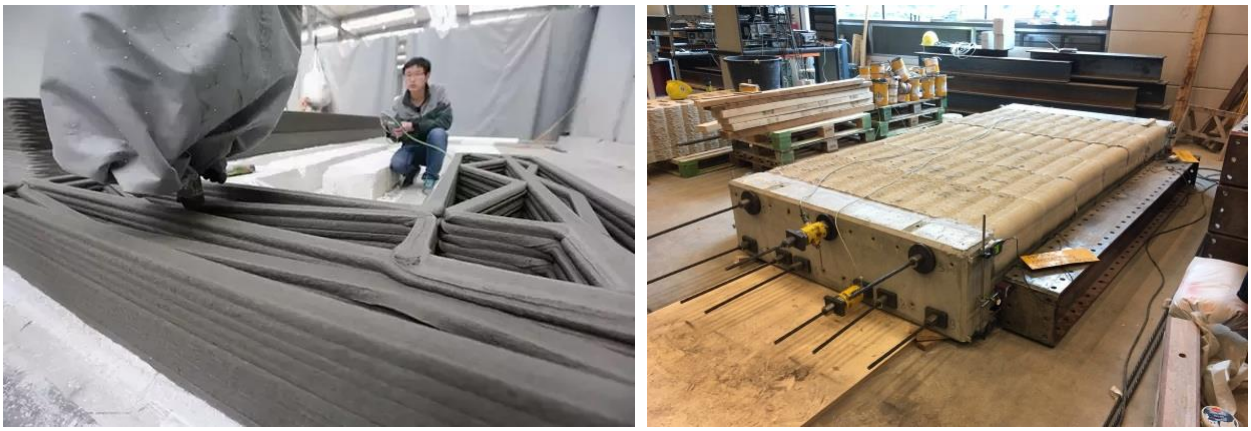

Figure 13 Left: WinSun printing hollow elements, Right: Prestressing 3DCP bridge elements TU/e

Another potential benefit of printing elements rather than buildings, is the upgrade in resolution. A smaller nozzle can depose material more precisely and therefore develop more freely designed models. (van Alphen, 2017, p. 16) The layer thickness determines the resolution of the print, which in turn influences the processing time but also the surface quality and level of detail of the design (Strauss, 2013, p. 31). The doctoral thesis of Aremu shows that printing with a higher resolution can be beneficial for topological optimization (Topology Optimization for Additive Manufacture, 2013).

2.2.4. Variables

Printing with concrete has proven to be a complex procedure, dependent on many variables. What makes it even more complex is that the variables themselves are also dependent on one another. For example, the load bearing capacity of the concrete mixture increases over time, but the bonding strength between two layers decreases as more time passes between addition of the second layer.

Material mix

The curing process of concrete is what makes it suitable as a material for AM, it remains formable for a certain period of time before hardening. But the behavior during the process of hardening is also very influential on the printing process and therefore the concrete or mortar mix is one of the most important variables of 3DCP (Constanzi, 2016, p. 43). Four criteria on a mix for 3DCP could be qualified are defined T.T. Le et al (Mix design and fresh properties for high-performance printing concrete, 2012):

- Extrudability:
  The ability of the mixture to flow through the printing system
- Workability:
  The physical behavior of the wet mixture; the ability to bond layers homogeneously
- Open Time:
  The length of time in which the fresh concrete remains fluid enough to be pumped
- Buildability:
  The load bearing capacity of fresh concrete; the ability to stack layers

The characteristics of concrete or mortar mixes are determined for a large part by their water cement ratio and the aggregates used. These determine, amongst other things, the drying time and strength of the fresh concrete, which are very important parameters for the above listed criteria. Additives like plasticizers and retarders can change these properties of the mix, but usually influence more than just the desired criterium. For example, adding retarder to extend the open time will reduce the buildability (de Witte, 2015, p. 59).

Next to the mixture itself, environmental factors such as temperature and humidity also influence the setting behavior. These variables are hard to control in the concrete printing process, especially when printing on site. But the system of the printer is also emitting heat which results in a temperature gradient in the concrete, the effects of which are studied at Eindhoven University of Technology (Salet, Bos, Wolfs, & Ahmed, 2017).

Printer properties

As shown in paragraph 2.2.3, the properties of the printer determine for a large part the possibilities and limits of what is printable. Three elements of the printer are examined: the positioning system (the robot), the concrete pumping system and the printhead (extruder nozzle).

A. Positioning system

The system that positions the printhead controls the movement of the printer, which determines the limits of design dimensions. A gantry supported printer usually has a greater reach than a single CNC robot arm, but the 'canvas size' is not the only parameter under influence of the system. The speed at which the system can move is one of the variables controlling the print speed, but this parameter has a direct negative relation with the print resolution, faster printing leads to a reduction in resolution (Strauss, 2013, p. 76).

The precision with which the printer is able to move is an important factor in controlling the resolution of the printer. This is combined with freedom of movement, the ability to rotate and translate in every axis gives the robot arm a significant benefit over a gantry supported printer, which can only translate in x-,y- and z-direction. Curvature radius and the ability to print slanted layers are controlled by the rotation capacity of the printhead, without this ability print paths will deform at introduced angles (see Figure 14) and clog and tear the concrete (Salet, Bos, Wolfs, & Ahmed, 2017, p. xlv).

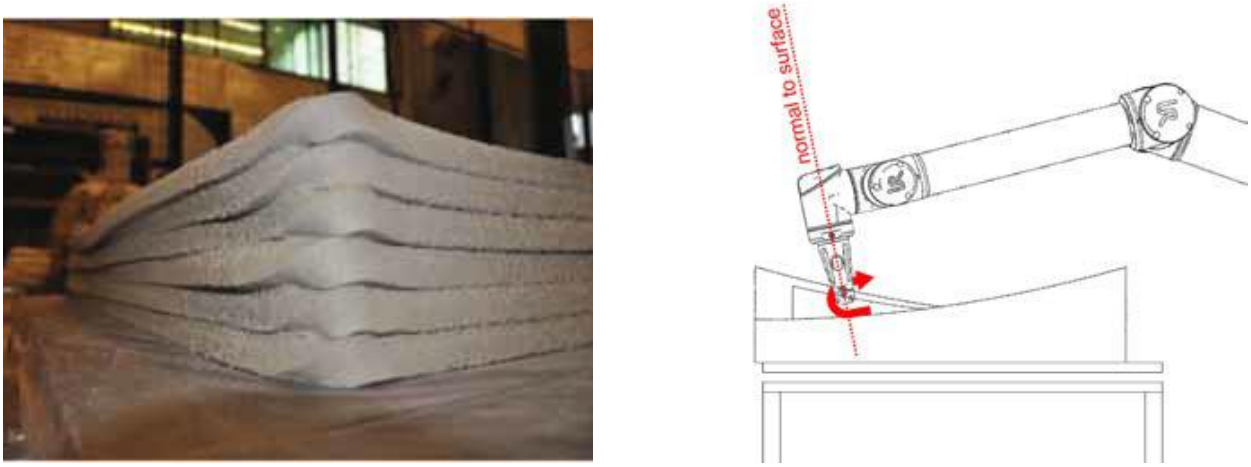

Figure 14 Left: Twisting of filament in corners, Right: Orientations of printhead when printing under angles

B. Pumping system

The print speed is limited by the amount of concrete that the pumping system can extrude through the printer nozzle. The pressure in the system together with opening of the nozzle influences the amount of extruded concrete, which in turn influences the layer dimensions (de Witte, 2015, p. 73). To provide more freedom in design, it is desired that the extrusion speed can vary throughout the process. In this way the dimensions of the layers can vary in the design, which is essential for local optimized designs. When the extrusion process can be stopped, the print path is no longer required to be continuous. It should be noted that the concrete must be prevented from setting in the printer (Marijnissen, 2016, p. 75).

Figure 15: Different variations in 3D print structure

C. Printhead

The shape of the nozzle on the printhead is very determining in the shaping of the layers. Constanzi and van Alphen concluded that square nozzle openings create easily stackable layers and a smoother surface finish (Constanzi, 2016, p. 50) (van Alphen, 2017, p. 59). Loughborough University (Lim, et al., 2009) and XtreeE on the other hand, use a circular nozzle opening to improve the resolution of the printed layers in the curved parts of the model (Figure 16). Replacing nozzles for different sized prints is a possible solution, but improvements in resolution are developing rapidly possibly making switching obsolete.

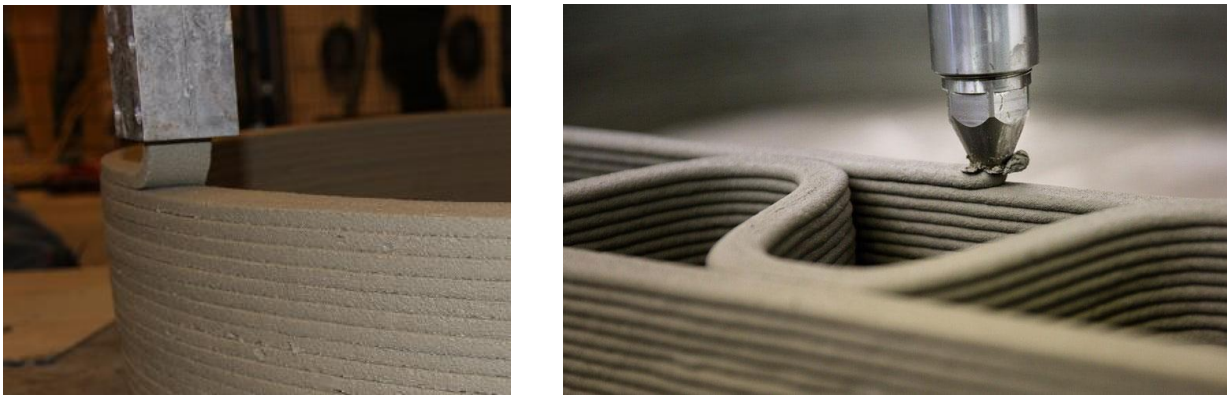

Figure 16 Left: Rectangular nozzle at TU/e, Right: Circular nozzle from XtreeE

Design variables

Designs for 3D concrete printed will (have to) be restricted by the limitations of the selected printing system, but the design can also influence the printability by adapting its shape. The geometry of the total structure can provide support for fresh concrete making complex shapes printable. Printing sloped surfaces for example is hard due to the low bond strength, but if the surface is curved in the xy-plane it can prevent the structure from collapsing during printing (van Alphen, 2017, p. 62).

Another manner in which design alterations can benefit the printability is by adding support where needed. This can be done by increasing the layer thickness locally to provide more material, but also supporting structure can be printed along the structure. As visible in Figure 16, a curved line is printed in between the straight lines to stabilize to total structure. Often these additions in design also benefit the structural loadbearing capacity in the end result.

A final aspect to take in to account when modeling designs for 3DCP, is the print path. The length of the print path determines the time it will take for the printer to add the consecutive layer on the first, which can influence the bonding of the layers. In addition, intersection and interruptions in the print path can result in fresh printed concrete to be (re)moved by the print head, effectively deforming the structure (Constanzi, 2016, p. 57).

2.3. Change the chain from 'design to realization'

The digitalization of the construction industry can provide great benefits both economically and on safety. Reduction of manual labor in one of the most hazardous working environment is one example of this. However, this proposes a great change in a well-established industry and requires a new look on the way things are designed and constructed integrally. The complete production chain from design to realization, with all involved parties in between, is affected by this revolution.

2.3.1. Design

What is the influence of a more digital world on the designer? Oxman concluded that digital design has a great impact on design process and its results, which lead to *digital design thinking.* In this way of thinking the designer no longer relates to typologies but focusses more on adapting multiple forms of data and design parametrically. This has consequences for the role of the designer in the process, which will involve more information handling (Oxman, 2005, p. 261). The theory of a new mindset for a digital world is underlined by the concept of computational thinking, which van der Maas describes as creative tool of solving problems by using digital (programming) skills (van der Maas, 2016).

The demand from designers to manufacture complex geometries lead to the innovation in AM techniques, but then these techniques also influenced and retroacted on the design and its process. In Zurich (ETH) an investigation is conducted on the influence of these new production methods on architectural design. The setup is an automated and digital construction environment in which robots are programmed to manufacture building parts by additive and subtractive means. The result is the development of new architectural systems and logics that are related to the new automated production processes (Strauss, 2013, p. 87) (Gramazio & Kohler, 2017).

For 3DCP as one of the digital fabrication techniques in a future automated construction industry, it is hard to predict what its influences will be on the design product and process. Marijnissen assumes that arch structures that are loaded primarily in compression will be the leading language of form, due to the poor tensile strength of concrete (Marijnissen, 2016, p. 41). The ribbed surface that is a direct result of the layered fabrication could become iconic for 3DCP if designers are willing to except it as an intrinsic property of 3DCP. The architectural structures and textures that we now relate to 3D printing might very well differ in a few years when the technique evolves to adapt new abilities.

Many researches on 3DCP conclude that a design for the AM technique require a new design strategy. Strauss refers to "designing for AM" (AM Envelope - The potential of Additive Manufacturing for façade construction, 2013) and Wolfs claims that a reverse engineering approach is required (3D printing of concrete structures, 2015). The necessity for this new approach comes from the possibilities of the technique on the one hand and its restrictions on the other. The technique produces freeform designs, but the shapes directly influence the printability due to material and printer properties. This is why knowledge and understanding of the technique is essential for any designer in this field.

2.3.2. Building process

The automation of the construction will also impact the process from concept to realization, in which the design is checked and adapted to fulfill the requirements set by all involved parties. Especially the digitalization influences the stream of information from party to party, but fabricating for a digital fabrication method can also affect steps in the process. With the introduction of BIM (Building Information Modeling) the handling of information is envisioned to change vastly to a more integrated process.

Coenders clarifies that "BIM as a vision" is a strive towards a future building process in which all involved parties in design, engineering and construction (and maintenance) collaborate through digital models.

Management of the building process is done digitally by creating, sharing and manipulating information in a shared digital model or environment. Potential problems in construction can already be tackled in design since the fabricator can already anticipate on the production method. However, Coenders et al. also state that (BIM) software is not yet ready for a full integration in the building process in all phases, especially the initial design parts where essential parameters are altered more frequently (Coenders, 2010) (Rolvink, Mueller, & Coenders, 2014).

Although the software might not be ready yet, integration of disciplines is essential for the production in an automated construction such as 3DCP. When the building process comes to the file-to-factory cycle, where a design can be fabricated once it is modeled, the intermediate step of the disciplines (such as structural engineering) needs to find a new place in the process. Engineering must also be more automated to be able to calculate the mass-customized elements to make 3DCP implementation affordable in the building industry. It seems that the file-to-factory thinking requires a different mindset from all disciplines (Strauss, 2013, p. 127).

2.3.3. Construction

The final part of the building process, the actual construction, needs to endure the digitalization as much as the earlier phases. This requires production factories to be able to operate AM production techniques and handle digital models. Rather than fabricating generic elements of standard dimensions, mass production of uniquely designed elements will become the new procedure. Operating robots and reading digital models and G-code are skills that will have to be obtained by the factories that are willing to adapt 3DCP to their production line (Constanzi, 2016, p. 54).

Every producer in 3DCP will develop their own means of printing with its own set of benefits and restrictions. Constant research in upgrading the concrete mix and the printing device requires a different set of knowledge and therefore a different approach (Wangler, et al., 2016). A trend that can already be distinguished from the current 3DCP producers is the split in focus between two groups of developers in terms of scale. One group focusses on fast, full-scale and on-site 3DCP of buildings while the other focusses on building elements of high resolution and freeform design. (de Witte, 2015, p. 125).

2.4. Conclusions and recommendations

2.4.1. Conclusion

The inventions of fabrication techniques for the production of freeform concrete structures, are a direct result of the demand for constructing complex geometrical designs. The digitalization of the design world made designing the freeform structures more accessible, which raised this demand even further. Until today this could only be realized by constructing expensive formwork or by reducing the complexity and designing in a repetitive manner.

This gap in the market is an area in which 3DCP can reach its full potential in realizing freeform architecture. The introduction of 3DCP techniques such as Contour Crafting showed the capability of printing structures fast and with significant material reduction, effectively lowering costs. Simultaneously, the resolution and detail level of the technique are improved, making freeform fabrication feasible and affordable. Although the techniques are not yet fully developed, projects have been realized using this innovative fabrication procedure. But before the level of mass-production can be achieved the design chain needs to be reviewed for a more digital construction world.

The building process is adapting the digital and automated tools from both ends of the spectrum, design and manufacturing. But in order to obtain functional and affordable building components an integrated approach need to be established, which includes structural engineering. The roles of the disciplines

involved in a traditional building process might need to shift a little towards designing for AM. This requires a new design thinking from all parties in order to come to a printable model that fulfills all set requirements.

2.4.2. Recommendations

The potential for 3DCP in the building industry is great, but the technique can still be improved to increase its possibilities and applicability. In this paragraph, some potential upgrades in the near future are listed as opportunities for the technique to be adapted. It is recommended that these innovations are investigated and tested to prove their viability. For prognosed development of the 3DCP technology, de Witte charted the (future) development in a roadmap form (de Witte, 2015, p. 125).

Material optimization

Researches in the field of 3DCP have almost all started with investigating the proper mix for printable concrete. Fabricators have found different mixes and solutions that make printing in concrete possible, but the investigation should continue to improve the quality of the concrete on the aspects of curing process, mechanical properties and appearance. A suggested optimization by Wangler, is the ability to make concrete set on demand to increase the open time of the concrete. This could be tested by, for example, adding accelerator at the last instance or hardening by selective heating, as seen in plastic AM techniques (SLS) (Wangler, et al., 2016).

Support Material

Another opportunity for 3DCP that is found from looking at its predecessors in plastic AM techniques, is the ability to print support material. Without involving the need for formwork or molds, the printer (or an additional printer) could print structures to support hanging and cantilevering parts of the model, that would otherwise collapse due to the low strength of the fresh concrete. Preferably, this support material would we something easily removable such as the water-soluble PVA that is used in plastic 3D printing (FDM) (de Witte, 2015). Lim, et al., have already investigated the use of printed recyclable gypsum as support (Fabricating Construction Components using Layered Manufacturing Technology, 2009), but more materials could be investigated on their ability to support and effect on the surface finishing.

3D printer

The printer itself is under constant revision in this early phase of 3DCP development, which is why the effects of upgrades for the printer require investigation. Due to the uniqueness of every 3DCP device and its used material, not all results of every investigation is applicable to every printer. Nonetheless, the essence of the upgrade can often be applied to any device under the adjustment and calibrations for the specific device.

An example of one of these upgrades is the investigation of a live feedback system to the robot at the Eindhoven University of Technology. A device attached to the nozzle of the printer measures the height of the printer in real time. It then feeds this information back in to the system allowing the printer to adjust its height to any variations found in the printed model (Wolfs, Bos, van Strien, & Salet, 2017).

Reinforcement

The brittle nature of concrete makes safety a big issue in concrete design. Traditional designs resolve this undesired failure behavior by reinforcing the concrete with steel, allowing tensile force to be taken up by the reinforcement. An added effect is that the structure remains in one piece while it is structurally failing, due to the yielding of the steel. This ductility and tensile strength are qualities that the pure concrete from 3DCP still lacks and should be investigated to enable all freeform designed models to be constructed.

Traditional reinforcement seems out of the question due to its linear shape and the necessity to make the automated process of 3DCP discontinuous in order to place rebars. Alternatives are currently investigated such as fiber reinforced concrete (Wangler, et al., 2016) and reinforcing the layers individually by 'weaving' a cable through the concrete while printing (Salet, Bos, Wolfs, & Ahmed, 2017, p. liv). Currently most common ways to ensure structural safety in 3DCP produced projects are performed by using the concrete as formwork and applying reinforcement afterwards, either casted (as in CC) or post tensioned.

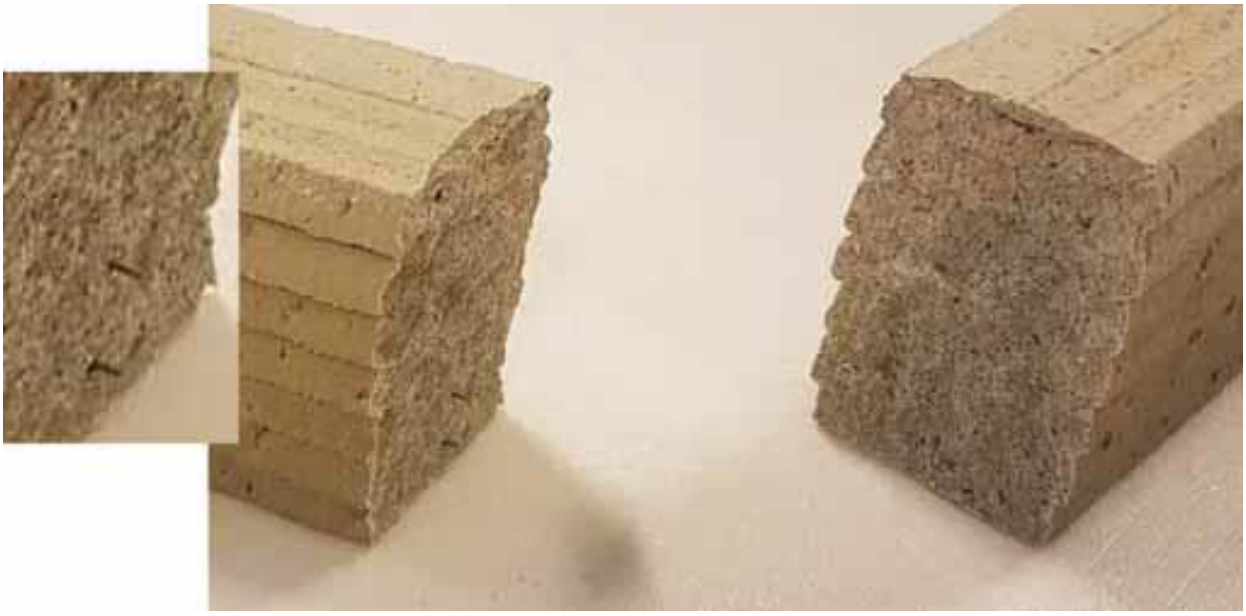

Figure 17: Embedded reinforcement from TU/e

3. Design

3.1. Introduction

The added value of freedom in design seems very beneficial for esthetical purpose which are an essential design criterium for exterior building enclosures. Other performance criteria for the façade however, also determine a large part of the restrictions and boundary conditions that are set for the design of the façade. In this paragraph the potential use of 3DCP for the fabrication of façade elements is studied based on the design performance criteria. For this study, first façade typologies are investigated after which requirements are specified for specific parts of a façade element.

The potential benefits and challenges that 3DCP brings in manufacturing façade elements are defined. Their possible implementation is analyzed by studying modern exterior enclosures based on predefined performance criteria. Three concept design types for 3DCP are suggested and their advantages and disadvantages are defined. Finally, these design types are reviewed for a basis of the case study that is part of the thesis research.

3.2. Façade typologies

Before a concept design is drafted, the functionality of the façade element must be defined. In general, what functions the façade must fulfill, and more specifically what parts are taken up by the printed element.

In the book Exterior Building Enclosures (Boswell, 2005), Boswell defines the primary *elements and forces* to which a building façade is exposed and relates this to the specific design aspects of the exterior enclosure. The influence of a force or element on a design requirement is described as primary, secondary or not applicable in Table 3.1. How these forces and elements influence the design of the case study, and to what extent, is determined by the selection of design requirements that are assigned to the façade. In other words, the desired functionality of the element defines the elements and forces to which the element is exposed.

EXTERIOR ELEMENTS AND FORCES

DESIGN	NATURAL						NATURAL & HUMAN		HUMAN CREATED	
	WIND	PRECIPITATION (INCL. HUMIDITY)	AIR INFILTRATION	TEMPERATURE	SUNLIGHT	SEISMIC	GRAVITY	NOISE	BLAST	BALLISTIC
STRUCTURAL	P	S	S	S	-	P	P	S	P	P
WEATHERTIGHTNESS	P	P	P	P	P	P	S	S	-	-
THERMAL COMFORT	S	P	P	P	P	S	-	S	-	-
MOVEMENT	P	P/S	P/S	P	P	P	P	-	S	S
LIGHT TRANSMISSION	-	-	-	P	P	-	-	-	S	S
ACCOUSTICS	S	S	S	S	S	-	-	P	S	S
SECURITY	-	-	-	S	S	-	-	-	P	P

P = Primary
S = Secondary
- = Not Applicable

Table 3.1: Primary exterior elements and forces and their influence on the enclosure design (Boswell, 2005, p.24)

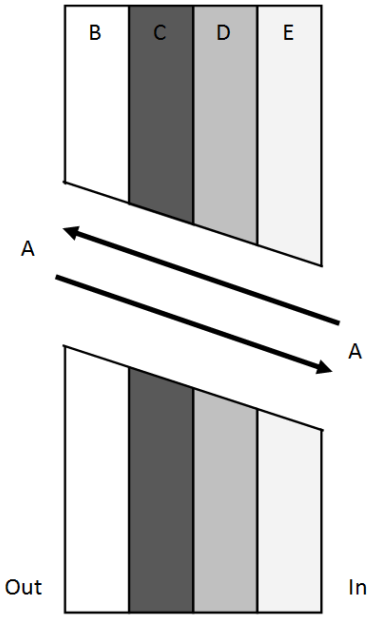

Figure 18: Building enclosure design requirements

A façade element does not necessarily fulfill all the requirements that are set for the exterior building enclosure as a whole. For example, the exterior cladding layer can prove to be functional in providing weathertightness but little to no thermal comfort. The shape and placing of an element within the buildup of the façade is related to its required functionality. A layered overview of the design performances is displayed in Figure 18 with the addition of esthetical design criterium. In order to determine which functionalities could be fulfilled by a 3DCP element, some façade designs (paragraph 3.4) and design types are analyzed on their ability to fulfill these requirements.

A. Light transmission and view
B. Esthetics
C. Weathertightness
D. Structural, movement and security
E. Thermal and acoustic comfort

The case study focusses mainly on the structural design requirements for the façade element, which requires mostly load bearing functionality. However, other performance requirements for the façade as a whole determine design (and fabrication) choices in the element. For example, the light transmission requires perforations in the concrete, demanding a certain flow of forces in the structural scheme of the façade. In this study these performance criteria are not defined in absolute numbers or restrictions, but conceptually considered in the design phase. These requirements are defined more specifically in the case study description, which is summarized in paragraph 4.3.

3.2.1. Infiltration design principles

Boswell defines four performance design principles for exterior enclosures, that each describe how the façade fulfills its design requirements in relation to its specific (layered) build up. These design principles are labeled: ***Barrier, Mass, Rain screen*** and ***Pressure equalized rain screen***. Their differences are mainly found in how they deal with exterior elements and forces which is depicted in Figure 19. The colored lines indicate where the exterior elements are blocked, blue for precipitation (dashed) and moisture (continuous), orange for wind (dashed) and air infiltration (continuous) (Boswell, 2005, p. 45).

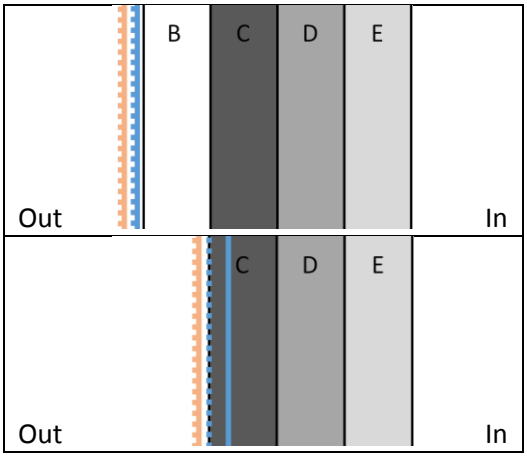

A **barrier**-type façade will block most exterior elements at the outmost edge of the enclosure, like a glass façade will seal the building and shield it from water and air infiltration. Only the outer layer is subjected to weathering, practically placing other layers inside the interior. Unless this outer layer is transparent, it also accounts for the façade appearance in terms of esthetics.

A **mass** design principle allows some of the exterior elements to partially penetrate the first exterior layer, such as in architectural concrete becoming wet up to a certain depth. The thickness of the elements prevents the external forces to enter the building. Printed concrete could fulfill this function if it covers the entire enclosure.

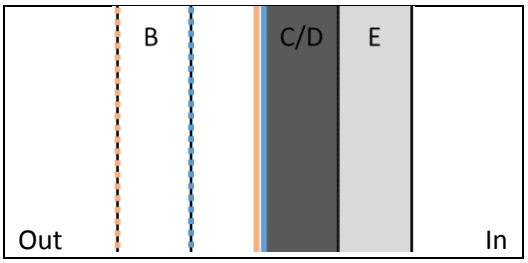

The (**pressure equalized**) **rain screen** design principles, assign the functions to zones within the buildup of the façade. This could be described as individual barrier layers which keep out specific elements, such as exterior cladding for rainwater (at B) and a more interior layer preventing air infiltration (at C). Open (perforated) printed concrete elements could prevent this type of wind and water protection if designed well.

Figure 19: Position of blockage of water and air in façade types barrier, mass and rain-screen.

3.2.2. Structural design principles

The structural system of a building has great influences on the dimensions of elements within the building. What part of building is part of the load bearing structure determines the loading on said elements, which in turn affect their design. For the case study the effect of the chosen structural system are relevant for the loads that are assigned to the façade. These systems can be categorized in the types: **center core-, tube-** and **loadbearing façade** systems. (Hallebrand & Jakobsson, 2016).

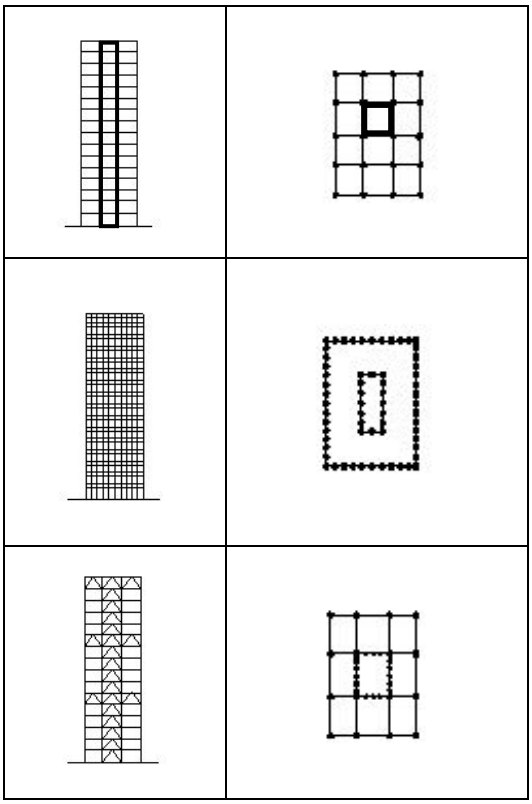

In a **center core** system with an internal frame, the vertical loads are distributed by beams and carried by columns. The lateral loads are transferred to one or multiple rigid cores which provide stability. In such a system the building enclosure functions only to transfer lateral loads to the structural frame directly. Façade panels are not part of the main load bearing structure.

Tube systems know many variations, for example the tube in tube system. One of the characteristics is the stiff frames in on the parameter of the building. This requires structural elements in (or near) the façade that can take up compression and tension forces and introduce bending moments in the rigid joints of the frame. The structural system is often integrated in the façade of the building.

Buildings with a **loadbearing façade** use the building enclosure as part of the structural system. Examples are outrigger systems and structural (dia)grid façades. As with tube systems, these buildings take up lateral forces by using loading the perimeter, which is loaded in compression and tension. Tension is compensated to some extend by the self-weight of the building.

Figure 20: Structural systems for high rise buildings

The load-bearing resistance that is required from the building perimeter, determines the necessity for and dimensions of structural elements in the façade. This influences the design of the façade, especially when the structure is integrated in the building enclosure.

3.3. Potentials and challenges

From the literature study of this thesis report it already became apparent that printing of concrete has a great potential for the construction industry. In this paragraph the potential benefits and challenges of applying 3DCP for the fabrication of elements for building façades are addressed.

3.3.1. Potentials

Mass-customization

The ability of the printer to automatically fabricate individually designed elements on a large production scale is referred to as mass-customization. For façade design this can eliminate the necessity of repetition in elements due to cost limitations. This enables the realization of designs on the scale of the entire building enclosure, which truly makes the façade a canvas for the designer. Some examples of this façade design type are shown in Figure 21. Such façade designs could be segmented into unique parts, which can be individually printed without additional costs for the uniqueness of each element.

Figure 21 Left: Edificio Mikimoto Ginza 2 (by Tokio Ito, 2005), Right: Brussels Parliament (by Skope Architects, 2013)

Form freedom

Another great potential for 3D printing is presented in the fabrication of geometrically freeform shapes, without the necessity of complex (and expensive) formwork. Although it should be noted that the system knows some restrictions, such as the limitation in printing cantilevering structures due to the physical properties of the fresh concrete. The ability to produce curved and double curved concrete shapes has a great potential in the construction of enclosures of geometrically complex architecture. But freeform shaping can provide benefits to more than just esthetics, curvature can be beneficial to the overall structural system of the building and can allow for great spans such as Figure 22 left. Experiments for producing double curved concrete elements by using 3DCP has already been tested.

Figure 22 Left: Thin shell structure (by Felix Candela) Right: Printed segments of turtle shells from 4TU project

Material reduction

By selectively printing concrete, material can be applied only where it is needed. This has the potential to reduce the waste of material in the building industry, which is currently one of the most wasteful industries. By locally increasing structural height or concrete cover for anchors elements can be optimized without over dimensioning the complete structure. Additionally, mass customization allows every element to be dimensioned individually, reducing the material abundancy even more. However, the printer works in line models, which should be taken in to consideration when the desired dimensions exceed the maximum print path width. One can design elements to be printed hollow (like hollow core slabs) (Figure 23) or functioning as formwork in order preserve material and maintain the freedom in shape.

Figure 23: WinSun printed hollow elements as walls floors and roofs

Integration of functions

Printing hollow elements also creates the opportunity for functions to be integrated within this element. This is a possibility that seems very beneficial for building enclosure as functions from many design performance criteria are assigned to the façade. Insulation and installations for example, could be implemented in the hollow sections of the product, effectively adding functionality to the element. Structural elements can be implemented in printed form work as well (figure), which creates the possibility of using 3DCP for façade elements that integrate load bearing functionality.

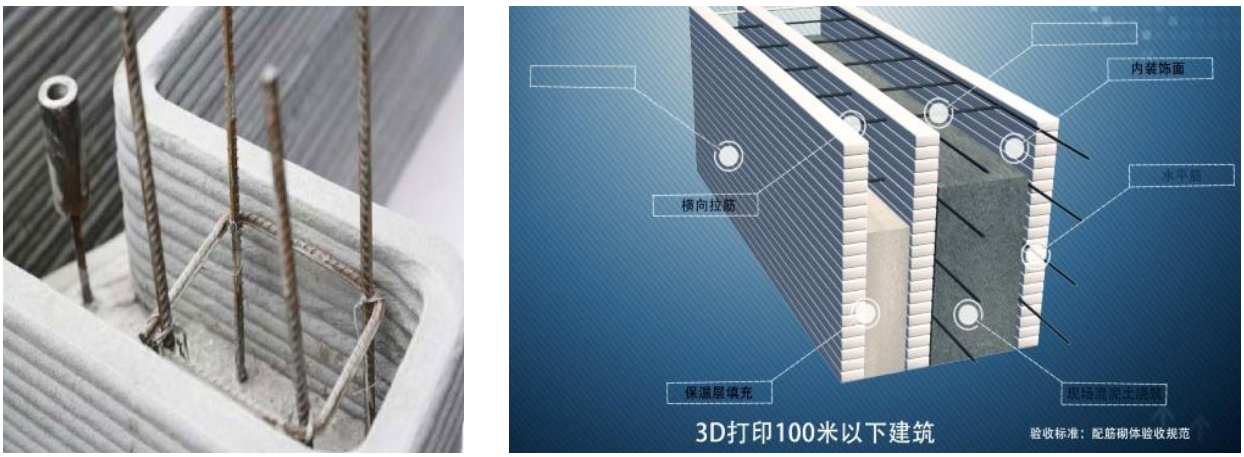

Figure 24: WinSun integrating components into hollow segments of printed concrete

3.3.2. Challenges

Although the technique is very promising and seems to provide a lot of opportunities in the building construction industry, some challenges require attention when considering 3DCP as a fabrication technique. As with any new technique, many challenges will be reduced or even completely resolved over time due to research and development, but other design restrictions will stay as they are inherent to the production process.

Integration of other materials

Most benefits of the technique lie in the automation of the construction process, reducing the production time and cost significantly. Subsequently many challenges also lie in maintaining an automated production process while trying to add steps or materials. The addition of materials and elements to the production process is essential when one wants to create an integrated façade element with full functionality on all design performance criteria. As an example, the integration of structural reinforcement in the printed concrete is examined. But the following claims also hold true for the integration of insulation, glass, finishing, connective details and many other materials and elements in the process.

To provide structural safety and ductility, reinforcement is the traditional addition to concrete. Post tensioning has proven to be a successful supplement to 3DCP elements (Figure 25), but researches are focused on the integration of reinforcement in the automated printing process. To maintain the automated flow of production, the handling, placing or even fabrication of the reinforcement should be controlled by robotlike machinery. One possibility is envisioned by a production line in which specific robots apply their specific functionality. But to fully integrate reinforcement into the concrete, it would ideally be integrated in to the concrete mix, like fibers and wired reinforcement. The challenge of improving the tensile strength perpendicular to the printed layer direction however, remains.

Figure 25: Post tensioned 3DCP bridge

Besides maintaining an automated production line, curvature that is introduced by freeform design creates challenges for added materials and elements to 3DCP fabrication. Where traditional elements are often linearly shaped and have standardized dimensions, 3DCP finds great potential in crafting geometrically complex shapes. The integration of these elements requires them to be custom shaped as well, for example by laser cutting the elements. Liquid materials provide a solution for some materials, for example casting liquid insulation (PUR) in printed formwork or embedding elements by casting more concrete. But windowsills and elements alike require intensive preparation before fitting in custom perforations.

Finally, as with any unification of two elements in the building industry, tolerances play a big role in connecting them. The tolerances of 3DCP are relatively big compared to other automated techniques such as laser cutting. This is due to the setting of concrete and the addition of loading during while the concrete is still fresh, in the production process. The ribbed texture from the AM technique can be challenging to connect linear elements directly onto, such as exterior reinforcement (e.g. carbon strips). One solution seems to lie in integration in the production process, which XtreeE shows in Figure 26.

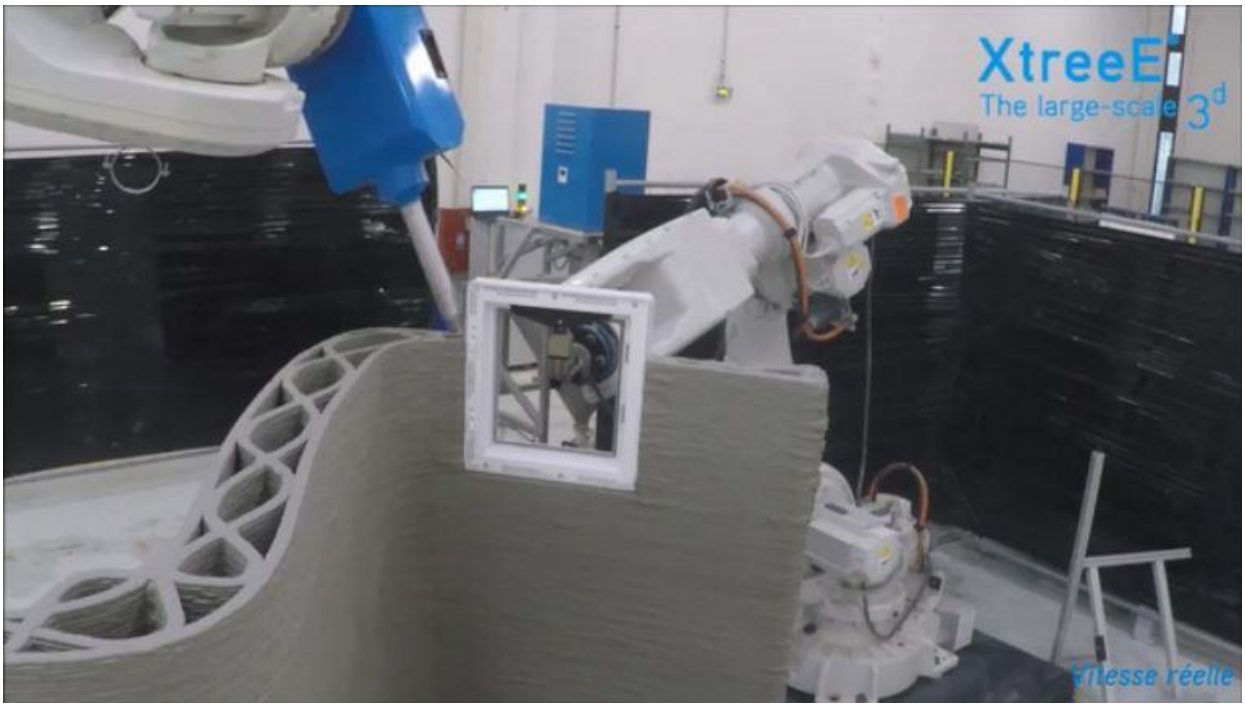

Figure 26: XtreeE placing component in printed wall during automated fabrication process

Modular

On the topic of sustainability, 3DCP has a big advantage on the reduction of material use and waste. But another aspect of sustainability in the construction industry is reusability and circular construction. This is more of a challenge for concrete. The advantage of printing in elements could be the creation of modular reusable elements, but a question should be asked is whether custom items are really reusable, since they are created for one specific design. Another is the connection of the elements, here dry connections (by post tensioning for example) have an advantage over wet connections (which is the case when 3DCP is used as formwork) when considering this modular aspect. Additionally, monolithic connections can create thermal bridges and unwanted clamped connections (as seen in Figure 23).

3.4. Analysis of printable façades

The design performance criteria and structural demands that are defined for a façade, form boundary conditions for designing façade elements (also for the case study). Selecting a fabrication method for elements manufactured by 3DCP also determines a large set of design restrictions. In this paragraph three fabrication methods are described as concepts and analyzed to see what option is best fit for the case study as well as for future research and possibly the construction industry. For these methods, the possible functionality of the printed element is analyzed using the in paragraph 3.2 design requirements and types. Additionally, existing building enclosures that are reviewed on the possibility of recreating similar façades using 3DCP.

One of the most influential fabrication choices is choosing the print direction, as this has a major impact on selection of buildable shapes. Another influence can be found in the distinction between prefabricated façade elements and in-situ casted enclosures in traditional construction methods. This is also a distinction that should be made when considering 3DCP because of the influence on the design and construction process. For this case study, and considering the printer range, the design for a prefabricated element is analyzed.

3.4.1. Concept 1: Panel

Fabrication

The first fabrication concept is for the fabrication of façade panels that are printed flat on the print table. In this method the print table functions as a canvas for creating panels from printed lines. The print path forms the contours of the panel as well as any pattern of shape that is designed in the panel. Two examples are produced by Bruil (Figure 27) and XtreeE (Figure 28), the latter was created during the research of this thesis. The panel from Bruil is designed as a continuous line that forms the motif inside the element. XtreeE's panel are designed by multiple different shapes that are later connected by casting concrete in the hollow sections of the element.

Figure 27: Facade elements from printed concrete, fabricated by Bruil

Figure 28: Elements printed and casted, fabricated by XtreeE

As visible from the examples, patterns and shapes that are designed in the vertical plane of the panel are virtually unlimited in design freedom. This method allows for form free and mass customized elements production, which is something that could benefit the esthetical characteristics of a façade element greatly. The appearance of a building is determined for the greatest part by its exterior enclosure, patterns and shapes on the façade influence this appearance greatly. For the overall panel however, the geometric freedom is restricted somewhat to the flatness of the panel (especially when casted).

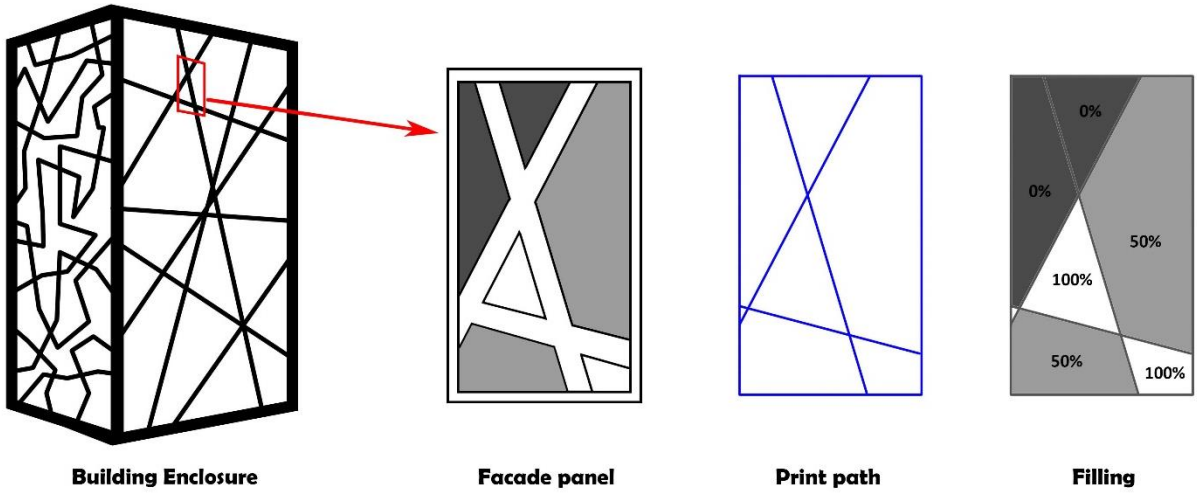

Figure 29: Concept facade panel design, by façade segmentation

Altering shape of the panel edges by slightly tilting printed contour, enables a curvature in the façade by segmentation (Figure 30). This can compensate for the lack of curvature in the horizontal plane of the elements individually. It also allows for interlocking shapes to be designed, in which one panels contour fits into the second, reducing the number of joints necessary in the building enclosure as a whole.

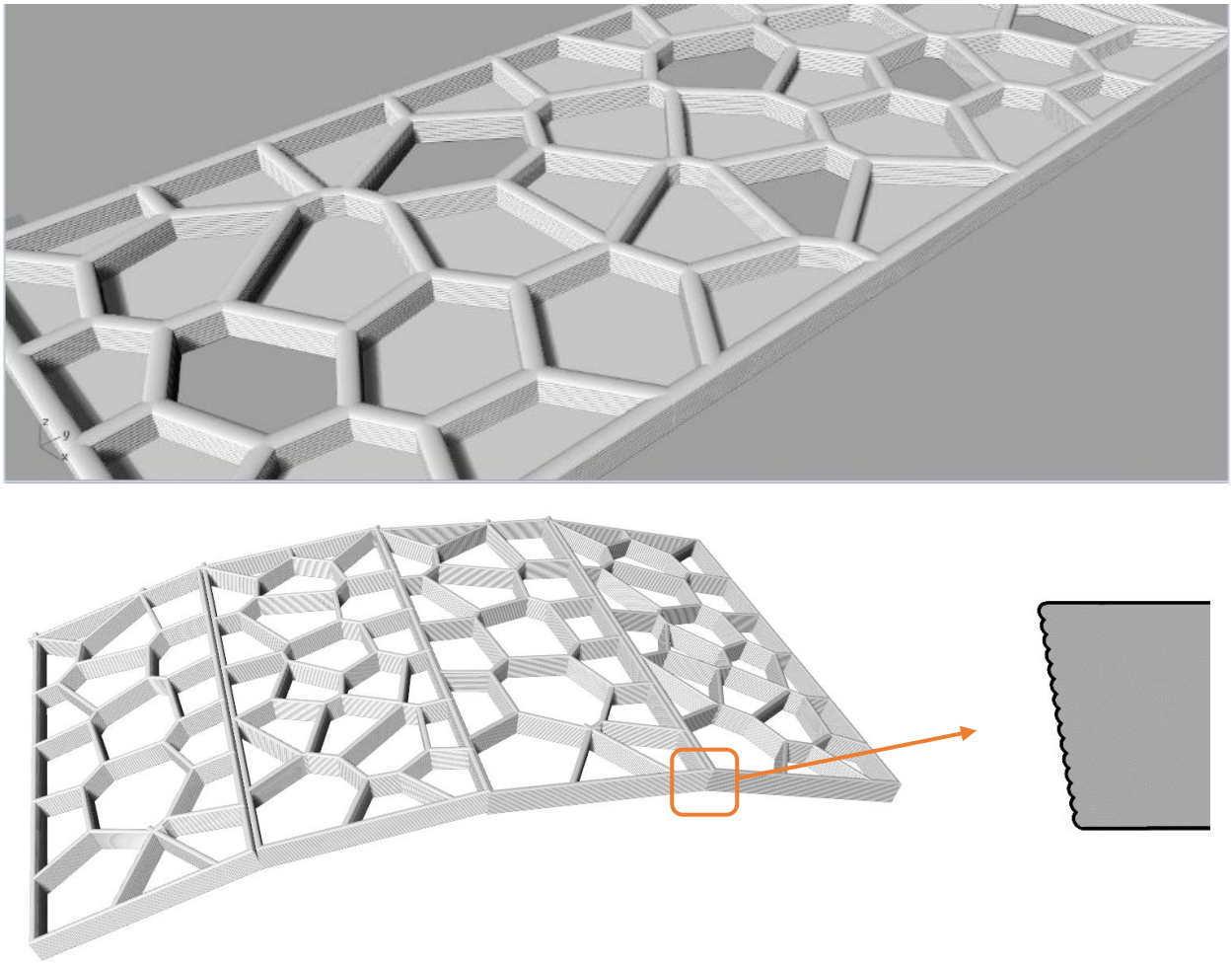

Figure 30: Slanted edges in layered build up to create curved building enclosures

Façades

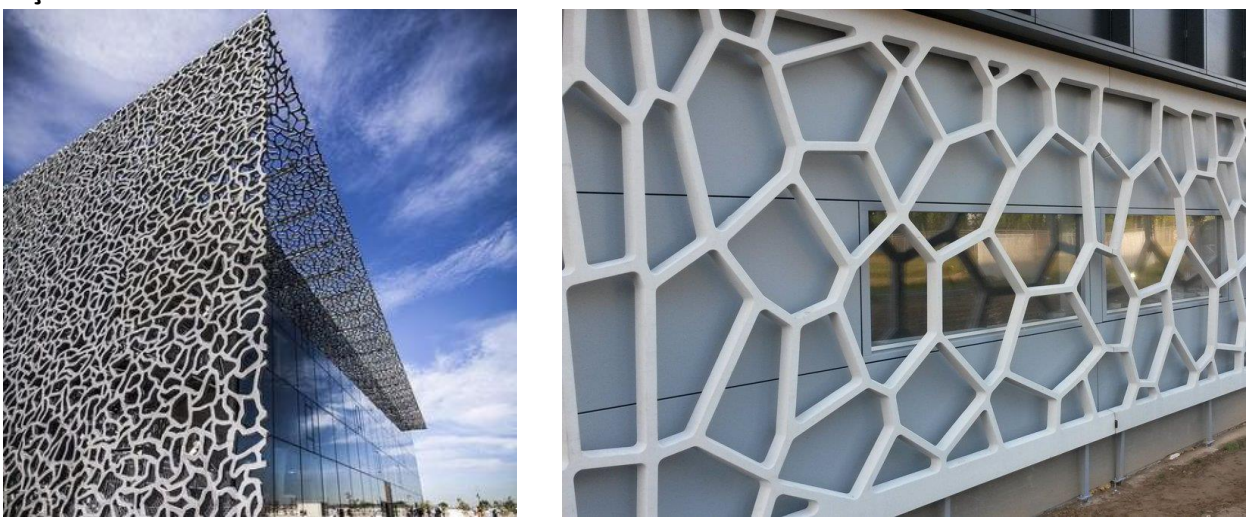

Figure 31: (left) MuCem in Marseille by architect Rudy Ricciotti shows a delicate filigreed concrete exterior skin, (right) Accsys office in Arnhem applied high performance concrete (Hi-Con) in decorative façade panels.

In Figure 31, two exterior finishes are shown that fulfill only a decorative function (possibly also shading), both fabricated using concrete. Both façades present a random pattern on the most exterior layer of the building enclosure, giving the façade a texture or structure. The limitation of functionality of the element allows for a lot of design freedom in shaping patterns on the façade. However, this does require a fully functional exterior enclosure behind this cladding since the cladding does not fulfill any other design requirement.

The examples are both very suitable for 3DCP due to their non-repetitive character. Printing these patterns on a 2D plane would be beneficial to casting due to elimination of many custom formworks. The limitation of functionality, purely decorative, results in little interaction with other elements and materials (such as windows) which results in a simple production process. There is no necessity of integrating elements in the printing process if the end result is an un-reinforced 3DCP panel that is placed in front of a fully functional exterior enclosure. The element sizing and supporting system are two points that still need to be considered, this comes down to the connection between the elements and between the element and the rest of the façade.

Another point is the finishing of printed concrete, which characterize a distinct layered texture (as is the case for most AM products). The layers present as ribs on the sides of the elements and the interior of the pattern lines. These ribs could provide a challenge in connecting the elements to each other or to the building structure due to the tolerance it requires from the connecting material or element. Removing or hiding the texture does require additional processing and could be labor intensive and costly.

Figure 32: Deloitte office "Barcode" in Oslo designed by Snøhetta has a façade consisting of open and closed polygon facets.

When the panels are shifted more to the interior side of the building enclosure, it becomes more integrated in the skin of building. This in turn requires more functionality of the element as the enclosure also protects the building from exterior forces and elements such as wind, temperature and water.

The façade in Figure 32 integrates the pattern structure more inwards into the enclosure compared to previous examples. This would be classified as a barrier type enclosure, as it keeps all exterior elements out at the outmost edge of the building. It requires more from the façade panels than is required from the previous examples, such as weathertightness and thermal comfort. Also, an integration between the glass and closed panels becomes an important detail in the façade.

For this façade image, two parts can be considered for fabrication by 3DCP:

1) the closed polygon shaped panels
2) an integrated element with open (glass) and closed panels

In the first case, panels could be printed as a whole, or only the outline as formwork and later filled to increase surface smoothness. The only advantage 3DCP has over traditional fabrication techniques in this case, is the ability to produce every panel in a unique shape without an increase of production time and cost. However, considering laser cutting on metal sheeting might be a preferable option reducing weight and thickness.

When a frame the size of one story is fabricated by 3DCP, it can reduce assembling time on site and improve weathertightness of the element as a whole. It does however require the integration of glass into the element, which brings about challenges of connecting the two and dealing with tolerances and deformation differences. The frame can function as a windowsill for the glazing or even a loadbearing framework when the entire enclosure is designed as such. In both cases connections are the most challenging part in the product, for this is where all requirements come together.

3.4.2. Concept 2: Bricks

Fabrication

Fabricating individual modular elements which can be stacked or interlocked like masonry bricks is the principle that describes concept 2. Contrary to the panel concept, the print direction is not predetermined for this fabrication method. 3DCP can fabricate shapes that perfectly interlock and, if designed well, transfer loads in compression only. As an example, the printed hollow bricks of WinSun are shown in Figure 33. When various polygon shapes such as in the example, are printed individually they can be stacked to form a modular wall.

Figure 33: WinSun stacked elements block wall

Individually shaped bricks have the possibility to provide a unique texture and shape for a building enclosure. The shape and dimensions of the bricks have a great influence on whether 3DCP is an effective technique to produce the element. The mass customization potential is not really effective on the scale of masonry bricks for example as it would require a great deal of labor on site as well as logistics. Besides, interlocking Lego-like bricks are more efficiently produced by casting with reusable molds.

With brickwork masonry like structures come to mind, which are not common in high rise buildings. Used as cladding, bricks can be applied if they are supported per level stacked on steel profiles. Fixating the bricks to each other and the building is labor intensive and preferably done off site, which would result in prefabricated panels. The only clear advantage that this concept has over the first concept (panels), is the geometric freedom (possible curvature) in the horizontal plane.

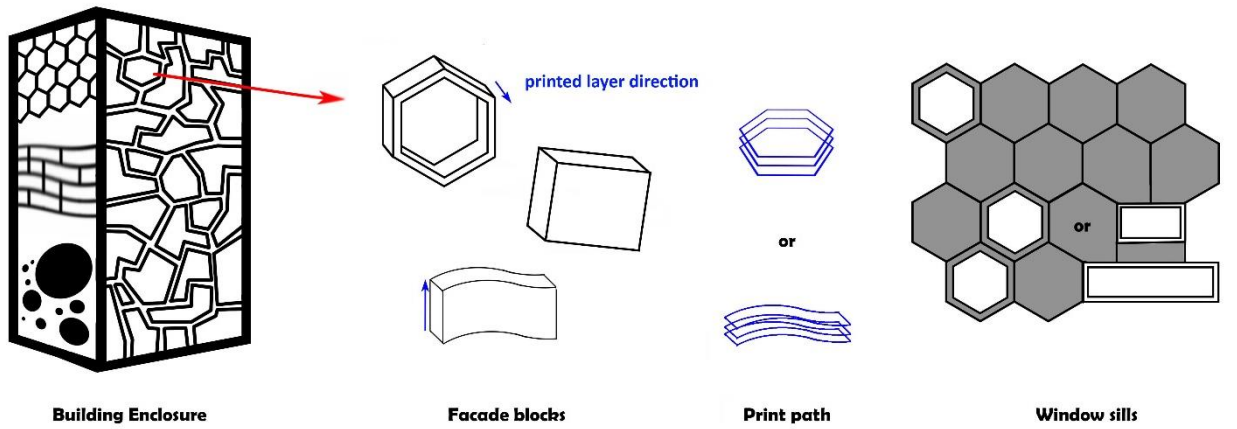

Figure 34: Concept design for customized bricks shaping a block façade

Façades

Figure 35 shows to façade claddings that are structured like building blocks, as is the principle of concept 2. The texture that is created by the application of these larger double curved blocks is more abundant than that of the examples of concept 1. For this effect a larger thickness of the elements, and thereby the façade, is required, resulting in a heavier design. It is clear that motifs and figures can still occur on the façade plane by designing open and closed parts with these elements. The second example from (Figure 35 right) shows the posibility of combining different shaped blocks to form a single façade design. With concrete printing even more variation in the element is possible without an increase in production cost.

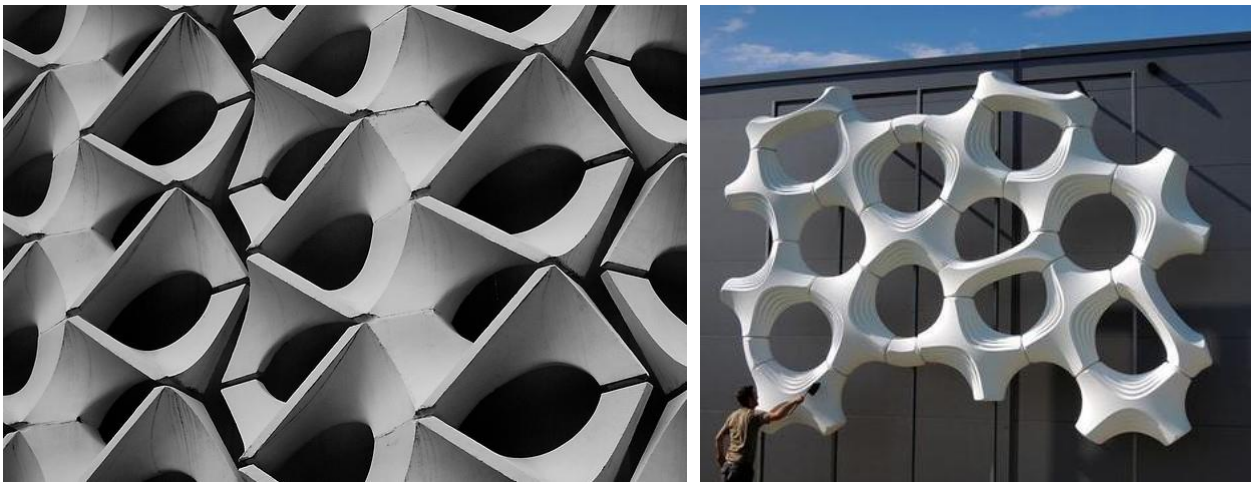

Figure 35 Left: Chemnitz Façade (by Schiefelbein), Right: Concrete eating CO2 (by Elegant Embellishments)

For fabrication of such elements using 3DCP, the print direction is not limited, but could be either horizontal or veritcal. It should be noted however that stacking or connecting the elements is preferred on a smooth surface, which is mostly produced on the top and bottom of printed elements. The elements in the example seem to be fixated to the building via a frame structure behind the elements from which they are hung.

Both examples are used as decorative cladding only, resolving no other criterium or functionality (except perhaps providing shading). The perforations in either design is not designed to classify them as a rainscreen type façade. When more functionality is assigned to the elements, more integration of other materials is required. This is not much different from the panel concept besides the fact that components such as window sills could be modularly installed in the façade.

3.4.3. Concept 3: Walls

The final concept for the fabrication of façade elements by printing concrete, is that of printing walls. For this method, the printing direction is vertical, meaning that the elements are fabricated in the same orientation as their ultimate in-use state in as part of the exterior enclosure. This concept lies closest to the original idea of Contour Crafting as it literally manufactures the contours of a building. A difference in production however is that wall segments can also be prefabricated rather than produced on site.

Figure 36 Left: Hollow circular wall segment (by Rudenko), Right: Profiled hollow wall segment (by SCG Thailand)

Many examples of this production method exist today as this is one of most common printing techniques. Two examples of concept 3 are depicted in Figure 36, more examples can be found throughout this document. The printed element of Rudenko (left) shows a hollow wall element that shows great curvature in the horizontal plane. The second example, SCG uses the small cantilevering

capabilities of the fresh concrete to create a unique texture on the wall element. Both show the potential of freeform fabrication and material reduction.

As discussed previously (paragraph 3.3.1), the potential for integrating functions and system in the hollow segment of printed walls is great. Especially when the hollow sections are continuous, elements for reinforcement, insulation, ventilation and electricity can be installed within the element. If specified zones are enclosed, integration by casting locally becomes possible, preventing the necessity of filling the entire element. It should be noted however, that this can cause thermal bridges in the exterior enclosure if not designed well. A challenge that is present even without casting: due to the segmentation of the façade in wall elements, the print path will inevitably connect interior to exterior at some point.

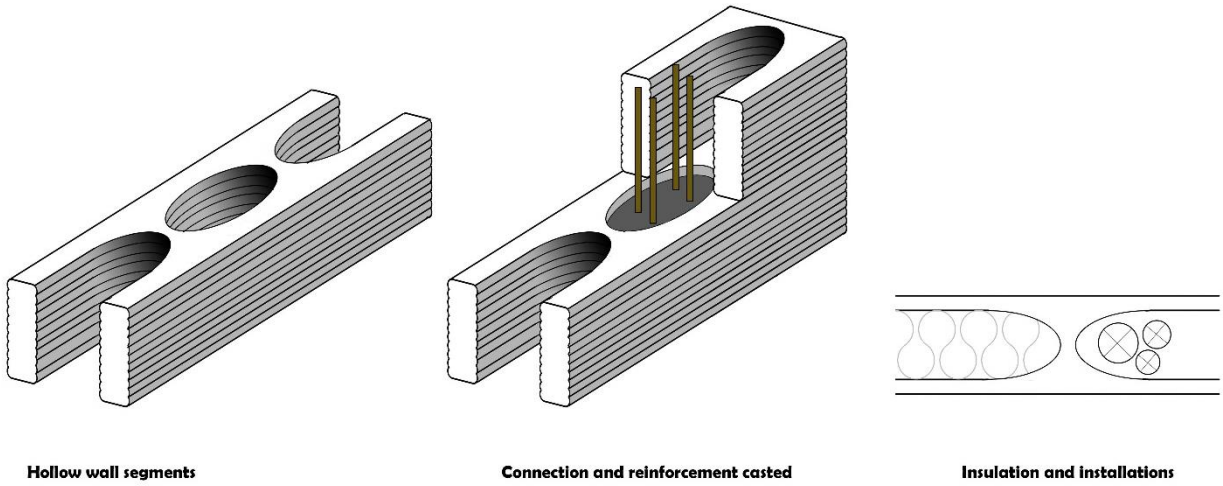

Figure 37: Concept design for 3DCP hollow wall segments

In high rise building, installing wall elements can be a challenge. The design of the connection of the element determines the installation procedure. Walls can be stacked as blocks and receive only horizontal support from the main structure. This might not be the best solution for high-rise buildings as any deformation in one element would affect the entire façade of 20+ stories. Alternatively, the elements are supported per floor level either directly on the floor or supported by a frame structure. Due to the thickness of the elements, a bigger support structure might be necessary compared to that for the panels of concept 1.

Finally, providing perforation in vertically printed elements remains a challenge due to the incapability of producing larger cantilevers with fresh concrete. Solutions for this are found by applying lintels and beams during the production process to print over or installing windows during the manufacturing process (paragraph 3.3.1). The panel concept does have a clear advantage in providing perforations in the elements within the automated construction process.

Façades

Figure 38: Hannam-Dong office in Seoul by the System Lab architects has a double curved façade

As opposed to casted concrete elements, printed elements can provide curved elements without increasing production costs due to formwork. This curvature can be used to shape the building enclosure freely like in Figure 38, the curvature can even provide structural load bearing capacity or stiffness where needed. Earlier discussed challenge of applying reinforcement in curved concrete holds especially for loadbearing curved elements. Also, the element dimensions will likely exceed the maximum print path width, but both of these problems could be solved by printing hollow structures.

As the example shows, curvature in the horizontal plane of the façade leads to cantilevers in the structure. For high-rise building this can have large impacts on the loading on the façade carrying structure and the building itself. This is why larger cantilevers in high-rise are often supported by the main load bearing structure, shaping the entire building.

3.5. Conclusion

The three fabrication concepts are analyzed on their ability and potential to fulfill the set design performance criteria. From this analysis a concept is chosen as the start point for the design of the case study façade elements.

All three concepts seem to be able to create any of the four Boswell defined exterior enclosure types. Enclosing of the façade as a whole however requires good designing of the connective details to ensure weathertightness, as is the case for any façade. The properties of concrete make a mass type façade the most logical choice when the elements are placed on the exterior edge, this requires some thickness of the elements to deal with moisture. Sealing the concrete with chemical could also provide a barrier type façade, without too much change in design of the element. For the case study a mass type is selected.

Perforations allow light to enter the building and inhabitants to view the outside world. Printing flat allows great freedom in creating and shaping perforations (as seen in concept 1), while printing vertical brings (concept 3) great challenges in creating perforations in the façade plane. Modular bricks could allow for windows to be stacked between the modular blocks that form the façade, but this does require custom window panels.

The design criterium of esthetics is measured by the design freedom since the design is not determined. For panels (1) this lies primarily in freedom in the plane of the façade, while printing walls (3) allows for curvature out of plane. For high-rise buildings however, it is considered that curvature of the façade is

determined by the building and its structural system. The appearance of the exterior enclosure is therefore more dependent on the patterns on the façade, to which concept 1 and 2 have an advantage.

Weathertightness is best controlled when connections are limited, since the joining of two elements is always a weaker spot and can lead to leakage. The grading for this criterium is therefore easily determined by the number of connections that have to be made. Since the bricks (2) are smallest they score lowest. Element sizing for panels (1) and walls (3) are determined by the printer and transport but can be regarded as equal.

For the installation of additional components regarding structural load bearing capacity or ductility (reinforcement) as well as insulation, the hollow segments provide a clear possibility. Integration of components in panel elements however has the benefit of being traditionally shaped, therefore accommodating more elements that are found in the traditional building industry already (reinforcement netting, EPS insulation blocks).

Concept	Light trans-mission / view	Esthetics (freeform)	Weather-tightness	Structural	Insulation
	A	B	C	D	E
1. Panel	++	+	+	+	+
2. Brick	+	+	-	-	-
3. Wall	--	-	+	++	++

Table 2: Fulfillment of design performance criteria of concept designs façade elements

From Table 2 the conclusion is drawn that a panel shaped design for the case study is the best fit. Proving the feasibility of creation and use of said panels can provide a “way in” the conservative construction world for 3DCP, since the panels are closer to traditional elements. Currently used applications and systems for façade panels can be used for the printed panels as well. Thus, while the panel offers some of the advantages of additive manufacturing by using 3DCP, it also could fit into the current construction industry in terms of installation and transportation.

Figure 39: Transportation of facade panels by forklift and truck

4. Case Study

4.1. Introduction

In order to examine the feasibility of 3DCP as a fabrication method for façade elements in the current state and conditions, tangible evidence is necessary. A case study is set up to formulate a more concrete design assignment, which concerns the qualification of an element fabricated by 3DCP for the current building industry. The case study describes the context of a design assignment from which boundary conditions, restrictions and requirements are derived.

The goal of the case study is to design and engineer a façade element that is manufacturable by 3DCP that for which fulfillment of the set requirements is made conceivable. The design is then put to the test for both fabrication and structural behavior, in paragraph 5.5. By developing the façade panel for this case study, the different stages from design, production to testing are experienced. In all faces challenges and potentials are analyzed and serve as input for a prediction of a digital construction chain.

Figure 40: Visual representation of concept façade design for case study

4.2. Case Study Description

In this fictional case, a high-rise building is going to be built in Rotterdam, the Netherlands (Figure 40). For the exterior enclosure of this 20+ story building, façade elements will be designed which are to be fabricated using 3DCP. The potential of fabricating mass customized and geometrically freeform elements seems to create the possibility of realizing of virtually any façade design. Boundary conditions and a research scope are defined in order to guide the design in the right direction and come to a more concrete image.

The focus of the study is on the constructability by 3DCP and structural validation of the element, in line with the thesis research. In other words, the element should be printable and be able to withstand loading conditions that are prescribed for a façade panel. Most design restrictions and requirements are derived from these codes and norms, but to define the essential functionality of the façade element, some basic typologies and definitions must be specified first. The potential benefit of 3DCP fabrication is

analyzed by looking at existing façades and determining which parts could have been fabricated in 3DCP, and why this would be better.

Goal
This part of the case study focuses on the theoretical part of the façade element. The end result is a design can be installed on a high-rise building in Rotterdam at 80m altitude. Next to the design a prediction of its loadbearing capacity is engineered and a fabrication plan of how the element can be manufactured. The three focus points are dealt with individually in their related paragraphs:

1) Function
2) Engineering
3) Fabrication plan

Figure 41: Facade panel concept for case study

4.3. Program of demands

4.3.1. Functional demands

The panel must be installed on the exterior of building at 80 meters altitude as part of the exterior building enclosure. The design performance criteria that are considered are foremost structural and manufacturability. Secondary design performance criteria that are considered for the case study are thermal comfort and light transmission.

The design for the façade panels:

- is dimensioned to span one story for a residential high-rise building
- includes a detail design regarding the installation to the building
- includes functional insulation providing thermal comfort for the interior of the building
- provides 30% transparency for light transmission (protection from overheating, maximum chosen as base for the case study design to analyze behavior of printed slab element)

4.3.2. Structural demands

Norms (NEN) prescribe specific load cases for building designs, which the designed façade panel should be able to withstand. Additionally, in the event of structural failure due to an excessive loading condition, the element should not fall down in fragments and preferably provide a warning mechanism. Basically, brittle failure should be prevented and the elements must be installed securely.

The loading cases that are considered are

- Self-weight
- Wind loads
- Fall protection

The gravity loads that are a result of the weight of the element are always present on the element. How the element is supported however, determines the flow of forces in the element. The direction of the self-weight load is also dependent on how the panel is oriented, which can vary during transportation and installation. The elements need to be able to withstand these loading conditions without cracking.

The loading due to wind is specified per region and altitude in the national building codes. As this case study is hypothetically situated in Rotterdam, the region is described as wind area II (South Holland) and on built terrain. At an altitude of 80 meters, an extreme thrust of qz = 1.39 kN/m² is defined, which is used for calculating the load on the façade panel. Factors considering the building shape and the

considered surface area are applied conservatively since the façade design for the façade panel should suffice for anywhere on the exterior of the high-rise. The final surface load that the capacity of the designed panel required to bear is 1.95 kN/m² (suction) and 1.39 kN/m² (compression).

As an exterior enclosure, the façade element should also provide fall protection for anyone inside the building. For this specific function, a test is prescribed in national annex of Eurocode 1. This is often referred to as the sand-sack test as it can be performed by swinging a weight at a prescribed height to the element to simulate a falling load.

For the case study a load is modelled on the interior face of the element at the by the code specified height. The load is modelled as a line load of 0.8 kN/m or a point load (on a surface of 0.2 x 0.2m) of 1.0 kN at a height of 1.20 meters measured from the floor level (Figure 42).

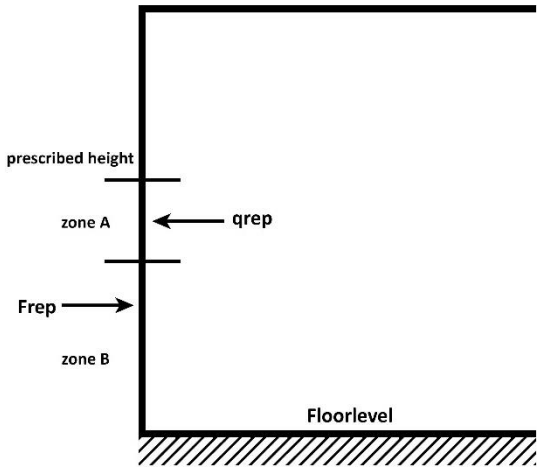

Figure 42: Load placing for fall protection

4.3.3. Fabrication demands

Dimensions of the façade panel are restricted by the fabrication; the reach of printer determines the maximum size of element. Additionally, transportation sets restrictions to the dimensions of an element, since the case study regards prefab façade panels (rather than on site fabrication). For the case study the selected printer system defines the boundaries with the size of the print table (1.5 x 4.0 m). A parametric design however, can take a potential upgrade of the system in to account and enable designs with larger dimensions.

Regarding the production process, the design should be such that completely automated manufacturing could be possible. For the case study, hand operations might be required for production but the fabrication plan for the design should consider automation of these steps. This requires elements and materials other than the printed concrete, to be integrated in the process and fixed to the concrete. Placing additional elements should not disturb the printing process or damage the printed element.

4.4. Design

4.4.1. Base design

The start point for the case study design is based on the design concept of panel elements as described in paragraph 3.4.1. Aiming for a feasible production and predictable structural behavior, geometric complexity is limited for the case study design. This means that no complex façade patterns are taken in to account for the design. The chosen element design is described as a rectangular panel with a single perforation (Figure 41). Adaptation to the design are made in accordance with test results that are performed for the case study, these tests are described in chapter 5.

Original design dimensions

Façade panels are designed digitally with the given requirements before printing tests for the case study are performed. The original design for the theoretical model is redesigned on the basis of test results that formed a variety of input factors. Both structural and fabrication requirements that are defined from analysis by experiments with 3DCP. With the purpose of analyzing the process from design to production, the change in design is also documented.

The height of the façade element is based on the floor-to-floor height of a standard residential building, which is between 3 to 4 meters. Based on the printer reach and the print tables the contours of the façade element are defined as a rectangle of 2.0 by 3.5 meters. This results in a surface area of 7m² and the maximum perforation (30% = 2.1m²) is defined as the surface by which the perforation shape is limited. The perforation is placed symmetrically in the center of the element (Figure 43).

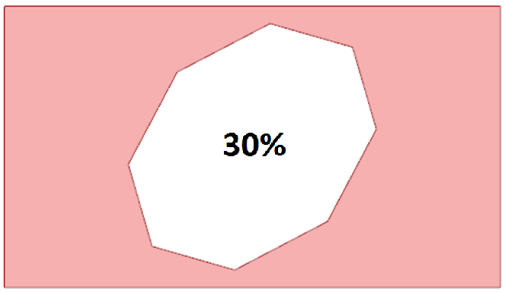

Figure 43:Visual perforation percentage

In the first stage of the research, the integration of reinforcement in printed concrete panels was conceptual and untested. Therefore, the thickness of the element in the original design is used as a parameter to influence the structural height. In a conceptual design the thickness of the element was a variable of the normative bending moment, increasing the section modulus (thereby the bending moment resistance) locally (Figure 44). The flexural strength of the printed concrete is an important input for dimensioning the façade panel in this design.

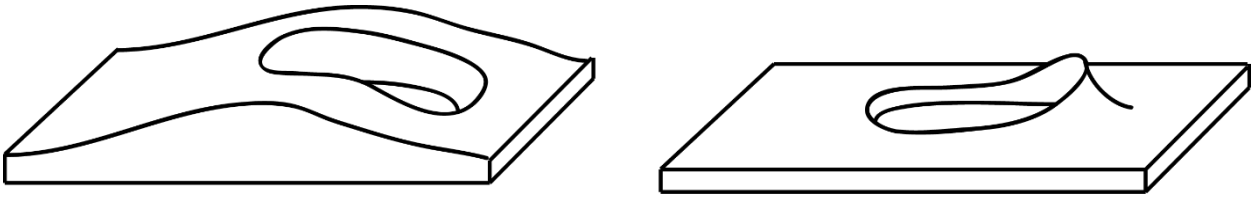
Figure 44: Concept designs using local deviations in element thickness as an advantage

Another method of profiting from the possibility of locally increasing the printed layers and shaping the element, is by printing exterior shading. When the contour of the perforation is extruded outwards on the top more, it can protect the building from heating due to direct sun light entrance (Figure 44). For this design, the impact of weather should be studied: wearing of concrete and water accumulation should be taken in to account. For this case study, this option is not investigated further.

Case study design dimensions

For the test panels different print tables are used to enable transportation of the printed elements without loading. These tables differ in dimensions (1.5 by 3.0 meters) and directly influence the printable contours for the element. The dimensions for the print path are designed at 1.2 by 2.9 meters (allowing for some deviations) with a print path width of 5cm. After fabrication the elements are measured at 1.23 by 2.96 meters each with a tolerance of ±1cm.

With the change in contour dimensions, the design maximum area of the perforation is also altered. In order to narrow the critical cross-section to one section, the perforation is changed to a circular shape. This results in the smallest cross-sectional area of the element being in the middle, which is beneficial for focusing the analysis during loading tests. The perforation is designed as an ellipse with two radii of 275mm (r_1) and 1125mm (r_2) (Figure 45).

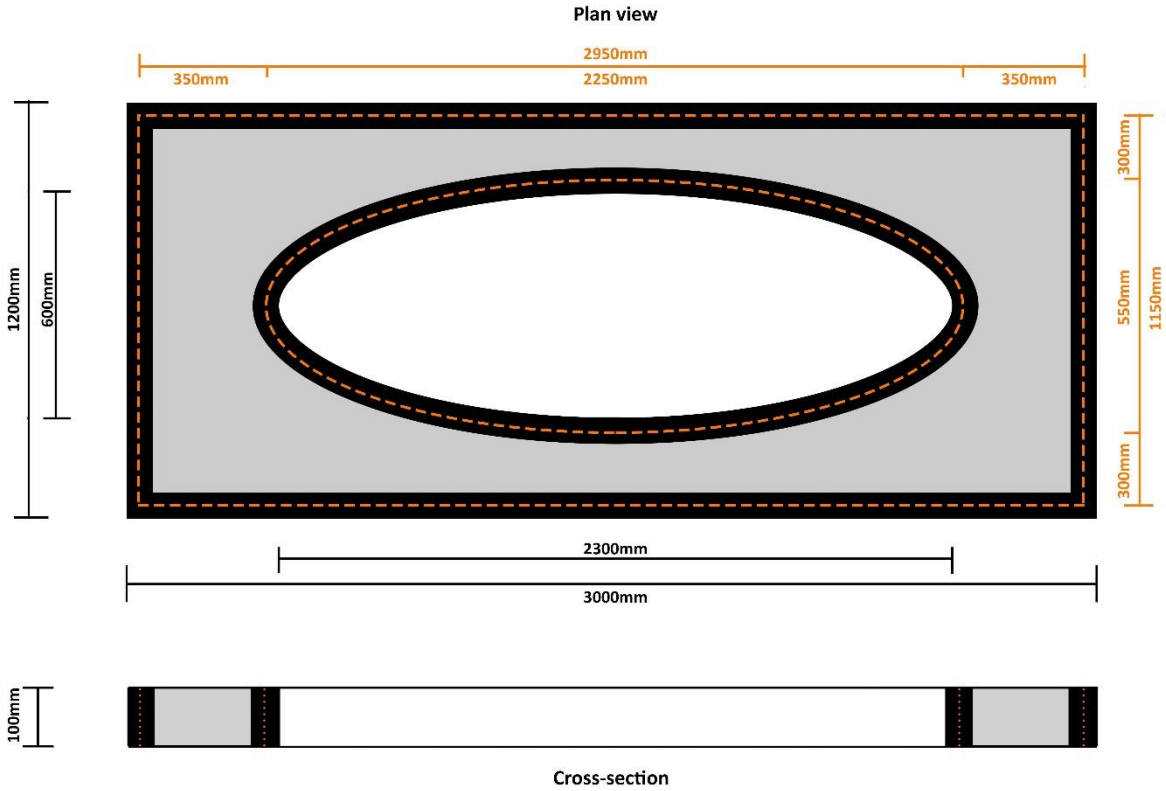

Figure 45: Designed dimensions of the printed test panels

From preliminary experiments 2 and 3 (paragraphs 5.3 and 5.4), the integration of reinforcement in the printing process was proven feasible. The design of the façade element was adjusted accordingly to account for reinforcement. The thickness of the element is no longer a variable of the bending moment but is determined by the necessary (minimum) concrete cover that is required by the reinforcement as protection from corrosion and for bonding strength. The element thickness in the case study design is set at 100mm for the entire panel.

4.4.2. Parameters

To envision the potential of the mass customization in the design, the elements are designed parametrically. The perforation is altered in dimensions, shape and position in the panel easily in the digital model designed in grasshopper (Figure 46). The shape of perforation is a symmetrical polygon defined by the number of corners (n) and the distance from the center to a corner (r). The shape can be deformed by scaling in x (rx*r) and (ry*r) direction and rotating around the center (phi). The center can be translated in x (x) and y (y) direction, repositioning the perforation.

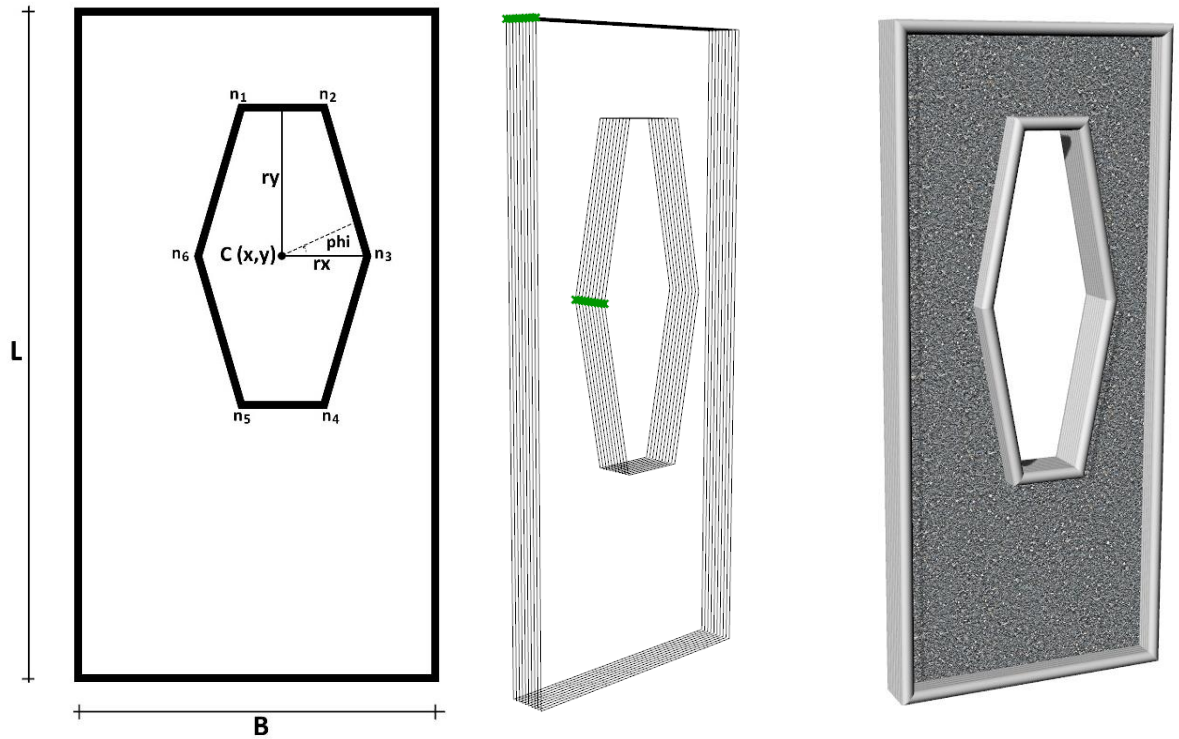

Figure 46: Design parameters of facade element and related models for print path and modelling

From the model the print path can easily be determined since it runs on the same software, Grasshopper® within Rhinoceros®. The print path lines lie in the center of the printed layers which requires a small offset from the outer dimensions from the design. Also, the thickness of the element is determined by the number of printed layers multiplied by the layer height. This is generated in the model by duplicating the lines vertically, with a spacing that represents the height of the printed layers (Figure 46 middle).

Alternatively, a flat shape (closed curve) can be imported or drawn and used as the contour for the perforation. This allows for more freeform design shapes to be added in the design. The digital model will adjust the panel design accordingly, but the size of the perforation is no longer restricted by the 30% area limit.

Design of the windowsill is not part of the scope of this case study, but for providing flat glazing in custom shapes many techniques are present to date. Integrating glass directly into the printed concrete is unadvisable, due to the complication in replacing glass when covered by hardened concrete. Printing on a window sill seems more feasible but would also require more research.

4.4.3. Details

For transportation of the element from the print table to the truck and maneuvering it on the building construction site, the element needs to be lifted. For this reason, the design includes anchors installed at the edge of the panel, on which cables can be temporarily fixed allowing cranes to tilt and lift the elements (Figure 47). In the original design the anchors are located on the top of the element, most useful for on-site transportation before installation. In the fabricated elements for the case study however, the anchors are installed on one side.

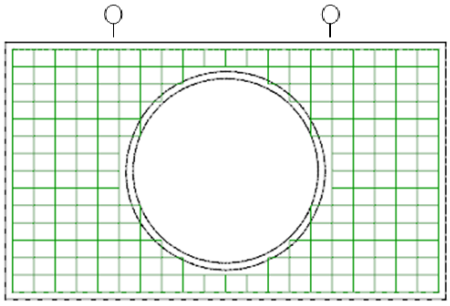

Figure 47: Placement of lifting anchors

The reason for the change is to reduce the bending moment in the element when tilting it from the print table. By reducing the span from anchors to table, (changing span from element width to element height) the lever arm is reduced (Figure 48).

Figure 48: Lifting the printed test panel on the longitudinal side using anchors

Connecting the elements directly to the floors or structure of the building creates thermal bridges. An insulation layer between the element and the building distances the element from the support fixation points on the building. This results in an eccentricity that acts as a lever for the self-weight introducing a bending moment on the anchors. To solve both the thermal bridge and the induced bending moment, anchors integrated element and in the insulation are designed (Figure 49 left). This demands for preparation of the insulation and the anchors before printing, more on this in fabrication plan (paragraph 4.6).

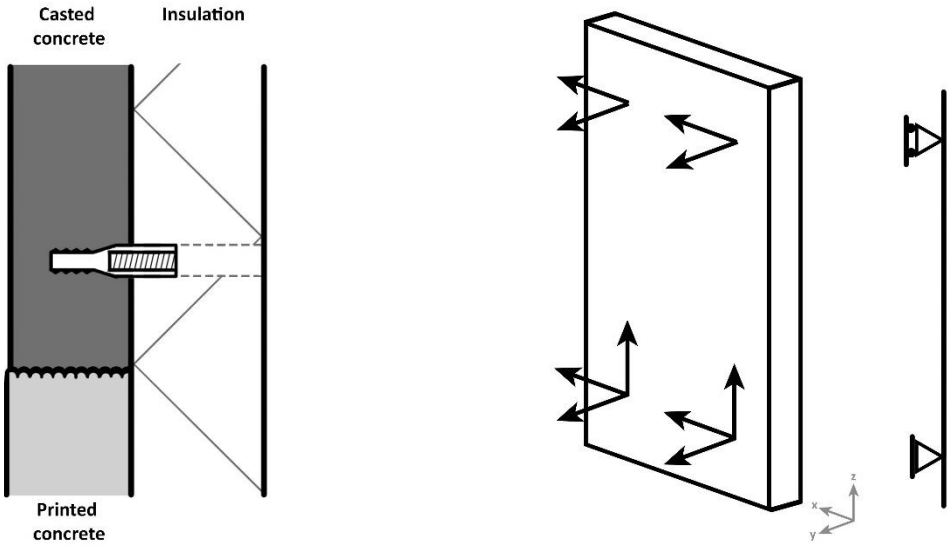

Figure 49 Left: detail for integrated anchor, Right: schematization support system for facade panel

The anchors that secure the panels horizontally to the building perforate the insulation layer only locally, limiting the thermal bridge. The design shows four fixation points of the element to the building, two at the top and two at the bottom, according to the schematized support system (Figure 49 right).

The lower supports take care of the weight of the element (loading in z-direction), all four supports restrain displacement in horizontal (x and y) direction. The vertical loading is only taken up by the lower supports to ensure that self-weight is carried by compression forces in the concrete.

4.4.4. Installation

The top anchors are single bolt anchor plates and the lower anchors are a bigger variant with four bolts. The top anchors only need to transfer horizontal loads but should also be designed for local buckling under wind compression forces. The lower anchors are bigger to accommodate heavier profiles that are subjected to the bending moment due to the eccentricity. Installation of the elements is done in the following sequence (see Figure 50):

1) Insert screw anchors and profile on element.
2) Attach leveling profiles to element.
3) Lift panel in place and fasten lower support to floor.
4) Fixate top support and secure element.
5) Finish sides and top with rubbers (and possibly glue kit).

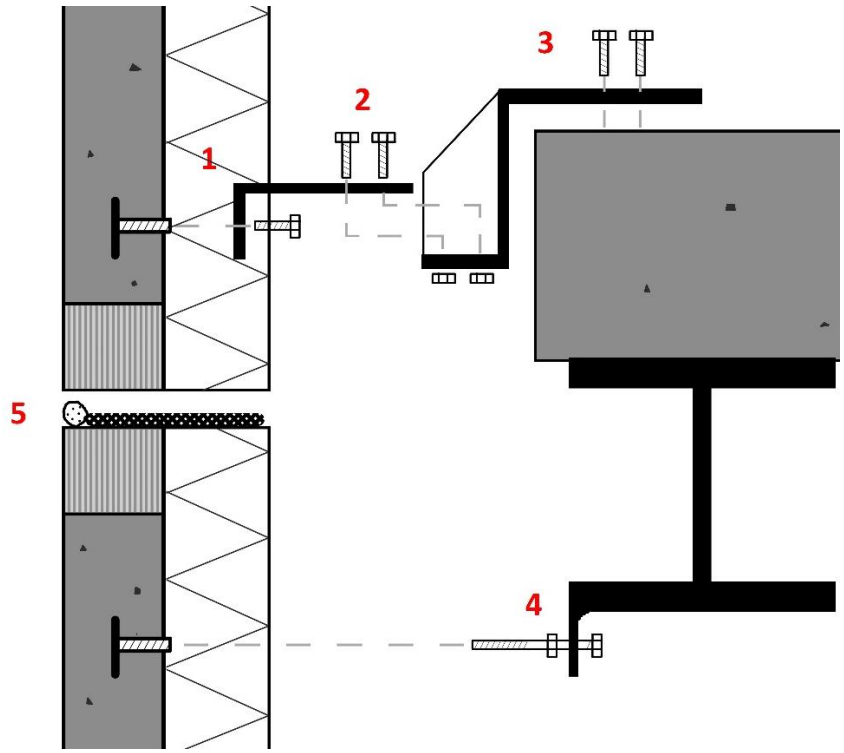

Figure 50: Installation detail of printed panels

The screw thread inside the bolt anchors allow different profiles to be installed onto the element after fabrication. This creates the possibility of using these fixations for transportation on site as well, making the anchors in the edge redundant (these are still used for the test panels however). For adjustments and exact positioning during installation, a connection from the panel to the building can be supported by façade carriers that are used for masonry cladding today (Figure 51). This can be applied as an intermediate profile between the floor and the profiles that are attached to the element directly.

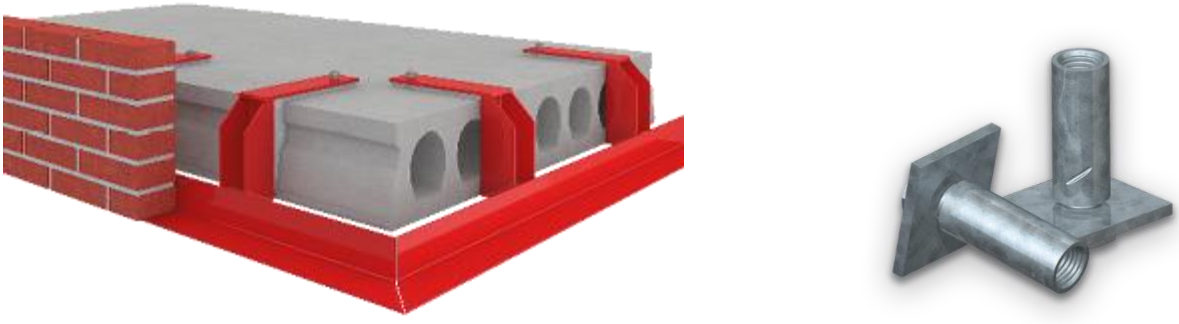

Figure 51:Left: Facade carrier system for masonry enclosures (by VEBO), Right: Bolt plate anchors

Enclosing the exterior requires rubbers to account for the tolerances that are produced by the ribs from the printing process. Even if the production process is upgraded, removing the ribs and reducing the tolerances, the rubbers are needed to compensate for any movements or deformations (sagging or creep). If this is not taken care of, load transfers between the panels might occur causing new load cases and possibly peak stresses that are unaccounted for. Glue is advised to seal the seams between the panels, ensuring weather tightness.

4.5. Engineering

4.5.1. Modeling

For engineering the façade panels, a slab model is drafted with similar support conditions as presented in Figure 49 earlier (two rolling supports, two hinged supports). The main concerns for the analysis of the structural models are the (tensile) stresses in the concrete and the acting bending moment versus the designed bending moment resistance. The tensile stress in the concrete indicates if cracking of the concrete will occur, and if so, at what load. The acting bending moment on the element is needed as an input for designing the reinforcement, which in turn provides input for the bending moment resistance of the (critical cross-section) of the element. More focus point for structural analysis could be considered (for example punching shear or reinforcement bonding failure) but are deemed abundant in the analysis of structural predictability given the test loading (three-point bending test).

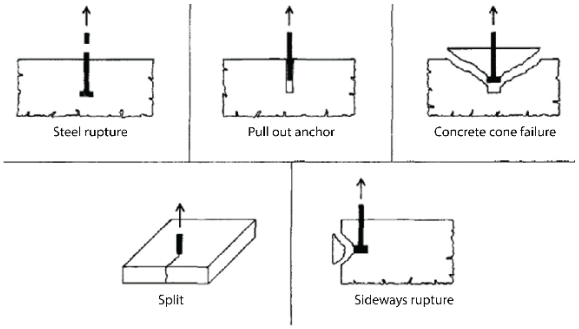

Figure 52: Anchor failure mechanisms

Nonetheless additional checks for anchors are performed to verify the potential of the design. This formed part of the analysis of the structural requirements for applying anchors in to printed concrete. CUR publication (25) describes the failure modes for anchors in concrete that need to be checked and an online tool from an international fabricator (Hilti) allows for quick modeling and checking of anchors. These calculations require a concrete cover that the print path width often cannot provide, but more on this later.

A clear distinction is made between the designed façade panel and the tested panels, due to differences in dimensions and loading conditions. For the designed panel, a parametric engineering model is described in which the structural model is directly influenced any alteration of dimensions or shape of the panel. For coherency, the dimensions of the element are not altered for imagery in this document but do differ from that of the tested panel. Through calculations the required reinforcement is determined based on traditional steel rebar netting. Load cases as defined in paragraph 4.3.2 are simulated.

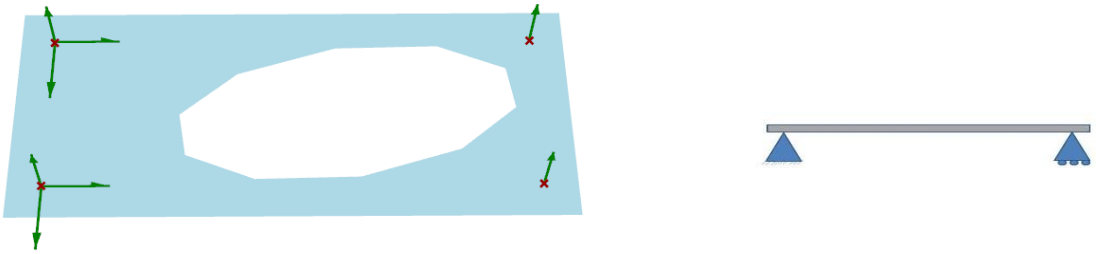

Figure 53 Left: Karamba model: Green arrows indicate the restricted translation direction by the modelled supports. Right: 2D schematic simplified view of supports

Self-weight

The self-weight is modelled as a surface (or mesh) load in two directions representing different phases in the construction process (Figure 54). When the element is lifted or transported horizontally, gravity will load the panel perpendicular to its face (cause out of plane bending). When the panel is installed, gravity will load the panel in-plane, causing mostly compressive forces, but these should be considered in combination with other load cases. The magnitude of the load is a direct function of the volume of the element multiplied by the density of concrete (2500 kg/m³) and is independent of the orientation

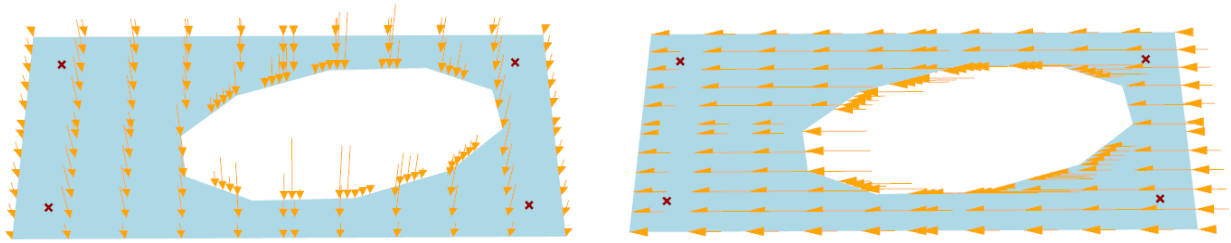

Figure 54 Left: Self-weight loading during transport *Right: Self-weight loading when installed*

Wind load

Load case 2 represents the wind loading on the façade panel, which is only modeled in one direction (perpendicular to the panel plane) due to symmetry. The magnitude of both suction and compression wind loads is conservatively considered equal, therefore resulting in similar structural analysis. The required reinforcement should be designed symmetrically as well, taking this consideration in mind using the generate concrete cover for both top and bottom netting.

Fall protection

The third load case simulates the sand bag test that analyzes the fall protection of the panel. This is modeled in two scenarios, the first is representing a point load that is applied to a surface of 20x20 cm, the second is a line load at a modifiable distance from the supports.

Figure 55: Visual representation of the modelled load cases considering fall protection.

Test load

Loading of the test panels in the three-point loading test for slabs is also modeled to predict the structural behavior and load bearing resistance of the case study panels. For this model different supports are used, as the panels are position on two rolling line supports a little of the outer edges. As the panel is placed horizontally, gravity loading is also present perpendicular to the panel (see self-weight). The test load is modeled as a surface load acting on 24x120cm at midspan, representing the HE240A beam that is used during testing.

4.5.2. Software strategy

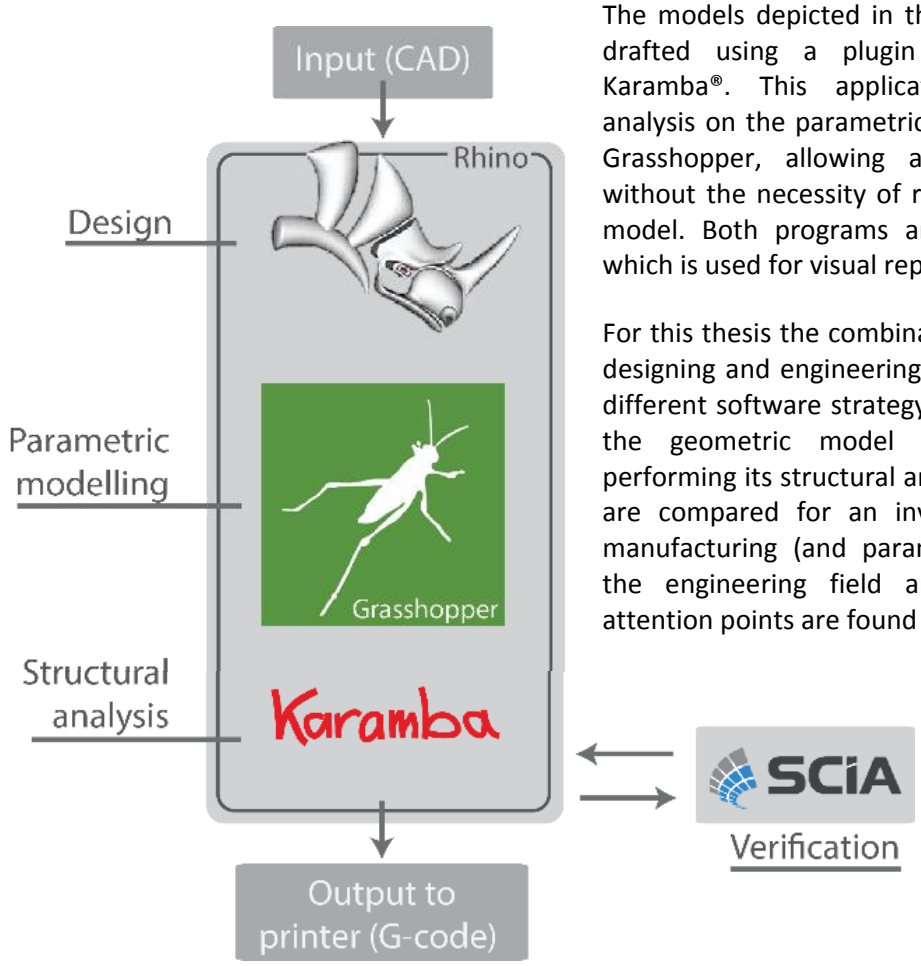

Figure 56: Software strategy

The models depicted in the previous paragraph, are drafted using a plugin in Grasshopper® called Karamba®. This application performs structural analysis on the parametric input that is generated in Grasshopper, allowing alterations of the design without the necessity of remodeling the engineering model. Both programs are run within Rhinoceros, which is used for visual representation of the models.

For this thesis the combination of the two is used for designing and engineering the panels. Additionally, a different software strategy is examined, by exporting the geometric model to SCIA Engineer® and performing its structural analysis. These two methods are compared for an investigation of how digital manufacturing (and parametric design) can impact the engineering field and what challenges and attention points are found in either strategy.

Karamba

In order to perform a structural analysis on the panel in Karamba, the panel is modelled in Grasshopper as a surface and then meshed to form input for the shell analysis of Karamba. As with any finite element analysis, correct mesh settings (especially refinement) are really important in order to obtain correct and accurate results. Grasshopper knows many ways of meshing geometric shapes (like BREPs) and redefining created meshes. Some focus points when checking meshes are the refinement (gridsize) and shape (triangular or quad) of the mesh elements. Errors can occur near boundary edges (see figure), which results in incorrectly calculated peakstresses.

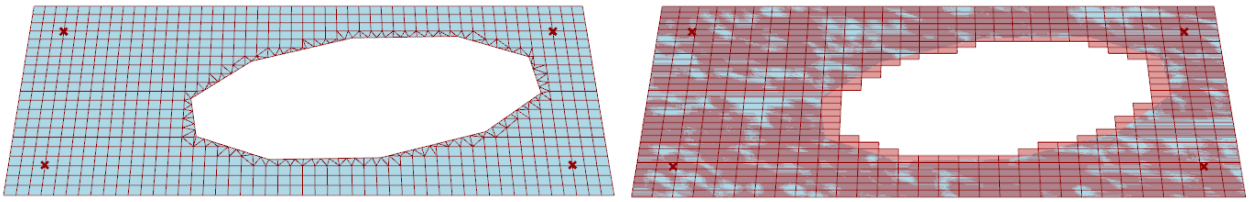

Figure 57 Left: Meshed panel using both quad and triangular mesh elements.
Right: Quad mesh incorrectly representing the designed surface near the edges.

The location of the supports and loads are defined in Grasshopper by modelling them as the required input for Karamba. The supports for example are defined by creating four points, to which a “support” component is assigned and set with the right restrictions in terms of translation and rotation. Similar

components are defined for the load cases, each labelled individually, as well as the selected material (concrete C50/60) and thickness. In this model the thickness of the panel is constant everywhere, virtually creating a slab like element.

The components are assembled and analyzed by the Karamba script, visual results are retrieved in Rhinoceros by the model and shell viewing components (Figure 58). While displaying stresses and displacements by using color scales is done easily, retrieving absolute values of any measurement at any selected location is rather difficult. This part of the software can definitely improve on user-friendliness.

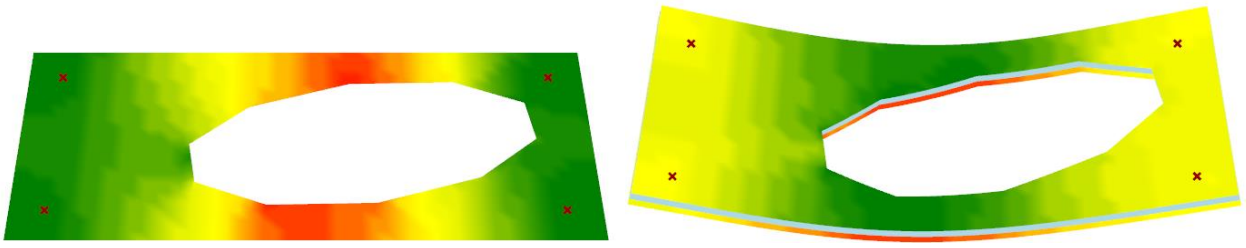

Figure 58 Left: Principle stresses displayed on a color scale green-red.
Right: Displacement displayed by scaled deformation of the model and utilization displayed by three layers in color scales

SCIA Engineer

As a more traditional and common structural analysis program, SCIA Engineer is used to analyze the panels as well. First annotation for modeling using this program is the limitation in design capabilities as it is restricted to creating easy polygon shapes. To overcome this obstacle, the model designed in grasshopper is exported, either as polyline geometry or as mesh, and imported into SCIA. This can then be used to define the boundaries of a slab element and a perforation within. Other settings, such as material and element thickness, are chosen similarly as in Karamba.

The exporting procedure does deprive the engineer from performing structural analysis parametrically. A solution for this is being developed on both ends: SCIA Engineer is developing a Grasshopper component that allows information transfer between the two programs. This reduces the procedure of exporting and importing to one click, however it still only transfers geometry requiring the user to define supports, loading and element specifications. A similar attempt is made by GeometryGym®, a plugin that links several FEM software programs to Grasshopper directly, including functional information such as material specifications and profiles.

When the same element and load case are modeled in both SCIA and Karamba, similar results are retrieved as expected. Absolute values are obtained from SCIA far easier than from Karamba and also more results are given (such as shear stresses and bending moments). Another benefit is the possibility of designing reinforcement into to element, which results in a better representation of the panel.

Hand calculations

To check if the model provides realistic results, hand calculations are performed on a simplified model. In this model the panels are reduced to a simply supported beam with a cross-section equal to the critical cross-section of the panel. By reducing the surface loads to distributed line loads, representative load cases are modelled. This results in a conservative model when looking at the loading and stresses at midspan, which is illustrated in Figure 59 and the example of self-weight load case:

Q_{rep} represents the surface load (q_G) as a line load with lower load at midspan due to the perforation. When the self-weight is distributed equally over the beam (Q_G), the loading at midspan (and thereby the bending moment and stress) is increased. Both simplifications (element and loading) are conservative in the sense that they result in a higher bending moment given the same input.

$$q_G = \rho \cdot g \cdot h \qquad [\text{kN/m}^2]$$

$$Q_G = \rho \cdot g \cdot h \cdot B \qquad [\text{kN/m}]$$

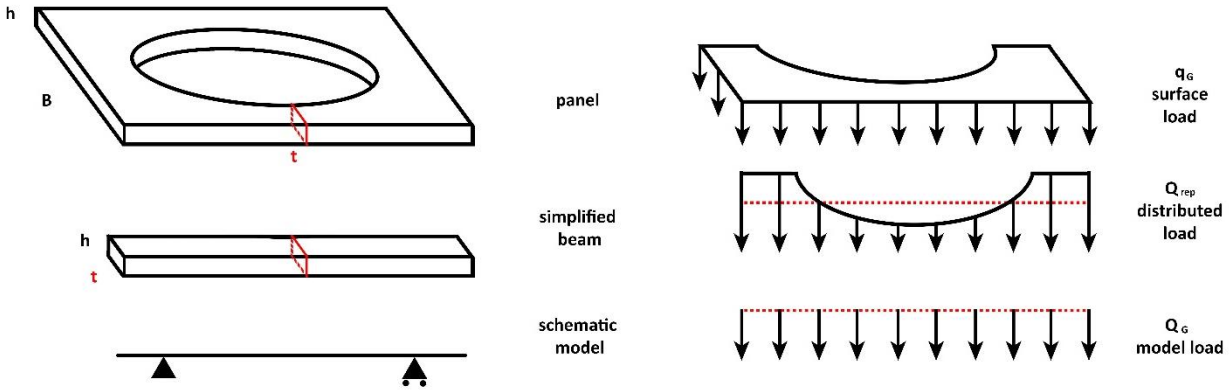

Figure 59 Left: Simplification of the panel model to a beam model. Right: Simplification of surface load to distributed line load.

The orange cross-section in Figure 59 is also used for designing the bending moment resistance to determine the required reinforcement. The resistance is determined by calculating the bending moment at which the reinforcement in the cross-section is subject to yielding due to tension force. This is done by common calculations for reinforced concrete, summarized below and in more detail in the attachments (9.3).

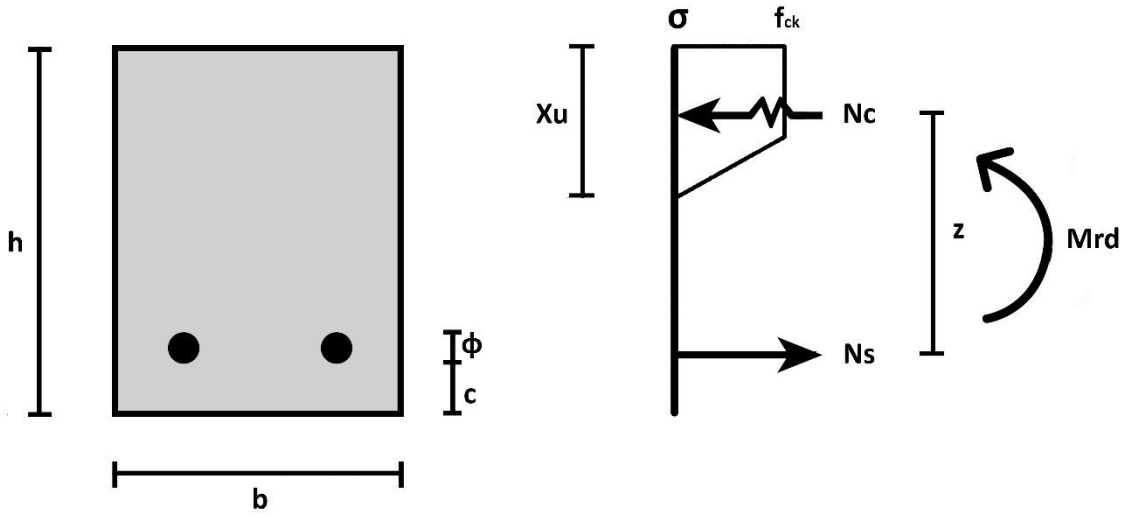

Figure 60: Reinforced concrete cross-section model and stress distribution at critical cross-section

The cross-section is simplified to a rectangle with (casted) height (h) and width (b) determined by the critical cross-section of the panel. Under the assumption that the steel will yield during failure, the tension force in the reinforcement (N_s) is equal to the yield strength of steel (f_{yd}) multiplied by the cross-sectional area of the reinforcement (A_s). During yielding the horizontal forces are in equilibrium, meaning that the compression in concrete (N_c) is equal to the tension in the steel (N_s). The compression in concrete is defined by the concrete compressive strength (f_{ck}) multiplied by the sectional area of the compression zone (with height X_u). This is the zone in which the concrete is not cracked but loaded in compression, which is determined using geometry (shape factors α and β). Now all parameters are filled in, the internal lever arm (z) is determined and finally the bending moment resistance (M_{rd}) is calculated:

$$N_s = N_c \;=\; A_s \cdot f_{yd} = \alpha \cdot X_u \cdot b \cdot f_{ck}$$

$$z = h - c - \frac{\varphi}{2} - \beta \cdot X_u$$

$$M_{rd} = N_c \cdot z$$

For a given design this a method for determining the bending moment resistance. The method is reversed in order to determine the required reinforcement (A_s) with a given bending moment (M_{ed}) that the panel should be able to endure. The input for these calculations are the material properties (f_{ck} and f_{yd}), the concrete cover (c) and the dimensions of the critical cross-section (h and b). During the case study testing, experiments with carbon grid reinforcement are also performed. For calculations of the bending moment resistance the same model is used, but the yielding stress of steel is replaced by the failure stress of the carbon grid.

These calculations are also scripted in to Grasshopper, from which the critical cross-section can be determined parametrically. This reduces the calculation time for the required reinforcement for each element individually as it is integrated in the design. When a parameter is altered, the model automatically gives the required reinforcement as an output.

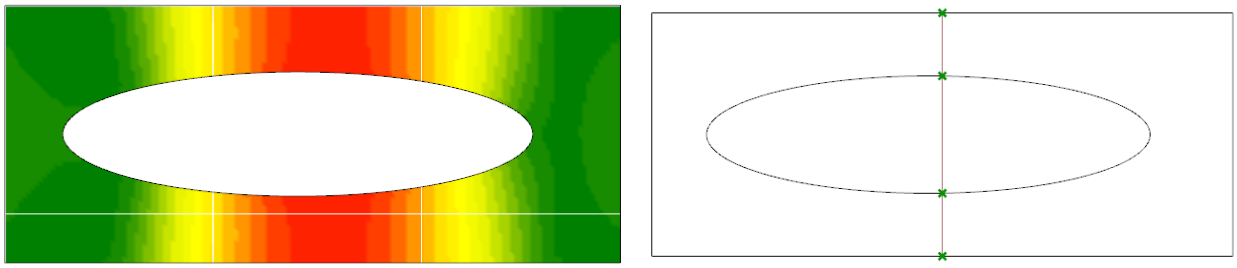

Figure 61: Karamba model determining the position and dimensions of the critical cross-section

4.5.3. Structural performance

Designed test panels

For the case study the face panels designed and modelled with the dimensions as illustrated in Figure 45. The outer dimensions are based on the dimensions of the print table, resulting in a contour of 2.9m by 1.2m as described earlier in paragraph 4.4.1. Using the given dimensions to model the element for structural analysis, the required reinforcement is determined as approximately 75mm² with a concrete cover of 35mm from the bottom fiber. This translates to a design of 4 rebars with a diameter of 5mm in the critical cross-sections at mid span.

The critical cross-section is designed 360mm wide and 100mm in height (see figure). This allows a placement of 4 rebars with a spacing of 100mm, leaving 25mm cover on the sides of the rebar. A steel netting with a grid of 100x100mm and rebar diameter of 5mm, a standardized production in the construction industry, is a perfect fit. The outer rebars in the cross-section are placed almost in the middle of the printed concrete, which is necessary to allow the printed formwork to operate as distancers in the production process. The outer rebars of the entire net are integrate over the entire length, strengthening the edges of the element and possibly increasing the structural interaction between casted and printed concrete.

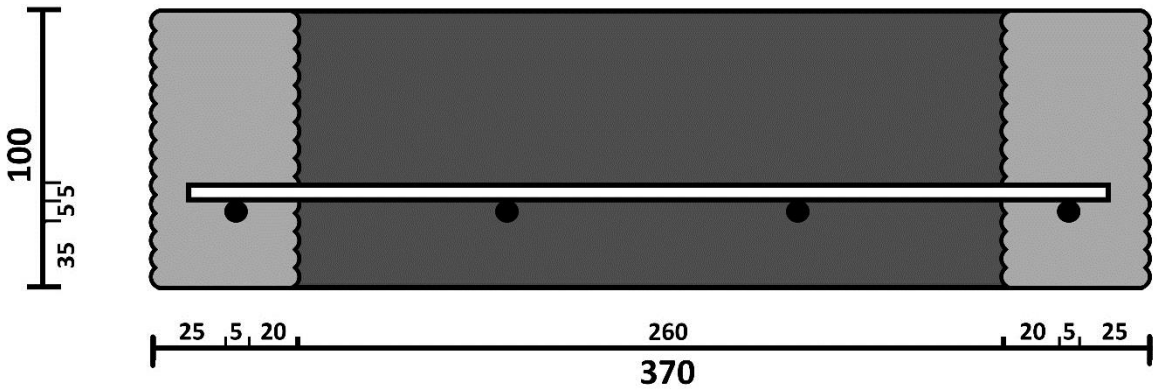

Figure 62: Designed reinforcement placing and cross-section dimensions of critical cross-section

The normative load case on which the reinforcement design is based, is the combination of all three load cases with safety factors as determined by the Eurocode. The wind load is multiplied by 1.5 and the line load for fall protection is multiplied by 1.35. As the self-weight (in the y-direction of the model) has no influence on the out-of-plane bending, but works favorable for in reducing tensile stress, it is multiplied by 0.9. This finally lead to a bending moment of 1.66kNm at one critical cross-section of width 360mm (see Figure 63). The calculated bending moment resistance of critical cross-section for the designed panels (M_{rd}) is 2.10 kNm which, verifying the structural safety of the design (UC=0.79).

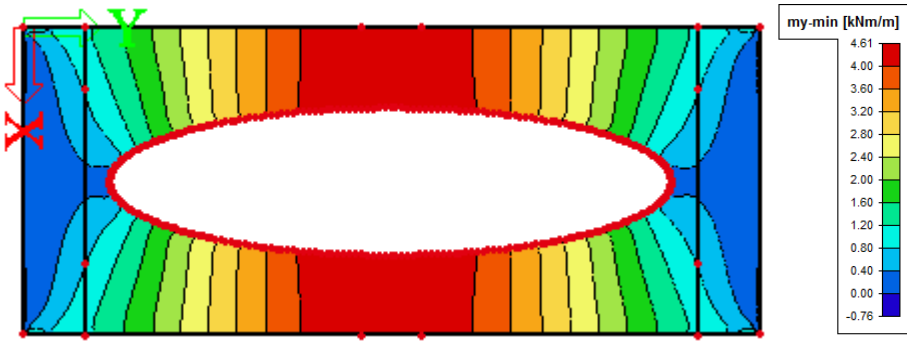

Figure 63: Out-of-plane bending due to normative load case as modelled in SCIA Engineer

Tested panels

In order to determine the load bearing of the test panels under the test case condition, a different model is used. The supports of the test case model are rolling line supports at 250mm from the outer edge, two corners are also restricted in x and y direction as kinematic constrains. The load case for testing is modeled without safety factors because the goal is to predict the failure load, not to guarantee safety. The self-weight of the element is modeled perpendicular to the plane (z direction in SCIA Engineer) since the element is tested horizontally. The test load is modelled as a line load at midspan.

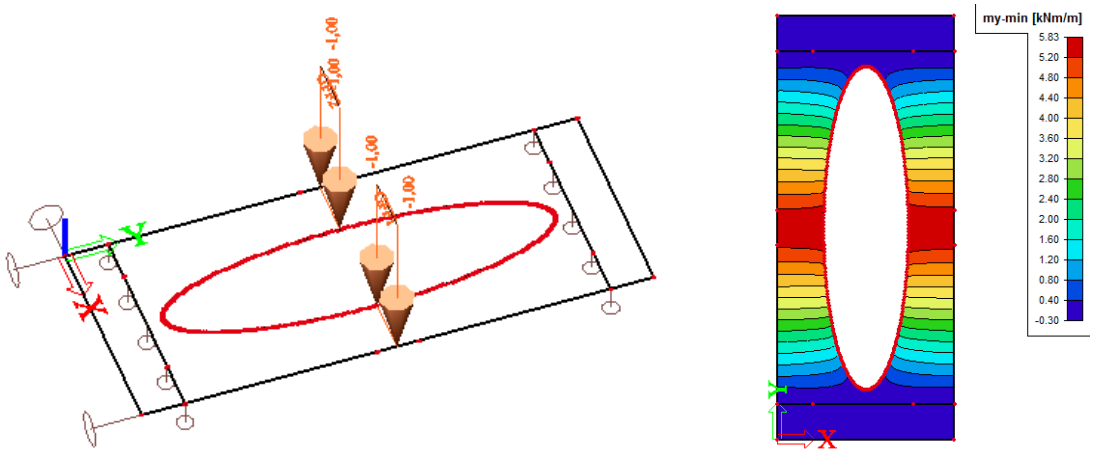

Figure 64 Left: Modelled test case loading for three point bending test. Right: Bending moments resutls (my)

The magnitude of the line load is increased until bending moment is equal to the resistance (M_{ed}=M_{rd}). The prediction is that the reinforcement will start yielding at this point and no further load bearing resistance is provided by the element. This occurs when the line load reaches 6.30 kN/m, which can be induced by distributing a point load of 4.54 kN over the width of the element (0.72m) at mid span.

The produced elements showed quite some deviations from the design due to the fabrication process. Dimensions of the critical cross-section and positioning of reinforcement is changed such that the calculated and modeled values no longer represent the test panel correctly. Therefore, the structural models are updated to better predict the load bearing resistance of the test elements (see attachment 9.4). The (lowest) newly calculated bending moment resistance is 1.46 kNm at the critical cross-section considering steel reinforcement (all panels are discussed in paragraph 5.5.4).

At 70% strength this test panel falls just short of the required load bearing capacity (1.66 kNm, UC=1.13). But more important for the panels is their performance under the test loading. With a load of 3.72 kN distributed over the width of the test elements at midspan, the weakest panel should fail. With this load, the calculated (14 day) tensile strength of 2 N/mm² of the casted concrete (SCC) would be surpassed, ensuring cracked concrete during failure loading. However, from prism test of the same specimen of SCC as used in the panels a far higher strength was measured (4.43 N/mm²), which would remain intact at failure load (reaching 2.7 N/mm²). If the concrete in the panels behave similarly, brittle failure could still occur as the cracking resistance is higher than the reinforced bending resistance (M_{cr}>M_{rd}).

4.6. Fabrication plan

For the production of the designed façade panels a procedure is described which describes any preparations and placement of components in the panel. The fabrication plan is a method for creating the parametrically designed panels and is therefore applicable for panels of different dimensions and shapes. The described process is idealized for automated production of integrated elements, it is inspired greatly by analysis of fabrication processes of the test cases (chapter 5). It differs from the production process of test panels because this automation is not yet achieved nor are the test panels fully integrated.

Theoretical design

Many steps in preparation are taken before the concrete printing occurs, this mainly consists preparing components that are to be installed during the printing process. Firstly, hard insulation (such as EPS) is cut into the desired dimensions, which is the equal to the outer dimensions of the designed concrete panel plus tolerances. This insulation block is then drilled at predetermined points, through which the

element can later be installed on to the building. The diameter of the drilled holes is such that the anchors which are later installed fit perfectly.

Next is the preparation of reinforcement. Netting is cut in the desired shape and dimensions, which are defined in the same model from which the print lines are generated. For steel reinforcement laser cutting is advised to automate this procedure and reduce errors. Any designed perforations in the elements are also cut out of the reinforcement.

Once all components are in the correct dimensions, the insulation blocks are placed level on (pallets on) the print tables. Objects (such as wooden beams or pallets) are placed between the insulation and the print table surface to enable easy lifting in a later phase. Distancers for the reinforcement are placed on the insulation. These are positioned such that they do not intersect the print path, their positions can be displayed by imprints on the insulation. The printer calibrates to the height of the placed insulation using a (infrared) sensor that is attached to the nozzle, before printing. Then concrete printing can commence. The contour and perforation are printed layer by layer, but the start/stop point for the lines are different for every layer.

After the printed concrete has reached the height of the designed concrete cover from the insulated side of the panel, the printer is temporarily paused. The reinforcement net is placed on the adjustable distancers, so that the edges are positioned just above the printed concrete. The distancers are lowered pressing the net slightly in to the fresh concrete without horizontal deformations occurring. Alternatively, the net can be placed by automated machinery, but this seems too cost intensive. After placement the printer continues printing until a second net is to be placed (if designed) or until the formwork is finished.

Once the printing is finished, the elements can be transported to make room for the production of new elements. Either the print tables are moved, or the printer system is operable enough to move to another position. Anchors are placed inside the drilled holes of the insulation and attached to the reinforcement nets. This seals off the holes and allows the insulation and printed concrete to be used as formwork for casting concrete.

The printed concrete is wetted to improve the attachment between the printed and casted concrete and prevent cracking. The segments of the panel that are designed to be closed are filled with a self-leveling concrete to the desired height. The top surface of the panel is treated with a sealant to prevent dehydration during the curing phase, which causes cracking. Alternatively, the mix of the poured concrete is altered so that it becomes tolerant to poor curing conditions (e.g. hot exterior climate). After the concrete has fully developed, the panels are ready for transportation to the construction site and installation on the building.

Production of test panels

The production procedure for fabrication of the panels that are designed for load testing is a modified version of the theory. The difference shows the potential of automating the process as well as attention points that should be considered in fabrication (or even design) with 3DCP. More on the fabrication process is found in paragraph 5.4.3.

The test panels are not printed on insulation, because it serves no purpose in the focus of defining the predictability of the structural behavior of the concrete under loading. This means that the panels are directly printed on (operable) print tables, requiring extra anchors for removal once the concrete is cured and hardened. Bolt plate anchors, like the ones that are designed for installation, are placed attached to the reinforcement of test panel 1 (Figure 65). These were hard to uncover after casting, a detail that requires attention when designing anchors.

Figure 65 Left: Placed bolt plate anchor on reinforcement net. Right: After casting

The preparation and placing of the reinforcement nets is done by hand, without the use of distancers. The nets are over dimensioned to ensure their attachment to the printed concrete. Placing the nets by hand reduced the accuracy of the positioning of the nets, resulting in bars extended out of the element and deformed printed concrete. More issues with reinforcement are discussed in the test in paragraph 5.3, but it is clear that this step is complex and requires attention in future production.

5. Testing and analyzing

5.1. Introduction

In order to analyze the feasibility of fabricating a façade element full scale by 3DCP, tests are defined and executed regarding specific aspects of the process. This practical research is divided in four tests each with a specified focus in the light of the production process and structural behavior of elements produced by 3DCP. The first experiment investigates the material behavior of the printed concrete, more specifically whether it responds monolithically, brittle and testing the flexural bending strength of the printed material. Experiment 2 examines the possibilities of applying reinforcement during the printing process and the effect on the elements structurally after fabrication. In experiment 3, several additions to 3DCP in the fabrication process are analyzed, that are regarded as possibilities for the production of the case study façade elements. Finally, experiment 4 consists of fabricating and testing full-scale façade elements as designed for the case study.

5.2. Experiment 1: Material behavior

An essential part of structural design is determining dimensions of elements to ensure structural safety. Material characteristics describing the mechanical behavior and resistance of printed concrete are fundamental for this part of the design. It is common practice to categorize and label materials on the basis of these characteristics, such as the concrete classes which are related to a specific compressive strength. In internationally agreed documents (such as NEN) tables can be found, relating material properties to that specific class, including tensile strength and Young's modulus. In this manner, a concrete producer can perform standardized tests on his concrete mix to classify it and guarantee certain properties to his buyer.

Such classes are not (yet) determined for 3D printed concrete due to its still short existence. The fabrication process can have a major influence on the mechanical behavior of the material. The material properties of printed concrete are nonetheless essential information for designing for 3DCP. For this thesis it is deemed sufficient to qualify the mechanical properties of printed concrete by performing a series of tests on a small sample batch. Afterwards the properties are related to an existing concrete class for comparison, this class is then used for the case study design.

For the first experiment the focus lies primarily on determining the flexural bending strength of the printed concrete. This specific test is chosen for a number of reasons, the first being that a façade element will be subject to bending by almost any load case. A second reason is that the tensile strength that can be determined from this test, is considered the most critical property of the material. The concrete is more likely to fail under tensile stress than compressive stress due to its relatively high compression strength. A third reason is that the tensile strength is thought to be influenced more by the production process than its compressive strength.

5.2.1. Research

To research the mechanical properties of printed concrete, experiments are setup analyzing the flexural strength of printed concrete samples. Due to the layered fabrication process, the monolithic and homogeneous behavior (as seen in casted concrete) is no longer guaranteed. The bonding strength between two printed layers could differ from the tensile strength in one layer of printed concrete. For this reason, three sets of experiments are set up:

I. Bending around y-axis
II. Bending around z-axis
III. Bending around x-axis

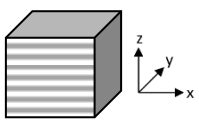

In these experiments the direction of movement of print nozzle for one layer is considered to be the parallel to the x-axis. The research goal is to determine if the flexural bending strength is related to the print direction and qualify printed concrete as monolithic or not.

Another effect of the fabrication method is a significant geometrical phenomenon, the ribbed texture that is created by layered extrusion. With additional experiments the influence of the ribs on the flexural bending resistance is tested. For an engineer it is logical to calculate the section modulus (W) using the reduced section profile without the ribs as a conservative assumption. This addition of the investigation analyzes whether the effect of the ribs is negligible in terms of bending moment resistance.

5.2.2. Method

In the Dutch norm for testing of hardened concrete, specific methods of testing are described. For these experiments the following codes are consulted: NEN-EN 12390-1, -2, and -5 (2009). They consider the dimensions, fabrication and handling, and testing of specimens respectively. The molds used for the fabrication of samples of casted concrete are dimensioned 40x10x10cm (Lxd_1xd_2) see Figure 66. The 3D printed specimens are dimensioned as closely as possible to these dimensions in an attempt to recreate the testing accurately.

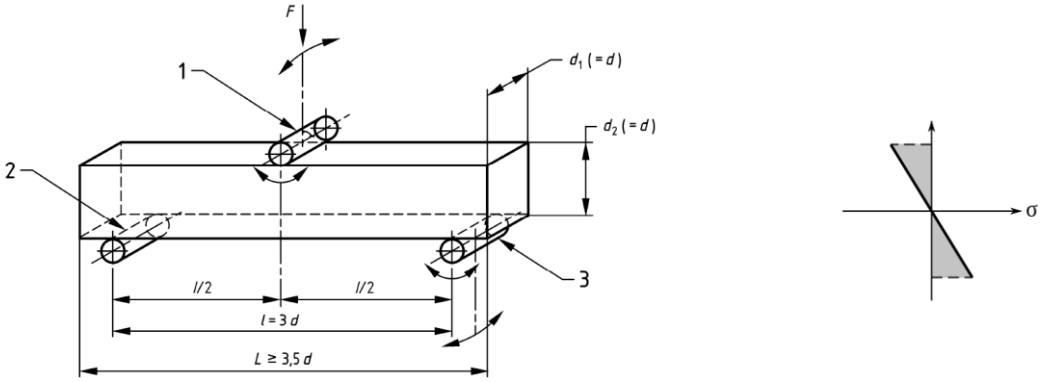

Figure 66: Three point bending test as prescribed by NEN

In this test the specimens are loaded by a point load in the center of the span. The elements are subject to bending and the bending moment will be highest directly under the applied load, at midspan. This bending moment causes a linear stress distribution over the height of the element (d_2). The unreinforced element will crack when the tensile stress in the bottom fiber reaches the tensile strength in the critical cross-section. The crack reduces the section modulus of this section and results in a progressive brittle failure of the element.

With this test the tensile stress can be derived as a result of the loading at failure (F_{ed}) and the dimensions of the cross-section of the specimen (d_1 and d_2). At failure the tensile stress (σ_t) and the tensile strength (f_t) are equal, therefore the strength is determined by calculating the stress at failure. In short the loading force at failure is related to the tensile strength following the formula:

$$f_t = \sigma_t = \frac{M_{ed}}{W} = \frac{\frac{1}{4} * F_{ed} * l}{\frac{1}{6} * d_1 * d_1^2}$$

Where;

- f_t is the tensile strength in N/mm²
- σ_t is the tensile stress at failure in N/mm²
- M_{ed} is the bending moment at failure in Nmm
- W is the section modulus in mm³
- F_{ed} is the loading at failure in N
- l is the span between the supports (l=3*d) in mm
- d_1 is the width of the element (d_1=d) in mm
- d_2 is the height of the element (d_2=d) in mm

For the three tests, different loading directions are required in relation to the print direction. The considered loading direction is indicated in the figures below, showing test I, II and III from left to right.

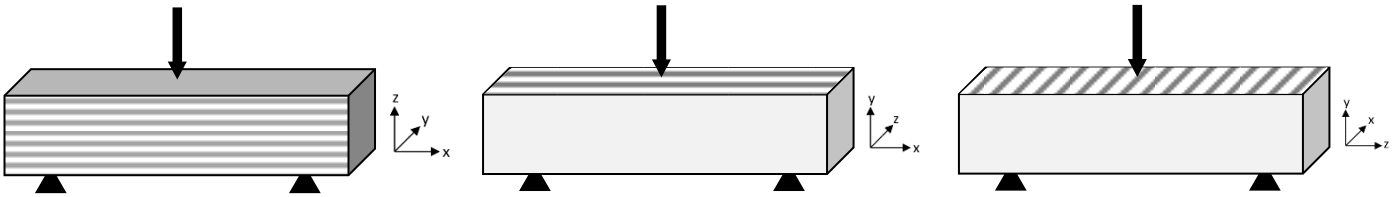

Figure 67: Direction of loading test specimen related to the orientation of the print direction

In test I the bottom printed layer is the first layer to fail under tensile stress if the layers work together to form a monolithic beam. If the bonding strength between layers is too low however, delamination of the layers might occur during loading. This should then be visible in the failure crack as gaps in the cross-section between the layers or possible concrete spalling. The shape of the crack can also be an indication of the layer bond strength: stepwise or continuous. If the bonding strength is low, the crack will form through the critical cross-section of each layer individually, creating a zigzag pattern over the z-axis. If the layers bond well, the shear strength between the layers will ensure a continuous crack pattern to form.

The bottom fibers in test II belong to different layers, but similar assumptions can be made as for test I. Delamination and stepwise crack pattern over the z-axis can occur when the bonding strength is too low to behave monolithic.

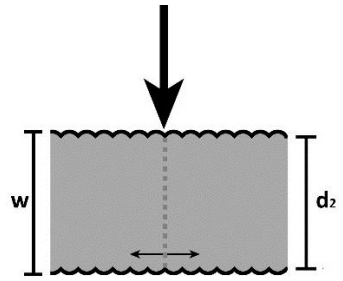

Figure 68: Critical cross-section

In test III the tensile stress in the bottom fiber pulls the layers from one another. This test can show if the bonding strength is significantly lower than the tensile strength of the concrete by separating layers “cleanly”. When this happens the failure crack is located exactly along the section between two layers. However, even if the beam is monolithic, the critical cross-section will most likely be in between two layers as it has the least structural height (d_2) in between two ribs. (Figure 68)

For the final test (IV), specimens without a ribbed texture need to be fabricated by printing. This can only be done after printing, because using formwork or trowels of any kind during printing could affect the compacting of the concrete during printing. Therefore, the specimens are fabricated similar to the others and the ribs are removed afterward. The specimens are loaded in the same manner as the specimens for test I.

5.2.3. Production

In order to print beams with the given dimensions of 40x10x10cm, the width of the print path needs to be adjusted to 10cm. However, the print path width of the selected printer is limited to approximately 9cm and an increase of width causes a decrease in resolution. A lower resolution results in less consistency in the cross-sections of the specimens, effectively reducing the accuracy of the experiment.

The increase in self-weight loading on the bottom layers causes slump of the cross-section of the fresh concrete. This results in a deformation of the cross-section from rectangular to trapezium shaped, with a small reduction in height (d_2) of the element and increase in in width (d_1) of the bottom layers. To compensate, the elements are modeled to 11cm in height. The model that is fed to the printer is that of 4 long beams (see Figure 69) of 11cm in height, requiring 15 printed layers (of ±7mm) each, and a print path width of 8cm is chosen.

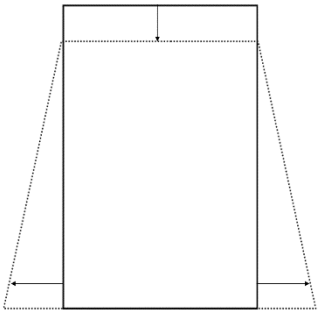

Figure 69: Fabrication and cutting of the test specimens

Just after the printer finished printing, the fresh concrete beams are cut easily in to segments of 40cm. At this stage the concrete is soft enough to cut with a butter knife, which is why the segments for the "un-ribbed" test IV are also prepared. For these specimens the ribs are removed using a handsaw, as seen in Figure 70.

Figure 70: Removing ribs from printed concrete specimens (IV)

For test III, a different model was needed because the length of the specimen (L) is now oriented in the z-direction of the print. The samples are fabricated by printing a wall of 50cm in height with a similar print width (±9cm) as the previous samples. Once hardened the specimens are sawn out of the concrete

wall in segments of 20cm wide. This results in beams with 40x20x8cm dimensions (Lxd_1xd_2). The increase of d_2 is chosen to reduce the effect of sawing on the printed concrete after hardening.

5.2.4. Sample testing

The (28 days) hardened specimens are placed on the loading bench, and slowly loaded until failure is reached. The apparatus indicates the largest measured resistance during loading, this is equal to the failure load that caused the element to fail under bending (F_{ed}). If the specimens are loaded too fast, the resistance is not measured properly and a lower indication for the failure load is given.

Figure 71: Set up for three point bending test on which the test specimens are loaded

Test I

The loading test in z direction (bending around y-axis) has the largest sample batch, because its specimens are closest to that of a casted specimen. It is therefore considered best comparable to the standardized test for hardened concrete, that are fabricated as casted prisms. The results of the visual inspection of test I are summarized as:

All specimens failed under bending at midspan as was expected. The failure behavior was a brittle tensile crack that split the element from bottom to top at once. All crack lines were continuous over the height (d_2) of the element, but often inclined to one side over the length of the element (as seen in Figure 72). No horizontal cracks between printed layers were found. All printed layers remained attached, no delamination occurred, and cross-section are (visually) monolithic.

Figure 72: Test specimen element showing diagonal crack after loading test

Test II

The loading test in y direction (bending around z-axis) had similar visual results as test I. Some notable differences are summarized:

The trapezium shaped cross-section prevented the specimens from being placed on their side straight (see Figure 73). Even though the supports were hinged, during loading some local crushing occurred before reaching failure load. This is also partly due to the ribbed texture; the loading caused the supports to flatten the ribs locally by crushing. The failure cracks of specimens of test II were all continuous over the height and, unlike test I, straight (parallel to the z-axis).

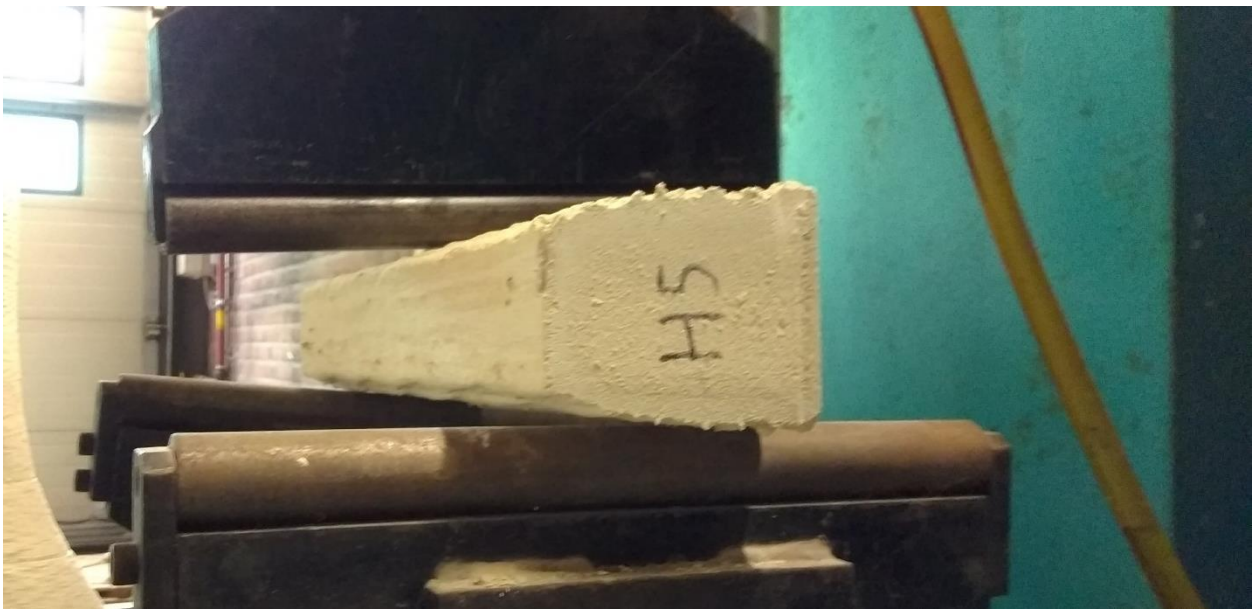

Figure 73: Test specimen under loading apparatus, tilting supports not making full contact

Test III

The samples for test III were bigger requiring more care with the handling and transport of the elements. Testing conditions were similar to previous tests, notable occurrence in visual results was the crack pattern: the failure cracks in the specimen went through multiple printed layers, between three to five layers (see Figure 74).

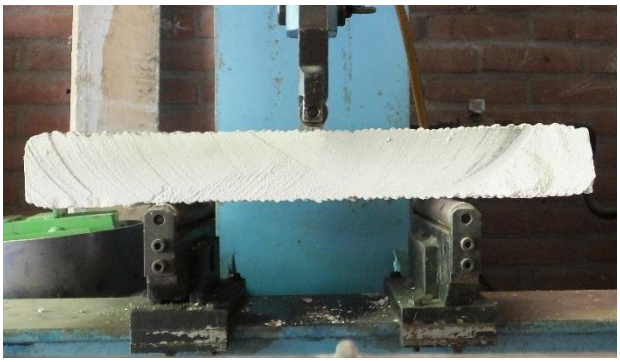
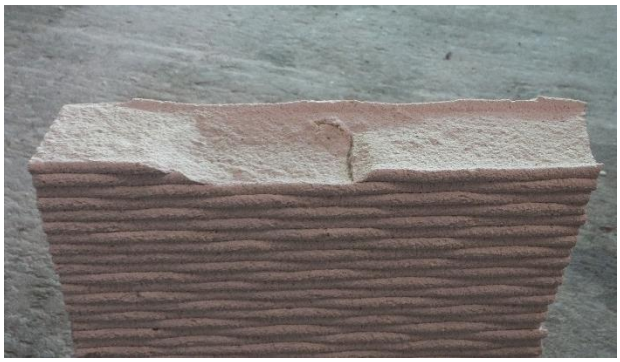

Figure 74: Test specimen from batch III during and after loading, showing crack through multiple layers

Test IV

The final test of this series, test IV, was performed on the specimen of which the ribs were removed after printing. The loading conditions were identical to those of test I and no notable visual difference in failure behavior were noted.

5.2.5. Analysis and conclusions

The results from the sample testing are used to calculate the tensile strength of the elements and are compared between sample batches (test groups). Due to the deformation of the cross-sections of the specimens, the presumed calculation of the section modulus (W) no longer holds true. For the calculations the cross-sections are modeled as trapeziums (see figure). The data and calculations from the sample testing can be found in attachment 9.1, a summary is presented in Table 3.

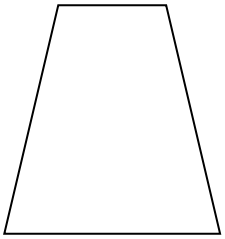

	Casted prisms	Test I	Test II	Test III	Test IV
Flexural stress	8.06 N/mm²	5.34 N/mm²	5.28 N/mm²	5.21 N/mm²	5.08 N/mm²
Batch size	10	8	8	5	3
Standard dev.	0.56 N/mm²	0.32 N/mm²	0.40 N/mm²	0.31 N/mm²	0.28 N/mm²
Percentage	100%	66%	66%	65%	63%

Table 3: Summarized results loading tests

The observed (average) tensile strength of the printed elements is significantly lower than that of the casted prisms, indicating that the printing process has a negative effect on the flexural bending strength of the concrete. Because the printing reducing the tensile strength to about 65%, it is concluded that casted prism tests are not indicative for printed concrete material properties, without additional safety factors. It is advisable to use additional material safety factors on material properties for the concrete classes (as defined by NEN) or defining the necessary material behavior by sample testing printed concrete.

The spread in results from the bending test is large leading to a statistical error of up to 20% for one sample. Larger batch sizes should be used than were used in this test for a better representation of the material properties (n>30). The spread in results is caused by the material on the one hand and the testing method on the other. Due to the high level of cement in the mortar mix and the open-air curing of the concrete, shrinkage occurs (autogenous and by dehydration). This results in the development of stress in the elements (mostly in the exterior layers) which influences the test results negatively. Another reason for the spread is the combination of a three-point bending test and the deviations in dimensions of cross-sections (due to ribs e.g.). The loading test generates the highest bending moment at midspan (see Figure 75), while the weakest cross-section might be slightly off center due to these tolerances in element dimensions. This results in an inaccuracy in the calculated bending moment (M_{ed}) and section modulus (W).

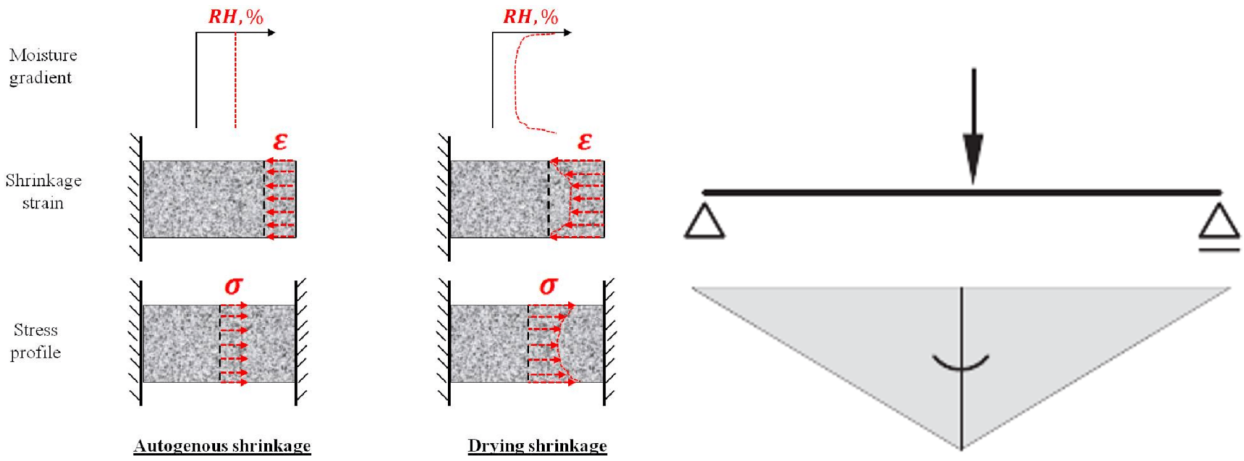

Figure 75 Left: Influence of moisture gradient in concrete on stresses and strains. Right: Bending moment line under three-point loading

Looking only at the results of the printed specimen, the differences in means of each batch are far lower and even within one standard deviation of one another. With a statistical t-test the results are compared: no significant indication is given that the print direction influences the flexural bending strength of the printed elements. The conclusion that the printed material behaves monolithic and homogenous is made presumable but cannot be confirmed with 95% certainty due to the small sample batch sizes. For the case study however, this assumption is taken as factual. An independent research at Bruil later confirmed this conclusion for printed concrete from specific mortar mixes.

Although the un-ribbed specimens (IV) showed less bending resistance than the un-cut specimens (I), the difference in average flexural bending strength is low (5%). Given that cutting the elements in the fresh concrete phase could also influence the results of the bending resistance of the elements, the difference is considered negligible. For calculating and engineering 3DCP elements it is advised to use the conservative minimal width of the cross-section, between the ribs, for determining the section modulus.

Finally, conclusions from the fabrication process are drawn. Tolerances in geometry of the printed elements (deviations in element dimensions) are greatest in print path width. These deviations are relatively high (up to 25% in this experiment) for small elements and therefore have a significant impact on the structural capacity of the element. Increasing the resolution reduces these tolerances, which can be done by reducing the designed print path width and changing several other printer settings.

It should be noted that the performed tests were all conducted on specimen fabricated with a specific mortar mix and printer settings, for which the results are representative. The absolute values of the results are therefore an indication of what is achievable rather than a constant value for printed concrete. Experiment 1 does verify that printing monolithic concrete elements is feasible and that it is possible to obtain representative material properties by sample testing.

5.3. Experiment 2: Reinforcement

Concrete is a very brittle material with a relatively low tensile strength, which is why concrete is commonly strengthened with reinforcement. For traditional casted concrete structures this is done by placing steel reinforcement bars or nets inside the cast before pouring the concrete. With 3DCP no formwork is used, and the geometrical freedom makes it difficult to integrate reinforcement in the process. Researchers at TU Eindhoven (Salet, Bos, Wolfs, & Ahmed, 2017) are investigating the possibility of wiring the concrete while printing and at ETH Zurich (Hack, Lauer, Gramazio, & Kohler, 2015) they examine the production of printing the reinforcement rather than the concrete. For this case study, with flat façade elements, linear reinforcement is possible. The feasibility of integrating reinforcement in 3DCP and its structural effect is analyzed to examine the possibility of adapting the selected techniques in the production of the case study element.

5.3.1. Research

To research the possibility of improving the ductility and tensile strength of printed concrete, some experiments are set up. Different types of reinforcement are implemented, tested and analyzed with the intent to document their respective impact on four points:

1) Fabrication process
2) Integration of reinforcement
3) Structural behavior under loading (ductility)
4) Strengthening

The focus of the first stage is on the implementation of the selected reinforcement in the concrete during the printing process. The ease with which the reinforcement is integrated in the process, can be an indication of the possibility of automating this step and working towards printing reinforced concrete elements. Difficulties that arise with implementing the reinforcement in the process can also appear when integrating other components in the process.

In the second stage, the integration of the applied reinforcement in the printed concrete is analyzed. By visual inspection, any deformations and notable deviations compared to unreinforced printed concrete are examined. Deviations can occur instantly after placing the reinforcement (i.e. deforming the fresh concrete) or during the hardening phase (i.e. crack formation). A second method of testing the integration is by testing the bonding of the reinforcement to the printed concrete. The bonding is examined by loading the elements until the reinforcement is either “pulled out” or fails under tensile stress.

The third stage is the ‘in use’ phase, when the element is finished and has to fulfill its structural purpose. The focus of the research in this phase is on the improvement of the structural qualities of the reinforced printed concrete. Testing whether the flexural resistance of the concrete element is improved, and if so, to what extent. If the reinforcement is integrated in the concrete correctly, the application could also affect the failure behavior of the element. Aspects that are researched for this point are brittleness (or ductility) and integrity of the element after cracking.

Reinforcement types

For this series of experiments the following types of reinforcements were selected:

Test	Reinforcement	Type	Material	Properties
V.	None	-	-	-
VI.	Plaster gauze	Net	Glass fiber	(see attachment 9.2 Knauf)
VII.	Wire-net	Net	Iron	(see 9.2 Handson) 0.65mm ϕ
VIII.	Rebar	Bar	Steel	Traditional 8mm ϕ rebar

IX.	Geogrid	Net	Polypropene	(see 9.2 Tensar) 5mm thickness
X.	Carbon grid	Net	Carbon fiber	(see 9.2 C-grid) 1.85mm² section
XI.	Plastic fibers	Fiber	PVA	(see 9.2 Fibers) 26micron ϕ

Table 4: Reinforcement types

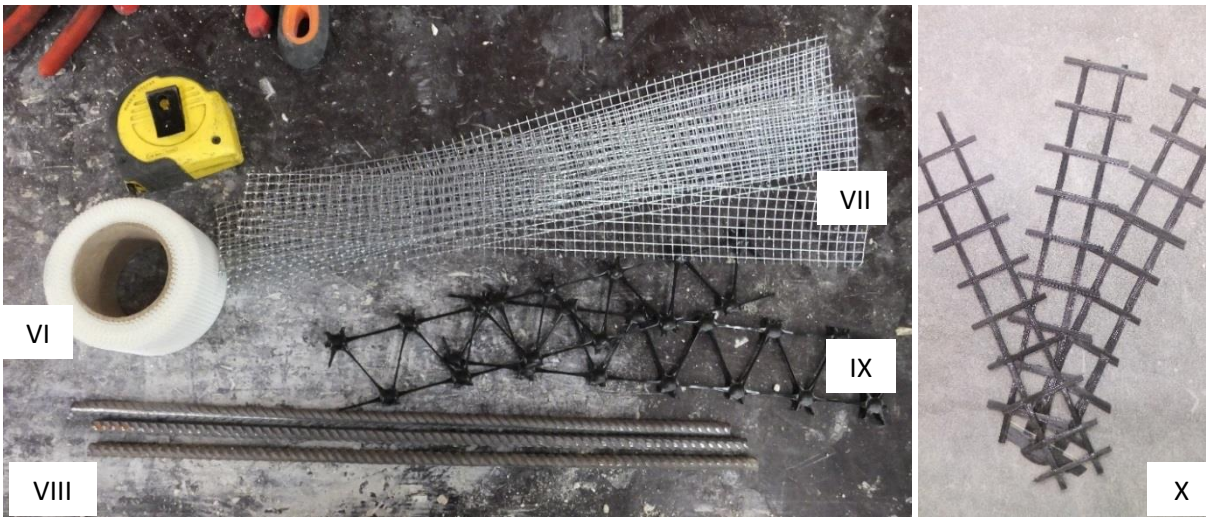

Figure 76: Reinforcement types VI, VII, VIII, IX and X

5.3.2. Method

The four stages are analyzed individually on the same specimen for the six sample batches. The first stage, fabrication, is analyzed by performing actual production of the sample specimen. The printing, placing of reinforcement, cutting and handling of elements are experienced in the production of the specimen and documented for analysis.

Through visual inspection the integration of the reinforcement is analyzed at first. Any deformation or sticking out reinforcement is documented, as are shrinkage cracks, rust formation and any other possible exterior notable changes to the specimen.

Finally, the samples will be loaded similarly as in test I of the first experiment (paragraph 5.2.2), using a center point loading bench. This will tell if and how the reinforcement type has any effect on the flexural bending resistance. Furthermore, the failure mechanism under this load is shown and reflects if the reinforcement has improved the ductility of the specimen compared to the unreinforced element. Filming the failure with a framerate allows further inspection of the crack formation.

The specimens are loaded after hardening 7 days, to investigate the strength development. Printed elements will often need to be transported from the fabrication site to a different location (to make room for new prints for example). The transporting these elements is done before the 28-day mark and the possibility of loading these elements in this time period is herewith examined.

5.3.3. Production

The sample elements for this test series are fabricated in a similar fashion as used in test series 1, by printing longer segments and cutting them in the correct length. A small reduction is made to the print width, to increase the resolution and thereby the test accuracy. Element dimensions are designed at 40x11x6cm (Lxd_2xd_1). A different mix was used to produce the printed concrete elements compared to that of Experiment 1.

Test V and XI

Fabrication of the specimens for the control test (V) is done as described in test series 1, tests I and II. The fiber reinforced specimens (XI) are printed and cut similarly but the preparation of the mortar mix

differs from the other tests. The selected fibers are added to the mixture before the concrete enters the printers pumping system. Not all fiber types are suitable for printing concrete, some can cause obstructions in the printer or are not able to flow through the nozzle. The printability of the fibers depends mainly on the material and dimensions of the fibers but is always depended on the printer system as well.

The selected fibers integrate easily into the concrete mix and form no problem in the printing process as they follow the printed structure perfectly. By visual inspection the fiber reinforced printed concrete shows no differences to the unreinforced prints. Only on thorough and zoomed in investigation can the fibers be detected without cutting the concrete. The fibers are randomly oriented, but always contained per printed layer, this could cause non-homogeneous behavior for fiber induced printed concrete. Cutting through fiber reinforced fresh concrete is no different compared to unreinforced fresh concrete and can be performed with a blunt knife.

Figure 77: Fiber induced concrete mix

Test VI – X

The specimens that are reinforced with more continuous elements, such as netting and rebars, require a small adjustment in the fabrication process. For the reinforcement to be integrated into the concrete, it needs to be placed during the printing process, in between layers. Especially for metal-type reinforcements that need to be protected from corrosion, the integration by concrete is important.

The chosen method for the fabrication of the specimen for test VI, VII, VIII, IX and X is summarized as: Line segments are printed in a continuous manner until the segments reach a height of four layers. Once the fourth layer is finished, the printer is paused in order to place the selected reinforcement in the desired dimensions on the related sample. After all reinforcement is placed, the final layers are printed on top of the previous layers, covering the reinforcement. Then the specimens are cut in segments of 400mm each (Figure 78).

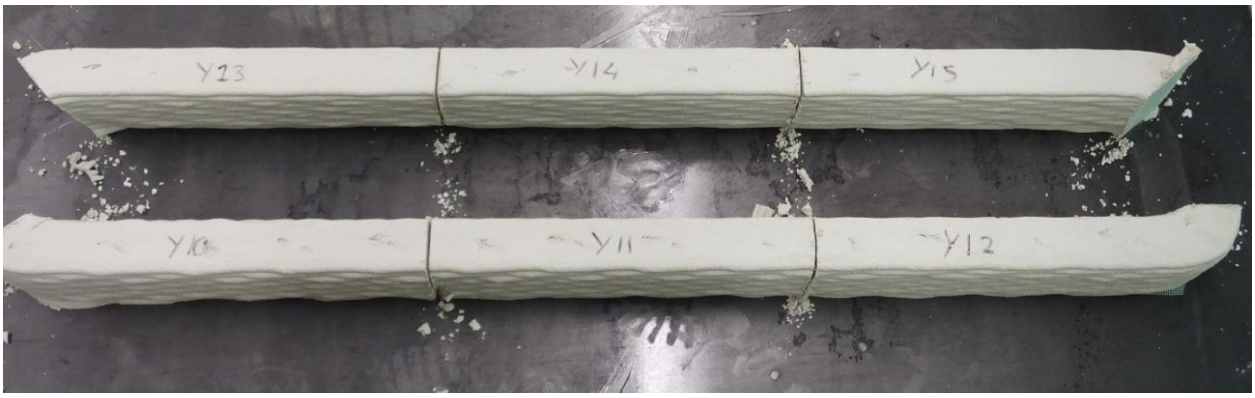

Figure 78: Test specimens for reinforced printed concrete test

For the chosen fabrication method, the selected reinforcement elements need to be prepared before printing, which demands cutting and shaping them in the desired dimensions. For the iron nets (VII) this includes straightening the nets by bending, since they were curved due to rolled up transport. If elements are not in the correct shape, they can form blockades in the print path and deform the specimens during printing. When the printing nozzle hooks on to a net, it can drag the reinforcement through the print, deforming the entire model. This occurs for both the plaster gauze and iron nets (VI and VII).

Another attention point is that when the printer is paused to enable the placing of the reinforcement, the concrete can harden inside the printing system. Since this is undesired for the remaining print and even damaging for the printer itself, this time frame should be minimized to a maximum of one or two minutes. In future processes, the preparation and placement of the reinforcement is ideally performed by machinery as well. This allows reinforcement to be shaped freely as the concrete and reduces tolerances and errors in the cutting and placing processes. If programmed well, the placing and printing can happen simultaneously.

5.3.4. Sample testing

Test V: Unreinforced

After seven days of hardening the elements are loaded under the three-point loading test. The unreinforced elements react similarly to those of experiment I: a bending crack at mid span caused the element to fail in a brittle manner. Due to the different mortar mix, the obtained flexural bending stresses differ greatly to those of experiment 1. The average flexural strength of test V is 8.39N/mm² compared to 5.24N/mm² of test I. To review strength development of the printed elements, a selection sample batch V was tested after hardening 28 days, for which the results were more in range: 8.66 N/mm². See Table 7 and attachment 9.1 for full results.

Test VI: Plaster gauze

Plaster gauze reinforced elements show no improvement in ductility and a slight reduction of bending moment resistance. The reinforcement has a lower tensile strength than the printed concrete, causing a brittle tensile failure in the reinforcement instantly after the concrete cracks. The failure behavior under loading is no different to that of unreinforced elements.

Test VII: Iron wire-net

The elements that are reinforced with iron nets showed a lower bending moment resistance on average than the unreinforced elements from test V. Four out of nine elements remained connected by one or more rods of the iron net through the developed concrete crack, but this provided no further bending resistance. The reinforcement showed no yielding, but failed brittle under tension, which is a common failure behavior for iron as it not a ductile material.

Test VIII: Steel rebar

Placing the rebar is done quickly and by pressing the reinforcement into the fresh concrete the bar is secured. The printer nozzle moves directly over the rebar and deposits more concrete, covering the reinforcement. After fabrication and hardening, no distinct differences are detected visually compared to the unreinforced elements from test V.

The reinforced elements can be loaded beyond concrete cracking, due to the rebar holding the element together (Figure 79 bottom). A concrete compression zone (uncracked) is visible at the top, while the cracks in the bottom fibers keep developing under continued loading. Eventually horizontal cracks develop at the height of the rebar which causes delamination of the concrete cover. The horizontal cracks form at the critical cross-section which is commonly between the ribs that are formed by printing (Figure 79 bottom and right). Diagonal shear cracks near the supports are also visible, a common crack pattern for reinforced concrete beams.

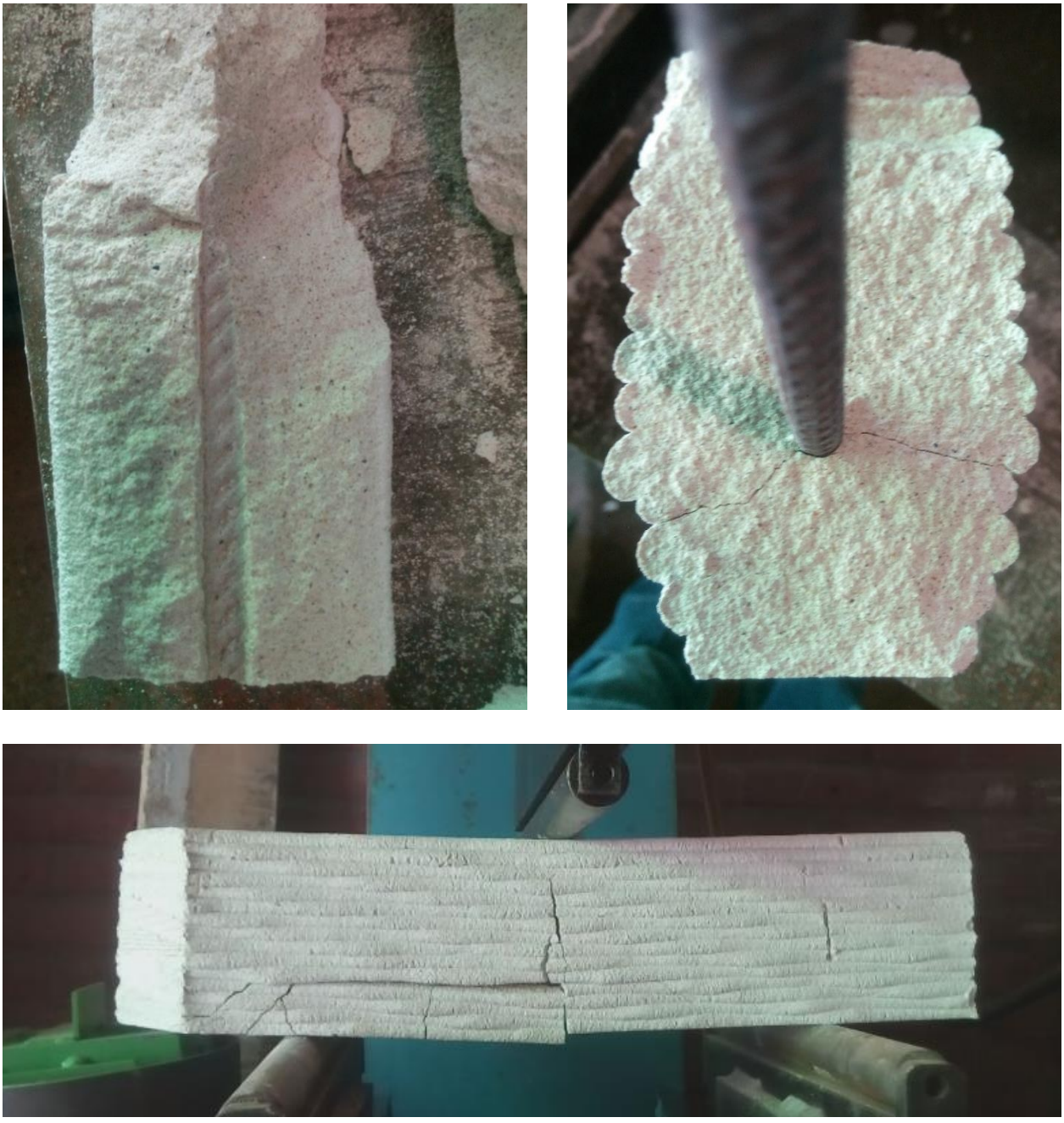

Figure 79: Specimen of test VIII during loading showing horizontal crack formation and pulled out reinforcement

Although delamination is easily accredited to lower bonding strength between printed layers, this is not the primary reason for cracking. Concrete cover spalling is common for casted beams under flexural loading as well. The reinforcement is loaded in tension and transfers this loading in shear forces to the concrete (Figure 80). The cracked concrete is delaminated on the shortest horizontal cross-section, providing the least resistance. This is not necessarily between two printed layers as seen in (Figure 79 right). Due to large deformations, linear calculations no longer hold true and eventually the element completely disintegrates.

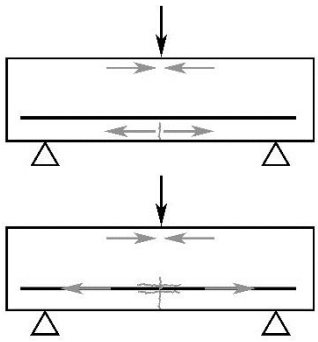

Figure 80: Cracking in concrete

After the concrete is spalled off, the rebar loses bonding strength and is eventually pulled out of the element on one side. The steel is therefore not loaded until breaking in these tests. From the spalled concrete it is clearly visible that the rebars are covered well by the concrete, leaving an imprint of the texture of the rebar in the concrete. The elements did outperform expectations from the calculations as average load bearing resistance of 21.6 kN was calculated (bending moment of 1.62 kNm), the elements were load up to at 31 kN on average (2.3 kNm) (attachment 9.1).

Test IX: Geogrid

The geogrid is difficult to obtain, which is why only two test specimens could be fabricated. The nets are prepared in the correct dimensions and slightly pushed into the fresh concrete to secure its position. After fabrication the layer on the nets are placed are deformed slightly, the rib texture is extended outwards more compared to the other ribs.

The geogrid reinforced elements performed similarly to the elements reinforced with iron nets (test VII): remaining intact after concrete cracking but providing no additional bending moment resistance. When the loading was continued after cracking phase, the plastic started to deform plastically, elongating significantly before breaking under tension. The reinforcement is not pulled out the element under loading but maintains integrated in the printed concrete.

Figure 81: Geogrid reinforced specimen shortly after failure with reinforcement still intact

Test X: Carbon grid

The carbon grid nets are light and easily placed in the concrete. The prepared samples remain sticking out of the printed elements after fabrication, but no deformations or cracks are found in the concrete.

During loading the reinforcement keeps the element together after concrete cracking and provided additional bending moment resistance. In two out of three tests the reinforcement was pulled out before it could reach tensile failure. The low concrete cover (sideways) decreased the bonding strength with the reinforcement, which is a reason for the pull-out failure type. During continued loading after initial concrete cracks, similar delamination occurred as in the steel rebar test (VIII).

Figure 82: Carbon fiber grid reinforced specimen after failure showing pulled out and failed reinforcement strands

After failure a horizontal cross-section of the specimen is visible, in which the imprint of the carbon grid is visible. Also, clearly visible is the lack of concrete cover on the sides of the reinforcement. The maximum measured load of the samples (average of 10 kN, or 0.75 kNm) is higher than the calculated load bearing resistance (average 5.95 kN, or 0.45 kNm).

Test XI: Plastic fibers

The fabrication of the elements that are printed with a fiber mixture does not differ to that of unreinforced concrete printing, also after fabrication the elements do not differ visually. Placing and using the fibers in the printing process is the most effortless and promising. It should be noted however that local strengthening is not possible with this method as the fibers are integrated throughout the entire elements.

The mortar mix with fibers differs from the mix of tests V to X and absolute values from loading tests are therefore not comparable. An additional batch was printed and tested by Bruil for the same mortar mix without the fibers for a comparison. The selected fibers provide no additional ductility in the bending test as all specimen failed in a brittle manner. The average tensile stress at failure is 5.62 N/mm² with fibers (standard deviation 0.97 N/mm²) compared to 5.15 N/mm² without fibers. For future research a wider variety of fibers could be tested, more on this in recommendations in chapter 6.

5.3.5. Analysis and conclusions

The test results are graded on the basis of the four focus points as described in paragraph 5.3.1. The grading is summarized in Table 5, and a summary of the reasoning is given in text below. The performance of the elements is graded positive (+), negative (-) or neutral (o).

	VI	VII	VIII	IX	X	XI
	Plaster gauze	Iron net	Steel rebar	Geogrid	Carbon grid	Fibers
Placing	-	-	+	+	+	++
Integration	+	+	-	o	-	++
Ductile	--	-	++	+	++	--
Strengthening	-	--	++	o	++	o
Total	---	---	++++	++	++++	++

Table 5: Performance of reinforcement types on the specified criteria

The placing of reinforcement in 3DCP process requires preparation of the reinforcement but is a feasible addition in the production process of printed concrete. Fibers integrated in the mortar mix (text XI) have a clear advantage over the other tests due to its ability to be applied easily in complex shapes. Any reinforcement that is placed during printing has the potential to be deformed by or deform the printed concrete in the printing process (test VI and VII).

Regarding the integration of the reinforcement in the printed concrete, again the fibers mixed in the concrete (XI) score highest. Only the two grids (IX and X) show visual deviations after fabrication on the exterior of the printed elements. The rebar and the carbon grid are pulled out in the loading process, indicating a low bonding strength (ideally, they break after yielding in tension). The bonding strength however is influenced greatly by the element dimensions (concrete cover) and can be improved by design of the element.

The behavior after concrete cracking determines the scoring of the reinforcement on the aspect of ductility. The rebar, geogrid and carbon grid (tests VIII, IX and X) were able to keep the element together after cracking for all samples. As for strengthening, only the steel rebar and carbon grid (VIII and X) added bending moment resistance to the element, both test performed as calculated. Placing plaster gauze and iron nets (VI and VII) actually reduced the tensile strength of the concrete element on average (Table 6).

	V	VI	VII	VIII	IX	X
	Blanco	Plaster	Iron net	Rebar	Geogrid	C-Grid
Flexural stress (at crack)	8.39 N/mm²	7.92 N/mm²	7.07 N/mm²	7.26 N/mm²	8.89 N/mm²	7.17 N/mm²
Batch size	10	14	9	3	2	3
Standard dev.	1.18 N/mm²	0.7 N/mm²	1.14 N/mm²	0.43 N/mm²	0.55 N/mm²	0.21 N/mm²
After con-crete crack	Failure	Failure	Failure/ intact	Bending resistance	Intact	Bending resistance

Table 6: Flexural stress in concrete and failure behavior during loading tests

To analyze the strength development of the printed concrete, test V was tested after seven days (8.39 N/mm²) and after 28 days (8.66 N/mm²). The average tensile strength did increase (3%) after allowing the elements to harden longer, but the difference is small. A bigger difference is found in the deviation of the results of both samples. After seven days, the range in results is almost 3 N/mm², while after 28 days this range has decreased to 0.7 N/mm². A similar result is found when looking at the standard deviations, from 1.18 N/mm² to 0.23 N/mm² (see Table 7).

	Casted prism	Casted prism	Test V	Test V
	7 days	28 days	7 days	28 days
Flexural strength	5.65 N/mm²	9.71 N/mm²	8.39 N/mm²	8.66 N/mm²
Batch size	2	7	10	5
Standard dev.	0.21 N/mm²	0.18 N/mm²	1.18 N/mm²	0.23 N/mm²
Percentage	63%	100%	81%	89%

Table 7: Flexural strength of casted prisms versus printed specimen after 7 and 28 days of curing

5.4. Experiment 3: Integrating materials

5.4.1. Research

One of the bigger challenges in adapting 3DCP in the building construction is the integration of other elements and materials in the automated production process. Embedding elements in the printed concrete sets requirements to the printed shape, the printing process and the element that is to be integrated. The goal of this test series is to investigate the possibility and challenges of integrating different materials. The focus of the research is on the production process and effects on the shape of the fabricated element. Due to the great variety of implemented materials and elements the structural effects fall outside the scope of this experiment.

5.4.2. Method

With the case study element in mind, four tests are performed which can produce useful information for fabricating a full-scale façade element. Firstly, the possibility to use printed concrete as a mold for casting concrete is examined, where the interaction between the materials is investigated. A second test is performed integrating reinforcement netting in printed concrete that is used as distancers. Different from experiment two, the reinforcement is now implemented in panel shapes as netting, rather than the beam shaped samples from previous tests. The third test investigates the integration of anchors in the printed concrete as well as in a casted panel. Lastly, printing on EPS panel is tested to analyze the ability to produce prefab façade elements with insulation, as suggested in the case study design. In summary:

XII. Printed and casted concrete
XIII. Reinforcement netting (in panels)
XIV. Lifting anchors
XV. Printing on insulation

5.4.3. Production

Test XII. Printed and casted concrete

By printing a circular print path up to 5cm in height, a mold for a circular panel is created. This is used as formwork in which leveling mortar is casted, the circle contains the liquid concrete and does not leak. As the printed concrete hardens very fast, it is usable as formwork quickly after printing without collapsing. The mortar is poured into the print after only one hour of hardening. After one day the panel (80cm diameter) is transportable. An important note is that the print tables on which the elements are fabricated are always sprayed with removal oil, to prevent the mortar from sticking to the table.

To check the interaction between the casted mortar and the printed formwork, the element is broken exposing the cross-section. (Figure 83) The ribs of the printed concrete are visible in the section, indicating that the casting did not deform the printed formwork. No air bubbles or detachments between the two materials is detected. The cracks from breaking go through both casted and printed material without detachment between the two occurring. Without quantifying, the bonding strength between the two mortars is enough to transfer stresses.

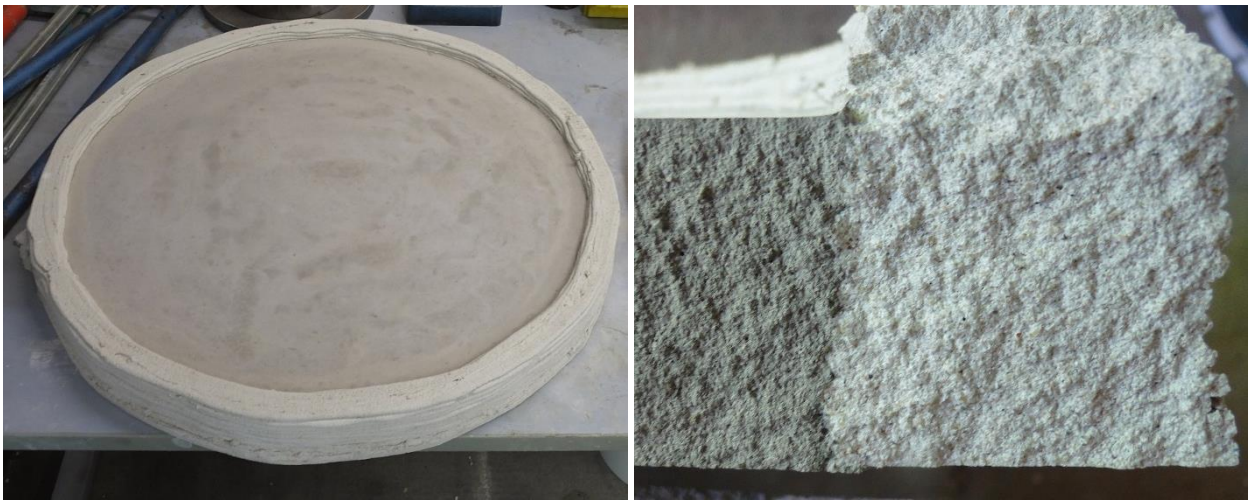

Figure 83 Left: Printed formwork in which concrete is casted, Right: cross-section of same element

Test XIII. Reinforcement netting

For the integration of reinforcement in printed concrete, experiment 2 (paragraph 5.3) already showed some of the difficulties in the production process and the structural benefit of steel and carbon fiber reinforcement. Using reinforcement netting for panels to be casted brings about additional challenges and consequences. For this test rectangular panels are printed placing a steel reinforcement net mid printing process in the printed formwork. The netting that was used is made of steel rebars (5mm diameter) with a mesh size of 10x10cm. Additional print path shaped as random patterns within the panel function both decoration as well as distancers for the reinforcement. The panels can then be casted even with colored mortars for esthetical reasons.

Figure 84: Façade panel with printed concrete formwork and casted concrete as infill

The panels are dimensioned 1m x 3m functioning also as a preliminary test run for the case study print in test XV. The panel requires reinforcement nets dimensioned to the panel size, which makes the nets large and difficult to place. This effect is similar to that of iron netting in test VII only on bigger scale. Furthermore, the weight of the steel nets presses them down a few print layers, distorting the printed formwork and effectively placing the rebars lower than the desired height (Figure 84). Dividing the net into lighter segments and providing more printed concrete as distancers could reduce this effect.

Another effect that is caused by applying reinforcement is cracking in the hardening phase, these vertical cracks occur at intersections with rebars locally (Figure 85). A logical explanation for this occurrence is the hindered deformation that is caused by the steel: while the concrete wants to shrink, the netting prevents this, causing tensile forces in the concrete. The cracking occurs mostly in the printed formwork and distancers, in both casted and empty (only printed formwork and reinforcement) elements.

Figure 85: Exposed reinforcement in printed formwork (without infill casted concrete)

After fabrication, a new challenge arises: transportation of the panels. Since the elements take up almost an entire print table, they should ideally be moved quickly to allow operation of the printer for production. However, the flat elements are mainly young concrete and cannot be lifted easily without breaking due to bending under self-weight (Figure 84). If the elements are fabricated on a moveable platform, the concrete can develop without disturbance of loads due to transportation. The panels still have to be removed from the platform at some point, for this (casted or integrated) anchors can provide a solution. Additionally, anchors allow transportation on the building site and potentially installation on the building.

Test XIV. Lifting anchors

Transporting and installing elements of said dimensions requires heavy machinery such as cranes. To enable lifting and installing of the elements, anchors can be installed in the printed concrete. A more detailed research on this topic is found in thesis report of M. Keizer (2018), for which Bruil also conducted research. For this test, the focus lies primarily on linear anchors, which are rebars with attached M12 screw thread head (Figure 86).

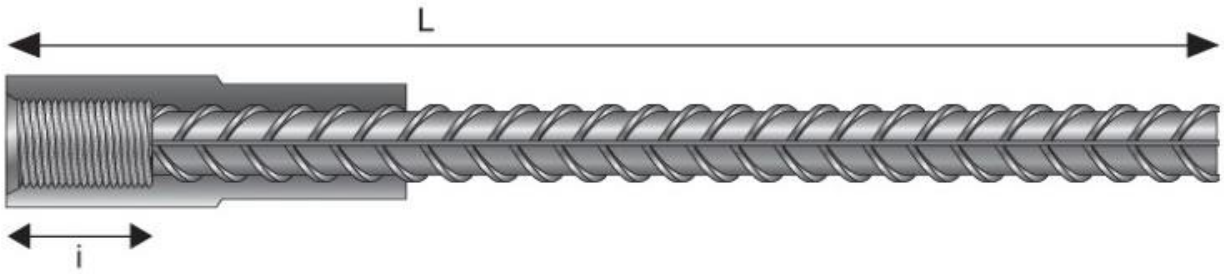

Figure 86: M12 screw thread head anchor

When placing anchors during the printing process, the orientation of the anchor relative to the print path is very important. The anchor can cause deformation of the printed element in the printing process

which influences the bonding of the anchor (Figure 87). The printer should be able to continue printing while moving over the anchor, requiring the anchor diameter not to exceed the layer height of the print. A challenge in this procedure is maintain enough concrete cover on the anchor at the outer end, because the anchor will most likely be longer than the print path width. However, for panels this should form no problem, since the casted concrete behind the printed formwork will form the concrete cover.

Figure 87: Anchors placed in printed concrete in different orientations to the printed layers

Pressing the anchors into the fresh concrete directly after the printer has finished, is an alternative that works well in vertical direction (perpendicular to the print path) (figure 2). This allows for longer anchors to be installed in the print without sticking out on the other end. The insertion does result in deformation of the printed concrete internally, but (if placed and performed correctly) this remains virtually invisible to the exterior of the print. The question remains whether the anchor receives full bonding contact with the concrete over its anchor length, since the concrete is pushed away by inserting.

It is also possible to embed the anchor between two printed layers (Figure 88 left), in order to gain enough concrete cover. Printing two layers parallel however does require more print time and material. If this fabrication method is chosen, the bonding between the two parallel printed layers should also be qualified. The layers are not subject to compression due to gravity as layers stacked vertically are. Pressing the anchors in horizontally, results in visible deformation of the printed concrete.

Figure 88 Left: Anchor placed between two printed layers, Right: Chemically bound anchor, sticking out of printed concrete

Lifting the elements by using the anchor should also be considered as a load case, this can influence the chosen direction of the anchor as well. For example, if the anchor on the right of Figure 88 is loaded vertically, it will introduce a bending moment due to its lever arm, which is undesirable. Norms to design anchors in concrete are present in CUR 25 which deals with given failure modes. However, these norms often require a certain concrete cover that cannot always be fabricated with 3DCP. In addition, the bonding strength between the anchor and the printed concrete should be tested. Possibly new models should be developed for these

Figure 89 Left: drilled hole in to printed concrete, Right: Anchors casted in infill of printed formwork element

Installing anchors after the printed concrete has hardened (instead of fresh) is also possible, for example by drilling in the hardened concrete and installing chemically bound (glued) anchors. Drilling in unreinforced concrete is done with care, in order not to break the element, but shows clean holes. Another option is installing the anchors by placing them in to the casted part of the panel, this allows easy integration with the reinforcement netting (if installed) and takes care of the concrete cover on the anchor. Methods like the latter are no different from installing anchors in traditionally casted elements.

XV. Printing on insulation

In order to print an integrated prefab façade element, insulation is needed. It seems optional to print double hollow elements and fill these with insulation afterwards, when printing vertical elements (such as 3D wall type,). For panels such as in the case study, integrating insulation can be done by simply printing on a hard insulation material. For this test blocks of EPS are placed on the print table, on which concrete panels are printed and afterwards casted (Figure 90).

Figure 90: Printed formwork and casted concrete on insulation blocks from EPS

The insulation sticks to the concrete making it possible to transport and install the insulated panel as one element. Preparations for removing the element off the print table (such as pallet or lifting bands) can be placed under the insulation without risking embedding in concrete. An additional benefit is that anchors can be preplaced into the insulation, so that they are fully integrated once the element is casted (Figure 91).

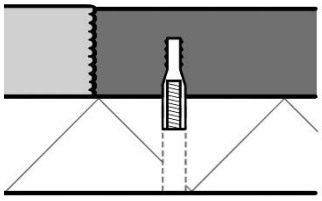

Figure 91: Anchor detail

5.4.4. Analyses and conclusions

Using printed concrete as formwork for the fabrication of panels is feasible in terms of production. The added value is that the formwork is freeform and actually adds to the element instead of being a waste product as traditional formwork. Additionally, the print can function as reinforcement distancers and anchors can be installed in the panel relatively easy. The type of reinforcement could be altered as steel nets show difficulties in placement and crack formation due to hindered deformation (shrinkage). Other methods to prevent cracking in the hardening phase, like post-treatment, could also provide a solution.

Handling and transportation of elements of these dimensions should be considered before manufacturing. Ideally, solutions such as anchors are already taken care of in the design phase, so that these can be used for transport and installation as well. Transportation can be planned in different phases, but it is best to let the concrete develop strength before subjecting it to loading due to transport.

To integrate insulation in the panel as a prefabricated element, it is possible to print on hard insulation board (specifically EPS). This allows for a more integrated product fabrication and could potentially also work for integrating other elements (for example custom windowsills). All in all, integrating materials and elements in the printing process is feasible for many standardized items by using the described method of casting in printed formwork.

5.5. Experiment 4: Façade element

The final test for the case study is the fabrication and loading of full scale developed façade elements. For this test the design as described in paragraph 4.4 is used. In short, the design is described as: concrete printed contours in the shape of a rectangle (exterior edge) and an oval (interior edge), between which reinforcement netting is placed and self-compacting concrete is casted (Figure 92). In this final test many aspects of previous experiments come together, but the main focus is on the production and structural predictability (verification of the engineering).

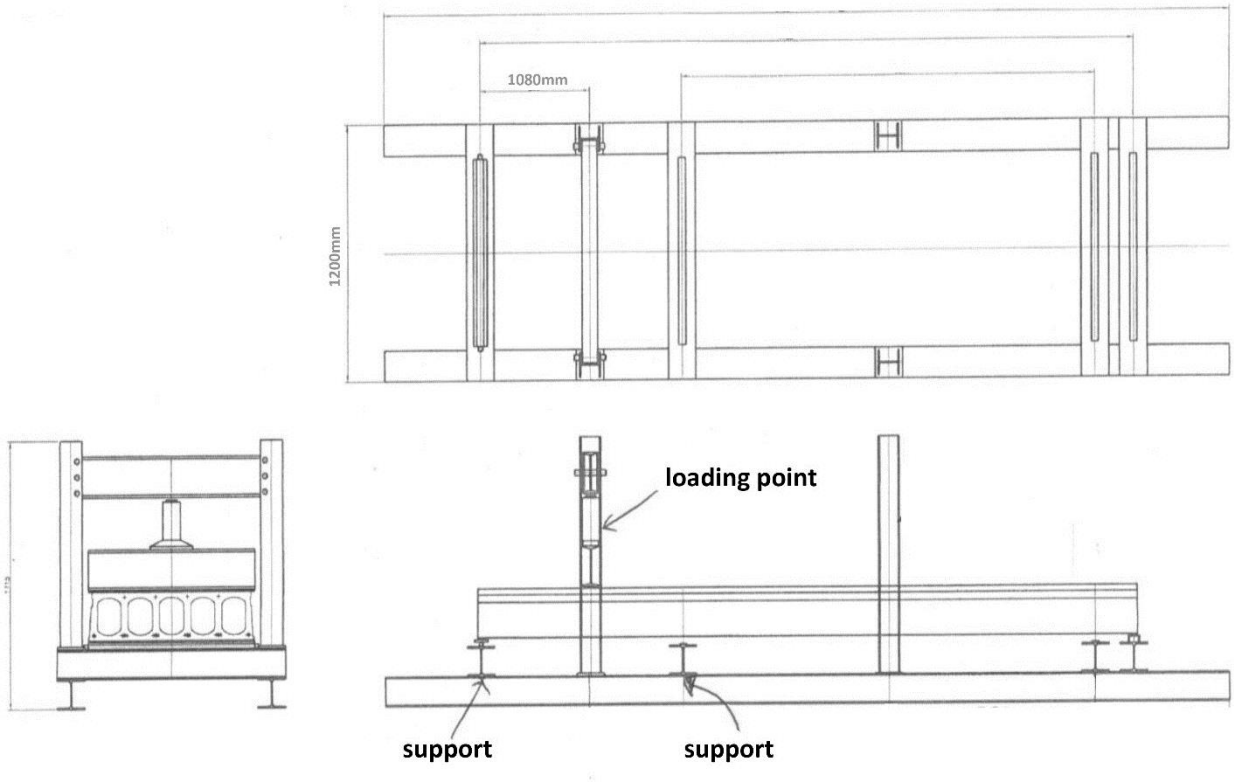

Figure 92: Three-point loading test setup for slab elements

5.5.1. Research

The two focus points of the test are described in two research goals which are related, both with individual subcategories. Both researches are described in their related chapter, Production 5.5.3 and Sample Testing 5.5.4.

Defining the potential of the chosen fabrication process for automated mass-production in the following production phases:

a. 3D concrete printing
b. Placement of (full scale) reinforcement and anchors
c. Casting Self-Consolidating Concrete (SCC)
d. Transportation and handling

Predictability of the structural behavior of the façade element under loading:

e. Load bearing capacity
f. Failure mechanism
g. Interaction between different materials

5.5.2. Method

The production process is examined by performing the paragraph 4.6 described fabrication process and defining any difficulties or noteworthy appearances in the process. Any deviations from the design are noted and their related causes defined. For comparison two types of reinforcements are used: steel reinforcement netting (two elements) and carbon fiber reinforcement netting (one element). These two options proved most promising in experiment test 2. The nets are fixed in the print and then covered by casting self-consolidating concrete (SCC) in the panels. This type of concrete flows easily and is almost self-leveling, enabling the mixture to flow into any panel shape and sticking to the (ribbed) printed formwork. It is used to prevent the need for vibration or temping after pouring, actions which could otherwise deform the formwork which is still fresh printed concrete.

The structural behavior of the elements under loading is analyzed by testing them with a three-point bending test. This test is similar to previous tests but scaled to the size of the elements. A setup is used that is also used for testing hollow core slabs with similar or bigger dimensions. The design of the element is such that the critical cross-section (lowest bending moment resistance, out of plane) is at mid span. Incidentally the three-point loading setup produces the highest bending moment at midspan, making the cracking and failure region predictable and easier to analyze. The bending will result in the concrete cracking, followed by the utility of the reinforcement and finally the failure of the element. The cracking (and potentially spalling) of the concrete under loading gives an indication of the safety of the element and the interaction between the two concrete types and the reinforcement.

5.5.3. Production

3D concrete printing

The fabrication process consists of many preparations and transformations to enable the final production of the façade element. Firstly, printer tables are exchanged for moveable tables to allow the elements to be moved for casting and hardening on a different location. This requires the printer to be recalibrated to the new table height. The tables that are used are not completely flat which directly effects the layer height of the first printed layer, and later the casting of the SCC (Figure 93). These deviations from the design are considered to have very little effect on the predictability of the structural behavior of the element. They do influence the appearance of the element esthetically, but in the case study design this is on the hidden (behind insulation) side.

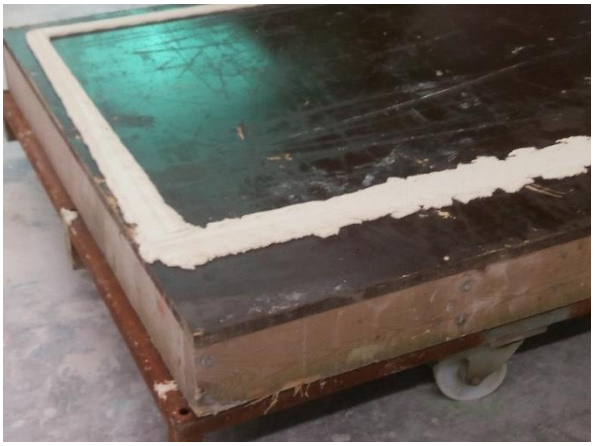

Figure 93: First printed layer on an unlevel print table

The print path is divided in rectangle and oval lines, the pump is stopped when switching paths, allowing a discontinued print path (Figure 94 right). The lines are printed one layer each, before moving to the second layer, instead of first printing the rectangle to full height before printing the oval. This allows both shapes to dry simultaneously and minimize difference in hardening phase. The stopping of the pump does decrease the print path width locally and creates a deformation at this location. After hardening it is clear that cracks occur at these weaker spots which does decrease the structural capacity locally (Figure 94 left). This effect could be reduced by printing a continuous line or relocating the start/stop moment differently per layer. In hindsight the start/stop point on the oval is chosen particularly unfavorable for the case study, as it weakens the critical cross-section.

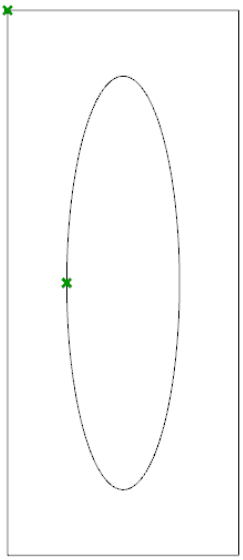

Figure 94 Left: Reinforcement in printed formwork and start/stop point of printing, Right: Print path with start/stop points

Reinforcement and anchors

After the printer has reached a certain number of layers (at the height of the desired concrete cover), the program directs the nozzle away from the print but continuous pumping concrete in a waste bucket (a solution to prevent hardening of the concrete in the printer). In this time the reinforcement and lifting anchors can be placed on the printed concrete. Due to a change in the layer height (10mm instead of 7mm) the height of the print at pausing is 50mm instead of the desired 35mm, placing the reinforcement far higher than originally intended. This effects the load bearing capacity for bending moment out of plane significantly.

The steel nets are big and difficult to place correctly by hand, conservatively the nets have been over dimensioned to ensure placement on the printer contour on all ends. Moving after placement results in deformation of the printed concrete, thus the reinforcement must be placed at once. The nets are not completely flat which results in some bars pressing deeper in the fresh concrete while others *float* above the print. For panel 2 the net is cut in two and placed in two sessions to ease this process. This only effects the process negatively as the print is even more distorted and the height of the rebars varies even more. Similar anchors (M12) as in test XIV (paragraph 5.4.3) are placed on the reinforcement, into the print path (Figure 95).

Figure 95: Reinforcement nets and anchors placed in printed concrete, deformation of the printed concrete locally

The carbon fiber net does not show these difficulties due to its (light) weight and flexibility. Once the net is in position, the system continues and finishes the print and is able to enclose the net within the printed layers (Figure 96).

Figure 96: Carbon fiber netting integrated in printed concrete formwork

After hardening, the elements with steel nets show cracking in the printed concrete near the rebars and significantly near around the anchors (Figure 99). The cracks are similar to those from test XIII (), but less wide. The difference can be explained by the placement of the rebar, in test XIII the rebars are embedded every 10cm whereas for test 4 the rebars are embedded over the length of the print path continuously. The stress caused by the hindered deformation (shrinkage) is now more spread out, causing more but smaller cracks. The element reinforced with carbon fiber netting does not show these types of cracks, because it hinders the shrinkage deformation less.

Casting SCC

Shortly after the prints are moved to the casting location, where the SCC is casted into the desired planes, covering the reinforcement. The moveable print tables, allow for the elements to be positioned directly under the spout of the SCC casting truck, making direct concrete casting possible. Prisms for compressive and flexural tests are also casted from the same specimen, in order to generate input for the engineering model. The elements are placed indoors to harden for fourteen days before testing (Figure 97).

Figure 97: Self compacting concrete pouring into the formwork on the print table

Because the print tables were not completely flat and level, the SCC pushed the printed concrete up locally (by 10mm) and went slightly under the print on one side (Figure 98). This deviation in shape should be avoided as it affects structural-, esthetical aspects and could be problematic when placing the elements on site. This effect only occurred on panel 3, which is reinforced with two half nets.

Figure 98: Casted concrete deforming the lower surface due to unlevel print tables

During hardening, the SCC shows significant (shrinkage) cracking in all three panels caused by dehydration in the concrete development phase. The cracks appear on the surface perpendicular to the printed concrete, but also between the printed and casted concrete, parallel to the print path (Figure 99). Eurocode 2 warns for this type of (autogenous) shrinkage 'specifically when new concrete is cast against hardened concrete.' These cracks can be reduced by wetting the printing concrete before casting, preventing the fresh SCC from extracting too much water from the printed concrete. Other options include a more careful post-treatment of the concrete with water, insulation material or curing compound, preventing water evaporation (dehydration) during the hardening phase.

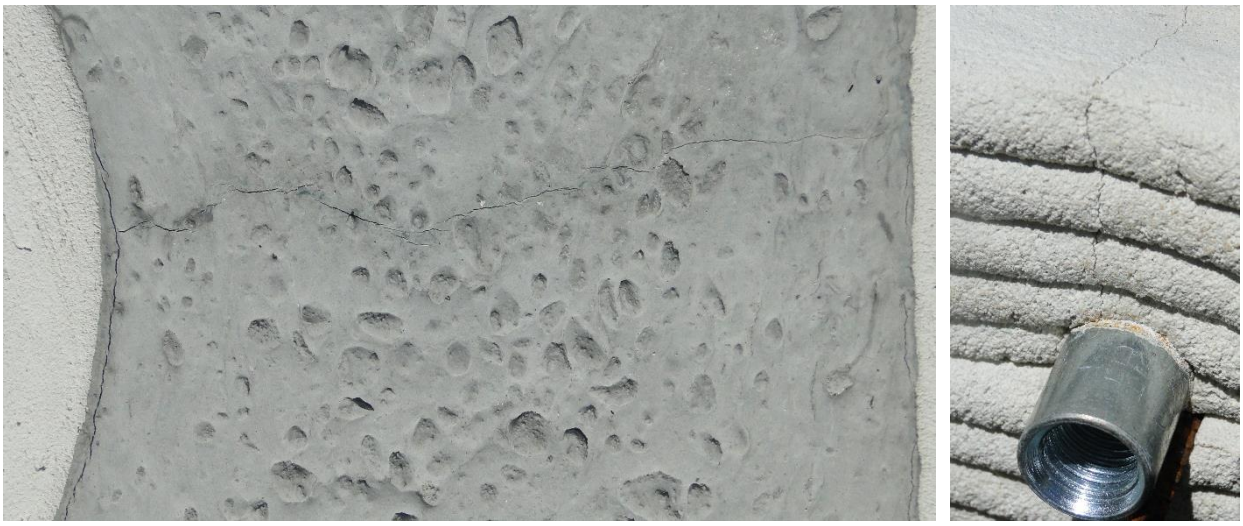

Figure 99 Left: Surface cracking of casted concrete in panel, Right: cracking of printed concrete locally

Transportation and handling

To move the elements to the testing site, they are lifted from the tables by tilting them using the anchors and by placing wooden beams between the element and the table. Once a panel is positioned on beams, forklifts can reach under them, lift them and place them on (pallets on) a truck (Figure 100). The forklifts are distanced such that bending under gravity loading is low, in this case as wide as possible. The elements are transported horizontally (as printed), separated by wooden pallets. Before testing, the reinforcement nets in the perforations are removed using a grinding machine and cutting the c-grid.

Figure 100: Transportation of test panels to load test area, lifting by forklift and horizontal transportation

5.5.4. Sample testing

On the testing site the elements are placed on a three-point loading bench (Figure 101). Positioning the heavy elements with precision is difficult and could not be done perfectly symmetrical: the elements are placed slightly off center (2 to 5cm). The loading setup is schematized in the sketch, spanning 2160mm between the supports. Loading the elements is done with a hand operated hydraulic piston press, that presses a HE240A beam on the element at midspan. The meter indicates the built-up pressure in the

press in bar, from which the load bearing resistance is later calculated. During loading, two cameras are used to capture the behavior under loading, one under the critical cross-section of the element and one mobile.

Figure 101: Load testing test panel by using a hydraulic press

During loading the crack development was recorded under the critical cross-section. All three panels showed no cracking before loading and developed cracks around critical cross-sections, going through both printed and casted concrete (Figure 102 left). For the steel reinforced elements, multiple parallel cracks developed next to the initial crack while panel 1 only further developed the first crack. The first crack formed at print start/stop point for panel 1 and 2, while the opposite site cracked first for panel 3. During cracking small segments of concrete spall off, the biggest pieces are retrieved and found to be no bigger than 2cm for any panel.

Figure 102: Crack patterns and deformation behavior under loading of the test panels

The elements are loaded until no increase in resistance is measured, when press loading is increased only deformation occurs. All three elements (reinforcement nets) remain intact after failing. Only the reinforcement of panel one (carbon grid) completely broke when it was removed from loading setup (Figure 105). Lifting causes upwards bending, cracking open any contact from the concrete compression zone. The reinforcement strands then had to carry the entire weight of the element when lifted, this caused breaking due to tension. No pull out of reinforcement occurred for any of the panels.

		Panel 1: Carbon		Panel 2: Steel (half)		Panel 3: Steel (full)	
Crack load	F_{cr}	4.25	kN	5.19	kN	7.80	kN
Flexural stress	σ_t	2.50	N/mm²	3.18	N/mm²	3.03	N/mm²
Failure load	F_{ed}	5.91	kN	*18.90*	kN	14.00	kN
Bending moment	M_{ed}	5.96	kNm/m	*12.14*	kNm/m	9.28	kNm/m
Bending resistance	M_{rd}	4.28	kNm/m	4.50	kNm/m	5.10	kNm/m

Table 8: Test loading results of tested panels under three point loading test

A summary of the test results is given in Table 8,for the full results and calculations see attachment 9.5. All panels cracked before reaching the tensile strength that was measured from the casted prism test (4.43 N/mm²). The ultimate load (F_{ed}) however exceeded expectations as all three panels resisted higher bending moments (M_{ed}) than was calculated (M_{rd}). For panel 3, a faulty measure was registered as the test setup was not properly arranged: a rebar that was sticking out hooked on the setup and provided additional resistance for the element.

5.5.5. Analyses and conclusions

From fabricating the test elements, it can be concluded that producing façade elements as designed for the case study is feasible in the prescribed fabrication process. Some attention points for the production process remain however:

Preparation of the printing setup, such as the platform and components that are to be integrated during the production process, is an essential step for creating elements as accurately as possible. Firstly, the printer setting should match that of the design including steps in the process (when to pause). Secondly a smooth and level printing surface reduces deviations in both printed and casted concrete. Placing components on printed concrete requires care and precision to prevent deformation of the fresh concrete. Ideally this step is automated for a more accurate result and reduction of production time and errors. Finally, as with any concrete fabrication technique, shrinkage of concrete should be taken care of during the hardening phase to prevent crack formation.

Both in the design and fabrication phases, transportation of the elements requires consideration. Anchor points for lifting (and installation) need to be positioned well in the element to be functional and operable during moving. Load cases for transportations should be modeled to prevent damaging of the element when lifted. Before fabrication, the transport of the elements should already be considered, because moving heavy objects takes heavy machinery and fresh or young concrete is fragile.

The structural behavior of the elements and its predictability is tested by loading. The cracking of composite (casted and printed) concrete section, due to exceeding the flexural strength, occurred earlier (under less loading) than was expected from prism tests. One explanation is the lack of treatment during the hardening phase, resulting in a lower concrete quality (and cracks) compared to casted prisms. Another reason is the larger deviations (from the model used for calculations) in cross-section dimensions. The printed and casted concrete attach well in the cross-section of the elements, show only cracking on the surface.

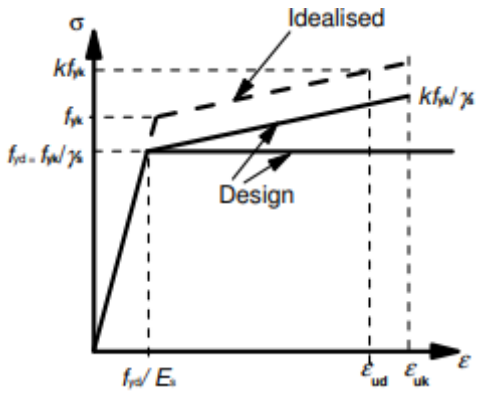

Figure 103: Stress strain relation of reinforced concrete in engineering model

The load bearing of the tested elements outperformed the expectations from engineered models (UC of 1.39 for carbon grid and 1.82 for steel). Both reinforcement types are appropriate in the production and use of printed concrete panels as fabricated for this case study. Additional load bearing resistance is provided by the applied reinforcement. A possible explanation is that no material safety factor for the reinforcement (of steel) is applied, meaning that the steel could be stronger than anticipated ($f_{yk}>f_{yd}$). Another is the assumption that yielding steel does not provide additional resistance once yielding, but this based on a simplified engineering model (see Figure 103).

A more realistic explanation is found when examining the failure behavior more carefully. The engineering model calculated the resistance from one cross-section that is subjected to yielding of the reinforcement. However as seen during loading, multiple cracks developed indicating that yielding occurred at more sections, likely due to larger deformations. When the bending moment at midspan reaches Mrd, the capacity is reached but the element continuous to deform plastically. The bending moment line chances from the left figure to the right figure (Figure 104). Additional resistance from surrounding cross-sections after the critical cross-section is in yielding phase, can explain the difference in calculations and measurement. A similar explanation is thinkable for carbon grid, but this would be due to elongation not yielding, which explains why its result is closer to the expectation.

Figure 104: Bending moment at midspan reaches plastic bending moment

Finally, the two reinforcement types are compared. Carbon grid reinforcement performs better in production process due to the ease and precision with which is placed. Also, in the hardening phase carbon shows great potential because it causes no shrinkage cracks as steel does. Carbon requires less concrete cover for protection against weathering since it does not corrode like steel does. This allows carbon netting to be placed lower in the element, increasing the internal lever arm and in effect increasing the bending moment resistance. Some concrete cover remains necessary however, to prevent the reinforcement from being pulled out. In structural phase however, steel has a clear advantage over the carbon as it provides a warning behavior during loading. Both reinforcements remained intact during the load test, but carbon failed brittle once loaded in opposite direction for removal (Figure 105).

Figure 105: Test panels after failure, panel 2 on the left and panel 1 on the right with carbon netting

6. Conclusion

6.1. Introduction

The final chapter of this thesis combines and summarizes the conclusions of the individual research topics from previous chapters. The results are interpreted as to what the technique can provoke in the digitization of the construction industry. Finally, recommendations are made for further research in this field.

6.2. Research questions

In order to reach a final thesis conclusion, the research question is answered. First the sub questions are reviewed and answered before the main question is regarded.

What is the current state of 3DCP?

From the literature research it is evident that many facilities over the world are investing in research in the field of concrete printing. A closing report of a Danish partnership on 3D printing provides a good overview (Jorgensen, et al., 2018). Due to many differences in systems, material and research focus from research groups, results are not always applicable one on one. As a general overview however, it can be concluded that printing systems and material mixes at this stage are developed far enough to allow fabrication for practical use. Some pioneering projects are proof of this and prognosis is that their number will grow exponentially. While current systems will be improved and optimized by research, it is the believe of the researcher of this thesis that most potential lies in developing an integrated production process, to realize the goal of mass production of custom elements. A goal that lies even further in the future is the standardization and national norming for 3DCP.

What is demanded from 3DCP façade design?

Due to the wide range of possibilities of additive manufacturing in terms of geometric freedom, 3DCP could produce elements for many specific functions. The true potential however lies in the integration of functions and the reduction of manual labor. Different designs accommodate different design requirements, where the case study panels focused on high-rise, the hollow walls concept is more applicable for low-rise freeform structures. The market potential is high, but it requires trust and knowledge of involved parties (client, designer, fabricators and engineers) to produce successful projects. The main focus for façade design using 3DCP is the interaction between printed concrete and other components or materials, and detailed design thereof.

What does it take to design and engineer a 3DCP façade element?

The panels that are produced for testing in the case study can be designed and engineered with traditional software, requiring only a digital geometry that the printer system can understand (and slice). For the production and verification of the customizable designed elements however, the design and engineering should be performed parametrically and ideally in the same software (to prevent information loss). For this, current software is practically ready but can still be improved to better integrate different disciplines (especially fabrication) in the design process. Additionally, the people involved in the project, need to be able to use and understand parametric software.

What can be expected of printed concrete as a structural material?

The printed concrete that is used in the case study tests performs homogenous as monolithic material and behaves similar to standard concrete under loading. Even when reinforced with steel or carbon, the printed concrete behaves as theory for casted reinforced concrete prescribes. The printed concrete from Bruil functions as a proof of concept for producing homogenous printed concrete, which should be a requirement for printed concrete from any institute in the future. Some other material properties do

distinguish the printed concrete from traditional concrete, such as shrinkage and strength development, but these are heavily dependent on the material mix and curing conditions. An attention point for fabrication with printed concrete are the tolerances of the dimensions of the printed elements.

What is the influence of 3D concrete printing on the design and construction process of building envelopes?

To conclude, additive manufacturing in the form of 3D concrete printing has a great potential in the current building construction industry. The invention of the technique is a logical step in the automation of construction process given the innovations in the field of AM techniques and the desires for complex architecture. Some of the more promising potentials that are accredited to 3D concrete printing include the ability of producing mass customized elements that integrate multiple functions. This new found freedom in design can evolve to produce a new design type where multiple disciplines influence the design phase. The envisioned result are integrated façade elements that fulfill all design performance criteria, providing freeform enclosure shapes without the necessity of repetition of elements.

Additionally, the technique lays the grounds for labor reduction in fabrication, which can result in a cost reduction, especially when considering that expensive formwork becomes abundant. This is a major step in the automation of the construction industry but comes with requirements: other phases of the total process are required to adapt to the technique for it to become successful. For example, other fabrication techniques need to fit the production process to allow automation as well as freeform fabrication. Subsequently design and engineering also need to evolve to the automation in order to prevent a shift of labor from production to design and engineering (which would limit cost efficiency). All considered fields are showing improvements in adapting to this change with new fabrication methods (AM is innovating many materials) and parametric design and engineering software.

From a structural engineering perspective, optimization of structures by freeform design resulting in material reduction is goal that seems achievable with 3DCP. Although this goal requires much more research before being applied in current construction processes, it is a worthy aspiration. With the fabrication and testing of the façade panels for this thesis a small step has been made in preparing the construction industry for the use 3DCP. With more projects in the planning, the technique is steadily integrating in the market and will eventually develop as a common fabrication method for buildings.

6.3. Conclusions

From this thesis some conclusions are formed on the aspect of 3DCP as a fabrication technique for the building industry in general and more specifically for the setup of Bruil. The contribution of this thesis research to field of building engineering is best reflected in these conclusions as it discusses several points including design, engineering and fabrication of building components. The main conclusion is that 3DCP as a fabrication technique for façade elements is feasible and that the technique is ready for (phased) implementation in the building industry.

Figure 106: Façade elements fabricated by 3DCP

6.3.1. Design

Designing for 3DCP requires the integration of fabrication restrictions in the design process. From the development of the case study façade element it is apparent that designing for 3DCP takes practice and practical knowledge of the technique. Even though more design shapes are available compared to traditional fabrication methods, the methodology demands and restricts in its own ways. The most practical aspect that should be concerned for any design for 3DCP, is that the printer works in print path lines rather than volumetric elements (which is more common with casting). But practical limitations in size and maximum overhang (curvature in vertical plane) determine design restrictions as well. In the design process, a check on feasibility in terms of fabrication is necessary almost constantly.

Analyzing the design process of the case study façade elements (paragraph 3.4) also leads to the conclusion that the print direction is a major influence on the design restrictions (such as perforations and curvature planes). In the case of printing building elements rather than buildings as a whole, the segmentation of the design as well as the individual element design shapes are important design parameters for the feasibility. Therefore, the disciplines of designer and manufacturer should work closely together in order to fabricate a design to its full potential.

6.3.2. Engineering

Applying reinforcement in 3DCP fabricated elements is possible, can provide additional load bearing capacity and even ductility. The case study and the loading tests associated with this thesis show that existing calculation models as used for (reinforced) concrete are also applicable for 3D printed concrete, for both steel and carbon reinforcement. When the material properties of the printed concrete are known, as well as the element dimensions, a good indication of the load bearing capacity can be calculated. Steel has the clear advantage of providing a warning mechanism, but its concrete cover determines the element dimensions. Carbon netting performs better in fabrication process and can lower the element thickness but breaks brittle and has a lower bonding strength.

The printing process at Bruil shows the possibility of creating homogenous concrete elements by 3DCP, with monolithic connections even between the layers. The results from the first test of printed concrete show high tolerances in both material properties as well as dimension deviations. Measured material properties such as strength and stiffness, vary per specimen due to the consistency of concrete and the “open air” curing that is part of the printing process (more detailed explanation in paragraph 5.2.5). In order to gain reliable material properties with which designs can be made and validated, load test specimen should be printed (not casted) in large batches (sample size n>30 for any new mortar mix).

The tolerances in material properties can be lowered by controlling environmental factors (temperature and humidity) during printing, to reduce the negative effect of open air curing. Tolerances in design dimension deviations are relative to element size and print resolution (print path height) but could also be lowered by applying trowels on the printer nozzle. Alternatively, safety factors could be determined higher than those used for traditional casted concrete classes, to ensure reliable engineering.

The ability to produce individually customized elements on a mass-productive scale, brings about some challenges to the engineering. Since differently dimensioned elements respond differently mechanically as well, each element needs to be structurally validated. To prevent the necessity of labor intensive hand calculations for individual elements, parametric engineering is necessary. Software which can calculate the mechanical behavior and load bearing capacity of elements directly by adjusting parameters exists but is not yet common and perfect. The next necessary step is integration of parametric design and engineering in one model or environment, requiring integration of design and engineering in the design process.

6.3.3. Fabrication

The end result of the case study provides a proof of concept, demonstrating the feasibility of the production of façade elements for 3DCP. A specific fabrication method is described, in which the printed concrete is used as formwork for casting concrete and distancers for the reinforcement nettings. This method enables production mass customized façade elements, which can be implemented in buildings today. From the results of multiple load tests, it can be concluded that mechanical behavior and load bearing capacity predicted for the elements that are produced with this production method. In other words, it is possible to manufacture façade elements with 3DCP that are structurally verified and applicable in the current building industry.

On the topic of integration of components in the 3DCP fabrication process, experiment 3 (paragraph 5.4) gives an indication of the possibilities. The conclusion from this experiment is that integration requires the production process to be thought through completely. Preparation, placing, integration and transportation are some steps in the process in which problems can arise. However, for the selected additions (reinforcement, insulation, anchors and casted concrete), integration is deemed feasible. For the specifically described production procedure, the casting of concrete provides a means for existing components (such as anchors) to be integrated in the panel, following existing norms and regulations. New connections and details with printed concrete should always be tested by prototype and loading tests. For integrated detail designs, interaction between the fabricator and engineer is necessary to design and test new connections on their structural competence.

With regards to installing reinforcement in elements fabricated by 3DCP, this thesis shows many potentials and challenges (paragraph 5.3 and 5.5). The most important conclusion is that, given the prescribed fabrication method of printing formwork and casting panels, installing reinforcement netting is possible and beneficial (to the load bearing capacity of the element). Traditional reinforcement steel bars or netting perform similarly in printed as in casted concrete and can improve ductility of an element when designed correctly. Three factors that should be considered when installing reinforcement in printed concrete are:

- *Deformation*: deformation of the freshly printed concrete due to the installing of the reinforcement should be limited;
- *Concrete cover*: The required concrete cover on the reinforcement is often more than one the width of one printed layer (for the printer from Bruil);
- *Curing:* During the curing of the reinforced printed concrete, cracking due to shrinkage can occur

In the research to find applicable reinforcement for printed concrete, different types and materials are tested. Carbon grid net proved to be applicable in the prescribed fabrication method, improving load bearing capacity (higher tensile strength than steel) and easy in instalment due its lightweight and flexible properties. Additionally, carbon does not corrode like steel, which lowers the required concrete cover for environmental protection. However, some negative factors considering carbon grid as a reinforcement material are also concluded: Carbon does not yield like steel does, therefore it does not provide ductility for the element. Furthermore, the bonding strength between the concrete and the carbon grid is lower compared to steel rebars. In conclusion, carbon grid can be used as reinforcement in façade panels produced by 3DCP but should be designed conservatively due to the lack of warning mechanism (ductility).

6.4. Recommendations

6.4.1. Research

To allow 3D concrete printing to further develop and integrate into the modern building construction industry, more research in this field is recommended. The technique is still young, and the research scope is still wide, some topics that are worth researching in an effort to reach this goal are:

Integration of components

Integration of materials and components proved promising when using printed concrete as formwork for casting and installing components. However, the adaptability is greatly dependent on the flexibility of the component or material to match the freeform design and accommodate the texture (and tolerances) of printed concrete the hollow wall design allows for freeform fabrication while maintaining the possibility of integrating functional elements in to the design. Many different materials and components are worth investigating for their possible integration, but a logical next step following this thesis would be the integration of insulation.

Fiber reinforcement

The application of linear reinforcement (bars and netting) is applicable for panels and slabs but is restricted in curved shapes. Fiber reinforcement clearly has an advantage for freeform but requires more research both in the field of fabrication and engineering. Researching different fiber types in size and material for their potential of being integrated in printed concrete can help determine if this is viable reinforcement method for 3DCP. Points of attention are the compatibility with the printer and the concrete, as well as the structural benefit and interlayer bonding. In the case study of this thesis, only one type was tested and performed well for fabrication purposes, but showed no structural benefit, but different fibers can achieve different results.

6.4.2. Production

Reinforcement

This thesis report shows that traditional steel reinforcement and carbon netting are applicable in the production of printed panels. In production, the (manual) placement of carbon netting is preferred significantly over that of steel netting. However, the warning mechanism of the yielding steel is regarded as an essential structural safety quality in the building industry. It is recommended to research the possibility of providing ductility to carbon reinforced panels (e.g. by using hybrid reinforcement of locally placed rebars) or improving the adaption of steel netting. The latter can be investigated on the use of (additional) distancers, lowering the rebar diameter (to lower deformations and required concrete cover) and automation of placement.

Concrete testing

Tolerances in the material properties play a big role in safely defining the strength of the printed concrete. Although Eurocode prescribes three sample tests of three batches of the same concrete to define the material characteristics, it is recommended to use more for defining those of printed concrete (especially for tensile behavior). It is essential to always test printed specimen from the same mortar mix batch from which an element is fabricated with, to verify its quality. More varied testing of the material is advised to define in stress strain behavior for example, for this displacement controlled tests (rather than load controlled tests) and data loggers are required. A four point bending test can be used to better examine reinforced printed concrete as it spreads the maximum bending moment over a longer segment of the element.

Concrete curing

To reduce tolerances and cracking in printed concrete elements, the curing phase of the concrete is essential. Controlling the environment in which the concrete is printed, and cures can benefit the concrete properties greatly and help reach a more consistent result. Preventing dehydration by wetting the concrete during this development phase can also prove to be a viable method. The effect of the climate and dehydration of the concrete on the material properties should be investigated.

6.4.3. Digital Chain

Design to construct cycle

This thesis shows how project analysis can be performed to define the viability of 3DCP for a product. Additionally, it prescribes necessary changes in the design process to make the cycle viable. Most significant is the required interaction between the three disciplines of designing, engineering and fabrication in the early phases of the design cycle (Figure 107). An integral (preferably parametric) model, containing information of all these fields is essential to comprehend the feasibility of the design by the related professions.

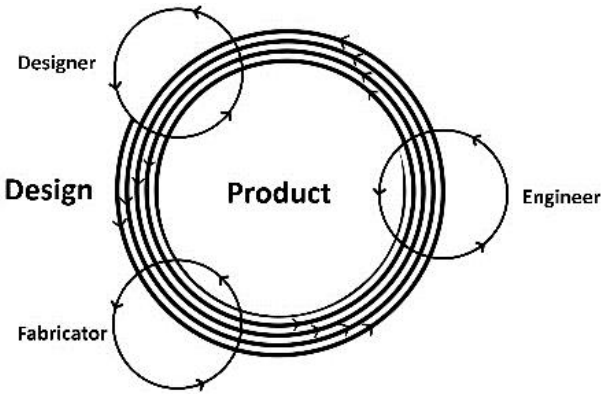

Figure 107: Integral design process

In this digital chain, design restrictions from each field need to be defined in the start of the process, setting the boundaries for the design. The selection of the fabrication method is a design step that defines the scope of the design early on in the process. During the design all disciplines are involved in shaping and verifying the design on the related qualities. When an alteration is made, the parametric model ideally confirms whether the other criteria (structural safety and manufacturability) are still met. The parameters that define the model should be set up in collaboration with all three disciplines in order to account for an integrated design and an operable process for every party.

For a future engineer, operating in a digital construction chain (from file to factory), it is vital to establish a position in the process in he can verify the structural safety of the model. In order to do so, he must understand the impact and influence of the fabrication technique on the structural qualities and thus work closely together with the fabricator. Meanwhile, the verification procedure should be relatively adaptable to changes to allow mass customization, without a significant increase in engineering labor (to remain economically viable). It is advisable to perform regular prototype testing to gain information on material properties and structural behavior regarding the development of 3DCP.

7. References

Aremu, A. (2013). *Topology Optimization for Additive Manufacture.* Loughborough : Loughborough University.

Barlett, S. (2013). *Printing Organs on demand.* The Lancet Respiratory Medicine.

Bos, F. P., Ahmed, Z. Y., Jutinov, E. R., & Salet, T. A. (2017). Experimental Exploration of Metal Cable as Reinforcement in 3D Printed Concrete. *NextGen Materials for 3D Printing*.

Bourell, D. L., Beaman, J. J., Jr., Leu, M. C., & Rosen, D. W. (2009). A Brief History of Additive Manufacturing and the 2009 Roadmap for Additive Manufacturing: Looking Back and Looking Ahead. *Workshop On Rapid Technologies* (pp. 5-11). TurkCadCam.net.

Cesaretti, G., Dini, E., de Kestelier, X., Colla, V., & Pambaguian, L. (2012). *Building components for an outpost on Lunar soil by means of a novel 3D printing technology.* Elsevier.

Coenders, J. L. (2010). *Parametric and associative design as a strategy for conceptual design and delivery to BIM .* Valencia: Editorial Universitat Politècnica de València.

Constanzi, C. B. (2016). *3D Printing Concrete onto Flexible Surfaces.* Delft: TU Delft: Architecture and the Built Environment.

de Witte, D. (2015). *Concrete in an AM process - Freeform concrete processing.* Delft: TU Delft: Architecture and the Built Environment.

Ding, L., Wei, R., & Che, H. (2014). *Development of a BIM-based automated construction system.* Wuhan: Elsevier.

Dini, E., Chlarugi, M., & Nannini, R. (2008). *United States Patent No. 0148683 A1.*

Eastman, C., Teicholz, P., Sacks, R., & Liston, K. (2011). *BIM Handbook: A Guide to Building Information Modeling for Owners, Managers, Designers, Engineers, and Contractors.* New Jersey: John Wiley & Sons, Inc.

Gramazio, F., & Kohler, M. (2017, 12 11). *Digitale Fabrikation, ETH Zurich, Architektur, Research*. Retrieved from Gramazio Kohler Research: http://gramaziokohler.arch.ethz.ch/

Hack, N., Lauer, W., Gramazio, F., & Kohler, M. (2015). Mesh Mould: Robotically Fabricated Metal Meshes as Concrete Formwork and Reinforcement. *11th International Symposium on Ferrocement and 3rd ICTRC* (pp. 1-13). Aachen: Rilem Publications Sarl.

Hallebrand, E., & Jakobsson, W. (2016). *Structural Design of High-Rise Buildings.* Lund: Lund University.

Huijben, F. (2016). *Vacuumatic formwork: a novel granular manufacturing technique for producing topology-optimised structures in concrete.* Berlin: Springer Verlag Berlin Heidelberg.

Iwamoto, L. (2013). *Digital Fabrication: Architecture and Material Techniques.* Princeton: Princeton Architectural Press.

Jorgensen, J., Holm, M., Goidea, A., Bergh, S. K., Dath, A., Blinkilde, H., . . . Lund-Nielsen, H. (2018). *Afslutningsrapport februar.* Kopenhagen: Parnerskabet 3D Printet Byggeri.

Khoshnevis, B. (2004). *Automated construction by contour crafting—related robotics and information technologies.* Los Angeles: Elsevier.

Khoshnevis, B., Russell, R., Kwon, H., & Bukkapatnam, S. (2001). Craftin Large Prototypes. *IEEE Robotics & Automation Magazine (Volume 8, Issue 3)*, 33-42.

Kolarevic, B. (2004). *Architecture in the Digital Age: Design and Manufacturing.* New York: Spon Press.

Le, T., Austin, S., Lim, S., Buswell, R., Gibb, A., & Thorpe, T. (2012). Mix design and fresh properties for high-performance printing concrete. *Material and Structures (Volume 45, Issue 8)*, 1221-1232.

Lim, S., Le, T., Webster, J., Buswell, R., Austin, S., Gibb, A., & Thorpe, T. (2009). Fabricating Construction Components using Layered Manufacturing Technology. *Global Innovation in Construction Conference* (pp. 512-520). Loughborough: CIB .

Marijnissen, M. P. (2016). *3D concrete printing in architecture: a research on the potential benefits of 3D concrete printing in the construction of resedential buildings in the Netherlands.* Eindoven: TU Eindhoven: Department of Architecture, Building and Planning.

Mattheck, C. (1998). *Design in Nature: Learning from Trees.* Berlin: Springer-Verlag Berlin Heidelberg.

Melnikova, R., Ehrmann, A., & Finsterbusch, K. (2014). *3D printing of textile-based structures by Fused Deposition Modelling (FDM) with different polymer materials.* IOP Conference Series: Material Science and Engineering.

Monolite, U. (2017, 11 15). *Vision*. Retrieved from D-Shape: https://d-shape.com/what-is-it/the-process/

Oxman, R. (2005). *Theory and design in the first digital age.* Haifa: Technion: Faculty of Architecture and Town Planning.

Papalambros, P. Y., & Wide, D. J. (2000). *Principles of Optimal Design: Modeling and Computation.* Cambridge: Cambridge University Press.

Pegna, J. (1997). Exploratory investigation of solid freeform construction. *Automation in Construction 5*, 427-437.

Rolvink, A., Mueller, C. T., & Coenders, J. (2014). State on the Art of Computational Tools for Conceptual Structural Design. *IASS-SLTE 2014 Symposium: "Shells, Membranes and Spatial Structures: Footprints".* Brasilia: International Association for Shell and Spatial Structures.

Rolvink, A., Mueller, C. T., & Coenders, J. L. (2014). State on the Art of Computational Tools for Conceptual Structural Design. *IASS-SLTE 2014 Symposium: "Shells, Membranes and Spatial Structures: Footprints".* Brasilia: International Association for Shell and Spatial Structures.

Salet, T. A., & Wolfs, R. J. (2016). Potentials and Challenges in 3D Concrete Printing. *Proceedings of the 2nd International Conference on Progress in Additive Manufacturing* (pp. 8-13). Singapore: Research Publishing.

Salet, T. A., Bos, F. P., Wolfs, R. J., & Ahmed, Z. Y. (2017). 3D Concrete Printing – A Structural Engineering Perspective. *Fib Symposium - High Tech Concrete: where Technology and Engineering Meet* (pp. xlii - lvii). Maastricht: Springer Cham.

Schipper, H. R. (2015). *Double-curved precast concrete elements: Research into technical viability of the flexible mould method.* Delft: TU Delft: Faculty of Civil Engineering.

Strauss, H. (2013). *AM Envelope - The potential of Additive Manufacturing for façade construction.* Delft: TU Delft: Architecture and the Built Environment.

The Third Industrial Revolution. (2012, April 21). *The Economist*, p. 14.

Ultimaker. (2017, 12 21). Retrieved from Ultimaker: http://www.ultimaker.com

van Alphen, J. M. (2017). *Structural optimization for 3D concrete printing.* Eindhoven: TU Eindhoven: Department of the Built Environment.

van der Linden, L. P. (2015). *Innovative joints for gridshells: joints designed by topology optimisation and to be produced by additive manufacturing.* Delft: TU Delft: Faculty of Civil Engineering.

van der Maas, H. (2016, 02 12). Computational thinking - 'Op een creatieve manier problemen oplossen'. (M. Eggink, Interviewer)

van Wolfswinkel, J. C., van 't Land, W., Stuit, H., Bastiaens, G., Ter Hall, L., van Beerendonk, W., . . . Attahiri, M. M. (2017). Design Process of a 3D-Printed Concrete Water Taxi Stop. *High Tech Concrete: Where Technology*.

Vizotto, I. (2010). *Computational generation of free-form shells in architectural design and civil engineering.* Campinas: UNICAMP: Faculty of Civil Engineering, Architecture and Urban Planning.

Volkers, N. J. (2010). *The Future for Additive Manufacturing in Facade Design: a stategic roadmap towards a preferable future.* Delft: TU Delft: Architecture.

Wangler, T., Lloret, E., Reiter, L., Hack, N., Gramazio, F., Kohler, M., . . . Flatt, R. (2016). *Digital Concrete: Oppertunities and Challenges.* Zurich: RILEM Technical Letters.

William, M. J. (2005). *Constructing Complexity.* Cambridge: MIT: School of Architecture and Planning.

Wolfs, R. J. (2015). *3D printing of concrete structures.* Eindhoven: TU Eindhoven: Department of the Built Environment.

Wolfs, R. J., Bos, F. P., van Strien, E. C., & Salet, T. A. (2017). A Real-Time Height Measurement and Feedback System for 3D Concrete Printing. *High Tech Concrete: Where Technology and Engineering Meet* (pp. 2474-2483). Maastricht: Springer, Cham.

Woodbury, R. (2010). *Elements of Parametric Design.* Vancouver: Routledge.

Wu, P., Wang, J., & Wang, X. (2016). *Automation in construction: A critical review of the use of 3-D printing in the construction industry.* Elsevier.

8. Image sources

Figure 1. Thesis author (2018). *Literature report structure*
Figure 2. www.archdaily.com *Heydar Aliyev, Baku (2013) by Zaha Hadid Architects*
Figure 3. Left: www.kuka.com *Automated assembly line of the automotive industry*,
Right: Iwamoto, Lisa: Digital Fabrications (2009). *Loewy Bookshop furniture by Jakob and MacFarlane (Paris)*.
Figure 4. Strauss, Holger: AM Envelope (2015). *Stereo Lithography Apparatus*
Figure 5. Strauss, Holger: AM Envelope (2015). *Fused Deposition Modeling*
Figure 6. Strauss, Holger: AM Envelope (2015). *Powder Bed Printing*
Figure 7. De Witte, Dennis: Concrete in an AM process (2015). *Clay printing by Langenberg*
Figure 8. Huijben, Frank: Vacuumatics (2014). *Vacuumatics*
Figure 9. Schipper, Roel: Double-curved Precast Concrete Elements. 2015 *Flexible mold by Koch*
Figure 10. Wangler, T. et al.: Digital Concrete (2016). *Mesh Mould produced reinforcement as formwork at ETH Zurich*
Figure 11. www.d-shape.com *D-Shape printing by Enrico Dini*
Figure 12. contourcrafting.com *Construction of conventional buildings using CC by Khoshnevis*
Figure 13. Left: futureofconstruction.org *WinSun printing hollow elements*
Right: www.tue.nl *Prestressing 3DCP bridge element at TU/e*
Figure 14. Left: Salet, T. et al.: 3D Concrete Printing (2017). *Twisting of filament in corners*
Right: Constanzi, C.B.: Printing onto Flexible Surfaces (2016). *Orientation of printhead*
Figure 15. Marijnissen, Marjolein: 3D Concrete Printing in Architecture (2016). *Different variations in 3D print structure*
Figure 16. Left: van Alphen, Jelle: Structural optimization for 3DCP (2015) *Rectangular nozzle TU/e*
Right: XtreeE.eu *Circular nozzle from XtreeE*
Figure 17. Salet, T. et al.: Potentials and Challenges in 3DCP (2016). *Embedded reinforcement TU/e*
Figure 18. Thesis author (2018). *Building enclosure design requirements*
Figure 19. Thesis author (2018). *Position of blockage of water and air in façade types*
Figure 20. Hallebrand, E. et al.: Structural Design of High-Rise Buildings (2016). *Structural systems*
Figure 21. Left: Tokio Ito (2015). *Edificio Mikimoto Ginza 2*
Right: Skope Architects (2013). *Brussels Parliament*
Figure 22. Left: Felix Candela. *Thin shell structure*
Right: www.tue.nl *Printed segments of turtle shells from 4TU project*
Figure 23. futureofconstruction.org *WinSun printed hollow elements as walls floors and roofs*
Figure 24. futureofconstruction.org *WinSun integrating components into hollow segments*
Figure 25. www.tue.nl and BAM. *Post tensioned 3DCP bridge*
Figure 26. XtreeE.eu *Placing component in printed wall during automated fabrication process*
Figure 27. wwwbruil.nl *Façade elements from printed concrete*
Figure 28. XtreeE.eu *Elements printed and casted*
Figure 29. Thesis author (2018). *Concept façade panel design, by façade segmentation*
Figure 30. Thesis author (2018). *Slanted edges in layered build up to create curved building enclosure*
Figure 31. Left: Rudy Ricciotti (2013). *Mucem in Marseille*
Right: Hi-Con (2018). *Accsys office in Arnhem*
Figure 32. Snohetta (2017). *Barcode in Oslo for Deloitte offices*
Figure 33. futureofconstruction.org *WinSun stacked elements block wall*
Figure 34. Thesis author (2018). *Concept design for customized bricks shaping a block façade.*

9. Appendices

9.1. Material test results Experiment 1 and 2

Experiment 1: Print direction

Results overview

	TEST I		TEST II		TEST III		TEST IV	
Flexural strength	Vertical		Horizontal		Perpendicular		Cut	
28 days	5,69	N/mm²	5,30	N/mm²	5,36	N/mm²	5,20	N/mm²
	5,77	N/mm²	5,02	N/mm²	5,52	N/mm²	4,77	N/mm²
	5,37	N/mm²	5,56	N/mm²	4,78	N/mm²	5,28	N/mm²
	4,77	N/mm²	5,56	N/mm²	4,99	N/mm²		
	5,41	N/mm²	4,74	N/mm²	5,38	N/mm²		
	5,39	N/mm²	4,92	N/mm²				
	5,11	N/mm²	5,85	N/mm²				
	5,17	N/mm²						
Average	5,34	N/mm²	5,28	N/mm²	5,21	N/mm²	5,08	N/mm²
Deviation	0,32	N/mm²	0,40	N/mm²	0,31	N/mm²	0,28	N/mm²
T-TEST			0,38	>0.05	0,24	>0.05	0,13	>0.05

TEST I: Vertical

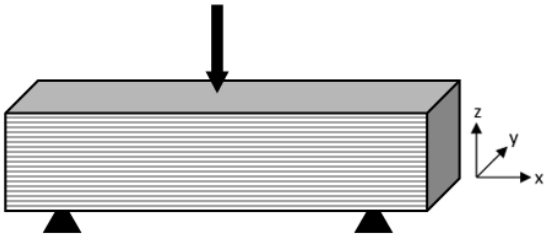

Specimen dimensions

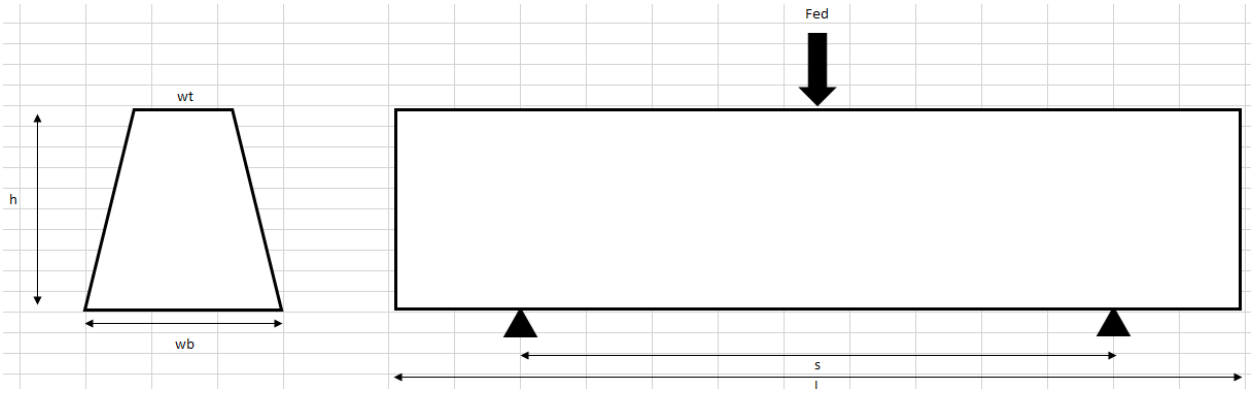

	Test	**Printed concrete**		**Vertical**	Date	09-02-2018		Setup	3 point loading test
Element	length	width top	width bot	height	span		Loading	Note	
	(L)	(wt)	(wb)	(h)	(s)		(Fed)		
#	mm	mm	mm	mm	mm		kN		
1	400	55	76	109	300		1,8	*Loaded too fast*	
2	400	55	75	109	300		0,5	*Loaded too fast*	
3	400	55	79	109	300		3,8	*Loaded too fast*	
4	400	55	81	106	300		9,0		
5	400	59	77	107	300		9,4		
6	400	59	82	107	300		9,0		
7	400	59	85	108	300		8,3		
8	400	58	84	107	300		9,1		
9	400	59	78	105	300		8,5		
10	400	59	83	105	300		8,3		
11	400	59	78	106	300		8,3		
X1	400	60	79	106	300		7,3	*Moved after printing*	
X2	400	59	78	106	300		6,7	*Moved after printing*	
X3	400	59	77	109	300		7,4	*Moved after printing*	
X4	400	57	70	109	300		9,4	*Moved after printing*	
X5	400	59	77	106	300		8,0	*Moved after printing*	

Inertia calculations

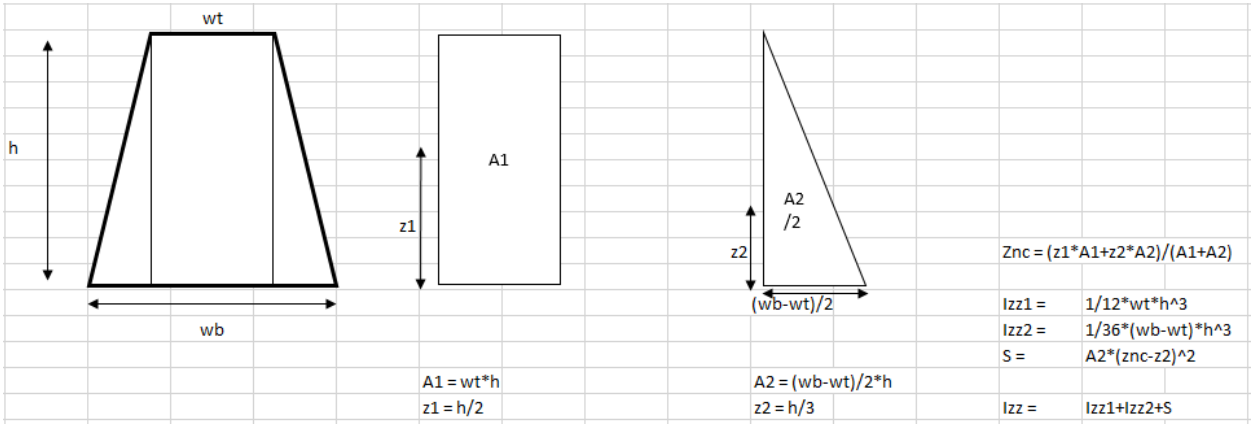

Element	width top (wt)	width bot (wb)	height (h)	Area 1 A1	Area 2 A2	z1	z2	Center Znc	Izz 1	Izz 2	S2	Inertia Izz
#	mm	mm	mm	mm²	mm²	mm	mm	mm	mm⁴	mm⁴	mm⁴	mm⁴
1	55	76	109	5995	1145	55	36	61	5,94E+06	7,55E+05	6,90E+05	7,38E+06
2	55	75	109	5995	1090	55	36	61	5,94E+06	7,19E+05	6,40E+05	7,29E+06
3	55	79	109	5995	1308	55	36	62	5,94E+06	8,63E+05	8,53E+05	7,65E+06
4	55	81	106	5830	1378	53	35	61	5,46E+06	8,60E+05	8,94E+05	7,21E+06
5	59	77	107	6313	963	54	36	58	6,02E+06	6,13E+05	5,00E+05	7,14E+06
6	59	82	107	6313	1231	54	36	60	6,02E+06	7,83E+05	7,25E+05	7,53E+06
7	59	85	108	6372	1404	54	36	61	6,19E+06	9,10E+05	9,07E+05	8,01E+06
8	58	84	107	6206	1391	54	36	61	5,92E+06	8,85E+05	8,91E+05	7,70E+06
9	59	78	105	6195	998	53	35	58	5,69E+06	6,11E+05	5,12E+05	6,81E+06
10	59	83	105	6195	1260	53	35	59	5,69E+06	7,72E+05	7,33E+05	7,20E+06
11	59	78	106	6254	1007	53	35	58	5,86E+06	6,29E+05	5,26E+05	7,01E+06
X1	60	79	106	6360	1007	53	35	58	5,96E+06	6,29E+05	5,22E+05	7,11E+06
X2	59	78	106	6254	1007	53	35	58	5,86E+06	6,29E+05	5,26E+05	7,01E+06
X3	59	77	109	6431	981	55	36	60	6,37E+06	6,48E+05	5,28E+05	7,54E+06
X4	57	70	109	6213	709	55	36	58	6,15E+06	4,68E+05	3,37E+05	6,96E+06
X5	59	77	106	6254	954	53	35	58	5,86E+06	5,96E+05	4,86E+05	6,94E+06

Determining stress

Element 0	length (L)	width top (wt)	width bot (wb)	height (h)	span (s)	Loading (Fed)	Bending Moment (Med)	Flexural stress (Sigma_fl)
#	mm	mm	mm	mm	mm	kN	kNm	N/mm²
1	400	55	76	109	300	1,8	0,14	1,11
2	400	55	75	109	300	0,5	0,04	0,31
3	400	55	79	109	300	3,8	0,29	2,30
4	400	55	81	106	300	9	0,68	5,69
5	400	59	77	107	300	9,4	0,71	5,77
6	400	59	82	107	300	9	0,68	5,37
7	400	59	85	108	300	8,3	0,62	4,77
8	400	58	84	107	300	9,1	0,68	5,41
9	400	59	78	105	300	8,5	0,64	5,39
10	400	59	83	105	300	8,3	0,62	5,11
11	400	59	78	106	300	8,3	0,62	5,17
X1	400	60	79	106	300	7,3	0,55	4,48
X2	400	59	78	106	300	6,7	0,50	4,17
X3	400	59	77	109	300	7,4	0,56	4,38
X4	400	57	70	109	300	9,4	0,71	5,89
X5	400	59	77	106	300	8	0,60	5,01

TEST II: Horizontal

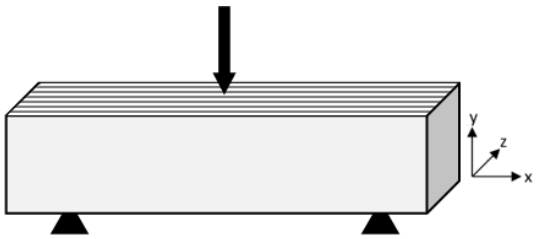

Specimen dimensions

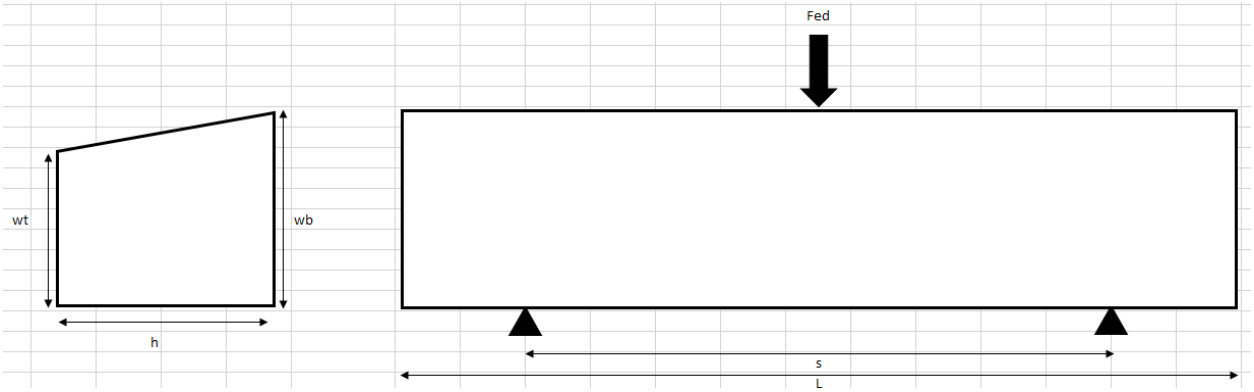

	Test	**Printed concrete**		**Horizont**	Date	09-02-2018		Setup	3 point loading test
Element	length	width top	width bot	height	span		Loading	Note	
	(L)	(wt)	(wb)	(h)	(s)		(Fed)		
#	mm	mm	mm	mm	mm		kN		
1	400	56	89	104	300		6,1		
2	400	59	85	104	300		5,8		
3	400	58	84	105	300		6,3		
4	400	59	86	104	300		6,5		
5	400	59	83	107	300		5,5		
6	400	59	83	105	300		5,6		
7	400	57	81	107	300		6,4		

Inertia calculations

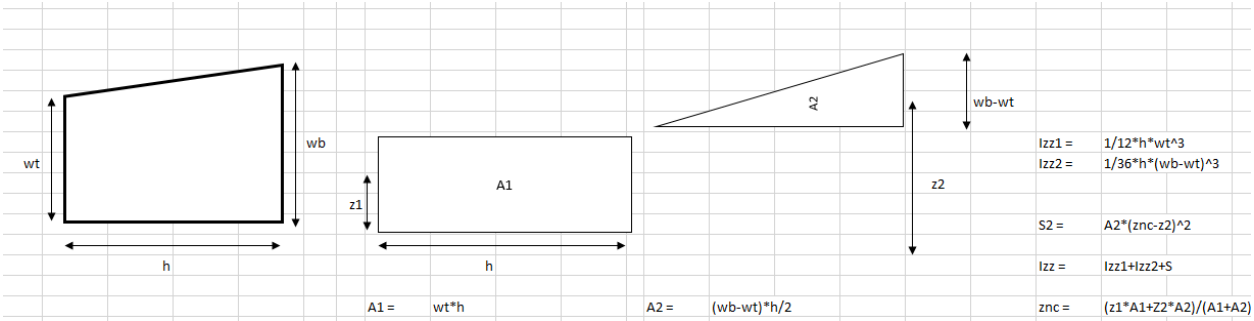

Element	width top	width bot	height		Area 1	Area 2			Center					Inertia
0	(wt)	(wb)	(h)		A1	A2	z1	z2	Znc		Izz 1	Izz 2	S2	Izz
#	mm	mm	mm		mm^2	mm^2	mm	mm	mm		mm^4	mm^4	mm^4	mm^4
1	56	89	104		5824	1716	28	67	37		1,52E+06	1,04E+05	1,56E+06	3,18E+06
2	59	85	104		6136	1352	29,5	68	36		1,78E+06	5,08E+04	1,32E+06	3,15E+06
3	58	84	105		6090	1365	29	67	36		1,71E+06	5,13E+04	1,29E+06	3,05E+06
4	59	86	104		6136	1404	29,5	68	37		1,78E+06	5,69E+04	1,38E+06	3,22E+06
5	59	83	107		6313	1284	29,5	67	36		1,83E+06	4,11E+04	1,25E+06	3,12E+06
6	59	83	105		6195	1260	29,5	67	36		1,80E+06	4,03E+04	1,22E+06	3,06E+06
7	57	81	107		6099	1284	28,5	65	35		1,65E+06	4,11E+04	1,17E+06	2,86E+06

Determining stress

width top	width bot	height	span		Loading		Bending Moment		Flexural stress
(wt)	(wb)	(h)	(s)		(Fed)		(Med)		(Sigma_fl)
mm	mm	mm	mm		kN		kNm		N/mm^2
56	89	104	300		6,1		0,46		5,30
59	85	104	300		5,8		0,44		5,02
58	84	105	300		6,3		0,47		5,56
59	86	104	300		6,5		0,49		5,56
59	83	107	300		5,5		0,41		4,74
59	83	105	300		5,6		0,42		4,92
57	81	107	300		6,4		0,48		5,85

Test III: Perpendicular

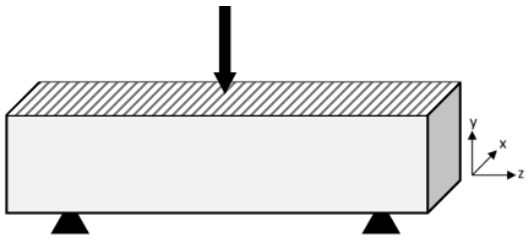

Specimen dimensions

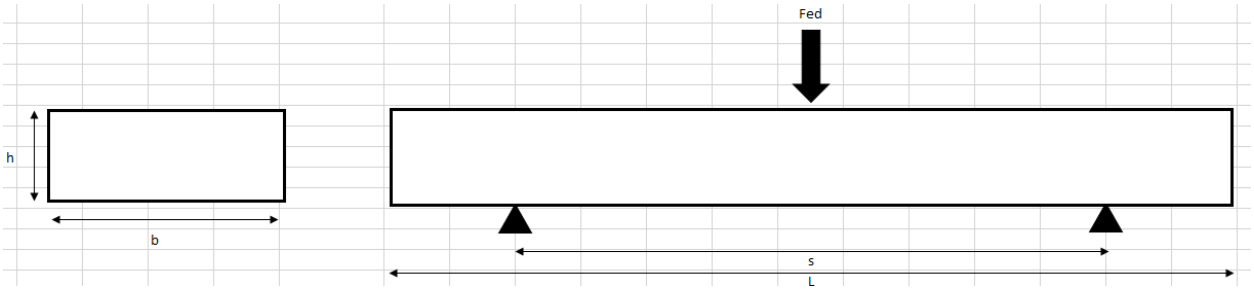

	Test	**Printed concrete**		**Vertical**	Date	09-02-2018		Setup	3 point loading test
Element	length	width top	width bot	height	span		Loading	Note	
	(L)	(wt)	(wb)	(h)	(s)		(Fed)		
#	mm	mm	mm	mm	mm		kN		
1	400	200	200	55	300		7,2		
2	400	200	200	56	300		7,7		
3	400	200	200	57	300		6,9		
4	400	200	200	57	300		7,2		
5	400	200	200	56	300		7,5		

Inertia calculations

Element		width top	width bot	height		Area 1	Center			Inertia
		(wt)	(wb)	(h)		A1	Znc		Izz 1	Izz
#		mm	mm	mm		mm^2	mm		mm^4	mm^4
1		200	200	55		11000	28		2,77E+06	2,77E+06
2		200	200	56		11200	28		2,93E+06	2,93E+06
3		200	200	57		11400	29		3,09E+06	3,09E+06
4		200	200	57		11400	29		3,09E+06	3,09E+06
5		200	200	56		11200	28		2,93E+06	2,93E+06

Determining stress

Element	length	width top	width bot	height	span		Loading		Bending Moment		Flexural stress
0	(L)	(wt)	(wb)	(h)	(s)		(Fed)		(Med)		(Sigma_fl)
#	mm	mm	mm	mm	mm		kN		kNm		N/mm^2
1	400	200	200	55	300		7,2		0,54		5,36
2	400	200	200	56	300		7,7		0,58		5,52
3	400	200	200	57	300		6,9		0,52		4,78
4	400	200	200	57	300		7,2		0,54		4,99
5	400	200	200	56	300		7,5		0,56		5,38

Test IV: Cut

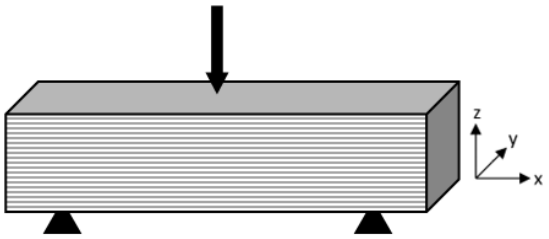

Dimensions

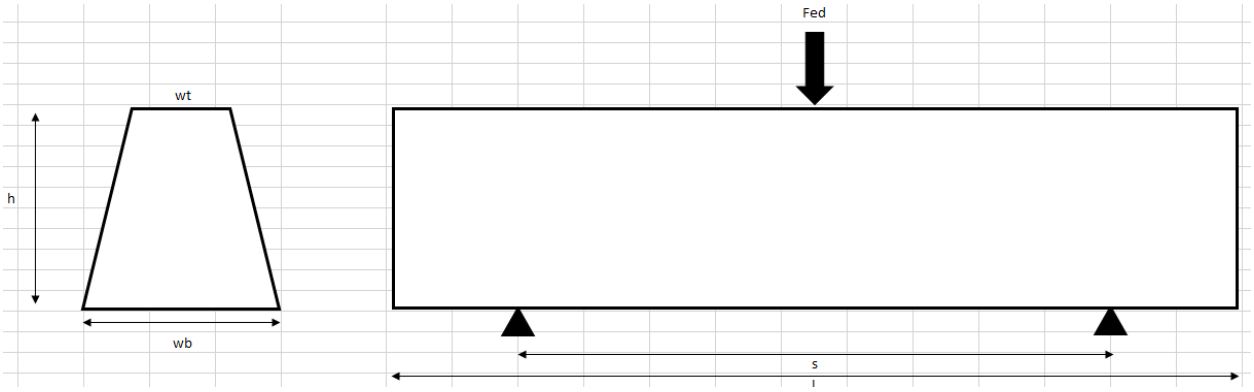

	Test	Printed concrete		Unribbec	Date	09-02-2018		Setup	3 point loading test
Element	length	width top	width bot	height	span		Loading		
	(L)	(wt)	(wb)	(h)	(s)		(Fed)		
#	mm	mm	mm	mm	mm		kN		
1	400	55	58	108	300		7,5		
2	400	59	67	110	300		7,8		
3	400	55	55	108	300		7,6		

Calculating inertia

Element		width top	width bot	height		Area 1	Area 2			Center					Inertia
		(wt)	(wb)	(h)		A1	A2	z1	z2	Znc		Izz 1	Izz 2	S2	Izz
#		mm	mm	mm		mm²	mm²	mm	mm	mm		mm⁴	mm⁴	mm⁴	mm⁴
1		55	58	108		5940	324	54	36	55		5,77E+06	1,05E+05	1,23E+05	6,00E+06
2		59	67	110		6490	880	55	37	59		6,54E+06	2,96E+05	4,58E+05	7,30E+06
3		55	55	108		5940	0	54	36	54		5,77E+06	0,00E+00	0,00E+00	5,77E+06

Determining stress

Element	length	width top	width bot	height	span		Loading		Bending Moment		Flexural stress
0	(L)	(wt)	(wb)	(h)	(s)		(Fed)		(Med)		(Sigma_fl)
#	mm	mm	mm	mm	mm		kN		kNm		N/mm²
1	400	55	58	108	300		7,5		0,56		5,20
2	400	59	67	110	300		7,8		0,59		4,77
3	400	55	55	108	300		7,6		0,57		5,28

Experiment 2: Reinforcement

	TEST V		TEST VI		TEST VII		TEST VIII	
Flexural strength	Blanco		Plaster gauze		Iron net		Rebar (crack)	
7 days	9,89	N/mm²	7,74	N/mm²	5,85	N/mm²	7,68	N/mm²
	9,31	N/mm²	8,25	N/mm²	7,64	N/mm²	6,74	N/mm²
	7,67	N/mm²	7,61	N/mm²	5,70	N/mm²	7,32	N/mm²
	6,97	N/mm²	6,95	N/mm²	5,80	N/mm²		
	7,24	N/mm²		*(faulty)*	6,57	N/mm²		
	9,65	N/mm²	9,14	N/mm²	7,26	N/mm²		
	9,79	N/mm²	7,05	N/mm²	8,18	N/mm²		
	7,04	N/mm²	6,66	N/mm²	8,81	N/mm²		
	8,54	N/mm²	8,55	N/mm²	7,79	N/mm²		
	7,83	N/mm²	7,60	N/mm²				
			8,15	N/mm²				
			8,70	N/mm²				
			8,21	N/mm²				
			7,99	N/mm²				
			8,20	N/mm²				
Average	8,39	N/mm²	7,92	N/mm²	7,07	N/mm²	7,25	N/mm²
Deviation	1,18	N/mm²	0,70	N/mm²	1,14	N/mm²	0,47	N/mm²

		TEST IX		TEST X		TEST XI	
Flexural strength		Geotex		C-grid		Fibermix	
7 days		8,59	N/mm²	7,40	N/mm²	4,44	N/mm²
		9,37	N/mm²	7,12	N/mm²	4,63	N/mm²
				6,99	N/mm²	4,32	N/mm²
						4,63	N/mm²
						6,70	N/mm²
						5,49	N/mm²
						5,42	N/mm²
						6,06	N/mm²
						6,09	N/mm²
						5,78	N/mm²
						6,88	N/mm²
						7,03	N/mm²
Average		8,98	N/mm²	7,17	N/mm²	5,62	N/mm²
Deviation		0,55	N/mm²	0,21	N/mm²	0,97	N/mm²

Test V: Blanco

Dimensions and loadig

Test	**Printed Concrete**		**Unreinforced (7d)**		Date	30-04-2018		Setup	3 point loading test
Element	length	width top	width bottom	height	Span		Loading		Days
	(l)	(wt)	(wb)	(h)	(s)		(Fed)		
#	mm	mm	mm	mm	mm		kN		
1	400	55	70	111	300		16,0		7 days
2	400	56	70	112	300		15,5		7 days
3	400	56	63	113	300		12,6		7 days
4	400	58	62	111	300		11,3		7 days
5	400	57	55	109	300		10,5		7 days
6	400	55	60	106	300		13,6		7 days
7	400	56	65	113	300		16,2		7 days
8	400	56	59	114	300		11,6		7 days
9	400	58	60	112	300		14,0		7 days
10	400	50	58	115	300		12,0		7 days
11	400	50	59	110	300		12,2		28 days
12	400	57	57	109	300		13,2		28 days
13	400	60	62	110	300		14,7		28 days
14	400	56	65	111	300		13,5		28 days
15	400	58	63	109	300		12,9		28 days

Calculating inertia

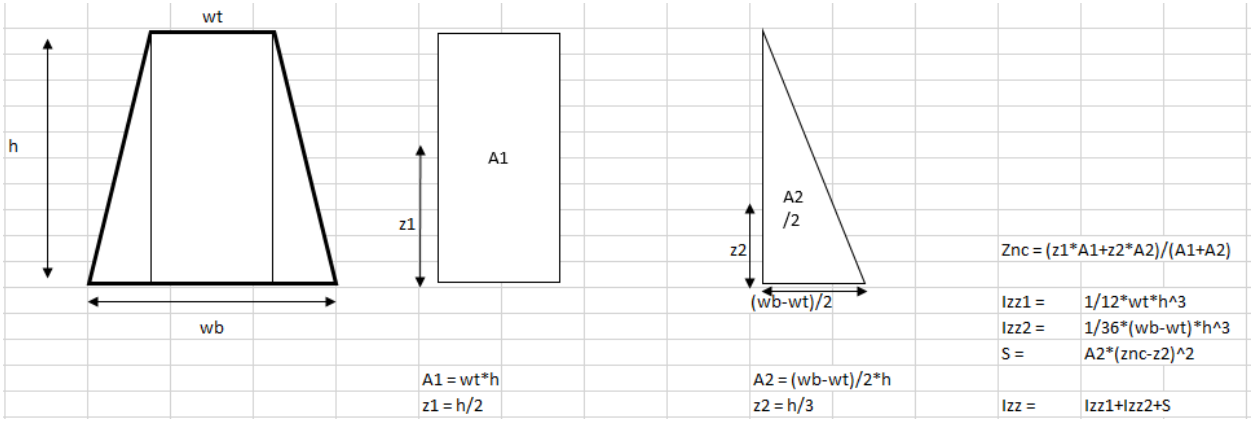

Element		width top	width bot	height		A1	A2	z1	z2	Center		Izz 1	Izz 2	S2	Inertia Izz
#		mm	mm	mm		mm²	mm²	mm	mm	mm		mm⁴	mm⁴	mm⁴	mm⁴
1		55	70	111		6105	832,5	55,5	37	60		6,27E+06	5,70E+05	4,40E+05	7,28E+06
2		56	70	112		6272	784	56	37	60		6,56E+06	5,46E+05	4,07E+05	7,51E+06
3		56	63	113		6328	395,5	56,5	38	58		6,73E+06	2,81E+05	1,69E+05	7,18E+06
4		58	62	111		6438	222	55,5	37	56		6,61E+06	1,52E+05	8,26E+04	6,84E+06
5	Differs	57	55	109		5668	275	57	3	57		5,34E+06	5,73E+02	8,03E+05	6,15E+06
6		55	60	106		5830	265	53	35	54		5,46E+06	1,65E+05	9,35E+04	5,72E+06
7		56	65	113		6328	508,5	56,5	38	59		6,73E+06	3,61E+05	2,31E+05	7,33E+06
8		56	59	114		6384	171	57	38	58		6,91E+06	1,23E+05	6,51E+04	7,10E+06
9		58	60	112		6496	112	56	37	56		6,79E+06	7,81E+04	3,97E+04	6,91E+06
10		50	58	115		5750	460	57,5	38	60		6,34E+06	3,38E+05	2,15E+05	6,89E+06
11		50	59	110		5500	495	55	37	58		5,55E+06	3,33E+05	2,19E+05	6,10E+06
12		57	57	109		6213	0	54,5	36	54		6,15E+06	0,00E+00	0,00E+00	6,15E+06
13		60	62	110		6600	110	55	37	55		6,66E+06	7,39E+04	3,76E+04	6,77E+06
14		56	65	111		6216	499,5	55,5	37	58		6,38E+06	3,42E+05	2,19E+05	6,94E+06
15		58	63	109		6322	272,5	54,5	36	56		6,26E+06	1,80E+05	1,01E+05	6,54E+06

Determining stress

Element	length	width top	width bot	height	Span		Loading		Med		Sigma
#	mm	mm	mm	mm	mm		kN		kNm		N/mm²
1	400	55	70	111	300		16,0		1,20		9,89
2	400	56	70	112	300		15,5		1,16		9,31
3	400	56	63	113	300		12,6		0,95		7,67
4	400	58	62	111	300		11,3		0,85		6,97
5	400	57	55	109	300		10,5		0,79		7,24
6	400	55	60	106	300		13,6		1,02		9,65
7	400	56	65	113	300		16,2		1,22		9,79
8	400	56	59	114	300		11,6		0,87		7,04
9	400	58	60	112	300		14,0		1,05		8,54
10	400	50	58	115	300		12,0		0,90		7,83
11	400	50	59	110	300		12,2		0,92		8,66
12	400	57	57	109	301		13,2		0,99		8,72
13	400	60	62	110	302		14,7		1,11		9,05
14	400	56	65	111	303		13,5		1,02		8,54
15	400	58	63	109	304		12,9		0,98		8,33

Results after 28 days

	Sample V	
Flexural	Blanco	
28 days	8,66	N/mm²
	8,72	N/mm²
	9,05	N/mm²
	8,54	N/mm²
	8,33	N/mm²
Average	8,66	N/mm²
Deviation	0,23	N/mm²

Test VI: Plaster gauze

Dimensions and loading

Test	Printed Concrete	Plaster Gauze						Date	30-04-2018		Setup	3 point loading test
Element	length	width top	width bottom	width middle	height	Reinforce	Position	Span		Loading	Crack load?	
	(l)	(wt)	(wb)	(wm)	(h)		(c)	(s)		(Fed)	(Fcr)	
#	mm	mm	mm	mm	mm	Type	mm	mm		kN	kN	
1	400	57	57	68	113		32	300			13,4	
2	400	58	58	60	114		32	300			14	
3	400	59	60	65	113		32	300			13,3	
4	400	56	56	62	110		44	300			10,8	
5	400	45	56	56	111		79	300			7,4	*faulty measure*
6	400	53	50	61	108		41	300			12,8	
7	400	38	58	65	110		72	300			10,5	
8	400	58	55	62	110		36	300			10,4	
9	400	56	50	60	109		33	300			12,4	
10	400	55	60	70	113		29	300			13,5	
11	400	52	54	57	114		24	300			12,9	
12	400	55	55	60	113		25	300			14,1	
13	400	56	48	60	110		30	300			12	
14	400	60	48	64	108		28	300			11,8	
15	400	60	50	60	108		25	300			12	

Calculating inertia

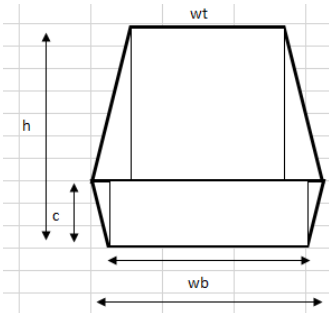

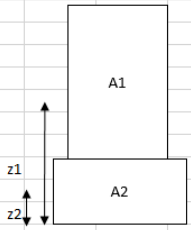

A1 = wt*(h-c)
z1 = (h-c)/2+c

A2 = wb*c
z2 = c/2

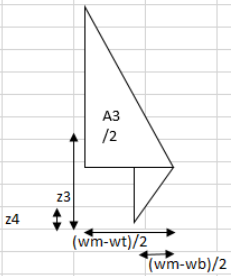

A3 = (wm-wt)/2*(h-c)
z3 = (h-c)/3+c

A4 = (wm-wb)/2*c
z4 = 2/3*c

Element		width top	width bot	width mid	height	Position									Center											Inertia
		wt	wb	wm	h	c		A1	A2	A3	A4	z1	z2	z3	z4	Znc		Izz 1	S1	Izz 2	S2	Izz3	S3	Izz4	S4	Izz
#		mm	mm	mm	mm	mm		mm²	mm²	mm²	mm²	mm	mm	mm	mm	mm		mm⁴	mm⁴	mm⁴	mm⁴	mm⁴	mm⁴	mm⁴	mm⁴	mm⁴
1		57	57	68	113	32		4617	1824	445,5	176	72,5	16	59	21	56		2,52E+06	1,29E+06	1,56E+05	2,89E+06	1,62E+05	4,62E+03	1,00E+04	2,09E+05	**7,24E+06**
2		58	58	60	114	32		4756	1856	82	32	73	16	59	21	57		2,66E+06	1,24E+06	1,58E+05	3,10E+06	3,06E+04	5,02E+02	1,82E+03	4,04E+04	**7,23E+06**
3		59	60	65	113	32		4779	1920	243	80	72,5	16	59	21	56		2,61E+06	1,30E+06	1,64E+05	3,07E+06	8,86E+04	2,19E+03	4,55E+03	9,61E+04	**7,34E+06**
4		56	56	62	110	44		3696	2464	198	132	77	22	66	29	55		1,34E+06	1,82E+06	3,98E+05	2,65E+06	4,79E+04	2,48E+04	1,42E+04	8,57E+04	**6,38E+06**
5		45	56	56	111	79		1440	4424	176	0	95	40	90	53	54		1,23E+05	2,40E+06	2,30E+06	9,55E+05	1,00E+04	2,21E+05	0,00E+00	0,00E+00	**6,01E+06**
6		53	50	61	108	41		3551	2050	268	225,5	74,5	21	63	27	54		1,33E+06	1,48E+06	2,87E+05	2,31E+06	6,68E+04	2,28E+04	2,11E+04	1,62E+05	**5,68E+06**
7		38	58	65	110	72		1444	4176	513	252	91	36	85	48	53		1,74E+05	2,10E+06	1,80E+06	1,18E+06	4,12E+04	5,20E+05	7,26E+04	5,86E+03	**5,90E+06**
8		58	55	62	110	36		4292	1980	148	126	73	18	61	24	55		1,96E+06	1,37E+06	2,14E+05	2,73E+06	4,50E+04	4,52E+03	9,07E+03	1,22E+05	**6,45E+06**
9		56	50	60	109	33		4256	1650	152	165	71	17	58	22	55		2,05E+06	1,10E+06	1,50E+05	2,44E+06	4,88E+04	1,75E+03	9,98E+03	1,79E+05	**5,97E+06**
10		55	60	70	113	29		4620	1740	630	145	71	15	57	19	55		2,72E+06	1,19E+06	1,22E+05	2,84E+06	2,47E+05	2,69E+03	6,77E+03	1,84E+05	**7,32E+06**
11		52	54	57	114	24		4680	1296	225	36	69	12	54	16	56		3,16E+06	7,54E+05	6,22E+04	2,54E+06	1,01E+05	1,20E+03	1,15E+03	5,85E+04	**6,68E+06**
12		55	55	60	113	25		4840	1375	220	62,5	69	13	54	17	56		3,12E+06	8,12E+05	7,16E+04	2,61E+06	9,46E+04	6,43E+02	2,17E+03	9,69E+04	**6,81E+06**
13		56	48	60	110	30		4480	1440	160	180	70	15	57	20	56		2,39E+06	9,33E+05	1,08E+05	2,37E+06	5,69E+04	1,93E+02	9,00E+03	2,28E+05	**6,09E+06**
14		60	48	64	108	28		4800	1344	160	224	68	14	55	19	55		2,56E+06	8,28E+05	8,78E+04	2,24E+06	5,69E+04	6,15E+00	9,76E+03	2,93E+05	**6,08E+06**
15		60	50	60	108	25		4980	1250	0	125	66,5	13	53	17	55		2,86E+06	6,70E+05	6,51E+04	2,25E+06	0,00E+00	0,00E+00	4,34E+03	1,83E+05	**6,03E+06**

Determining stress

Element	length	width top	width bot	width mid	height	Span		Loading	Crackload		Med		Sigma
#	mm	mm	mm	mm	mm	mm		kN	kN		kNm		N/mm²
1	400	57	57	68	113	300		13,4	13,4		1,01		7,74
2	400	58	58	60	114	300		14,0	14,0		1,05		8,25
3	400	59	60	65	113	300		13,3	13,3		1,00		7,61
4	400	56	56	62	110	300		10,8	10,8		0,81		6,95
5	400	45	56	56	111	300		7,4	7,4		0,56		5,01
6	400	53	50	61	108	300		12,8	12,8		0,96		9,14
7	400	38	58	65	110	300		10,5	10,5		0,79		7,05
8	400	58	55	62	110	300		10,4	10,4		0,78		6,66
9	400	56	50	60	109	300		12,4	12,4		0,93		8,55
10	400	55	60	70	113	300		13,5	13,5		1,01		7,60
11	400	52	54	57	114	300		12,9	12,9		0,97		8,15
12	400	55	55	60	113	300		14,1	14,1		1,06		8,70
13	400	56	48	60	110	300		12,0	12,0		0,90		8,21
14	400	60	48	64	108	300		11,8	11,8		0,89		7,99
15	400	60	50	60	108	300		12,0	12,0		0,90		8,20

Test VII: Iron net

Dimensions

Test	**Printed Concrete**		**Reinforcement bar**					Date	30-04-2018	Setup	3 point loading test
Element	length	width top	width bottom	width middle	height	Reinforce	Position	Span		Crack load?	
	(l)	(wt)	(wb)	(wm)	(h)		(c)	(s)		(Fed)	
#	mm	mm	mm	mm	mm	Type	mm	mm		kN	
1	400	50	56	56	112		33	300		8,9	
2	400	50	51	51	113		30	300		11	
3	400	51	55	55	114		33	300		8,9	
4	400	56	45	65	110		39	300		8,4	
5	400	55	45	63	109		38	300		9,2	
6	400	55	47	60	108		30	300		10,1	
7	400	55	55	55	114		41	300		13	
8	400	56	56	56	113		40	300		14	
9	400	54	54	60	115		40	300		12,8	

Calculating inertia

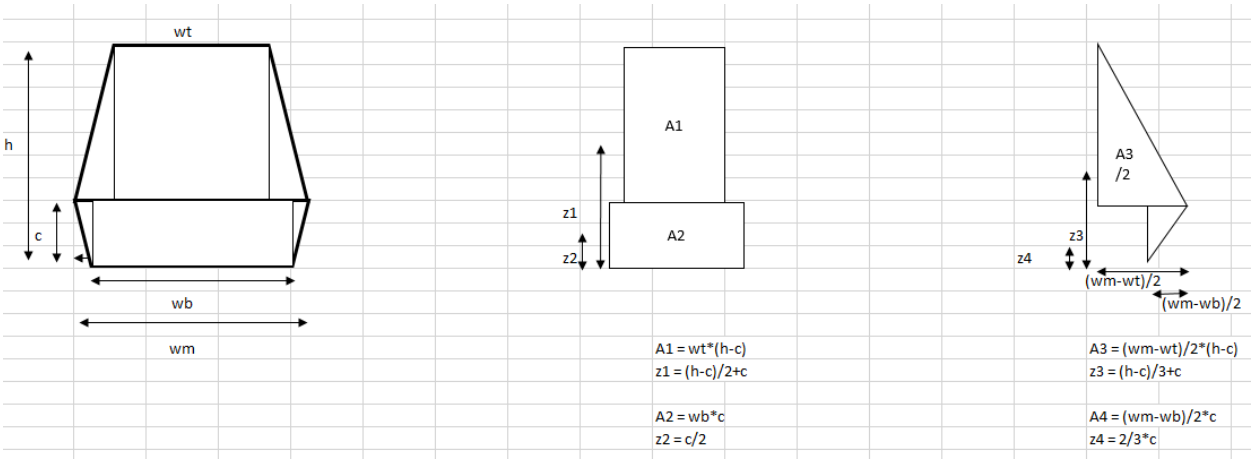

A1 = wt*(h-c)
z1 = (h-c)/2+c

A2 = wb*c
z2 = c/2

A3 = (wm-wt)/2*(h-c)
z3 = (h-c)/3+c

A4 = (wm-wb)/2*c
z4 = 2/3*c

Element	width top	width bot	width mid	height	Position									Center									Inertia
0	(wt)	(wb)	(wm)	(h)	(c)	A1	A2	A3	A4	z1	z2	z3	z4	Znc	Izz 1	S1	Izz 2	S2	Izz3	S3	Izz4	S4	Izz
#	mm	mm	mm	mm	mm	mm²	mm²	mm²	mm²	mm	mm	mm	mm	mm	mm⁴	mm⁴	mm⁴	mm⁴	mm⁴	mm⁴	mm⁴	mm⁴	mm⁴
1	50	56	56	112	33	3950	1848	237	0	72,5	17	59	22	55	2,05E+06	1,23E+06	1,68E+05	2,72E+06	8,22E+04	4,80E+03	0,00E+00	0,00E+00	6,26E+06
2	50	51	51	113	30	4150	1530	41,5	0	71,5	15	58	20	56	2,38E+06	9,60E+05	1,15E+05	2,61E+06	1,59E+04	7,86E+01	0,00E+00	0,00E+00	6,08E+06
3	51	55	55	114	33	4131	1815	162	0	73,5	17	60	22	56	2,26E+06	1,24E+06	1,65E+05	2,86E+06	5,90E+04	2,33E+03	0,00E+00	0,00E+00	6,58E+06
4	56	45	65	110	39	3976	1755	319,5	390	74,5	20	63	26	56	1,67E+06	1,36E+06	2,22E+05	2,34E+06	8,95E+04	1,42E+04	3,30E+04	3,51E+05	6,08E+06
5	55	45	63	109	38	3905	1710	284	342	73,5	19	62	25	55	1,64E+06	1,28E+06	2,06E+05	2,26E+06	7,95E+04	1,12E+04	2,74E+04	3,09E+05	5,82E+06
6	55	47	60	108	30	4290	1410	195	195	69	15	56	20	55	2,18E+06	9,00E+05	1,06E+05	2,20E+06	6,59E+04	4,32E+02	9,75E+03	2,32E+05	5,69E+06
7	55	55	55	114	41	4015	2255	0	0	77,5	21	65	27	57	1,78E+06	1,69E+06	3,16E+05	3,00E+06	0,00E+00	0,00E+00	0,00E+00	0,00E+00	6,79E+06
8	56	56	56	113	40	4088	2240	0	0	76,5	20	64	27	57	1,82E+06	1,64E+06	2,99E+05	2,98E+06	0,00E+00	0,00E+00	0,00E+00	0,00E+00	6,73E+06
9	54	54	60	115	40	4050	2160	225	120	77,5	20	65	27	57	1,90E+06	1,67E+06	2,88E+05	2,99E+06	7,03E+04	1,37E+04	1,07E+04	1,12E+05	7,05E+06

Determining stress

Element	length	width top	width bot	width mid	height	Span		(Fed)		Med		Sigma
#	mm	mm	mm	(wm)	mm	mm		kN		kNm		N/mm²
1	400	50	56	mm	112	300		9,3		0,70		6,11
2	400	50	51	56	113	300		11,0		0,83		7,64
3	400	51	55	51	114	300		8,9		0,67		5,70
4	400	56	45	55	110	300		8,4		0,63		5,80
5	400	55	45	65	109	300		9,2		0,69		6,57
6	400	55	47	63	108	300		10,1		0,76		7,26
7	400	55	55	60	114	300		13,0		0,98		8,18
8	400	56	56	55	113	300		14,0		1,05		8,81
9	400	54	54	56	115	300		12,8		0,96		7,79

Test VIII: Rebar

Dimensions

Test	**Printed Concrete**		**Reinforcement bar**					Date	30-04-2018		Setup	3 point loading test
Element	length	width top	width bottom	width middle	height	Reinforce	Position	Span		Loading	Crack load?	
	(l)	(wt)	(wb)	(wm)	(h)		(c)	(s)		(Fed)	(Fcr)	
#	mm	mm	mm	mm	mm	Type	mm	mm		kN	kN	
1	400	55	50	57	107	BAR	30	300		35	10,5	
2	400	58	55	60	105	BAR	30	300		25	9,5	
3	400	56	64	61	110	BAR	30	300		32	12,0	

Calculating inertia

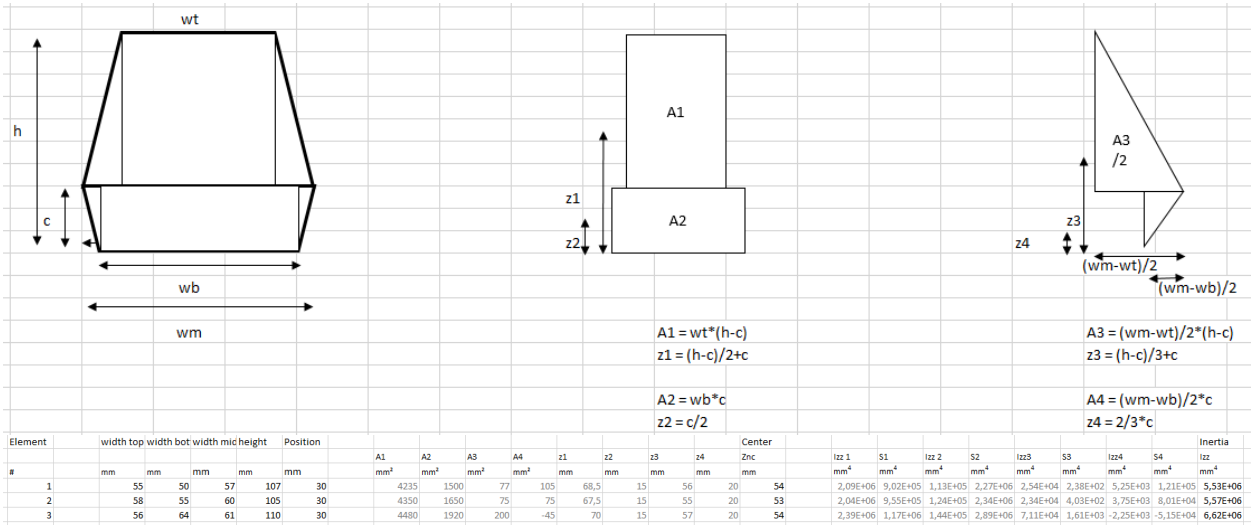

Element	width top	width bot	width mid	height	Position									Center										Inertia
						A1	A2	A3	A4	z1	z2	z3	z4	Znc	Izz 1	S1	Izz 2	S2	Izz3	S3	Izz4	S4	Izz
#	mm	mm	mm	mm	mm	mm²	mm²	mm²	mm²	mm	mm	mm	mm	mm	mm⁴	mm⁴	mm⁴	mm⁴	mm⁴	mm⁴	mm⁴	mm⁴	mm⁴
1	55	50	57	107	30	4235	1500	77	105	68,5	15	56	20	54	2,09E+06	9,02E+05	1,13E+05	2,27E+06	2,54E+04	2,38E+02	5,25E+03	1,21E+05	**5,53E+06**
2	58	55	60	105	30	4350	1650	75	75	67,5	15	55	20	53	2,04E+06	9,55E+05	1,24E+05	2,34E+06	2,34E+04	4,03E+02	3,75E+03	8,01E+04	**5,57E+06**
3	56	64	61	110	30	4480	1920	200	-45	70	15	57	20	54	2,39E+06	1,17E+06	1,44E+05	2,89E+06	7,11E+04	1,61E+03	-2,25E+03	-5,15E+04	**6,62E+06**

Calculating load bearing resistance

Element	length	width top	width bot	height	Reinforce	Position	Span		Loading		Reinforce	Yield	Force	factor	Concrete	Compress	Lever arm	Moment	Resistance
0	(l)	(wt)	(wb)	(h)	0	(c)	(s)		(Fed)		As	fyd	Ns = Nc	alpha	fcb	Xu	z	Mrd	Frd
#	mm	mm	mm	mm	Type	mm	mm		kN		mm²	Mpa	N		Mpa	mm	mm	Nmm	kN
1	400	55	50	107	BAR	30	300		35		50,26548	435	21865,48	0,75	60	9,255232	73,39046	1604718	**21,39624**
2	400	58	55	105	BAR	30	300		25		50,26548	435	21865,48	0,75	60	8,599994	71,646	1566575	**20,88766**
3	400	56	64	110	BAR	30	300		32		50,26548	435	21865,48	0,75	60	8,098328	76,84165	1680180	**22,4024**

Resistance	**Loading**	**Capacity**
Frd	**Fed**	**Fed/Frd**
kN	**kN**	**%**
21,39624	**35**	**164%**
20,88766	**25**	**120%**
22,4024	**32**	**143%**

Calculating stress

Element	length	width top	width bot	width mid	height	Span		Loading	Crackload		Med		Sigma_crack
#	mm	mm	mm	mm	mm	mm		kN	kN		kNm		N/mm²
1	400	55	50	57	107	300		35,0	10,5		0,79		7,68
2	400	58	55	60	105	300		25,0	9,5		0,71		6,74
3	400	56	64	61	110	300		32,0	12,0		0,90		7,32

Test IX: Geotex

Dimensions

Test	Printed Concrete	Geotextile						Date	30-04-2018	Setup	3 point loading test
Element	length	width top	width bottom	width middle	height	Reinforce	Position	Span		Crack load?	
	(l)	(wt)	(wb)	(wm)	(h)		(c)	(s)		(Fed)	
#	mm	mm	mm	mm	mm	Type	mm	mm		kN	
1	400	58	65	65	111		30	300		14,9	
2	400	55	60	60	105		30	300		13,5	

Calculating inertia

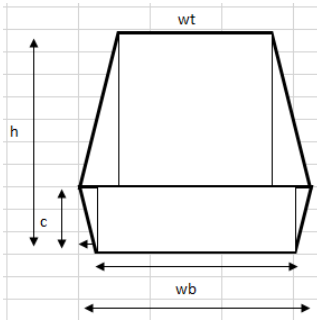

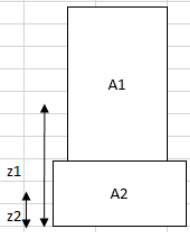

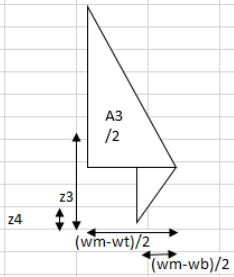

A1 = wt*(h-c)
z1 = (h-c)/2+c

A2 = wb*c
z2 = c/2

A3 = (wm-wt)/2*(h-c)
z3 = (h-c)/3+c

A4 = (wm-wb)/2*c
z4 = 2/3*c

width top	width bot	width mid	height	Position									Center										Inertia
(wt)	(wb)	(wm)	(h)	(c)	A1	A2	A3	A4	z1	z2	z3	z4	Znc	Izz 1	S1	Izz 2	S2	Izz3	S3	Izz4	S4	Izz	
mm	mm	mm	mm	mm	mm²	mm²	mm²	mm²	mm	mm	mm	mm	mm	mm⁴	mm⁴	mm⁴	mm⁴	mm⁴	mm⁴	mm⁴	mm⁴	mm⁴	
58	65	65	111	30	4698	1950	283,5	0	70,5	15	57	20	54	2,57E+06	1,23E+06	1,46E+05	3,02E+06	1,03E+05	2,01E+03	0,00E+00	0,00E+00	7,06E+06	
55	60	60	105	30	4125	1800	187,5	0	67,5	15	55	20	52	1,93E+06	1,04E+06	1,35E+05	2,42E+06	5,86E+04	2,10E+03	0,00E+00	0,00E+00	5,58E+06	

Determining stress

Element	length	width top	width bot	width mid	height	Span		(Fed)		Med		Sigma
#	mm	mm	mm	(wm)	mm	mm		kN		kNm		N/mm²
1	400	58	65	mm	111	300		14,9		1,12		8,59
2	400	55	60	65	105	300		13,5		1,01		9,37

Test X: C-grid

Dimensions

Test	Printed Concrete		C-Grid					Date	30-04-2018	Setup	3 point loading test	
Element	length	width top	width bottom	width middle	height	Reinforce	Position	Span		Crackloaf	Failure load	
	(l)	(wt)	(wb)	(wm)	(h)		(c)	(s)		(Fcr)	(Fu)	
#	mm	mm	mm	mm	mm	Type	mm	mm		kN	kN	
Blanco	400	42	50	50	102			300		8,8		
C1	400	42	55	54	94	C-grid	35	300		7,5	8,7	*Torn out
C2	400	44	55	54	96	C-grid	35	300		7,6	9	*Torn out
C3	400	43	52	51	100	C-grid	35	300		7,7	12,3	*Tensile break

Calculating inertia

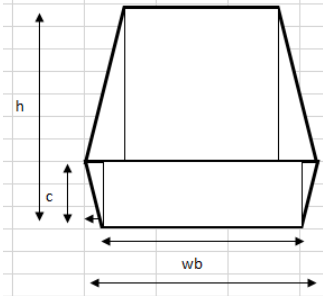

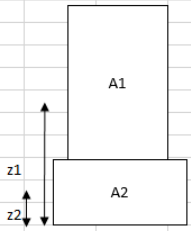

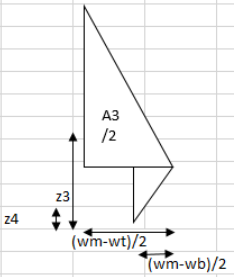

A1 = wt*(h-c)
z1 = (h-c)/2+c

A2 = wb*c
z2 = c/2

A3 = (wm-wt)/2*(h-c)
z3 = (h-c)/3+c

A4 = (wm-wb)/2*c
z4 = 2/3*c

Element		width top	width bot	width mid	height	Position									Center									Inertia
	0	(wt)	(wb)	(wm)	(h)	(c)	A1	A2	A3	A4	z1	z2	z3	z4	Znc	Izz 1	S1	Izz 2	S2	Izz3	S3	Izz4	S4	Izz
#		mm	mm	mm	mm	mm	mm²	mm²	mm²	mm²	mm	mm	mm	mm	mm	mm⁴	mm⁴	mm⁴	mm⁴	mm⁴	mm³	mm⁴	mm⁴	mm⁴
Blanco		42	50	50	102	0	4284	0	408	0	51	0	34	0	50	3,71E+06	9,36E+03	0,00E+00	0,00E+00	2,36E+05	9,83E+04	0,00E+00	0,00E+00	4,06E+06
C1		42	55	54	94	35	2478	1925	354	-17,5	64,5	18	55	23	45	7,19E+05	9,59E+05	1,97E+05	1,44E+06	6,85E+04	3,43E+04	-1,19E+03	-8,09E+03	3,41E+06
C2		44	55	54	96	35	2684	1925	305	-17,5	65,5	18	55	23	46	8,32E+05	1,01E+06	1,97E+05	1,58E+06	6,31E+04	2,57E+04	-1,19E+03	-9,11E+03	3,69E+06
C3		43	52	51	100	35	2795	1820	260	-17,5	67,5	18	57	23	48	9,84E+05	1,03E+06	1,86E+05	1,73E+06	6,10E+04	1,80E+04	-1,19E+03	-1,09E+04	3,99E+06

Calculating load bearing capacity

Element	length	width top	width bot	height	Reinforce	Position	Span	0	Crackloaf		Reinforce	Yield	Force	factor	Concrete	Compress	Lever arm	Moment	Resistance
0	(l)	(wt)	(wb)	(h)	0	(c)	(s)	0	(Fcr)		As	fyd	Ns = Nc	alpha	fcb	Xu	z	Mrd	Frd
#	mm	mm	mm	mm	Type	mm	mm	0	kN		mm²	Mpa	N		Mpa	mm	mm	Nmm	kN
C1	400	42	55	94	C-grid	35	300	0	7,5		3,7	2000	7400	0,75	60	3,390607	57,67766	426814,7	**5,690863**
C2	400	44	55	96	C-grid	35	300	0	7,6		3,7	2000	7400	0,75	60	3,32211	59,70438	441812,4	**5,890832**
C3	400	43	52	100	C-grid	35	300	0	7,7		3,7	2000	7400	0,75	60	3,461988	63,64982	471008,7	**6,280116**

Resistance	Loading	Capacity
Frd	Fed	Fed/Frd
kN	kN	%
5,690863	7.5	132%
5,890832	7.6	129%
6,280116	7.7	123%

Determining stress

Element	length	width top	width bot	width mid	height	Span		(Fcr)		Med		Sigma
#	mm	mm	mm	(wm)	mm	mm		kN		kNm		N/mm²
Blanco	400	42	50	50	102	300		8,8		0,66		8,05
C1	400	42	55	54	94	300		7,5		0,56		7,40
C2	400	44	55	54	96	300		7,6		0,57		7,12
C3	400	43	52	51	100	300		7,7		0,58		6,99

Test XI: Fiber reinforced concrete

Dimensions

Test	**Printed Concrete**		**Fibre reinforced**		Date	20-04-2018		Setup	3 point loading test
Element	length	width top	width bottom	height	Span		Loading		
	(l)	(wt)	(wb)	(h)	(s)		(Fed)		
#	mm	mm	mm	mm	mm		kN		
1	400	55	58	98	300		5,4		
2	400	55	60	94	300		5,3		
3	400	55	59	97	300		5,2		
4	400	50	56	93	300		4,8		
5	400	59	61	95	300		8,1		
6	400	60	61	100	300		7,4		
7	400	56	59	95	300		6,3		
8	400	50	60	100	300		7,6		
9	400	54	59	95	300		7,0		
10	400	60	60	100	300		7,7		
11	400	60	63	93	300		8,2		
12	400	55	60	100	300		9,1		

Calculating inertia

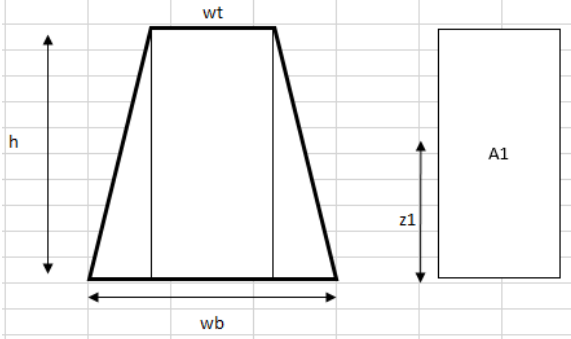

Znc = (z1*A1+z2*A2)/(A1+A2)

Izz1 = 1/12*wt*h^3

Izz2 = 1/36*(wb-wt)*h^3

S = A2*(znc-z2)^2

Izz = Izz1+Izz2+S

A1 = wt*h

z1 = h/2

A2 = (wb-wt)/2*h

z2 = h/3

width top	width bot	height						Center					Inertia
			A1	A2	z1	z2		Znc		Izz 1	Izz 2	S2	Izz
mm	mm	mm	mm^2	mm^2	mm	mm		mm		mm^4	mm^4	mm^4	mm^4
55	58	98	5390	147	49	33		49		4,31E+06	7,84E+04	3,72E+04	**4,43E+06**
55	60	94	5170	235	47	31		46		3,81E+06	1,15E+05	5,28E+04	**3,97E+06**
55	59	97	5335	194	48,5	32		48		4,18E+06	1,01E+05	4,72E+04	**4,33E+06**
50	56	93	4650	279	46,5	31		46		3,35E+06	1,34E+05	5,97E+04	**3,55E+06**
59	61	95	5605	95	47,5	32		47		4,22E+06	4,76E+04	2,30E+04	**4,29E+06**
60	61	100	6000	50	50	33		50		5,00E+06	2,78E+04	1,37E+04	**5,04E+06**
56	59	95	5320	142,5	47,5	32		47		4,00E+06	7,14E+04	3,39E+04	**4,11E+06**
50	60	100	5000	500	50	33		48		4,17E+06	2,78E+05	1,15E+05	**4,56E+06**
54	59	95	5130	237,5	47,5	32		47		3,86E+06	1,19E+05	5,44E+04	**4,03E+06**
60	60	100	6000	0	50	33		50		5,00E+06	0,00E+00	0,00E+00	**5,00E+06**
60	63	93	5580	139,5	46,5	31		46		4,02E+06	6,70E+04	3,19E+04	**4,12E+06**
55	60	100	5500	250	50	33		49		4,58E+06	1,39E+05	6,35E+04	**4,79E+06**

Determining stress

width top	width bot	height	Span		Loading		Med		Sigma
mm	mm	mm	mm		kN		kNm		N/mm²
55	58	98	300		5,4		0,41		4,44
55	60	94	300		5,3		0,40		4,63
55	59	97	300		5,2		0,39		4,32
50	56	93	300		4,8		0,36		4,63
59	61	95	300		8,1		0,61		6,70
60	61	100	300		7,4		0,56		5,49
56	59	95	300		6,3		0,47		5,42
50	60	100	300		7,6		0,57		6,06
54	59	95	300		7,0		0,53		6,09
60	60	100	300		7,7		0,58		5,78
60	63	93	300		8,2		0,62		6,88
55	60	100	300		9,1		0,68		7,03

9.2. Material specifications

Pleisters en gevelisolatiesystemen

K445

Technische fiche 09/2016

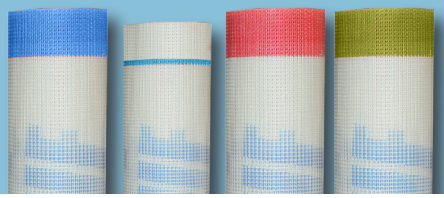

Knauf Gitex - Gitex LW - Autex - Isoltex

Glasvezelweefsels voor de wapening van pleisterlagen

Productbeschrijving

Knauf Gitex - Gitex LW - Autex - Isoltex zijn gaasvormige glasvezelweefsels met een alkalibestendige kwaliteit en een hoge weerstand tegen trekkrachten. Zij worden geleverd onder de vorm van rollen in diverse breedtes.

Toepassingsdomein

Knauf Gitex - Gitex LW - Autex - Isoltex zijn glasvezelweefsels die lokaal (vb. ter plaatse van sleuven, barsten of gaten in de ondergrond, van de overgang van verschillende ondergronden, van hoeken van ramen of deuren, …) of volvlakkig (vb. op labiele ondergronden zoals oude metselwerken, op isolatiematerialen, …) worden toegepast als wapening in pleisterlagen. Zij worden toegepast daar waar er scheurvorming in de pleisterlaag kan verwacht worden.

- Knauf Gitex wordt uitsluitend gebruikt in binnenbereik en in combinatie met gipsgebonden pleisters zoals Knauf Goldband, Goldband XT, Goldband Quick, Rotband, MP 75, MP 2, ECOfin of DUO-Light . Het wordt o.a. toegepast in het geval van muurverwarmingsystemen, ondergronden bestaande uit EPS, houtwolcementpanelen, ...
- Knauf Gitex LW wordt uitsluitend gebruikt in binnenbereik en in combinatie met gipsgebonden pleisters, daar waar er weinig spanningen in de ondergrond te verwachten zijn en waar een geringere weerstand tegen trekkrachten in het glasvezelweefsel volstaat.
- Knauf Autex wordt gebruikt in binnen- en buitenbereik in combinatie met cement-, kalk-, of kalkcementgebonden pleisters. In het geval van toepassingen in buitenbereik wordt in het buitenpleister systematisch een strook (ca. 40 x 50 cm) van dit glasvezelweefsel voorzien, diagonaal, ter plaatse van alle hoeken van ramen en deuren.
- Knauf Isoltex wordt voornamelijk toegepast als volvlakkig glasvezelweefsel in de wapeningsmortels (vb. SupraCem, SupraCem PRO, Lustro, Sockel SM, Sockel SM PRO, ...) van de gevelisolatiesystemen Knauf A1, B1, Volamit of Diffutherm. Systematisch en bijkomend wordt een strook (ca. 40 x 50 cm) van dit glasvezelweefsel voorzien in de wapeningsmortel, diagonaal, ter plaatse van alle hoeken van ramen en deuren

Verwerking

Knauf Glasvezelweefsels in de gewenste maat snijden met behulp van een mes of een cutter. Zij worden steeds in de verse pleisterlaag ingebed. Het wapeningsnet dient net onder het pleisteroppervlak geplaatst te worden, op 1/3 van de dikte van de pleisterlaag naar buiten toe. Ter plaatse van de aansluitingen van de weefsels dient er steeds een overlapping van minimaal 10 cm voorzien te worden. Het wapeningsnet dient overal met pleister bedekt te zijn.

Opmerkingen

Door het gebruik van Knauf Glasvezelweefsels wordt het risico op barstvorming in de pleisterlaag beperkt. Het kan echter niet volledig uitgesloten worden aangezien dit steeds afhankelijk blijft van de stabiliteit en de bewegingen van de ondergrond. Uitzettings- en bewegingsvoegen in de ondergrond dienen ten allen tijde overgenomen te worden in de pleisterlaag en kunnen niet met behulp van pleisters en glasvezelwapeningen overbrugd worden.

Technische gegevens

Naam	Kleur	Breedte (mm)	Lengte per rol (m)	Maaswijdte (mm)	Gewicht	Trekkracht (N/50 mm)
Gitex	Wit en blauw	1000, 500, 250, 125 of 100	100	ong. 5,5 x 6	ong. 105	ong. 1100
Gitex LW	Wit met blauwe streep	1000, 500, 250, 125 of 100	100	ong. 5 x 5	ong. 60	ca. 850
Autex	Wit en rood	1000	50	ong. 6,5 x 7	ong. 200	ong. 2400
Isoltex	Wit en olijfgroen	1000	50	ong. 5 x 5	ong. 200	ong. 2500

Contacteer ons
Technische dienst:
Tel.: +32 (0) 427 3 83 02
technics@knauf.be

www.knauf.be

Knauf Rue du parc Industriel 1, B-4480 Engis

Specificaties

Product	
Productsoort	Vogelgaas
Productnummer	536806
Hoogte product	50.0 cm
Breedte product	2.50 m
Lengte product	1 mm
Merk	Handson

Algemeen	
Kleur	Zilver
Kleurfamilie	Zilver
Type gaas	Rol
Materiaal	Ijzer

Afmetingen	
Maaswijdte	6.35 mm

Technische kenmerken	
Draaddikte horizontaal	0.65 mm
Draaddikte verticaal	0.65 mm

Environmental Product Declaration

as per ISO 14025 and EN 15804

Owner of the declaration:	Tensar International Limited
Publisher:	Kiwa BCS Öko-Garantie GmbH – Ecobility Experts
Programme operator:	Kiwa BCS Öko-Garantie GmbH – Ecobility Experts
Declaration number:	EPD-Tensar-001-EN
Date of issue:	20.06.2017
Valid to:	19.06.2022

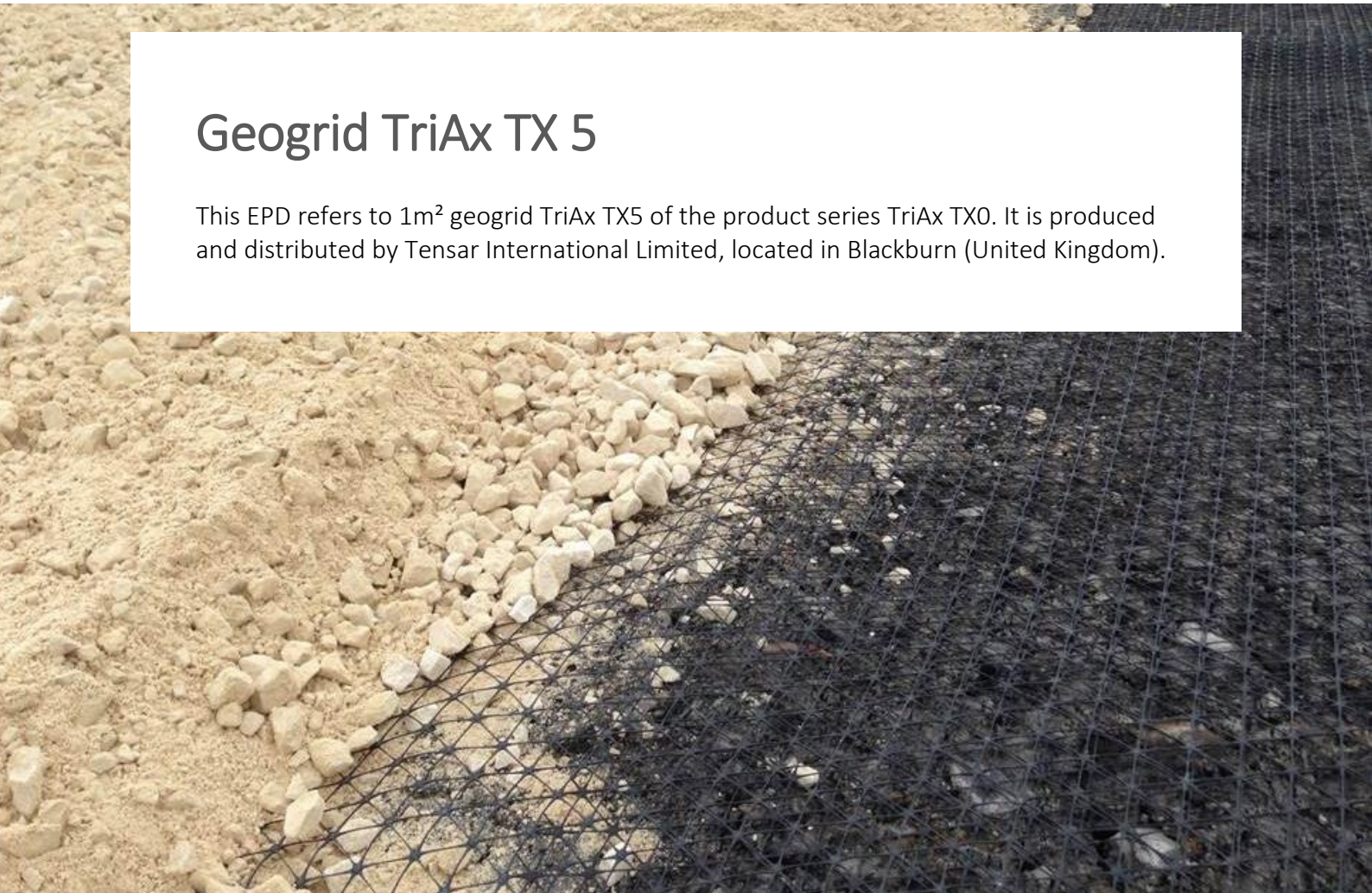

Geogrid TriAx TX 5

This EPD refers to 1m² geogrid TriAx TX5 of the product series TriAx TX0. It is produced and distributed by Tensar International Limited, located in Blackburn (United Kingdom).

Tensar TriAx®

1. General information

Tensar International Limited	Geogrid TriAx TX 5
Programme Operator Kiwa BCS Öko-Garantie GmbH – Ecobility Experts Marientorbogen 3-5 90402 Nürnberg Deutschland/Germany	**Owner of the Declaration** Tensar International Limited Units 2-4 Cunningham Court Shadsworth Business Park Blackburn, United Kingdom
Declaration number EPD-Tensar-001-EN	**Declared product /declared unit** **1 m^2 geogrid**
This declaration is based on the Product Category Rules: Anforderungen an Umweltproduktdeklaration für Geokunststoffe/-textilien (Ausgabe 2017-06) (PCR tested and approved by the independent expert committee)	**Scope** TriAx TX5 geogrid is a product of the product series TriAx TX0. It is produced and distributed by Tensar International Limited, located in Blackburn (United Kingdom). The EPD refers to the specific product. The owner of the declaration is liable for the underlying information and evidence; the Kiwa BCS Öko-Garantie GmbH – Ecobility Experts shall not be liable with respect to manufacturer information, life cycle assessment data and evidences.
Issue date: 20.06.2017	**Verification** The CEN Norm EN 15804 serves as the core PCR. Independent verification of the declaration according to ISO 14025 ☐internally ✓externally
Valid to: 19.06.2022	

Signature
Prof. Dr.-Ing. Roland Hüttl
(President of Kiwa BCS Öko-Garantie GmbH – Ecobility Experts)

Signature
Prof. Dr. Frank Heimbecher
(Chairman of the independent expert committee)

Signature
Matthias Schulz,
(Independent verifier appointed by the independent expert committee)

2. Product

2.1 Product description

The geogrid is comprised of multiple hexagons formed by equilateral triangular apertures. These apertures are defined by a structure of monolithic, multi-directional tensile elements of defined orientation, size and shape.
The hexagonal geogrid is manufactured from an extruded polypropylene sheet, which is then punched and orientated in three equilateral directions so that the resulting ribs of the triangular apertures have a high degree of molecular orientation which continues through the mass of integral node.

2.2 Intended Use

The intended use of the geogrid is to stabilize granular layers in order to minimize deformations during trafficking, to improve the load bearing capacity and to increase the design life of the granular layer in or under a construction in roads, railways and other trafficked areas, taking into account prevailing national regulations on design methodologies.
The combination of the geogrid and the aggregate creates a mechanically stabilized composite layer with significantly improved properties and performance capabilities in response to dynamic and static loading compared with aggregate layers alone. When installing, the manufacture's installation procedures shall be observed, as well as the respective national practices.
The geogrid is installed in five steps.

1. Site preparation
2. Placing and overlapping geogrid
3. Tensioning and pinning
4. Dumping and spreading aggregate fill
5. Compacting

More information is provided by the specific installation guide for Tensar TriAx geogrids.

2.3 Technical data

The technical data for the TriAx TX5 geogrid is shown in the following table.
These values were determined to receive an European Technical Approval (ETA). The ETA demands, that the actual product values are above the lowest value of the tolerance range, because product specific data can vary due to operating conditions or raw material specific features. It is assumed that all product requirements are assured, if the actual product parameters are above the values which were determined for the ETA. The products are limited to a minimum but not to a maximum.

Name	Value	Tolerance	Unit
Weight of product /TR 041 B.1/	205	-35	g/m2
Radial Secant Stiffness at 2% strain /TR 041 B.4/	250	-65	kN/m
Radial Secant Stiffness at 0,5% strain /TR 041 B.1/	360	-75	kN/m
Radial Secant Stiffness Ratio /TR 041 B.1/	0,80	-0,15	-
Junction Efficiency /TR 041 B.2/	100	-10	%
Static Puncture Resistance/EN ISO 12236/	n.r.	-	kN
Characteristic Opening Size	n.r.	-	mm
Water Permeability/EN ISO 11058/	n.r.	-	Velocity Index (VIH50) ms-1
Chemical Resistance	n.r.	-	-
Hexagon Pitch /TR 041 B.4/	80	±4	mm
Resistance to weathering /EN 12224/	Maximum time for exposure after installation of 1 month		
Resistance to oxidation and to acid and alkali liquids /EN ISO 13438/ and /EN 14030/	Resistant for 50 years when used in soil temperature of 25°C and 100 years when used in soil temperature of 15°C for soils with pH between 4 and 9		
Specific dimension of the finished rolls (width x length)	4 x 75	-	m x m

2.4 Placing on the market / Application rules

For quality assurance the geogrids TriAx TX0 series are regulated in accordance with the European Technical Assessment (ETA) 12/0529 and marked with a CE mark by the manufacturer.
In the EU/EFTA (excluding Switzerland) the placing of geogrids on the market is covered by Regulation (EU) No. 305/2011 of 9 March 2011. For the product use the respective national provisions shall apply. The product is packed and transported as roll.

2.5 Base materials / Ancillary materials

TriAx geogrids are manufactured from a homopolymer or a copolymer of Polypropylene.
Polypropylene (PP) is a thermoplastic polymer. It belongs to the group of polyolefins and is partially crystalline and nonpolar. PP is prepared by polymerisation of propene. It is rugged and unusually resistant to many chemical solvents, bases and acids.

Name	Quantity	Unit
Polypropylene (PP)	95	%
Masterbatch	5	%

2.6 Manufacturing

The manufacturing is located in Blackburn, United Kingdom.
The geogrids are made from polypropylene granulate. In the first step granulate is melted and then extruded. After this the extruded sheet passes the punching process. Depending on the specific product the punches differ in size. The punched sheet is then stretched.
The result is the specific triangular structure of each geogrid. The products are rolled and then packaged.
The manufacturing process is shown in the following figure:

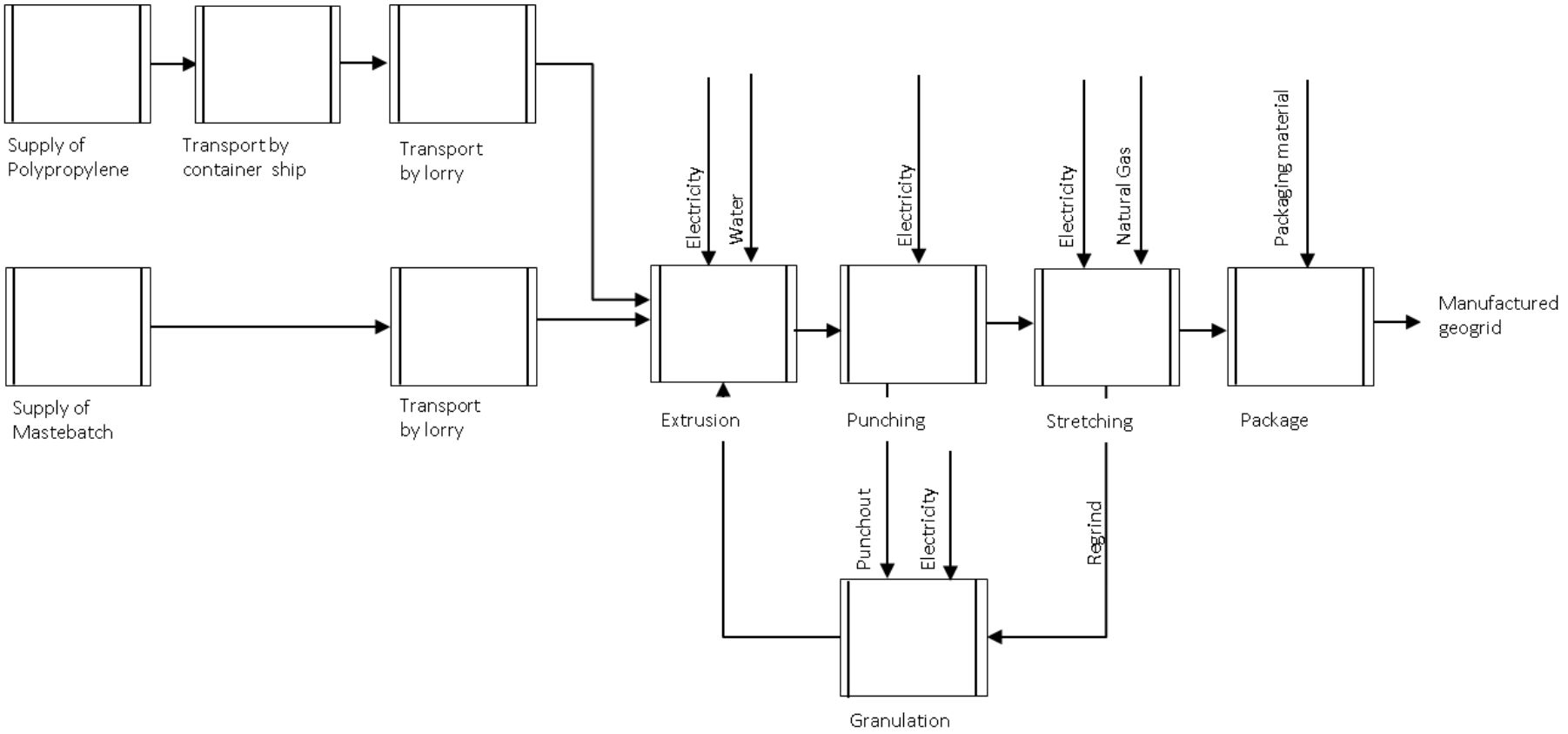
Supply of Polypropylene
Transport by container ship
Transport by lorry
Supply of Mastebatch
Transport by lorry
Electricity
Water
Extrusion
Electricity
Punching
Electricity
Natural Gas
Stretching
Packaging material
Package
Manufactured geogrid
Punchout
Electricity
Granulation
Regrind

2.7 Reference service life

A reference service life does not have to be declared, because this LCA does not declare the entire life cycle. Therefore it is a voluntary statement. According to the manufacturer the reference service lifetime of TriAx TX0 series is about 100 years.

3. LCA: Calculation rules

3.1 Declared unit

This declaration of the product TriAx TX5 refers to 1 m² geo grid with a mass per unit area of 189 g/m². The declared unit of TriAx TX5 is within the tolerance range of the ETA. All calculations refer to this declared unit.

Name	Quantity	Unit
Declared unit	1	m^2
Conversion factor to 1 kg	5,29	-
Mass per unit area	0,189	kg/m^2

3.2 System boundary

The Environmental Product Declaration is a cradle-to-gate EPD. It contains all the potential environmental impacts caused in the production stage. According to EN 15804 these are the production phases A1 to A3.

The environmental impacts caused by the infrastructure are neglected because of the high mass flow. Furthermore only the use of energy related to the production processes is considered (excluding offices, social rooms etc.).

The production stage includes:

- A1: Extraction and processing of the raw materials (Polypropylene, Masterbatch)
- A2: Transport to the production site
- A3: Processing of the geogrids (Extrusion, Punching, Stretching) and Packaging (including packaging material)

The production does not contain secondary materials or fuels.

The system boundaries, including the modules A1 to A3, were made in accordance with the PCR. The study does not contain any information about the modules A4, A5, B1 to B7, C1 to C4 and D.

3.3 Estimates and assumptions

If it was not possible to choose data sets with the geographic reference of the United Kingdom, a data set with a similar geographic reference was used.

The distance for the transport of raw materials as well as the types of transport could be determined. For the transport by road a truck with a payload of 27 tons, total weight 40 tons from generation EURO 4 was assumed. As utilization factor 85% was selected.

3.4 Cut-off criteria

All flows whose influence is higher than 1% on the total mass, energy or environmental impact are included in the Life Cycle Assessment. It is assumed, that the total neglected input flows are much less than 5% of energy usage and mass.

All process specific data could be determined and modelled by the use of generic data (GaBi-database). The polypropylene is bulk delivered in 24 tons batches – the pellet is blown into to silo. Therefore there is no packaging waste for the polypropylene.

The masterbatch is delivered in octabins made of cardboard and a thin polythene liner. Cardboard

and liner are recycled afterwards. As the amounts for the masterbatch packaging are quite small referred to the overall mass flow this packaging was neglected. It is assumed that the residues of the extrusion, punching and stretching processes are less than 1% of the total mass, energy or environmental impact. Therefore these residues are within the cut-off criteria and were neglected.

3.5 Background data and data quality

For all processes primary data was collected and provided by Tensar International Limited. The primary data refers to year 2014. For the data, which is not influenced by the manufacturer, generic data is used. The GaBi-database was used for the generic data. This database is updated regularly. The power sources were chosen from data for the UK in 2011, in accordance with the geographical and time representativeness. The study does not consider any other energy sources due to the fact, that just conventional power mix is used.
The modelling was made by using the LCA software GaBi 6, which was developed by thinkstep AG. Due to the comparability of the results all used data sets are consistent and documented. The documentation is available online (GaBi-documentation). Therefore the process specific and the generic data meet requirements of EN 15804.

3.6 Period under review

All process specific data were collected in 2014. The data is based on 1 year of averaged data.

3.7 Allocation

Allocations were avoided as far as possible. Tensar uses polypropylene (PP) for several products as a raw material and all PP residues, which occur during the manufacturing, are recycled. The residues are not mandatorily used again for the product from which they occurred. The material can also be used for products from another series.
For Example: 5 % residues of polypropylene occur during the manufacturing of geogrid A. These 5 % are recycled, but due to operating conditions, it can be that 4 % is reused for geogrid A and 1 % for geogrid B.
For this calculation it was assumed, that the generated punchout and the regrind material of a specific geogrid is reused in a closed loop recycling for the analysed geogrid. This was done to avoid product specific shifts of potential environmental impacts. It was also assumed that the recycled PP substitutes virgin PP after a regranulation without any quality losses during the process.

3.8 Comparability

A comparison or an evaluation of EPD data is only possible if all the data sets to be compared were created according to /EN 15804/ and the building context, respectively the product-specific characteristics of performance, are taken into account. The used background database has to be mentioned.

4. LCA: Scenarios and additional technical information

No other scenarios were considered in this EPD.

5. LCA: Results

The next tables show the environmental impact potentials for the different parameters, for the material flows as well as for the waste and other outputs. The results refer to the declared unit of 1 m^2 geogrid.

Description of the system boundary (X = included in LCA)																
Product stage			Construction process stage		Use stage							End of life stage				Benefits and loads beyond the system boundary
Raw material supply	Transport	Manufacturing	Transport	Installation process	Use	Maintenance	Repair	Replacement	Refurbishment	Operational energy use	Operational water use	De-construction / demolition	Transport	Waste processing	Disposal	Reuse-, Recovery-, Recycling potential
A1	**A2**	**A3**	**A4**	**A5**	**B1**	**B2**	**B3**	**B4**	**B5**	**B6**	**B7**	**C1**	**C2**	**C3**	**C4**	**D**
X	X	X	-	-	-	-	-	-	-	-	-	-	-	-	-	-

Results of the LCA – Environmental impact: 1 m² geogrid TriAx TX5		
Parameter	unit	A1 – A3
Global warming potential	[kg CO2-Eq.]	5,12E-01
Depletion potential of the stratospheric ozone layer	[kg CFC11-Eq.]	3,91E-11
Acidification potential of land and water	[kg SO2-Eq.]	1,30E-03
Eutrophication potential	[kg $(PO4)^3$-Eq.]	1,27E-04
Photochemical Ozone Creation Potential	[kg Ethen-Eq.]	1,78E-04
Abiotic depletion potential for non-fossil resources	[kg Sb-Eq.]	1,01E-07
Abiotic depletion potential for fossil resources	[MJ]	1,52E+01

Results of the LCA – Resource use: 1 m² geogrid TriAx TX5		
Parameter	unit	A1 – A3
Renewable primary energy as energy carrier	[MJ]	4,02E-01
Renewable primary energy resources as material utilization	[MJ]	IND
Total use of renewable primary energy resources	[MJ]	4,02E-01
Non-renewable primary energy as energy carrier	[MJ]	7,87E+00
Non-renewable primary energy as material utilization	[MJ]	8,13E+00
Total use of non-renewable primary energy resources	[MJ]	1,60E+01
Use of secondary material	[kg]	IND
Use of renewable secondary fuels	[MJ]	IND
Use of non-renewable secondary fuels	[MJ]	IND
Use of net fresh water	[m^3]	2,01E-03

Results of the LCA – Waste and output flows: 1 m² geogrid TriAx TX5		
Parameter	unit	A1 – A3
Hazardous waste disposed	[kg]	1,83E-06
Non-hazardous waste disposed	[kg]	4,84E-01
Radioactive waste disposed	[kg]	3,32E-04
Components for re-use	[kg]	IND
Materials for recycling	[kg]	IND
Materials for energy recovery	[kg]	IND
Exported electrical energy	[MJ]	IND
Exported thermal energy	[MJ]	IND

6. LCA: Interpretation

The table “LCA: Interpretation” shows the influence of the phases A1, A2 and A3 on the production stage and it can be seen that the analysed impact categories are mainly influenced by the raw material supply (A1). The share varies from 50-96 % depending on the impact category. The supply of polypropylene is identified as the most significant parameter for the raw material supply in all analysed impact categories. Another significant parameter results from the emissions which occur through the use of energy.

The manufacturing phase (A3) is identified as another influential phase of the production stage, whereas the influence varies from 4 to 35 % The share of this stage on the total Global warming potential (GWP), Acidification (AP) and Eutrophication potential (EP) of the production stage is between 34 – 35 % and for the categories Depletion potential of the Stratospheric ozone layer (ODP), Photochemical Ozone Creation Potential (POCP) and Abiotic depletion potential for fossil resources (ADP_f) the share is between 16 – 17 %.

The emissions based on the transport are marginal for all impact categories, except for the Eutrophication (EP) and Acidification potential (AP) with 14 and 16 %.

LCA: Interpretation			
Parameter	A1	A2	A3
Global warming potential	64%	2%	34%
Depletion potential of the stratospheric ozone layer	83%	0%	17%
Acidification potential of land and water	51%	14%	35%
Eutrophication potential	50%	16%	34%
Photochemical Ozone Creation Potential	79%	4%	17%
Abiotic depletion potential for non-fossil resources	96%	0%	4%
Abiotic depletion potential for fossil resources	83%	1%	16%

7. Requisite evidence

In 2008 TriAx TX 160 was tested concerning its leaching behaviour using the trough method. Due to this method the institute “Prüftechnik CDL” could determine the direct environmental impacts to the local environment (soil and groundwater). No parameters from the Bundes-Bodenschutz- und Altlastenverordnung (BBodSchV) were found in the 5. eluate, except from phenol. The analysed phenol concentrations are with 12 µg below the threshold value of the BBodSchV.

In accordance to the criteria of the BBodSchV the environmental soundness of the geogrid could be confirmed. This result can be transferred to all the other types of geogrids referring to the product series TX0, so as well to TriAx TX5.

8. References

GaBi 6: Software und Datenbank zur Ganzheitlichen Bilanzierung. LBP, Universität Stuttgart und PE INTERNATIONAL, 2015

CML-IA April 2013 – Characterisation factors developed by Institut of Environmental Sciences (CML): Universität Leiden, Niederlande - http://www.cml.leiden.edu/software/data-cmlia.html

Klöpffer & Grahl 2009 – Ökobilanz (LCA): Ein Leitfaden für Ausbildung und Beruf. Wiley-VCH Verlag GmbH & Co. KGaA; Auflage: 1. Edition

European Technical Assessment ETA-12/0529, TriAx TX 0 series, Tensar International Ltd, Kiwa K76037, EOTA 2012

ISO 14040: 2006: ISO/TC 207/SC 5: Environmental management -- Life cycle assessment -- Principles and framework, International Organization for Standardization, 2006

ISO 14044: 2006: ISO/TC 207/SC 5: DIN Deutsches Institut für Normung e.V.: Environmental management -- Life cycle assessment -- International Organization for Standardization, 2006

ISO 14025: 2006: ISO/TC 207/SC 5: Environmental labels and declarations -- Type III environmental declarations -- Principles and procedures International Organization for Standardization, 2006

BS EN 15804:2012: Sustainability of construction works. Environmental product declarations. Core rules for the product category of construction products; Beuth Verlag. Berlin, 2012.

BS EN 12224: 2000: Geotextiles and geotextile-related products - Determination of the resistance to weathering; BSI

BS EN 3249ff: 2001: Geotextiles and geotextile-related products. Characteristics required for use in the construction of roads and other trafficked areas (excluding railways and asphalt inclusion), BSI

Regulation (EC) No. 305/2011 of the European Parliament and of the Council; 2011-03

Kiwa BCS Öko-Garantie GmbH – Ecobility Experts (Hrsg):

Produktkategorieregeln für Geokunststoff/-textilien: Anforderungen Umweltproduktdeklarationen für Geokunststoff/textilien; 2017-06

Allgemeine Produktkategorieregeln für Bauprodukte: Rechenregeln für die Ökobilanz und Anforderungen an den Hintergrundbericht; 2017-06

Allgemeine Programmanleitung aus dem EPD-Programm der Kiwa BCS öko-Garantie GmbH – Ecobility Experts; 2017-06

	Publisher Kiwa BCS Öko-Garantie GmbH – Ecobility Experts Marientorbogen 3-5 90402 Nürnberg Deutschland/Germany	E-Mail Web	ecobility@bcs-oeko.de www.kiwabcs.com/ecobility
	Programme operator Kiwa BCS Öko-Garantie GmbH – Ecobility Experts Marientorbogen 3-5 90402 Nürnberg Deutschland/Germany	E-Mail Web	ecobility@bcs-oeko.de www.kiwabcs.com/ecobility
	Author of the Life Cycle Assessment Kiwa GmbH Voltastr. 5 13355 Berlin Germany	Tel. Fax. E-Mail Web	+49(0)30/467761-43 +49(0)30/467761-10 info@kiwa.de www.kiwa.de
	Owner of Declaration Tensar International Limited Units 2-4 Cunningham Court Shadsworth Business Park Blackburn, United Kingdom	Tel. Fax. E-Mail Web	+44(0)1254 262431 +44(0)1254 266868 info@tensar-international.com www.tensar.co.uk

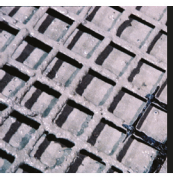

C50 – 1.8 x 1.6

Carbon Fiber Reinforcing Grids for Concrete Structures

C-GRID® REINFORCED

DESCRIPTION C-GRID® C50 – 1.8 x 1.6 is one of the C50 Series of high strength carbon fiber/epoxy grids for reinforcing concrete structures. Large high strength carbon strands are aligned in both longitudinal and transverse directions.

FEATURES

- Non-corrosive; can be used with as little as 1/4" (6 mm) of cover
- Requires less concrete cover leading to lighter structures
- Lightweight, easy to handle and use; can be cut to fit using conventional tin snips
- High tensile strength and modulus
- Outstanding mechanical bond with concrete; requires a mimimum 1/4" (6 mm) to develop its strength

APPLICATIONS

- Slabs-on-grade
- Thin topping slabs and overlays
- Marine structures
- Concrete repair and shotcrete
- Silos and concrete storage tanks
- Balconies
- Precast concrete, including architectural and wall panels

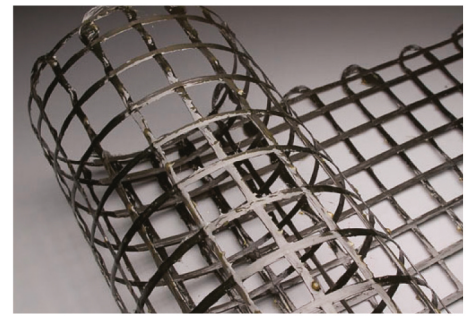

PHYSICAL PROPERTIES

Composition	carbon fiber and epoxy resin
Color	black
Grid geometry (longitudinal x transverse spacing)	1.8" x 1.6" (46 mm x 41 mm)
Supply form (custom widths and lengths also available)	47.5" (or 95") x 450 yd (1.2 m x 411.5 m) rolls

TYPICAL MECHANICAL PROPERTIES

	LONGITUDINAL PROPERTIES		TRANSVERSE PROPERTIES	
Individual strand cross-sectional area	0.002860 in^2	(1.85 mm^2)	0.002860 in^2	(1.85 mm^2)
Average number of strands per unit width	6.67 strands/ft	(21.87 strands/m)	7.5 strands/ft	(24.61 strands/m)
Area of strands per unit width	0.019067 in^2/ft	(40.36 mm^2/m)	0.021450 in^2/ft	(45.4 mm^2/m)
Strand tensile strength	830 lbs	(3.7 kN)	730 lbs	(3.25 kN)
Grid tensile strength per unit width	5,530 lbs/ft	(80.75 kN/m)	5,480 lbs/ft	(79.9 kN/m)
Tensile modulus of elasticity	34,000 ksi	(234,500 MPa)	34,000 ksi	(234,500 MPa)
Elongation at break	0.76%	(0.76%)	0.76%	(0.76%)

Application Use Note: C-GRID® remains a relatively novel material without the extensive performance history of traditional construction materials. Reported properties are average values, not design values. Structures and applications using C-GRID® should be designed using appropriate safety factors or load and strength reduction factors. All applications utilizing C-GRID®, including critical life safety and fire rated structures, should be designed and reviewed by a licensed engineer experienced with FRP materials. The data expressed herein is believed to be accurate at the time of publication; however, it is subject to change without notice.

Notes:

1. Centerline-to-centerline spacing between strands is nominal and based on the average number of strands per unit width. Actual spacing may vary by ± 0.10" (± 2.5mm).
2. The longitudinal direction is in the direction of the roll, and the transverse direction is across the width of the roll. For example, if a roll of C-GRID® is 47.5" wide, the carbon strands in the transverse direction are 47.5" in length. If a roll of C-GRID® is 500 yards long, the longitudinal strands are 500 yards in length.
3. Individual strand cross-sectional area is normalized to the cross-sectional area of the fibers in accordance with ACI 440.2R. The actual measured thickness and width are larger and shall not be used for design purposes.
4. Reported tensile strengths are based on the average minus two standard deviations (AVG-2σ) of a large population of test results. Tensile modulus values are based on properties reported by the carbon fiber supplier. C-GRID® exhibits linear elastic behavior, so failure strains are estimated using Hooke's Law.

Production

CHOMARAT

Our world is textile

Exclusive distribution

B&R BUILDING MATERIALS

Innovative Solutions & Support

Hoge Mauw 460 | B-2370 Arendonk | T +32 14 68 91 50 | F +32 14 68 91 51
www.benrbuildingmaterials.be | BE0546 916 484
Christophe De Saeger | T +32 474 74 07 59 | christophe.desaeger@benrbuildingmaterials.be

Mortar properties without fibers

De gemiddelde waarden van de onderzochte eigenschappen van het geprinte beton zijn samengevat:

Tabel 2. Gemiddelde waarde onderzochte eigenschappen geprint beton

Eigenschap (eenheid)	**M1 mengsel zonder vezel**			
	opentijd			
	kort (K)		lang (L)	
	||| (A)	≡ (B)	||| (A)	≡ (B)
	1KA*	1KB*	1LA*	1LB*
Druksterkte (MPa)	68,6	73,9	71,5	75,7
Splijttreksterkte (MPa)	4,7	5,2	5,4	5,1
Vol. massa (kg/m^3)	2132	2120	2144	2157
Hechtsterkte (MPa)		2,0		1,9
Therm. uitz.coef. ($^oC^{-1}$)		18.10^{-6}		
Waterabs VDZ (%m/m)		0,61		
Scaling VDZ (kg/m^2)		0,009		
E_n/E_0 na VD-proef (%)	101 (geen schade)			

* K/L = korte/lange 'open tijd'; A/B = parallel aan/loodrecht op geprinte laagjes mortel

Fiber specifications

het materiaal = polyvinylalcohol (pva).
lengte = 6 mm
diameter = 26 micron
treksterkte = 1,6 GPa
rek bij breuk = 6 %
density = 1,3 g/cm3
Young's modulus = 39 GPa
dosering = 3,0 kg/m3

9.3. Grasshopper and Karamba script

Grasshopper and Karamba script

<u>Design parameters panel:</u>

The panel size is controlled by the parameters L and B which are determined by the print table (or transport restrictions).

The perforation of the panel is governed by 6 parameters as visible in the figures. They shape and position one perforation in the panel and check the total perforation percentage.

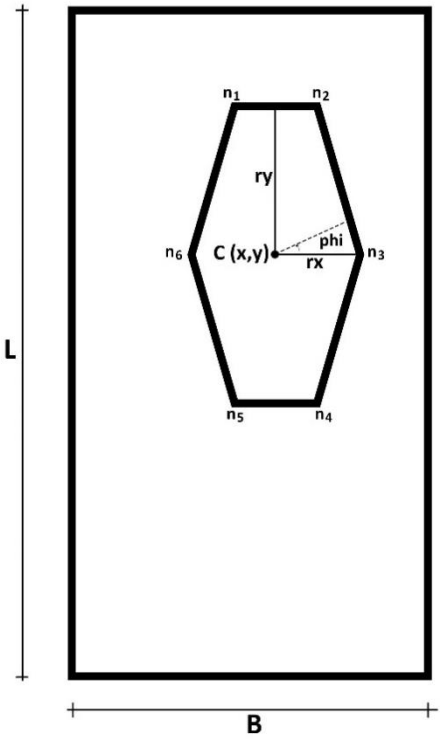

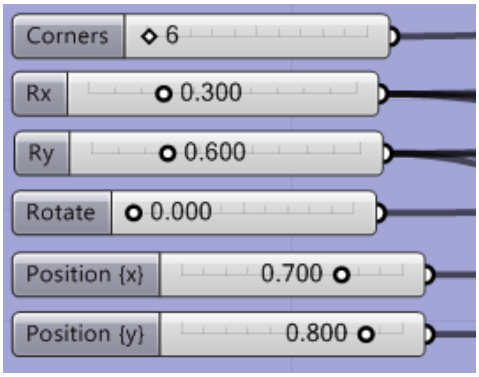

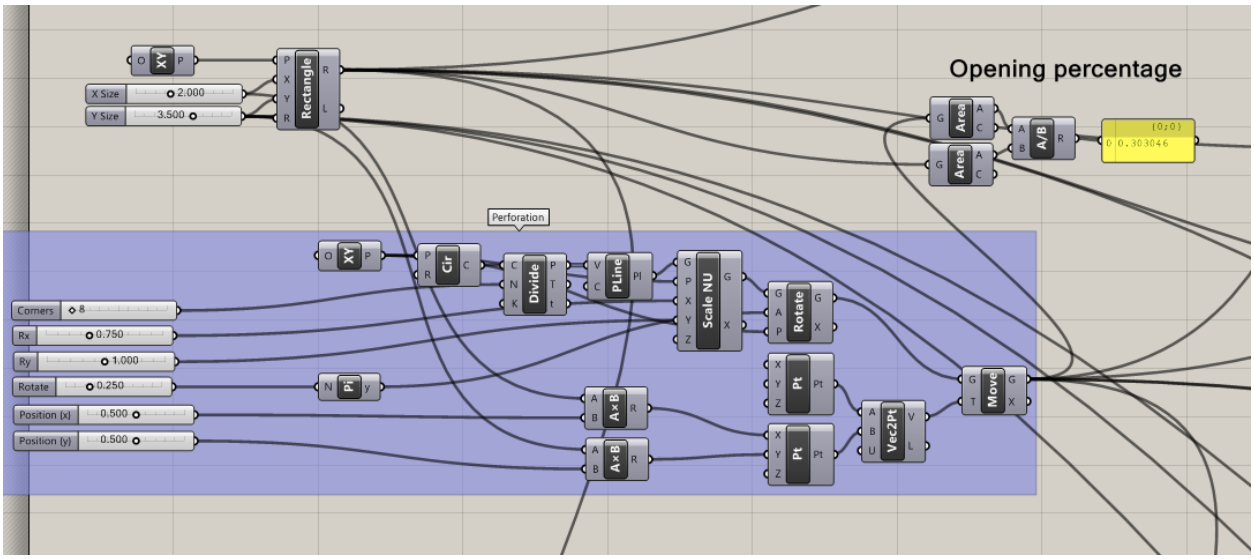

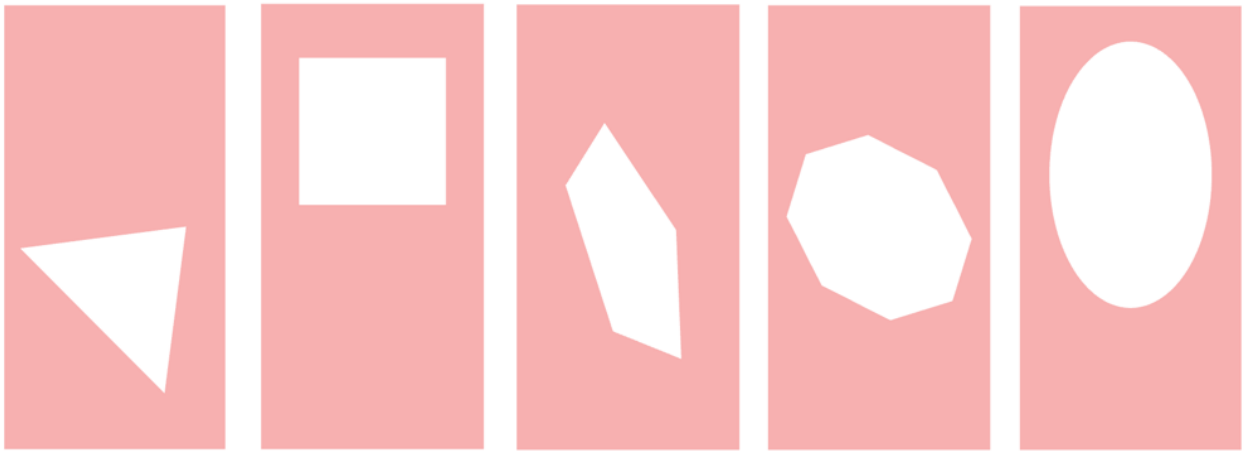

Mesh

The panel is now defined as a surface from which the perforation is split. But in order to perform structural calculations on the model, the surface needs to be transformed to a mesh (mesh Brep). Using custom mesh settings, the mesh refinement can be determined, which needs to be high in order to achieve an accurate result and lower the (false) peak stresses at sharp mesh edges.

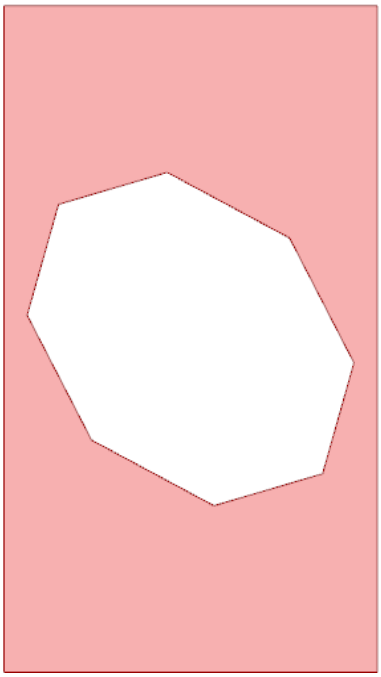

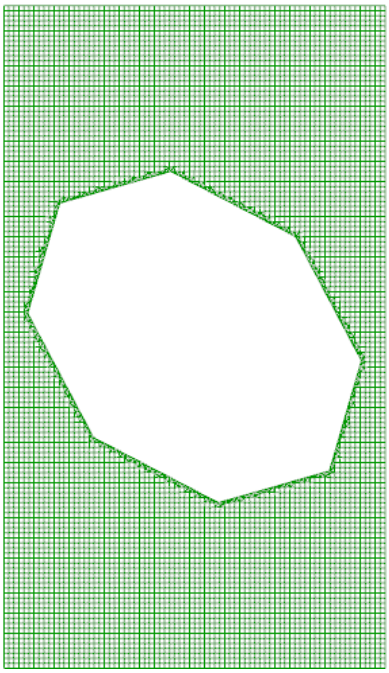

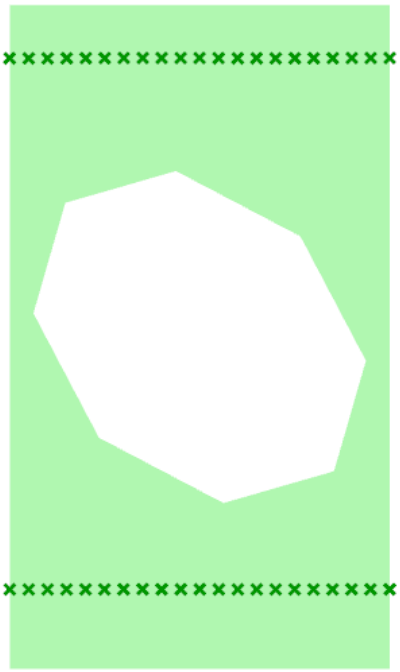

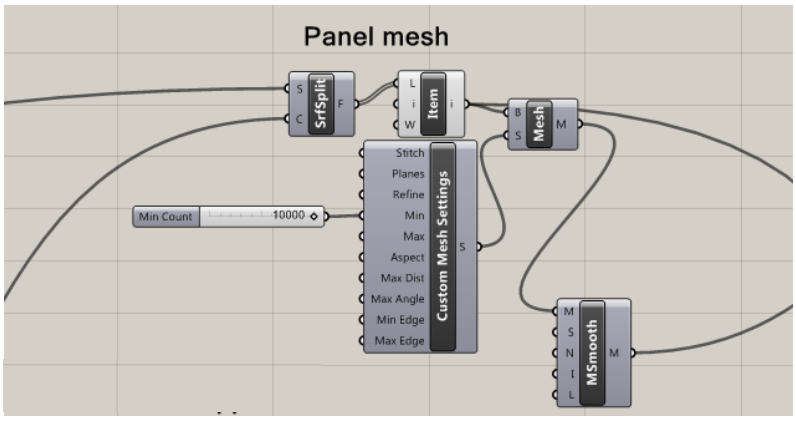

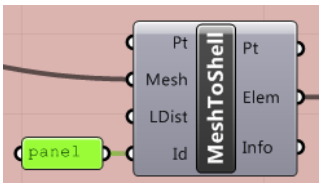

The mesh forms input for the Karamba model and is interpreted as a shell element. The cross section of the panel is defined as a constant over the length and width of the element, and determined by a parameter in cm.

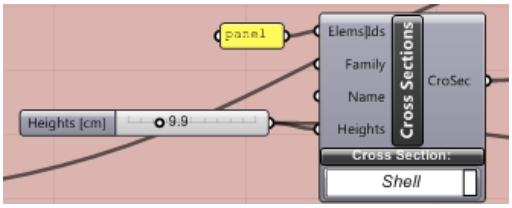

Supports

The supports are located on intersection of the mesh grid. For the case study loading these are defined as two line supports on the indicated positions on the previous page. The position of the lines can be altered by two individual sliders which indicated the distance from the edge of the panel.

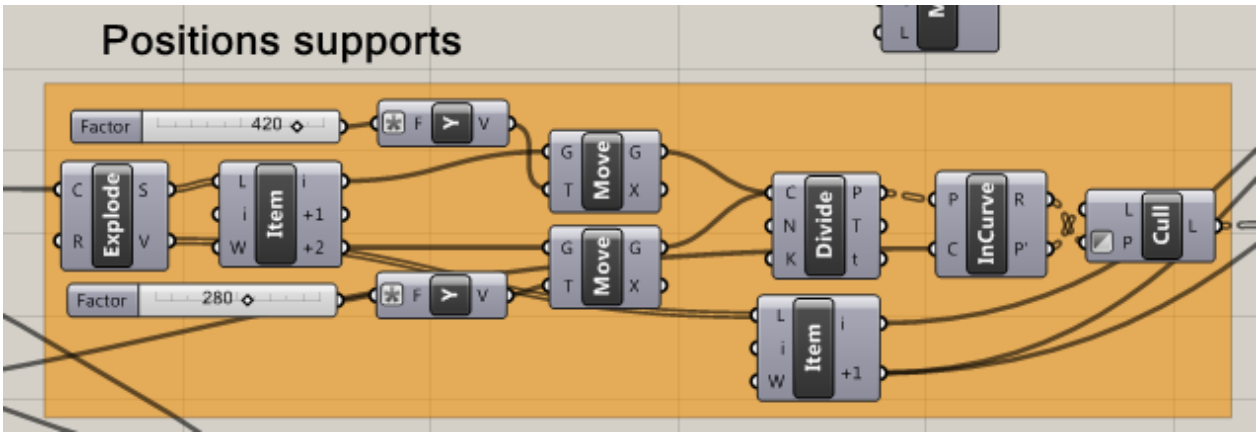

The supports are defined as restrictions in translation in z-direction by Karamba. Two corner points of the panel are also restricted in x and y direction in order to make the model kinematically determinant.

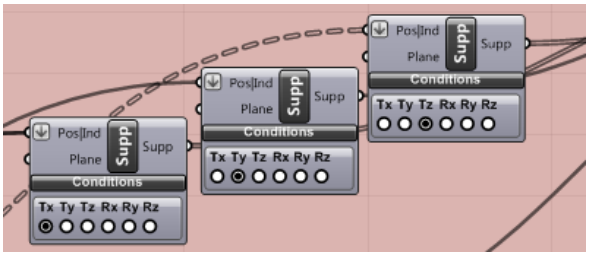

Loads

Different load cases are defined, in order to analyze each:

- Gravity load is defined by the panel mesh

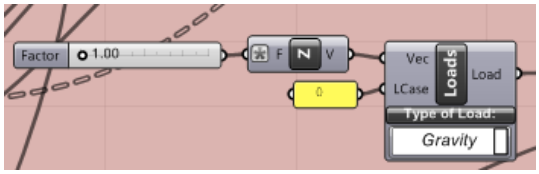

- A line load A line load is simulated by a mesh load on the panel by defining a small segment of the mesh at midspan as the surface on which the load is acting. The amplitude of the load is governed by a slider.

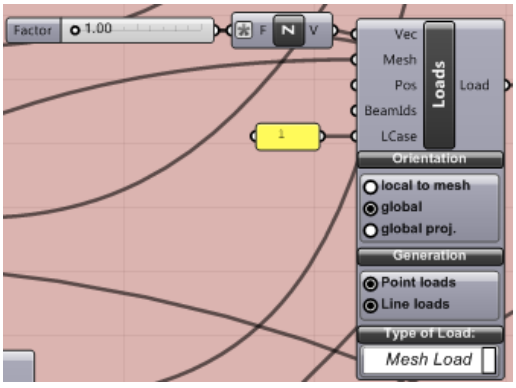

Gravity in z and x direction:

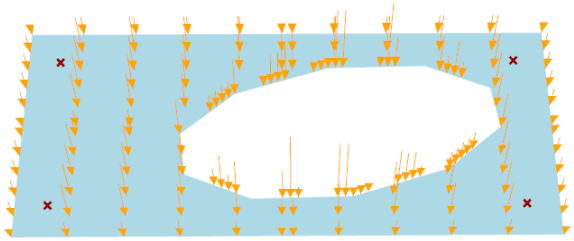

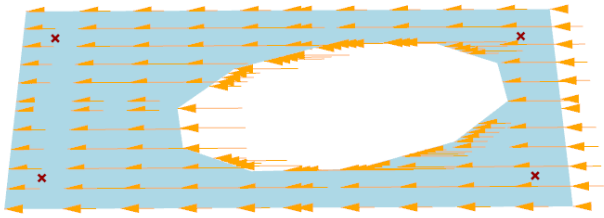

Fall protection loading as point (20x20cm) and line load:

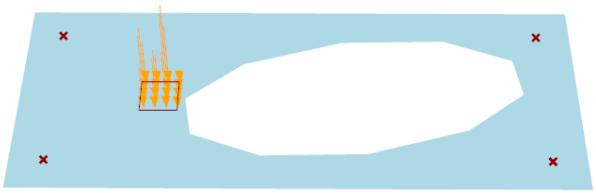

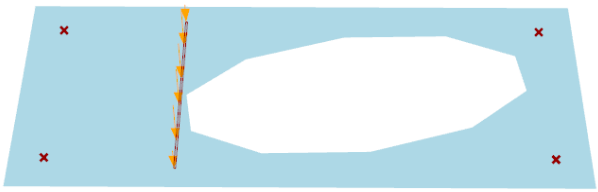

Material

The material is set to concrete C50/60, but the “utilization” output from Karamba is not used.

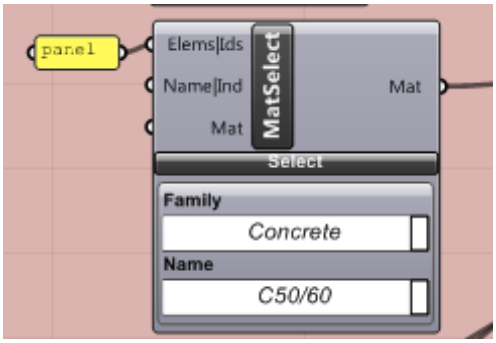

Output

The Karamba model is assembled and analyzed. A color gradient is defined to represent the stresses which are displayed by the shell view component. A legend is retrieved from which the stresses can be quantified.

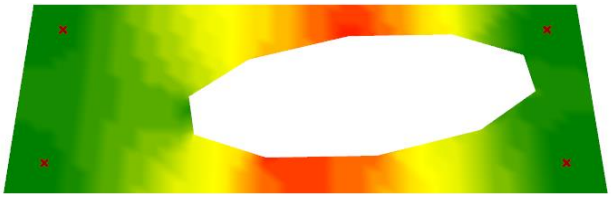

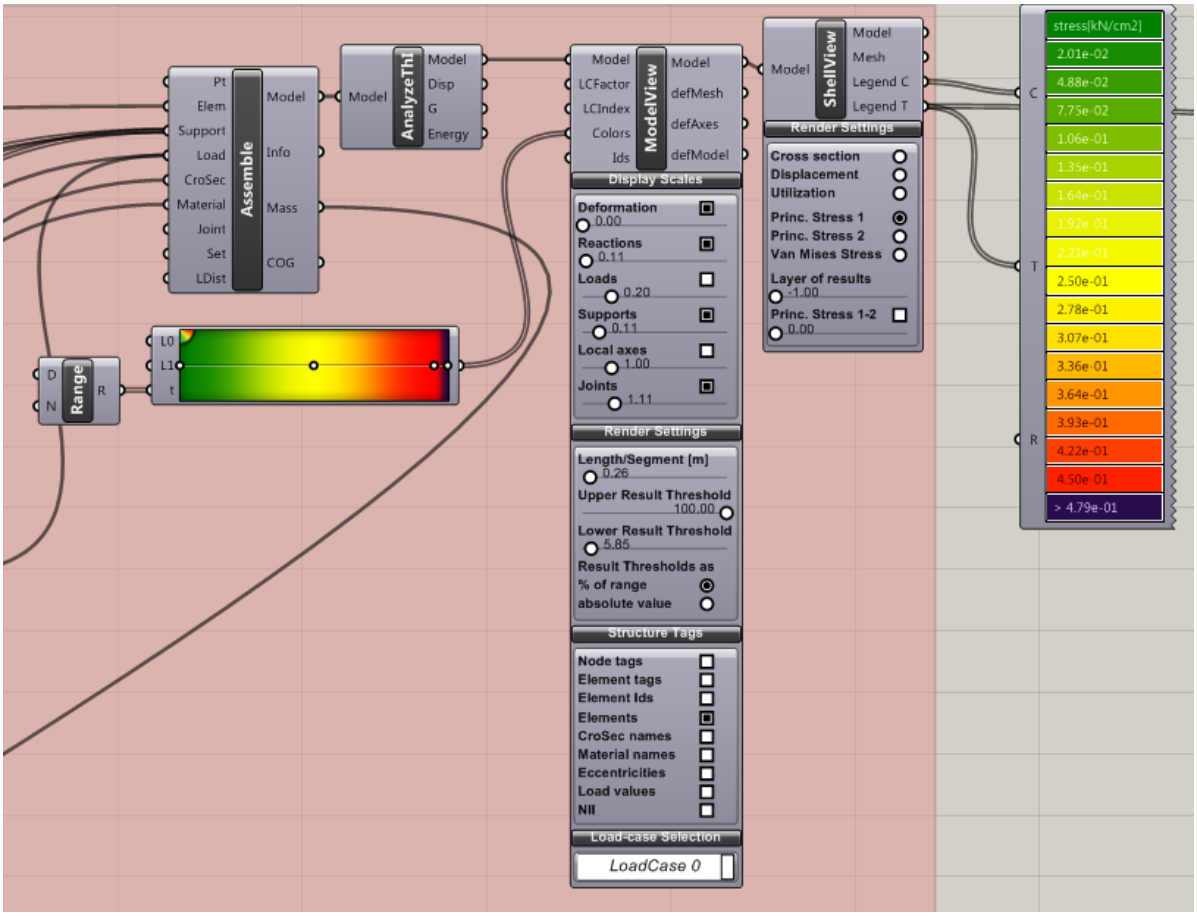

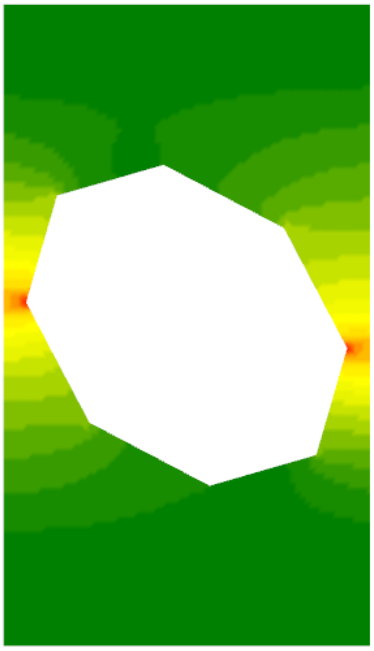

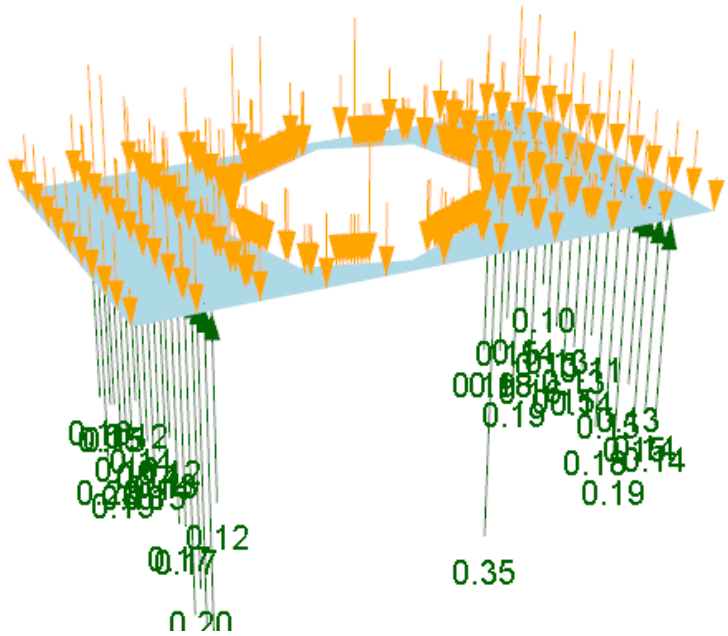

The maximum stress and deflections are checked with SCIA for specific models and given load cases in order to determine whether the mesh is correct and the model fully functional. Some rounding errors occurred, and overall the system is very sensitive to mesh shape and refinement.

Hand calculations

Reducing surface loads to line loads and reducing the element to a beam with given critical cross section:

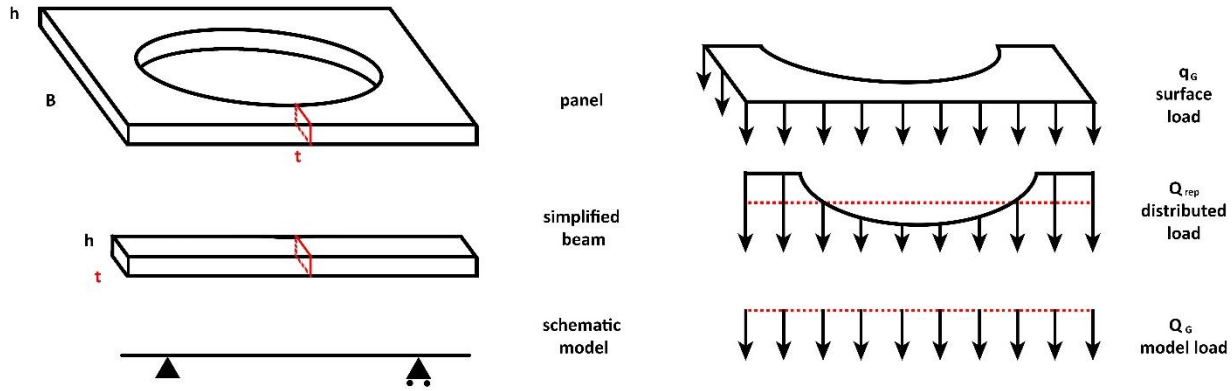

Defining bending moment at midspan using simplified model:

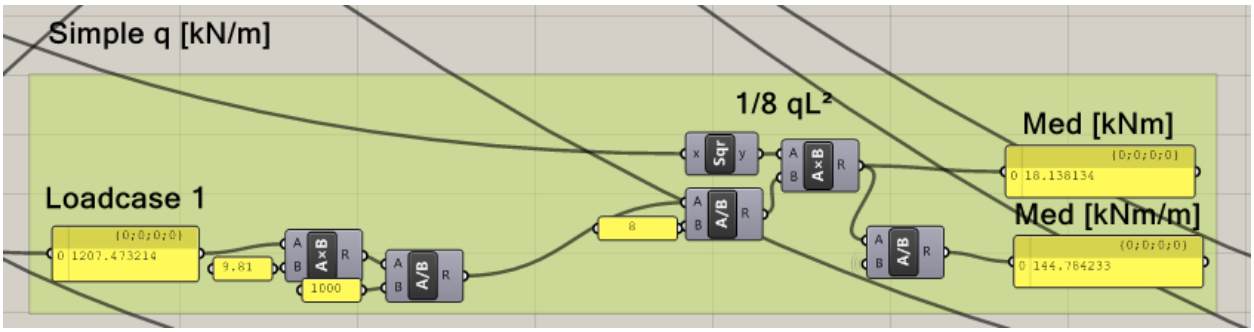

Calculating Required reinforcement

The bending moment (Med) is then used to calculate the required reinforcement. This is done by defining the critical cross-section and performing reinforced concrete calculations according to the model below.

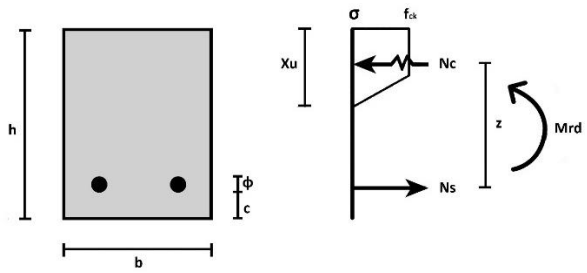

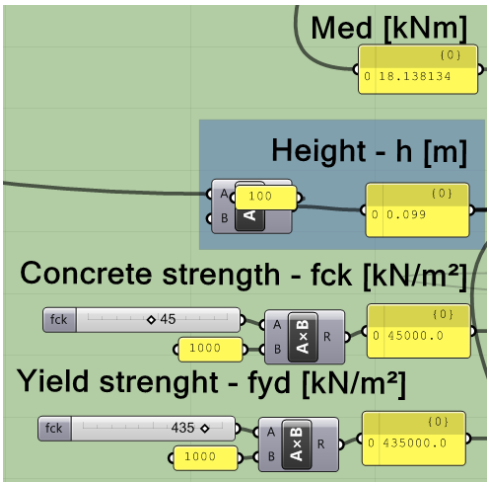

Finding the critical cross-section

The panel is cut at 30 points over the width. At each cut the length of the section is determined, and the shortest segment is defined as the width of the critical cross-section. This is then used as input for the section modulus of the simplified beam.

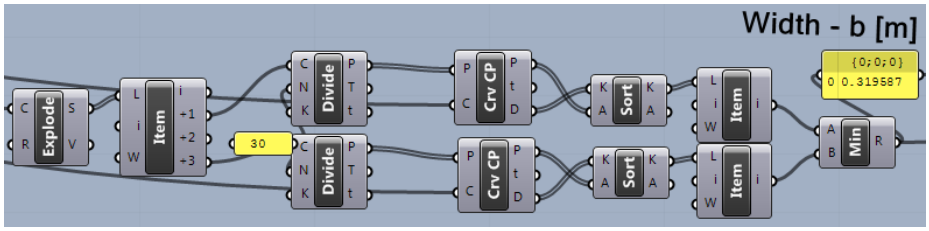

Given the number of bars that can be placed in the critical cross-section and the required concrete cover, the model determines the minimum rebar diameter that is necessary to give the element sufficient load bearing capacity.

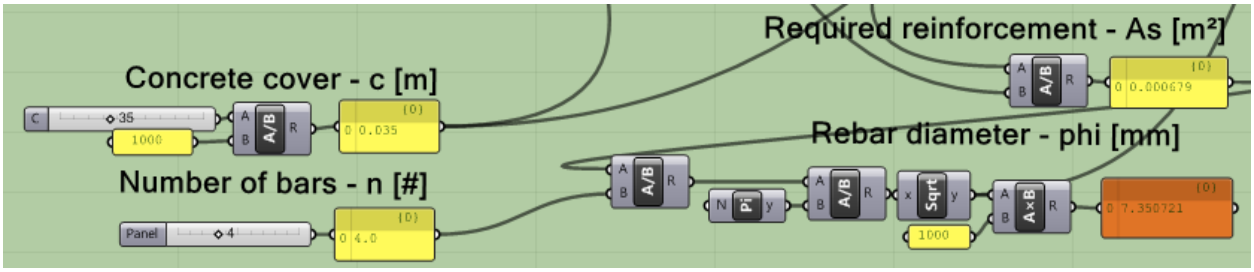

For the case study design, the reinforcement was designed given the load combination:

- **Wind: Surface load in z-direction of 1.95 kN/m²**
- **Gravity: Surface load in y-direction**
- **Fall protection: line load in z-direction of 1 kN/m**

Four rebars with a diameter of 5mm each are found sufficient for the given panel design

9.4. Bending Moment Resistance Case Study Panels

Input
Panel 1: 3D printed panel, casted with ZVB concrete, carbonfiber reinforcement netting.
Design: rectangluar outline, oval perforation of 30% surface area.
Phase: Testing (final)

Geometry panel

$L := 2.955m$ Length element

$B := 1.235m$ Width element

Critical cross-section

$b := 320mm$ Cross-section width

$h := 99mm$ Cross-section height

Reinforcement: C-Grid carbonfiber net in critical cross-section (left)

$Ar := 1.85mm^2$ Cross-sectional area per strand

$s := 46mm$ Spacing strands

$n := 7$ Number of strands

$c := 45mm$ Concrete cover (bottom)

$Nrt := 3.7kN$ Tension strength per strand

$\frac{Nrt}{Ar} = 2 \times 10^3 \cdot MPa$ Tensile strength carbon fiber

Concrete: Self compacting concrete (14 days)

$fck := 45 \frac{N}{mm^2}$ Concrete compression strength (ZVB after 14 days)

$fctm := 4.43 \frac{N}{mm^2}$ Concrete tensile strength (ZVB after 14 days)

$Ec := 35000MPa$ Youngs modulus concrete

$\rho := 2500 \frac{kg}{m^3}$ Concrete density

$\alpha := 0.75$ Shape factors for concrete compression zone

$\beta := 0.389$

Calculation
Bending moment resistance

$Nr := Nrt \cdot n = 25.9 \cdot kN$ — Tension force in C-grid

$Nc := Nr$ — Concrete compression force

$Xu := \frac{Nc}{\alpha \cdot fck \cdot b} = 2.398 \cdot mm$ — Concrete compression zone height

$z := h - c - \beta \cdot Xu = 53.067 \cdot mm$ — Internal lever arm

$Mrd := Nc \cdot z = 1.374 \cdot kN \cdot m$ — Bending moment resistance

$Mrdm := \frac{Mrd}{b} = 4.295 \cdot kN \cdot \frac{m}{m}$ — Bending moment resistance per meter

$Mcr := fctm \cdot \frac{b \cdot h^2}{6} = 2.316 \cdot kN \cdot m$ — Bending moment at cracking of concrete

$Mcr > Mrd = 1$ — Check if concrete cracks before reaching failure
1 = uncracked, 0 = cracked

Load bearing capacity:
simplified panel to simply supported beam with cross section bxh of critical cross-section
The supports are set at distance S from either end of the beam

$S := 400mm$ — Distance of support from element edge

$Ls := L - 2 \cdot S = 2.155\,m$ — Span length

$qrd := \frac{Mrd}{\left[\frac{1}{(8)} \cdot Ls^2 - \frac{1}{2} \cdot S^2\right]} = 2.746 \cdot \frac{kN}{m}$ — Load bearing capacity for a linear distributed load over the length of the simplified beam

Check loading for test

The panel is simplified to a simply supported beam with cross-section bxh
The supports are set at distance S from either end of the beam
The selfweight is distributed equally over the length of the beam (conservative approach)

Self weight

$Weight := L \cdot B \cdot h \cdot 0.7 \cdot \rho \cdot g = 6.2 \cdot kN$ Total weight of the panel

$qself := \frac{Weight}{2 \cdot L} = 1.049 \cdot \frac{kN}{m}$ Representative linear distributed load for self weight

$Mspan := \frac{qself}{8} \cdot Ls^2 - \frac{qself}{2} \cdot S^2 = 0.525 \cdot kN \cdot m$ Bending moment at midspan due to self weight

$Mcr > Mspan = 1$ Test if concrete is cracked under self weight alone
1 = uncracked, 0 = cracked

$Mrest := Mrd - Mspan = 0.849 \cdot kN \cdot m$ Remaining bending moment resistance for test load

$Frd := 4 \cdot \frac{Mrest}{Ls} = 1.577 \cdot kN$ Load bearing capacity for panel in 3 point bending test under self weight

Maximum deflection

$I := \frac{b \cdot h^3}{12}$ Inertia of critical cross-section

$uz := \frac{5}{384} \cdot \frac{qself}{Ec \cdot I} \cdot Ls^4 - \frac{1}{16} \frac{qself}{Ec \cdot I} \cdot S^2 \cdot Ls^2 = 0.272 \cdot mm$ Maximum deflection before loading

Input
Panel 2: 3D printed panel, casted with SCC concrete, steel reinforcement netting.
Design: rectangluar outline, oval perforation of 30% surface area.
Phase: Testing (final)

Geometry

$L := 2.96m$ Length element

$B := 1.23m$ Width element

Critical cross-section

$b := 325mm$ Cross-section width

$h := 94mm$ Cross-section height

Reinforcement in critical cross-section (left)

$r := \frac{5}{2}mm$ Rebar radius

$s := 100mm$ Spacing bars

$n := 4$ Number of bars

$c := 50mm$ Concrete cover (bottom)

$fyd := 435 \frac{N}{mm^2}$ Steel yield strength

Concrete: Self compacting concrete (14 days)

$fck := 45 \frac{N}{mm^2}$ Concrete compression strength
(Tested SCC prism after 14 days)

$fctm := 4.43 \frac{N}{mm^2}$ Concrete tensile strength
(Tested SCC prism after 14 days)

$Ec := 35000MPa$ Youngs modulus concrete

$\rho := 2500 \frac{kg}{m^3}$ Concrete density

$\alpha := 0.75$ Shape factors for concrete compression zone

$\beta := 0.389$

Calculation
Bending moment resistance

$As := \pi r^2 \cdot n = 78.54 \cdot mm^2$ Reinforcement sectional area

$Ns := As \cdot fyd = 34.165 \cdot kN$ Yielding tension force in steel bar

$Nc := Ns$ Concrete compression force

$Xu := \frac{Nc}{\alpha \cdot fck \cdot b} = 3.115 \cdot mm$ Concrete compression zone height

$z := h - c - \beta \cdot Xu = 42.788 \cdot mm$ Internal lever arm

$Mrd := Nc \cdot z = 1.462 \cdot kN \cdot m$ Bending moment resistance

$Mrdm := \frac{Mrd}{b} = 4.498 \cdot kN \cdot \frac{m}{m}$ Bending moment resistance per meter

Check minimal and maximum reinforcement

$Asmin := \frac{b \cdot h^2}{6} \cdot \frac{fctm}{fyd \cdot z} = 113.914 \cdot mm^2$ Minimum reinforcement cross-sectional area

$Mcr := fctm \cdot \frac{h^2}{6} = 6.524 \cdot kN \cdot \frac{m}{m}$ Bending moment at cracking of concrete

$Mcr > Mrdm = 1$ Check if concrete cracks before reaching failure
1 = uncracked, 0 = cracked

Load bearing capacity:
simplified panel to simply supported beam with cross section bxh of critical cross-section
The supports are set at distance S from either end of the beam

$S := 400mm$ Distance of support from element edge

$Ls := L - 2 \cdot S = 2.16\,m$ Span length

$qrd := \frac{Mrd}{\left[\frac{1}{(8)} \cdot Ls^2 - \frac{1}{2} \cdot S^2\right]} = 2.905 \cdot \frac{kN}{m}$ Load bearing capacity for a linear distributed load over the length of the simplified beam

Check loading for test

The panel is simplified to a simply supported beam with cross-section bxh
The supports are set at distance S from either end of the beam
The selfweight is distributed equally over the length of the beam (conservative approach)

Self weight

$Weight := L \cdot B \cdot h \cdot 0.7 \cdot \rho \cdot g = 5.873 \cdot kN$ Total weight of the panel

$qself := \frac{Weight}{2 \cdot L} = 0.992 \cdot \frac{kN}{m}$ Representative linear distributed load for self weight

$Mspan := \frac{qself}{8} \cdot Ls^2 - \frac{qself}{2} \cdot S^2 = 0.499 \cdot kN \cdot m$ Bending moment at midspan due to self weight

$Mcr \cdot b > Mspan = 1$ Test if concrete is cracked under self weight alone
1 = uncracked, 0 = cracked

$Mrest := Mrd - Mspan = 0.963 \cdot kN \cdot m$ Remaining bending moment resistance for test load

$Frd := 4 \cdot \frac{Mrest}{Ls} = 1.783 \cdot kN$ Load bearing capacity for panel in 3 point bending test under self weight

Maximum deflection

$I := \frac{b \cdot h^3}{12}$ Inertia of critical cross-section

$uz := \frac{5}{384} \cdot \frac{qself}{Ec \cdot I} \cdot Ls^4 - \frac{1}{16} \frac{qself}{Ec \cdot I} \cdot S^2 \cdot Ls^2 = 0.298 \cdot mm$ Maximum deflection before loading

Input
Panel 3: 3D printed panel, casted with SCC concrete, steel reinforcement netting.
Design: rectangluar outline, oval perforation of 30% surface area.
Phase: Testing (final)

Geometry

$L := 2.960\,m$ Length element

$B := 1.235\,m$ Width element

Critical cross-section

$b := 320\,mm$ Cross-section width

$h := 95\,mm$ Cross-section height

Reinforcement in critical cross-section (left)

$r := \frac{5}{2}\,mm$ Rebar radius

$s := 100\,mm$ Spacing bars

$n := 4$ Number of bars

$c := 46\,mm$ Concrete cover (bottom)

$fyd := 435\,\frac{N}{mm^2}$ Steel yield strength

Concrete: Self compacting concrete (14 days)

$fck := 45\,\frac{N}{mm^2}$ Concrete compression strength
(ZVB after 14 days)

$fctm := 4.43\,\frac{N}{mm^2}$ Concrete tensile strength
(ZVB after 14 days)

$Ec := 35000\,MPa$ Youngs modulus concrete

$\rho := 2500\,\frac{kg}{m^3}$ Concrete density

$\alpha := 0.75$ Shape factors for concrete compression zone

$\beta := 0.389$

Calculation
Bending moment resistance

$As := \pi r^2 \cdot n = 78.54 \cdot mm^2$ Reinforcement sectional area

$Ns := As \cdot fyd = 34.165 \cdot kN$ Yielding tension force in steel bar

$Nc := Ns$ Concrete compression force

$Xu := \frac{Nc}{\alpha \cdot fck \cdot b} = 3.163 \cdot mm$ Concrete compression zone height

$z := h - c - \beta \cdot Xu = 47.769 \cdot mm$ Internal lever arm

$Mrd := Nc \cdot z = 1.632 \cdot kN \cdot m$ Bending moment resistance

$Mrdm := \frac{Mrd}{b} = 5.1 \cdot kN \cdot \frac{m}{m}$ Bending moment resistance per meter

Check minimal and maximum reinforcement

$Asmin := \frac{b \cdot h^2}{6} \cdot \frac{fctm}{fyd \cdot z} = 102.615 \cdot mm^2$ Minimum reinforcement cross-sectional area

$Mcr := fctm \cdot \frac{b \cdot h^2}{6} = 2.132 \cdot kN \cdot m$

Load bearing capacity:
simplified panel to simply supported beam with cross section bxh of critical cross-section
The supports are set at distance S from either end of the beam

$S := 400mm$ Distance of support from element edge

$Ls := L - 2 \cdot S = 2.16\,m$ Span length

$qrd := \frac{Mrd}{\left[\frac{1}{(8)} \cdot Ls^2 - \frac{1}{2} \cdot S^2\right]} = 3.243 \cdot \frac{kN}{m}$ Load bearing capacity for a linear distributed load over the length of the simplified beam

Check loading for test

The panel is simplified to a simply supported beam with cross-section bxh
The supports are set at distance S from either end of the beam
The selfweight is distributed equally over the length of the beam (conservative approach)

Self weight

$Weight := L \cdot B \cdot h \cdot 0.7 \cdot \rho \cdot g = 5.96 \cdot kN$ Total weight of the panel

$qself := \frac{Weight}{2 \cdot L} = 1.007 \cdot \frac{kN}{m}$ Representative linear distributed load for self weight

$Mspan := \frac{qself}{8} \cdot Ls^2 - \frac{qself}{2} \cdot S^2 = 0.507 \cdot kN \cdot m$ Bending moment at midspan due to self weight

$Mcr > Mspan = 1$ Test if concrete is cracked under self weight alone
1 = uncracked, 0 = cracked

$Mrest := Mrd - Mspan = 1.125 \cdot kN \cdot m$ Remaining bending moment resistance for test load

$Frd := 4 \cdot \frac{Mrest}{Ls} = 2.084 \cdot kN$ Load bearing capacity for panel in 3 point bending test under self weight

Maximum deflection

$I := \frac{b \cdot h^3}{12}$ Inertia of critical cross-section

$uz := \frac{5}{384} \cdot \frac{qself}{Ec \cdot I} \cdot Ls^4 - \frac{1}{16} \frac{qself}{Ec \cdot I} \cdot S^2 \cdot Ls^2 = 0.298 \cdot mm$ Maximum deflection before loading

9.5. Final test results

	Pressure load	Load	Dist. load	Surf load		Span	Self-weight	Bending moment	
				on 240mm				Hand Calc	SCIA
Panel 1	bar	kN	kN/m	kN/m²		m	kN/m	kNm/m	kNm/m
Crack	5,9	4,25	6,65	27,69		2,16	2,00	4,76	4,69
Failure	8,2	5,91	9,24	38,49		2,16	2,00	6,15	5,96
Panel 2									
Crack	7,2	5,19	8,05	33,53		2,16	2,00	5,55	5,52
Failure	*18,9*	*13,63*	*21,13*	*88,03*		*2,16*	*2,00*	*12,66*	*12,14*
Panel 3									
Crack	7,8	5,62	8,72	36,33		2,16	2,00	5,91	5,79
Failure	14	10,09	15,65	65,21		2,16	2,00	9,68	9,28
	Stress	Stress							
	left	right							
Panel 1	Mpa	Mpa							
Crack	2,50E+00	2,50E+00							
Panel 2									
Crack	3,18E+00	3,38E+00							
Panel 3									
Crack	3,03E+00	3,09E+00							

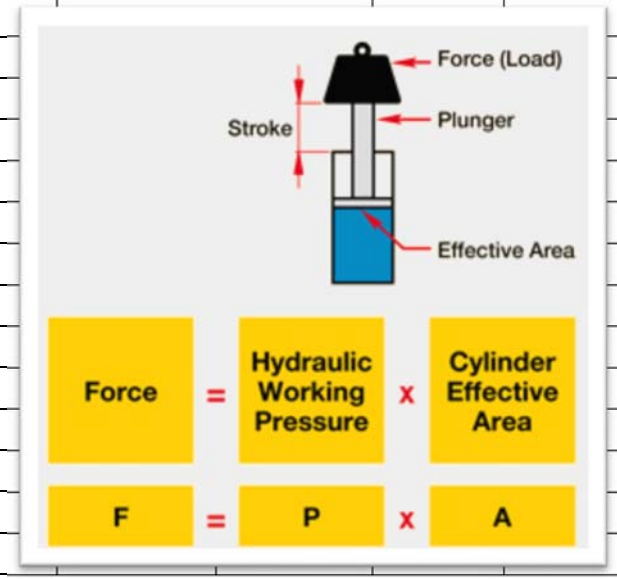

	Contour		Left		Right		Top		Bottom	
	Length	Width	Height	Width	Height	Width	Height	Width	Height	Width
	mm	mm	mm	mm	mm	mm	mm	mm	mm	mm
Panel 1	L	B	hl	wl	hr	wr	ht	wt	hb	wb
Element	2955	1235	106	320	106	320	110	420	108	280
Casted			99		99		103		99	
Panel 2	L	B	hl	wl	hr	wr	ht	wt	hb	wb
Element	2960	1230	102	325	99	320	102	350	105	350
Casted			94		98		98		103	
Panel 3	L	B	hl	wl	hr	wr	ht	wt	hb	wb
Element	2960	1235	107	320	106	325	110	420	111	280
Casted			101		*95**		*95**		107	

*(concrete stuck out underneath)

Section modulus		Tensile strength	Crack resistance		Cracking moment			Bending resistance		Bending moment		Unity Check	
Left	Right	SCC	Left	Right	Left	Right		Left	Right	Left	Right		
mm4	mm4	N/mm²	kNm	kNm	kNm	kNm		kNm	kNm	kNm	kNm		
W	W	fctm	Mrcr	Mrcr	Mcr	Mcr		Mrd	Mrd	Med	Med	UC left	UC right
5,99E+05	5,99E+05	4,43	2,65	2,65	1,52	1,52		1,37	1,37	1,91	1,91	1,4	1,4
5,23E+05	5,23E+05	4,43	2,32	2,32									
W	W	fctm	Mrcr	Mrcr	Mcr	Mcr		Mrd	Mrd	Med			
5,64E+05	5,23E+05	4,43	2,50	2,32	1,80	1,77		1,46	1,87	3,95	3,88	2,7	2,1
4,79E+05	5,12E+05	4,43	2,12	2,27									
W	W	fctm	Mrcr	Mrcr	Mcr	Mcr		Mrd	Mrd	Med			
6,11E+05	6,09E+05	4,43	2,71	2,70	1,85	1,88		1,63	1,84	2,97	3,02	1,8	1,6
5,44E+05	4,89E+05	4,43	2,41	2,17									